Identification of Pharmacogenomic and Functional Biomarkers for Antidepressant Treatment Outcome in Patients-Derived Lymphoblastoid Cell Lines

Dissertation

zur

Erlangung des Doktorgrades (Dr. rer. nat.)

der

Mathematisch-Naturwissenschaftlichen Fakultät

der

Rheinischen Friedrich-Wilhelms-Universität Bonn

vorgelegt von

Abdul Karim Barakat

aus Hama

Bonn 2022

Angefertigt mit Genehmigung der Mathematisch-Naturwissenschaftlichen Fakultät der Rheinischen Friedrich-Wilhelms-Universität Bonn

1. Gutachterin: Prof. Dr. Julia Stingl

2. Gutachter: Prof. Dr. Ulrich Jaehde

Tag der Promotion: 02.03.2023

Erscheinungsjahr: 2023

Für meine Familie

Abstract

Major depression is the most prevalent mental disorder worldwide. Pharmacological management of the disease is considered a cornerstone in treatment guidelines adopted by many industrialized countries. However, response and remission rates remain moderate to low, leaving a major proportion of patients without sufficient symptomatic improvement. Moreover, almost 15% of patients will develop treatment resistant depression resulting in a substantial burden to the health and social systems. An early clinical evaluation of individual therapy outcome is hampered by a delay in clinical improvement of several weeks. Therefore, the aim of this work was to identify rapidly determinable predictive biomarkers for the clinical outcome of antidepressant therapy and to provide insights in the molecular mechanisms underlying antidepressant effects. For this purpose, the observational Munich Antidepressant Response Signatures (MARS) study was chosen as a study cohort, in which depression patients had been previously treated in real-world practice settings and documented for their individual weekly clinical improvement in addition to their clinical response and remission status. From MARS patients, lymphoblastoid cell lines (LCLs) generated from B-lymphocytes were employed in this work as an *in vitro* model for transcriptional profiling using directed candidate gene and undirected whole-transcriptome analyses. Differential gene expression was tested under control and antidepressant short-term incubations using citalopram as a prototype antidepressant drug. After step-wise analyses of gene hits using predetermined methodologies and a validation in a larger MARS cohort, *GAD1*, *TBC1D9 and NFIB* could be determined as tentative predictive genes for clinical response, clinical remission and for improvement in depression scores, respectively. Pathway analysis of citalopram-altered gene expression revealed response-status-dependent transcriptional reactions. Whereas in clinical responders neural function pathways were primarily up- or downregulated after incubation with citalopram, deregulated pathways in non-responders LCLs were less specific to the nervous system and mainly involved cell adhesion and immune response. For determination of predictive biomarkers for treatment-resistant depression, LCLs from the interventional Sequenced Treatment Alternatives to Relieve Depression (STAR*D) study were employed. The particular sequential 4-level-treatment design of the study enabled us to select patients representing the clinical edge groups, i.e. first-line responders and treatment-

resistant patients, for pursuing transcriptional biomarker analyses. Hits detected from MARS cells showed only a tendency to association of *NFIB in* STAR*D cells, whereas associations with further genes were not significant.

Furthermore, the pharmacologically functional target of antidepressants, the serotonin transporter (SERT) was systematically studied on the genetic variants level and the transcriptional level, as well as on the total and surface protein expression levels in LCLs from the MARS and STAR*D studies for associations with response and treatment resistance status of the donor patients. Genetic investigations of the SERT-coding gene (*SLC6A4*) polymorphisms 5-HTTLPR and rs25531 did not reveal associations with the clinical outcome of the donor patients. Transcription and total protein analysis did not show static or reactional (i.e. changes upon antidepressant incubation) differences in SERT expression between LCLs from patients with different clinical outcomes. However, surface SERT demonstrated a stably higher expression in LCLs from treatment-resistant patients than in those from first-line responding patients from the STAR*D cohort. Ubiquitination of SERT did not reveal definite patterns to be associated with clinical outcome.

This work provides deeper insights in personalization of treatment in depressed patients based on response patterns. Our whole-transcriptome results propose the existence of distinct pathway regulation mechanisms in responders vs. non-responders and suggest that tentative predictors for clinical response, full remission, and improvement in depression scale, do not overlap as predictors of different therapy outcome phenotypes. Whereas no transcriptional biomarker for treatment resistance could be identified, our SERT analyses suggest an association of this clinical phenotype with higher cell surface expression of SERT.

Table of Contents

List of Figures

List of Tables

List of Abbreviations

18S rRNA	18S ribosomal RNA
AADAT	Aminoadipate aminotransferase
ACTB	β Actin
ACTH	Stimulates adrenocorticotropic hormone
AD(s)	Antidepressant(s)
AMPA	α-amino-3-hydroxy-5-methyl-4-isoxazolepropionic acid
AP	antipsychotics
BCA	bicinchoninic acid
BDNF	Brain-derived neurotrophic factor
BF	Bound fraction
BMP7	Bone morphogenetic factor
BP	Bipolar disorder
BZD	benzodiazepines
CHL1	Close homolog to L1
CNS	Central nervous system
Cp	Crossing point
CRE	cAMP Response Element
CREB	cAMP responsive element binding protein
CRF	corticotrophin-releasing factor
CTNNA2	catenin alpha 2
CTP	Citalopram
Ctrl	Control
CV%	Coefficient of variation
Cy3	Cyanin-3-cytidine triphosphate
DA	Dopamine
DMSO	Dimethyl sulfoxide
DOPAC	Dihydroxyphenylacetic acid

DRN	Dorsal raphe nucleus
DSM-5	The Diagnostic and Statistical Manual of Mental Disorders, version 5
EBV	Epstein-Barr virus
ELISA	Enzyme-linked immunosorbent assays
EPHB2	EPH receptor B2
EtOH	Ethanol
FC	Fold change
|FC|	Absolute value of fold change
FCS	Fetal calf serum
FGF7	Fibroblast growth factor 7
FKBP5	FKBP prolyl isomerase 5
FSC	Forward scatter
FYB	FYN binding protein 1
GABA	Gamma aminobutyric acid
GAD1	Glutamate decarboxylase 1
GAPDH	Glyceraldehyde 3-phosphate dehydrogenase
GRIN2A	Glutamate ionotropic receptor NMDA type subunit 2A
GSRD	The European Group for the Study of Resistant Depression
GWAS	Genome-wide association studies
HAMD	Hamilton's depression score
HAMD-21	The 21-item Hamilton depression score
HPA	Hypothalamic–pituitary–adrenal axis
HPRT1	Hypoxanthine-guanine phosphoribosyltransferase
ICD-10	International Statistical Classification of Diseases, version 10
IFNγ	Interferon gamma
IP	Immunoprecipitation
ITGB6	Integrin subunit beta 6
LCLs	lymphoblastoid cell lines

LME	Linear mixed-effects regression model
MADRS	Montgomery–Åsberg Depression Rating Scale
MAOI	monoamine oxidase inhibitors
MARS	Munich Antidepressant Response Signatures
MDD	Major depression disorder
MPI	Max-Plank-Institute for Psychiatry
MRI	Magnetic resonance imaging
MS	mood stabilizers
NARI	Noradrenergic reuptake inhibitors
NaSSA	Noradrenergic and Specific Serotonergic Antidepressant
NCBI	National Center for Biotechnology Information
NFIB	Nuclear factor I B
NINL	Ninein like
NMDA	N-methyl-D-aspartate
NR	Non-responding patient
NRP1	Neuropilin 1
OCD	Obsessive-compulsive disorder
OTH	other antidepressants
PBMCs	Peripheral blood mononuclear cells
PCR	Polymerase chain reactions
PFC	Prefrontal cortex
PITX1	Paired like homeodomain 1
PKC	Protein kinase C
PKG	Protein kinase G
QIDS	Quick Inventory of Depressive Symptomatology
RAMP1	Receptor activity modifying protein 1
RBPMS	RNA binding protein, mRNA processing factor
RESP	Responding patient

RIN	RNA integrity number
RPL13A	Ribosomal Protein L13a
SED	Sedatives
SERT	Serotonin transporter
SLC6A4	Solute carrier family 6 member 4 (Serotonin transporter)
SMAD7	Mothers against decapentaplegic homolog 7
SMPD1	Sphingomyelin phosphodiesterase 1
SMURF1	SMAD specific E3 ubiquitin protein ligase 1
SMURF2	SMAD specific E3 ubiquitin protein ligase 2
SNRI	serotonin norepinephrine reuptake inhibitors
SSC	Side scatter
SSRE	selective serotonin reuptake enhancer
SSRI	selective serotonin reuptake inhibitors
STAR*D	Sequenced Treatment Alternatives to Relieve Depression
TBC1D9	TBC1 domain family member 9
TBP	TATA-box binding protein
TCA	tricyclic antidepressants
TET1	TET methylcytosine dioxygenase 1
TGFB1	transforming growth factor beta 1
TGFBR1	Transforming growth factor beta receptor 1
TMD	Transmembrane-domain
TPH	Tryptophan hydroxylase
TR	Treatment resistant patient
UCHL5	Ubiquitin C-terminal hydrolase L5
UF	Unbound fraction
UNC13C	unc-13 homolog C
VNTR	Variable number tandem repeat
YLD	Years lived with disability

Chapter I Introduction

I.1. Major Depressive Disorder

Major depressive disorder (MDD) is the most prevalent mental disorder worldwide. Among one billion people suffering from mental and addictive disorders on the globe, MDD is estimated to affect over 320 million patients[1-3]. Socioeconomic consequences of depression are immense. Almost 7.5% of years lived with disability (YLD) in 2015 were attributed to depressive disorders[4]. Outlooks for the future labor population prophesy a growing threat of depression for society. The reported disease rates from 2005-2017 show steep increases in morbidity of 52 and 63 per cent in adolescents and young adults, respectively[5]. Pathologically, MDD is considered a heterogeneous disorder with respect to the symptomatic manifestations, underlying causes and clinical response. In practice, diagnosis is based on subjective symptoms with almost complete lack of objectively observable, quantifiable signs. According to the fifth Diagnostic and Statistical Manual of Mental Disorders (DSM-5), MDD is diagnosed when during a 2-week period an individual experiences five or more of the following symptoms: sad mood, diminished interest, concentration and/or energy, markedly changed appetite and/or weight, persistent feeling of worthlessness, guilt, and suicidal ideation[6]. Several depression-specific rating scales are available to measure severity of symptoms including Hamilton Depression Rating Scale (HAMD), Montgomery–Åsberg Depression Rating Scale (MADRS) and Quick Inventory of Depressive Symptomatology (QIDS)[7-9]. Depression is believed to be inherited. Younger age at onset, psychosis comorbidity and high recurrence seem to be at least partially heritable[10, 11]. Inheritance is, however, considered multifactorial and is further conditioned by the environment[12, 13]. Association of genetic variants with depression has been heavily analyzed[14]. However, solid findings of pathologic genetic alterations are still lacking[15]. Moreover, individual clinical response to antidepressants is largely unpredictable, heterogeneous and of poor rates[16]. The first chapter of the work is dedicated to present the state of art of our understanding of depression pathophysiology, of relevant serotonin transporter implication, of the mechanism of action of antidepressants and of recent research conducted on predictive biomarkers for antidepressant response.

I.2. Pathogenesis Hypotheses and the Antidepressant Mechanism of Action

Despite tremendous efforts over the past decades, the molecular underpinnings of depression remain not fully deciphered. Various hypotheses have nevertheless emerged in attempts to explain depression pathogenesis. Emergence of these hypotheses depended to a great extent on experiments using already available antidepressants. Thus, studies on depression pathogenesis and on antidepressant mechanism of action are often found as a duality in literature. Since an individual's response to a pharmacological treatment is believed to correlate to a change in the pathophysiological state of this individual, and the observation and measurement of this change can be employed as a predictive biomarker, an overview of hypotheses of depression pathophysiology is given in the following sections.

I.2.1. The Monoamine Hypothesis of Depression

The monoamine hypothesis is considered the earliest evidence-based hypothesis on depression and dates back to 1965. At those times, the hypothesis speculated that depression evolves due to a declined monoamine transmission, in particular of Serotonin (also 5-hydroxytryptamine, 5-HT) and norepinephrine (NE)[17, 18]. In the central nervous system, the two monoamines exert overlapping but still, to a considerable extent, distinct functional profiles. While 5-HT is involved in complicated cognitive processes such as memory, learning, affection and emotional states[19-22], NE increases arousal and alertness[23, 24]. Shortly after presenting the monoamine hypothesis, 5-HT drew more attention as the key neurotransmitter of the disease. This was supported by works demonstrating that concomitant administration of monoamine oxidase inhibitors (MAOIs) with tryptophan (precursor of 5-HT) elevated mood in patients and potentiated the antidepressant effect of MAOI[25]. Additionally, the therapeutic effect of MAOIs and tricyclic antidepressants (TCAs) was later shown to be counteracted by giving 5-HT synthesis inhibitors[26, 27]. The subsequent success of the Selective Serotonin Reuptake Inhibitors (SSRIs) in becoming the first-line antidepressants conferred significant weight on the role of 5-HT. Nevertheless, the observation that antidepressants produce immediate effects on monoamine transmission whereas the therapeutic effects appear with a delay of several weeks challenged the hypothesis for decades[28-30]. The current version of the hypothesis proposes increased monoamine transmission caused by antidepressants to be an initial event followed by a sequence of

intracellular signaling cascades modulating neuronal function, growth and structure in a process known as neuroplasticity[31, 32]. Our understanding of the latter developed with time to eventually raise a neuroplasticity hypothesis for depression and antidepressant effects, *per se*.

I.2.2. The Neuroplasticity Hypothesis of Depression

Neuroplasticity refers to the ability of the nervous system to sense, respond and adapt to internal and external stimuli[33]. This ability leads to structural and functional alterations in the nervous system including formation of novel neurons (neurogenesis), new synapses (synaptogenesis) and neuronal remodeling[34]. Active neurogenesis is implicated in the neurodevelopment in early life but also in adults[35] e.g. in the dentate gyrus in the hippocampus[36], the neocortex[37], and the amygdala[38]. Within the complex chemistry of neurogenesis, the serotonergic system, neurotrophic factors[39] and adrenal steroids[40] seem to dominate its regulation. Reminding of the monoamine hypothesis, inhibition of 5-HT synthesis and depletion of serotonergic neurons were found associated with reduction in numbers of newly generated cells in the dentate gyrus[41]. In contrast, increasing serotonergic activity via chronic treatment with antidepressants elevated number of proliferating cells, of which 75% eventually differentiated to neurons[42]. Not surprisingly, serotonin transporter (SERT), the main target blocked by antidepressants, has been considered a major element in the scene. Short-term knockdown of *SLC6A4,* the transcript coding for SERT, decreased expression and function of 5-HT_{1A} autoreceptors, increased 5-HT in forebrain and reinforced neurogenesis in the hippocampus. In summary, 5-HT activity has been proven critical for naturally occurring cell proliferation in adult brain, and is a key element involved in its regulation. Nevertheless, the immediate steering agents of neurogenesis are believed to be the neurotrophic factors, which are neurodevelopmental growth factors that regulate plasticity within the adult brain. Out of these, studies particularly focused on the brain-derived neurotrophic factor (BDNF) and its transcription factor cAMP response element-binding protein (CREB). The two proteins were found to possess modulatory effects on neurogenesis of a dynamic nature. Hippocampal expression of CREB and BDNF was found to decrease in response to chronic stress and increase in response to antidepressants in animal studies[43-45]. Similarly, post-mortem studies showed that there are lowered expression levels in the PFC of depression patients[46]. Moreover, numerous studies described predictive potential of CREB and BDNF expression for

response to antidepressants[47-50]. Another protein, close homolog to L1 (CHL1), is a cell adhesion protein abundantly expressed in the nervous system, mainly in areas of high plasticity[51, 52]. It plays a key role in neuron migration, survival, synaptogenesis and myelination in the developing and in the adult brain[53-55]. Earlier findings implied also a therapeutic relevance of *CHL1* as genetic variants and transcription levels were found to predict response status to antidepressant treatment[47, 56-58]. Neurogenesis is furthermore known to be regulated by epigenetic factors including DNA methylation and histone acetylation[59]. Of several epigentic regulators, the methylcytosine dioxygenase TET1 was found to be heavily involved in neurogenesis, both in early life but also in adults [60-62]. Moreover, functional modification of TET1 was shown to alter behavioral phenotypes in animal models. Knockout in nucleus accumbens of adult mice produced antidepressant-like effects[63] and led to resistance to chronic stress[64]. These genes (*BDNF, CREB, CHL1* and *TET1*) are thus considered to play key roles in the neuroplasticity process as cumulatively evidenced from *in vitro, in vivo* and clinical research and have thus been subject of investigation within the current work.

I.2.3. The Inflammatory Hypothesis of Depression

Inflammation is the term typically used to describe the immunological reaction of the body to physical injuries, including infections. Although classically seen as a response to physical injury, there is growing evidence that systemic inflammation can be triggered by psychological stress perceived from modern social environment[65, 66]. The emerging neuro-inflammation evokes substantial cognitive changes including the initiation of depressive symptoms such as anhedonia, sadness, loss of interest, feeling of worthlessness, guilt, and decreased social behavior[67]. The hypothalamic–pituitary–adrenal axis (HPA axis) is the main interactional interface of the immune and the central nervous systems. It plays a key role in regulating the inflammatory process through secretion of the corticotropin releasing factor (CRF), adrenocorticotropic hormone (ACTH) and cortisol from the hypothalamus, the pituitary gland and the adrenal glands, respectively, eventually resulting in inhibition of the immune response. However, perception of sustained or frequent stress results in HPA axis dysregulation as the immune cells develop glucocorticoid insensitivity and restore their pro-inflammatory activity[68]. The compensated pro-inflammatory activity, together with the chronic high levels of cortisol lead to neuronal atrophy

and volume decline of the hippocampus, a phenomenon repeatedly observed associated with depression[69-71]. In this context, FKBP5, a co-chaperone with inhibitory effects on the cortisol receptor, the glucocorticoid receptor (GR), has been repeatedly shown to be involved in regulation/dysregulation of the HPA axis[72, 73]. *FKBP5* gene variants were further shown to associate with increased depression recurrence rapid antidepressant treatment response[74] risk for adult depression[75, 76] and for post-traumatic stress disorder[76, 77]. Recently, higher *FKBP5* expression levels were observed in non-responders after six-week antidepressant treatment[78]. These findings point out to *FKBP5's* potential in predicting antidepressant response. On the other hand, reports on involvement of the cytokines (inter-cellular messengers of the immune system) indicate pivotal roles of the transforming growth factor beta (TGFβ) pathway in depression[79, 80]. Unlike many cytokines, which usually possess consistent pro- or anti-inflammatory effects, TGFβ is seen as a pleiotropic cytokine with both regulatory and inflammatory activities. It acts through binding to the TGFβ receptor complex which in turn phosphorylates intracellular second messengers known as the SMAD family[81]. In a clinical trial, lower levels of SMAD7 were observed in peripheral blood of antidepressants responders[82]. Our previous work (unpublished) on a small sample of blood cell lineages derived from depression patients showed similar, consistent tendencies of higher *SMAD7* expression in responders. However, a closer interpretation of these results warrants the study of further function-modulating molecules. This is due to the fact that SMAD7 function highly depends on its next interaction. Whereas an interaction with Smurf1/2 would result in termination of TGFβ signaling through promotion of receptor degradation, an interaction with UCH37 would stabilize the TGFβ receptor and maintain its action[83]. Thus, the study of the expression patterns of TGFβ, SMAD7, Smurfs 1/2 and UCH37 is of critical importance in biomarker research.

I.2.4. Converging the Pathogenesis Hypotheses of Depression

Together, the presented pathogenesis conceptions can serve as a comprehensive outline of further, more specific hypotheses mentioned elsewhere in literature which can be sub-categorized under one, or more, of the above mentioned hypotheses. An overlap between the single distinct hypotheses can already be noticed above at more than one level, e.g. implication of the serotonergic system in neurogenesis (section I.2.2) and decreased hippocampal volume

upon sustained cortisol secretion (section I.2.3). The link between the three presented hypotheses has been additionally empirically demonstrated through the observation of intracellular pathway regulation upon treatment with antidepressants. Incubation of hippocampal progenitor cells with sertraline, an SSRI, increased growth of immature neuroblasts and mature neurons. This effect was abolished by blocking the glucocorticoid receptor[84]. This and other data prove that depression pathophysiology is versatile, so that it can only partially be explained by each of the hypotheses with any one hypothesis standing alone not being able to fully decipher the disease underpinnings.

I.3. Treatment of Major Depression Disorder

Depression treatment aims to reduce the duration and relapse of a current episode and, in the long term, to reduce the recurrence of new episodes[85]. Pharmacotherapy is considered an effective component of depression treatment. MAOIs and TCAs were the first drugs used against depression. However, the frequent food- and drug-drug interactions of MAOIs and adverse effects of TCAs limited their usage, especially in comorbid patients. The later developed selective serotonin reuptake inhibitors (SSRIs) had a more favorable safety profile and were at least as effective. Further antidepressants classes followed, including serotonin and norepinephrine reuptake inhibitors (SNRIs, e.g. venlafaxine), noradrenergic and specific serotonergic antidepressants (NaSSAs, e.g. mirtazapine) and norepinephrine reuptake inhibitors (NARIs, e.g. reboxetine; see Table 1). These classes differ from each other according to the set of transporters and receptors they affect and the affinity of the drugs to those targets. This is clinically observed as distinct pharmacological and clinical properties (e.g. adverse and/or secondary effects), sometimes within one drug family[86-89]. Most current antidepressants have been mainly, if not solely, developed based on the monoaminergic hypothesis of depression etiopathogenesis. Yet they are far from being ideal. Although they produce immediate effects on monoamine transmission, therapeutic effects need several but no less than 2 weeks to fully occur and are still often accompanied by unwanted adverse effects[14]. Moreover, treatment outcomes are suboptimal leaving a major proportion of patients without sufficient response. It has been estimated that about one to two thirds of patients adequately treated MDD did not respond to first-line antidepressant treatment, of whom, 15 - 33% did not respond to multiple interventions

and could be considered as treatment resistant[90]. The current treatment strategies applied in the psychiatric practice continue to depend on a trial and error principle[91], leaving more patients with prolonged periods of symptoms, increasing complication rates and health care costs[92]. Thus, finding biomarkers that predict a patient's response is of utmost importance to clinicians, patients and the health care system. In this context, identification of pathways and structures possibly differentially targeted by antidepressants in patients with different clinical outcome is of great interest, as it can provide insights into the genomic and functional correlates of heterogeneous therapeutic successes[93]. If these target structures and their biological variations are known, it will be possible in the future to create personalized concepts optimally matched to each patient's biological profile. This will save time of unsuccessful therapy attempts and reduce the treatment costs[94]. In order to achieve this goal, efforts are also underway on the development of antidepressant classes that affect targets other than the monoamines including the HPA axis and neurogenesis and are supposed to have an antidepressant effect[95].

Table 1. Main antidepressant drug classes.

Class	**Prototype drug**	**Proposed mechanism of action**
TCA	Amitriptyline Imipramine Clomipramine	Inhibition of serotonin and norepinephrine transporters, modulation of serotonergic, adrenergic, glutamatergic, cholinergic and histaminic receptors
MAOI	Phenelzine Tranylcypromine	Inhibition of monoamine oxidase
SSRI	Citalopram Fluoxetine	Inhibition of serotonin transporters
SNRI	Venlafaxine	Inhibition serotonin and norepinephrine transporters
NaSSA	Mirtazapine	Modulation of adrenergic and serotonergic receptors
NARIs	Reboxetine	Inhibition of norepinephrine reuptake transporters

TCA - tricyclic antidepressants, TeCAs - tetracyclic antidepressants, MAOI - monoamine oxidase inhibitors, SSRI - selective serotonin reuptake inhibitors, SNRI - Serotonin-norepinephrine reuptake inhibitors, NaSSA - noradrenergic and specific serotonergic antidepressant, NARIs - norepinephrine reuptake inhibitors

I.3.1. Biomarkers for Antidepressant Treatment Outcome

The term biomarker can be defined as an objectively measurable feature of an individual that provides information on a disease state, predicts the outcome of a treatment or predicts the likely course of the disease in untreated individuals[96, 97]. Accordingly, biomarkers can be divided into diagnostic biomarkers, treatment-predictive biomarkers and prognostic biomarkers. Treatment-predictive biomarkers may be present at baseline, or, alternatively, may change shortly after treatment initiation in such a way as to predict the ultimate response. In the latter case, the biomarker should be measured at baseline and again early in the course of therapy. Biomarkers are typically biological features (e.g. genome variation, plasma concentration of a protein, etc.), but do not have to be limited in this manner (e.g. functional biomarkers)[98].

I.3.1.1. Predictive Genetic Biomarkers

Genetic epidemiological studies observed that MDD runs in families with a 2-3 fold higher prevalence in first-degree relatives of a depression patient. A meta-analysis study with 21000 individuals revealed a genetic contribution of 37% for MDD[11]. Considering illness factors like severity, relapse and early onset increases heritability up to 70%[99]. The Munich Antidepressant Response Signature (MARS) and the Sequenced Treatment Alternatives to Relieve Depression (STAR*D) studies are two clinical studies that investigated genetic biomarkers in depressive disorders and from which cell lines employed in the current work were derived (more details on the two studies can be found under section III.2.2). Analyses conducted over the course of the two studies reported correlations between several genetic variants and different clinical endpoints observed in patient subgroups. Thereof, polymorphisms within the *FKBP5* (a co-chaperone that regulates glucocorticoid receptor sensitivity) were found to modulate the association of increased expression with depressive symptoms relapse in MARS patients[78]. In a prospective MARS sample, carriers of the G variant at the rs7905446 SNP in the *HTR7* (serotonin receptor 7) were found to more consistently respond to paroxetine and fluoxetine[100]. A further

analysis tried to replicate earlier findings of the STAR*D study by testing response and remission of depressive symptoms in about 300 MARS patients against 82 *GRIK4* (glutamate receptor, ionotropic, kainate 4) and 37 *HTR2A* (serotonin receptor 2A) SNPs. Previously reported SNPs, however, turned to show negative results, with some associations with the opposite risk alleles. On the other hand, different variants of *GRIK4* and *HTR2A* not previously reported showed associations with clinical endpoints[101]. Further analyses identified variants in the *BDNF* (brain-derived neurotrophic factor), *NTRK2* (BDNF receptor), *ABCB1*, *GAD2* (glutamate decarboxylase 2) or *SLC6A15* as potential biomarkers for treatment outcomes and the susceptibility to develop depressions[102-105]. A genome-wide association study (GWAS) conducted on 1116 STAR*D patients to study biomarkers for sustained therapy response identified strongest association with a single nucleotide polymorphism (SNP; rs10492002) within the acyl-CoA synthetase short-chain family member 3 gene (ACSS3)[106]. A further GWAS conducted on 1491 patients to study common DNA variation influencing citalopram response and remission identified three SNPs associated with response near *UBE3C* (rs6966038), *BMP7* (rs6127921), and a third that is intronic in the *RORA* gene (rs809736). In an analysis targeting gene variants of the opioid mu- receptor, only one SNP, rs540825, showed an association with specific citalopram response that endured Bonferroni correction[107]. Yet, it can be noticed that genome-wide association studies could not define single reproducible risk genes[108]. Likewise, tremendous efforts could not detect gene-sets, poly-genic risk scores predictive for antidepressant treatment response[109, 110]. No less than 8 single large-scale GWAS with individual sample sizes of over 9100 patients, along with their later meta-analyses could not identify reliable genetic predictors of antidepressant treatment outcome[109-117]. This might suggest that clinical response could be regulated by factors other than stable germline genetic variants e.g. gene expression, protein expression, trafficking and turnover.

I.3.1.2. Peripheral Transcriptomic Biomarkers

Studying of gene expression in the brain is hampered by the difficulty of access to cerebral tissues for specimen collection. A number of studies investigated RNA derived from post-mortem cerebral tissue[118]. However, gene expression can be largely confounded by agonal and post-mortem factors[119]. On the other hand, peripheral blood cells are easily accessible and are in contact with body's tissues. While gene expression in blood is not believed to mirror that of the

neuronal cells, an overlap between the transcriptome in peripheral blood and brain has been reported. Rollins and co-workers showed that over 4,000 transcripts are co-expressed in post-mortem brain tissue and peripheral blood cells[64]. In a further genome-wide analysis, a co-expression as high as 81% between human peripheral blood and cerebral tissue was observed[120]. Quantitatively, a study of transcriptional profiling of 79 human tissues for 33,698 genes showed an intermediate median correlation between whole blood and 16 CNS tissues (r=0.52), higher than that with muscle and peripheral nervous tissues (r=0.48, 0.36, respectively) but, not unexpectedly, below that with the immune system (r=0.64)[121].

Research on transcriptional biomarker in peripheral blood has covered diverse neuropsychiatric disorders including Parkinson's disease, Huntington's disease, post-traumatic stress disorder, schizophrenia, bipolar disorder, and major depression (reviewed by Menke 2013[122]). Biomarkers for antidepressant response have also been subject of several investigations. Noteworthy examples include two studies by Mamdani *et al.*, which identified expression of *IRF7* as predictor for improvement in HAMD scores after treatment with citalopram, and expression of *SMAD7* and *SIGLECP3* as predictors for remission[123]. In an interesting longitudinal study design of initially healthy patients, Belzeaux *et al.* identified *PPT1, TNF, IL1b* and *HIST1H1e* as predictors of antidepressant treatment response[124]. Hennings *et al.* conducted a 2-phase screening for predictive transcriptomic biomarkers in an exploratory (n=12) followed by a replication (n=142) patient cohorts. The researchers could identify expression of retinoid-related orphan receptor alpha (*RORa*) as a candidate predictive biomarker[125].

The next sub-section gives a short review on lymphoblastoid cell lines that should warrant their use as an *in vitro* model in this work.

i. Lymphoblastoid Cell Lines (LCLs) as *in vitro* Cell Models in Antidepressant Response Biomarker Research

Lymphoblastoid cell lines (LCLs) emerge upon treating the peripheral blood mononuclear cells (PBMCs) with Epstein Barr virus (EBV) *in vitro*, resulting in the virus selectively infecting, transforming and consequently immortalizing the B-lymphocytes subpopulation. Subsequently, an individual-specific lymphoblastoid cell line (LCL) arises[126]. LCLs are gaining popularity as an *in-vitro* model for the inherent human genome natural diversity. Although comparisons between

LCLs and their primary cellular peers showed that EBV transformation altered gene expression profiles in about half of the genes tested, yet the changes remained minimal (<1.5 folds) and, more importantly, inter-individual differences were maintained[127, 128]. Moreover, the fact that LCLs emerge from one subpopulation of leucocytes, the inter- and intracellular impact of the presence of other leucocytes subpopulations is minimized. The utility of LCLs in biomarker research began as these cell lines had been used in studies searching for gene-expression markers for antineoplastic drug sensitivity reactions. Transcriptomes of 'edge' cell lines with the highest vs. lowest sensitivities to cytotoxic cancer drugs of interest were compared and candidate biomarkers were identified for several antineoplastic agents (reviewed by Morag *et al.* 2011[129]). The fact that serotonin transporter (SERT) is expressed in LCLs encouraged extending this concept to antidepressant drugs[22]. Moreover, LCLs have been shown to resemble neuronal cells in their gene expression regulation and produce a model that can be employed in follow-up studies[130-133]. Earlier studies from our group investigated gene expression of target genes in LCLs from patients with depressive episodes and identified *ITGB3* and *CHL1* to be candidate predictive biomarkers for clinical remission i.e. full clinical recovery[56]. Recently, functional neuroplasticity biomarkers have been investigated by studying *ex vivo* proliferation rates and gene expression profiles of LCLs from patients with depressive episodes after long-term (21-day) *in vitro* incubation with fluoxetine. Cell proliferation was found to correlate with treatment resistance i.e. when comparing responders to treatment-resistant patients, but not with response, i.e. when comparing responding to non-responding patients. Additionally, transcriptional biomarkers for treatment resistance and response could be identified. Expression levels of *WNT2B, ABCB1,* and *FZD7* were found predictive for treatment resistance while expression of *WNT2B, SULT4A* correlated with response suggesting *WNT2B* as a common predictor[134, 135].

I.3.1.3. Functional Biomarkers

In addition to our quickly growing knowledge of pharmacogenomics, newly emerging fields of research are gaining increasing interest, including studying of functional biomarkers. These include a heterogenous spectrum of quantifiable parameters that highly depend on the measuring methodologies. Thus, functional MRI biomarkers, EEG biomarkers and functional biological biomarkers emerged. The latter involve studying of functional aspects of target

molecules in an attempt to identify differences between individuals with distinct clinical manifestations[96]. For antidepressant therapy, SERT has been in focus for functional investigations; however, only in very few works. Since SERT exerts its transport function only when at the cell surface, this work was also dedicated to establish an investigational battery to study peripheral SERT total and surface expression as putative functional biomarker for treatment outcome.

I.4. Serotonin Transporter in Depression

I.4.1. Function, Topology and Physiology of Serotonin Transporter

Serotonin transporter (SERT, also 5-HTT and SLC6A4) is a membrane protein that is responsible for the active transport of serotonin from the extracellular space to inside the cell. In the CNS, this process involves the re-uptake of serotonin from synaptic cleft back to the presynaptic neurons resulting in a termination of serotoninergic neurotransmission. SERT possesses a 12-transmembrane-domain (TMD) topology, which resembles the typical structure found among members of the Na^+/Cl^--dependent solute carriers (SLC) family. The amino and carboxylic termini of the single peptide chain lie in the cytoplasm (Figure 1). Post-translational modifications include N-glycosylation, which mainly takes place at the large extracellular loop located between TMDs iii and iv. Further members of the SLC family include neurotransmitters (e.g. dopamine, norepinephrine, GABA), neuromodulators and osmolyte transporters[136-139]. SERT is abundantly expressed in the mammalian body. Its expression could be identified in blood lymphocytes[140], platelets[141], placental syncytiotrophoblasts[142] and epithelial cells of the gastrointestinal mucosa[143]. In the brain, immunohistochemistry studies detected SERT expression in the hippocampus, the olfactory bulb, cerebellum, amygdale, raphe nuclei and suprachiasmatic nucleus[144, 145]. These findings are especially intriguing owing to the role serotonin plays in modulating emotions, cognition and adult neurogenesis (see I.2.1 and I.2.2). SERT involvement in depression, anxiety, autism and obsessive-compulsive disorder (OCD) has been well established[146-148]. It is thus not surprising that SERT is targeted by several psychoactive drugs when antidepressant, anxiolytic, mood stabilizing, psychostimulating or even illicit intoxicating effects are sought[149-153]. Particularly, SERT is a main target of major, frequently prescribed antidepressant classes including the first line SSRIs, TCAs and SNRIs[154-157], see I.2 for details).

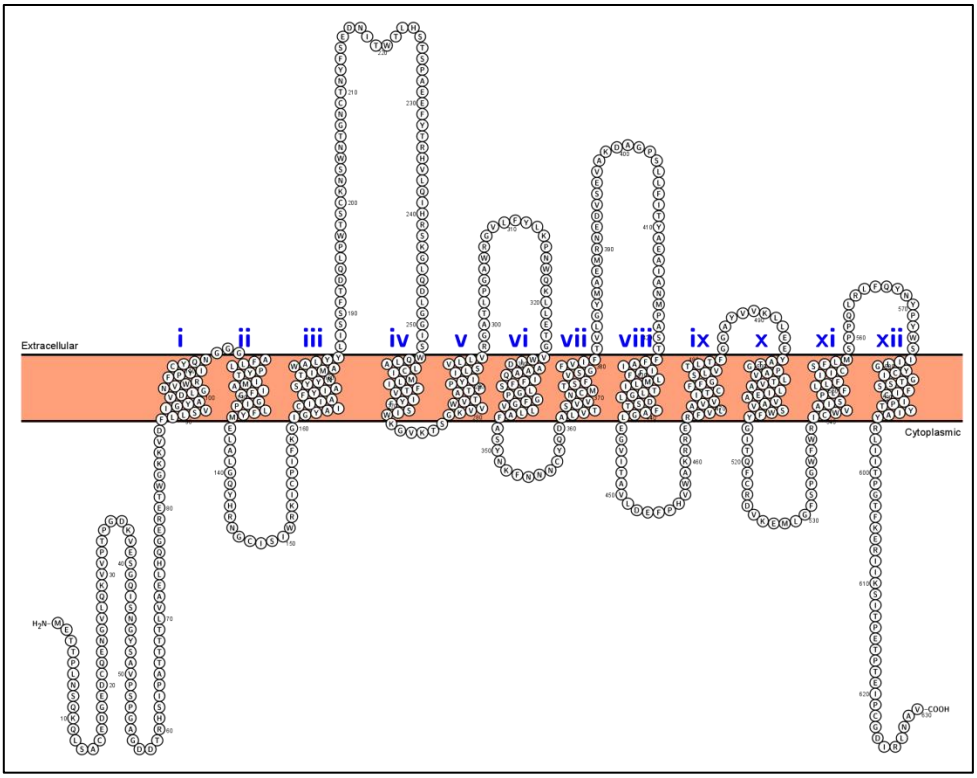

Figure 1. A topology diagram of SERT. The single amino acid chain of SERT spans the cytoplasmic membrane 12 times giving rise to 12 transmembrane domains (TMDs) connected by hydrophilic loops, a topology typical for Na^+/Cl^- symporters from the solute carrier (SLC) family. Both the carboxylic and the amino termini are predicted to hover in the cytoplasm. Antibody FL-N40 used in this work was raised against the large extracellular loop between TM vii and viii. The diagram was created using Protter[158] based on the UniProt SERT entry: P31645.

I.4.2. Gene Variants of Serotonin Transporter: 5-HTTLPR and rs25531 Polymorphisms

Human SERT is encoded by *SLC6A4* gene which was identified and sequenced for the first time in 1994 by Lesch *et al.*[159]. After several curations, the current RefSeq database (accessed on 17-07-2022) locates the gene to band 11.2 on the short arm of chromosome 17. This gene consists of more than 48 kb containing 15 exons that code for the 630 amino-acid-long, single chain protein. The gene was found to possess several polymorphisms that mainly affect its expression/function and rarely the protein structure[160]. One of the most studied polymorphisms is located within the gene promoter locus, almost 1 kb upstream from the 5´-UTR. This region, known as 5-HTT-linked polymorphic region (5-HTTLPR), contains a variable number of GC-rich, 20- to 23-bp-long tandem repetitive elements (VNTRs) (Figure 2). The polymorphism, lately designated rs1567826436, involves an insertion/deletion (indel) of a 43-bp-long sequence resulting in a short (S), 14-repeat, and a long (L), 16-repeat allele. The S and L alleles have the same protein structure since they

appear in the non-coding region, but they differently affect the expression of SERT. The S allele is believed to convey reduced transcription, resulting in lower transporter levels, and lower serotonin uptake, with putatively functional effects on neural circuits relevant to mood regulation[161]. This S/L bi-allelic subdivision of 5-HTTLPR was later replaced with a haplotype model as an A>G substitution SNP (rs25531), upstream to the indel polymorphism, was found to further condition SERT expression in L-allele carriers (Figure 2). The SNP renders only the A variant of the L allele (LA haplotype) as yielding high 5-HTT mRNA levels, but not the G variant (LG haplotype). Thus, the LG haplotype apparently behaves equivalent to the low-expressing S variant[162]. 5-HTTLPR has been extensively analyzed for associations with several psychiatric disorders including bipolar disorder, anxiety as well as depression[163-166]. However, 5-HTTLPR association with depression appears to be complicated by several factors including environmental stressors and ethnicity[148, 167-169]. Data on association with treatment outcome in depression patients remain to date inconsistent[170, 171]. Authors of several studies suggested future work to include stratifications by outcome phenotype (remission, response) and by antidepressant treatment to omit bias during the statistical detection of allele effect[172]. In the current work, efforts were focused on addressing this knowledge gap by investigating the rs25531 and the indel polymorphisms along with *SLC6A4* expression in LCLs from patients stratified by administered antidepressant therapy and clinical outcome.

	1	2	3	4	5	6	7	8	9	10	11	12	13	14	15	16	17	18	19	20	21	22	23	Number of bases	GC%
α	T	G	C	A	G	C	C	C	T	C	C	C	A	G	C	A	T	C	C	C	C	C	C	23	73.91%
β	T	G	C	A	A	C	C	T	C	C	C	A	G	C	A	A	C	T	C	C	C	-	-	21	61.90%
γ	T	G	T	A	C	C	C	C	T	C	C	T	A	G	G	A	T	C	G	C	T	C	C	23	60.78%
δ	T	G	C	A	T	C	C	C	C	C	A	T	T	A	T	C	C	C	C	C	C	C	-	22	63.64%
ε	T	T	C	A	C	C	C	C	T	C	G	C	G	G	C	A	T	C	C	C	C	C	C	23	73.91%
ζ	T	G	C	A	C	C	C	C	C	**R**	G	C	A	T	C	C	C	C	C	C	-	-	-	20	75.00%
o	T	G	C	A	G	C	C	C	C	C	C	C	A	G	C	A	T	C	T	C	C	C	C	23	72.73%
ζ	T	G	C	A	C	C	C	C	C	A	G	C	A	T	C	C	C	C	C	C	-	-	-	20	75.00%
η	T	G	C	A	G	C	C	C	T	T	C	C	A	G	C	A	T	C	C	C	C	C	-	22	68.18%
θ	T	G	C	A	C	C	T	C	T	C	C	C	A	G	G	A	T	C	T	C	C	C	C	23	65.22%
ι	T	G	C	A	A	C	C	C	C	C	A	T	T	A	T	C	C	C	C	C	C	-	-	21	61.90%
κ	T	G	C	A	C	C	C	C	T	C	G	C	A	G	T	A	T	C	C	C	C	C	C	2	69.57%
λ	T	G	C	A	C	C	C	C	C	C	A	G	C	A	T	C	C	C	C	C	C	A	-	22	72.73%
μ	T	G	C	A	C	C	C	C	C	G	G	C	A	T	C	C	C	C	C	C	-	-	-	20	80.00%
ν	T	G	C	A	C	C	C	C	T	C	C	A	G	C	A	T	T	C	T	C	C	T	-	22	59.09%
ξ	T	G	C	A	C	C	C	T	A	C	C	A	G	T	A	T	T	C	C	C	C	C	-	22	59.09%

Figure 2. Nucleotide sequence of the variable number of tandem repeat (VNTR) segments of the 5-HTT-linked polymorphic region (5-HTTLPR) of *SLC6A4*. Nucleotides shaded in black mark the 43-bp-long sequence involved in the indel polymorphism, which gives rise to the long (L) and short (S) alleles. SNP rs25531 is referred to as **R** in the sixth segment (ζ), where **R** = A or G. The figure is modified from Myint *et al.*[173].

I.4.3. Serotonin Transporter Total and Surface Expression as a Functional Biomarker

Evidence on pathological associations of SERT expression levels has been increasingly reported in literature in the context of depression, comorbid depression and OCD, to name a few[174, 175]. The fact that SERT expression in the lymphocytes and platelets is associated with its expression in the central nervous system made it a promising peripheral surrogate indicator[140, 176]. Previous works demonstrate a significant decrease in SERT binding in platelets from depression patients in comparison to healthy controls[177]. Likewise, lymphocytes of depression patients also demonstrate lower SERT expression[178]. However, growing research adopts the functional notion of SERT and investigates relating surrogates. Since SERT exerts its transport function only when at the cell surface, surface expression and intracellular localization of the transporter molecule rather than studying total SERT expression in a tissue has gained focus. SERT is on a continuous, dynamic distribution between the cell surface and intracellular compartments, yet the underlying controlling factors and mechanisms are not fully understood[179]. Meanwhile, it is known that 5-HT signaling, mainly through the G-protein coupled receptor 5-HT_{2A}R and the consequent protein kinase C (PKC) regulation should play a major role[180]. Other regulating kinases include p38 mitogen-activated protein kinase (p38 MAPK) and protein kinase G (PKG)[181, 182].

How SERT surface and total expression is related to antidepressant action and, more interestingly, clinical outcome remains insufficiently investigated. Some studies propose that antidepressants action involves, in addition to the functional blockade of monoamine transporters, a regulation of SERT expression[183-185]. An *in vitro* study on transfected HEK293 cells showed long-term exposure to citalopram to cause a downregulation of transport activity in which substrate affinity remained unchanged while a decrease in ligand binding sites in membrane SERT was observed[186]. In line with this, exposure of murine serotonergic neurons to SSRIs reduces SERT surface levels by internalization and redistribution into the soma which results in a decrement in 5-HT uptake[187]. In lymphocytes from depression patients, SERT has been demonstrated to build clusters that do not necessarily differ in number between patients and healthy controls but in size. Moreover, and within patients, these spatial distribution patterns associated with patients' responsiveness to antidepressant therapy[188]. More efforts were considered necessary for extensive establishment of peripheral SERT total and surface expression as treatment response biomarker. In a continuum

of the current research findings, one major aim of this work was dedicated to establish an investigational battery to study peripheral SERT total and surface expression as putative functional biomarker for treatment outcome.

I.4.3.1. Serotonin Transporter Ubiquitination

Ubiquitination is a post-translational protein modification that involves a covalent conjugation of an 8-kDa protein, ubiquitin, to lysine residues on a substrate protein. Proteins may undergo mono-ubiquitination events on several lysine residues or, alternatively, on the previously attached ubiquitin peptides resulting in multi-ubiquitination and poly-ubiquitination, respectively. What ubiquitination type a protein undergoes determines its consequent fate[189, 190] e.g. multi-ubiquitination was found to regulate internalization of surface proteins[191] while poly-ubiquitination through ubiquitin lysine residues 48 or 11 targets proteins for proteasomal degradation[192, 193]. Ubiquitin signals may also modulate protein activity e.g. kinase activation, signal transduction, endocytosis and DNA damage tolerance[194]. Since SERT is subject to complex intracellular processes including glycosylation, trafficking and degradation, studying of its ubiquitination patterns in parallel to investigating total and surface expression is of key interest for deciphering possible implication in antidepressant response. This is of special importance in light of paucity of relevant literature. Research to date has suggested that SSRI-resistant MDD patients may have higher SERT expression accompanied with lower ubiquitinated protein in comparison with sensitive patients. Although further research was suggested to generalize the findings, no similar study has been conducted to date[195].

Chapter II Aims of the Current Work

In the absence of solid antidepressant response predictors from recent genetic research[108], factors other than the stable germline genetic variants that may explain clinical response are currently in focus. Previous works from our group tested neuroplastic effects of antidepressants in lymphoblastoid cell lines (LCLs) from depression patients by studying cellular proliferative behavior under antidepressants. Results could identify transcriptional biomarkers that showed correlations with distinct treatment outcome phenotypes upon long-term (21-day) incubation of LCLs with antidepressants. The intention to the current work was thus to investigate more rapidly determinable transcriptional as well as functional, predictive biomarkers for the clinical outcome of antidepressant therapy. For this aim, LCLs derived from depression patients who were recruited in the observational MARS study and in the interventional STAR*D study were employed as an in-vitro model. We made use of the setups of the two studies by employing LCLs from different patient subgroups (cohorts) with distinct clinical characteristics to realize the following three specific aims of the work:

(I) Investigation of the association of the transcriptional levels of pre-selected key genes pertinent to the inflammatory and the neuroplasticity hypotheses on depression etiology with the antidepressant treatment outcome in a naturalistic, unstratified patient cohort.

(II) Determination of transcriptional predictors for the antidepressant treatment outcome using the transcriptome-wide technology in patient cohorts stratified on their clinical profiles with regard to therapy history.

(III) Systematically investigate genetic variants, gene expression, protein expression and localization of serotonin transporter in association with treatment outcome in patient cohorts stratified as in (II).

Chapter III Materials and Methods

III.1. Materials

Table 2. List of Instruments.

Product	Supplier
2100 Bioanalyzer	Agilent Technologies, USA
Centrifuge 5415 D	Eppendorf, Germany
Centrifuge 5415 R	Eppendorf, Germany
Centrifuge 5702	Eppendorf, Germany
Centrifuge 5804	Eppendorf, Germany
Centrifuge 5810 R	Eppendorf, Germany
Centrifuge, ultra (Avanti J-26 XP)	Beckman Coulter, Krefeld, Germany
ChemiDoc Touch Imaging system	Bio-Rad, Germany
CO2 incubator	Binder, Germany
Criterion™ gel chamber	Bio-Rad, Germany
Doumax 1030 shaker	Heidolph
Electrophoresis and blotting power unit	Bio-Rad, Germany
FACSCalibur	BD Biosciences, Germany
Hybridization oven	Agilent Technologies, USA
Imaging system Stella 3200	Raytest, Straubenhardt, Germany
Labsonic®	Sartorius AG
Laminar flow cabinet Herasafe	Heraeus, Hanau, Germany
LightCycler® 480 II	Roche, Switzerland
Magnet heating mixer	Heidolph
Mastercycler gradient	Eppendorf, Germany
Micropipettes	Eppendorf, Germany
Microscope, Inverse light	Axiovert 40C Zeiss, Germany
Milli-Q water system	MILLIPORE
MixMate plate stirrer	Eppendorf, Germany
MS3 Basic shaker	IKA®, Germany
Multipette® plus	Eppendorf, Germany
NanoDrop 1000 spectrophotometer	Thermo Scientific, USA
pH-Meter	Schott
Pico™ 17 Microcentrifuge	Heraeus, Hanau, Germany
Pipetboy	Integra, Switzerland
Safire² microplate reader	Tecan Group AG, Switzerland
Scale 1219 MP	Satorius
Scale LE244s	Satorius
SureScan Microarray Scanner	Agilent Technologies, USA
TC20™ cell counter	Bio-Rad, Germany
Thermomixer comfort MTP	Eppendorf, Germany

Ultra Centrifuge Optima L-80 XP	Beckman
Ultrassound water bath	BANDELIN
Vaccum pumpe PM 20405-86	VWR
Vortex	VWR
Water bath	GFL, Germany

Table 3. List of labware.

Product	Supplier
10% Criterion™ TGX Stain-Free™ Protein Gel, 18 well, 30 µl	Bio-Rad, Germany
Cell culture flasks T25 Suspen.	Sarstedt, Germany
Cell culture flasks T75 Suspen.	Sarstedt, Germany
Criterion™ 10.5-14% Tris-HCl Gel, 12+2 well	Bio-Rad, Germany
Cryo Tube vials	Nunc, Denmark
DMSO safe Acrodisc syringe filters	PALL, Germany
Immunoblot® PVDF membrane	Bio-Rad, Germany
LightCycler 480 384-well plate, white	4titude, UK
Microtubes 0.2 ml	Thermo Scientific, USA
Microtubes 1.5 ml	Thermo Scientific, USA
Mr. Frosty™ Freezing Container	Thermo Scientific, USA
Nunc™ MicroWell™ 96-Well Microtiterplates	Thermo Scientific, USA
Pipette tips, sterile with filter	Sarstedt, Germany
Pipettes (5-50 ml), sterile	Sarstedt, Germany

Table 4. List of Chemicals, Solutions and Buffers

Product	Supplier
10 x TBS (Tris buffered saline)	Bio-Rad, Germany
10 x TGS (Tris/glycerin/SDS) buffer	Bio-Rad, Germany
10% SDS (w/v)	Bio-Rad, Germany
10% Tween 20 solution	Bio-Rad, Germany
Citaloprma HBr	Sigma Aldrich, Germany
cOmplete Ultra mini tablets	Roche, Switzerland
Cyclosporine A	Sigma Aldrich, Germany
Dimethyl sulfoxide (DMSO)	Sigma Aldrich, Germany
DNA loading dye (6 x)	Thermo Scientific, USA
Dulbecco's PBS w/o Magnesium, w/o Calcium, sterile	Biowest, France
EDTA	Calbiochem, Germany
Ethanol for molecular biology	Merck, Darmstadt, Germany
FACS Clean	BD Biosciences, Germany
FACS Flow	BD Biosciences, Germany
FACS Rinse	BD Biosciences, Germany
Fluoxetine HCl	Sigma Aldrich, Germany
Formaldehyde, 10%, methanol free, Ultra Pure	PolySciences, Germany

Imipramine HCl	Sigma Aldrich, Germany
Laemmli buffer	Bio-Rad, Germany
L-glutamine 100X, 200mM	Biowest, France
Mirtazapine	Sigma Aldrich, Germany
Nuclease-free water	Thermo Scientific, USA
Paroxetine HCl	Sigma Aldrich, Germany
Penicillin-Streptomycin solution 100x, sterile	Biowest, France
RPMI-1640 culture medium, with phenol red	Biowest, France
Sodium Azide	Sigma Aldrich, Germany
SuperSignal™ West Femto Maximum Sensitivity HRP Substrate	Thermo Scientific, USA
SYTO® 61 Red Fluorescent Nucleic Acid Stain	Thermo Scientific, USA
TopVision Agarose	Roth, Germany
Triton X100	Sigma Aldrich, Germany
Trypan blue solution	Sigma Aldrich, Germany
β-Mercaptoethanol	Sigma Aldrich, Germany

Table 5. List of Kits and biological reagents

Product	**Supplier**
Blotting Grade Blocker (skimmed milk)	Bio-Rad, Germany
Bovine Serum Albumin	Sigma Aldrich, Germany
ELISA Kit for Serotonin Transporter (SERT)	CloudClone by Biozol, Germany
Fetal Bovine Serum FBS Superior	Biochrom, Merck, Berlin, Germany
GeneRuler 50 bp DNA Ladder	Thermo Scientific, USA
LongRange PCR kit	QIAGEN, Germany
MspI restriction enzyme	New England BioLabs Inc., USA
MycoAlert™ Mycoplasma Detection Kit	Lonza Cologne GmbH, Germany
NucleoSpin® RNA/Protein isolation kit	Macherey Nagel, Germany
Precision Plus Protein™ Dual color Standards	Bio-Rad, Germany
Protein A Agarose Beads 1 ml	Cell Signaling, Germany
Quantitect SYBR green PCR Kit	QIAGEN, Germany
Quantitect SYBR green PCR Kit	QIAGEN, Germany
Transcriptor First Strand cDNA Synthesis Kit	Roche, Switzerland
Tritest Kit	BD Biosciences, Germany

Table 6. List of Antibodies

Product	**Supplier**
Anti-SERT anitbody, Mouse Monoclonal, Alexa488-labeled(FL-N40)	Advanced-Targeting-Systems, USA
Anti-SERT antibody, rabbit anti-human (AB10514P)	Merck-Millipore, Germany
Pierce™ Goat anti-Mouse IgG (H+L) Poly-HRP Secondary Antibody, HRP conjugate	Thermo Scientific, USA

Pierce™ Goat anti-rabbit IgG (H+L) Poly-HRP Secondary Antibody, HRP conjugate	Thermo Scientific, USA
Ubiquitin Antibody, rabbit anti-human (3933)	Cell Signaling, Germany

Table 7 List of primers used in this work.

Gene	Primer name or sequence	Supplier	Cat#
Primers used in qPCR reference gene analysis			
18S ribosomal RNA (*18S rRNA*)	Hs_RRN18S_1_SG	QIAGEN	QT00199367
β Actin (*ACTB*)	Hs_ACTB_1_SG	QIAGEN	QT00095431
Hypoxanthine-guanine phosphoribosyltransferase (*HPRT1*)	Hs_HPRT1_1_SG	QIAGEN	QT00059066
Ribosomal Protein L13a (*RPL13A*)	Hs_RPL13A_1_SG	QIAGEN	QT00089915
Glyceraldehyde 3-phosphate dehydrogenase (*GAPDH*)	Hs_GAPDH_1_SG	QIAGEN	QT00079247
TATA-box binding protein (*TBP*)	Hs_TBP_1_SG	QIAGEN	QT00000721
qPCR primers used in project I: the candidate gene approach for response biomarker			
Brain-derived neurotrophic factor (*BDNF*)	Hs_BDNF_1_SG	QIAGEN	QT00235368
Close homolog to L1 (*CHL1*)	Hs_CHL1_1_SG	QIAGEN	QT00024801
Interferon gamma (*IFNG*)	Fwd: ATGACCAGAGCATCCAAAAGAG Rev: GCTTTGCGTTGGACATTCAAG	Eurofins	n/a
transforming growth factor beta 1 (*TGFB1*)	Fwd: CAACACATCAGAGCTCCGAG Rev: TATCGCCAGGAATTGTTGCTGT	Eurofins	n/a
Transforming growth factor beta receptor 1 (*TGFBR1*)	Fwd: TGTGAACAGAAGTTAAGGCCAA Rev: TGTAAGCCTAGCTGCTCCAT	Eurofins	n/a
Ubiquitin C-terminal hydrolase L5 (*UCHL5*)	Fwd: GTGGATCGGGGCGGTGT Rev: TCCATATTTCTTCTACTTGGGCT	Eurofins	n/a
SMAD specific E3 ubiquitin protein ligase 1 (*SMURF1*)	Fwd: AGACCCATCCACGACAATCTT Rev: TTGGCGGGAGATGTCGAAC	Eurofins	n/a
SMAD specific E3 ubiquitin protein ligase 2 (*SMURF2*)	Fwd: TATTACGGATCTCCCATCCAG Rev: AACAGAGGACAACGCAACAAG	Eurofins	n/a
FKBP prolyl isomerase 5 (*FKBP5*)	Fwd: ATCATCGGCGTTTCCTCACC Rev: AGAAAGCCCCACAGCCACT	Eurofins	n/a
Sphingomyelin phosphodiesterase 1 (*SMPD1*)	Fwd: ACCTACATCGGCCTTAATCCT Rev: ATGTTTGCCTGGGTCAGATTC	Eurofins	n/a
TET methylcytosine dioxygenase 1 (*TET1*)	Fwd: GGATCTCCCGTTCAACCAAG Rev: GGGGAGGAATTCTCTGATGG	Eurofins	n/a
cAMP responsive element binding protein 1 (*CREB1*)	Fwd: CACCTGCCATCACCACTGTA Rev: ATGTTTGCAGGCCCTGTACC	Eurofins	n/a
Mothers against decapentaplegic homolog 7 (*SMAD7*)	Fwd: TGAAACAGGGGGAACGAATTAT Rev: CTCTTGTTGTCCGAATTGAGC	Eurofins	n/a
Primers used in project II for qPCR validation of putative genes from whole genome expression analysis			
unc-13 homolog C (*UNC13C*)	Hs_UNC13C_3_SG	QIAGEN	QT01664733

TBC1 domain family member 9 (*TBC1D9*)	Hs_KIAA0882_1_SG	QIAGEN	QT00077994
catenin alpha 2 (*CTNNA2*)	Hs_CTNNA2_1_SG	QIAGEN	QT00999250
Glutamate decarboxylase 1 (*GAD1*)	Hs_GAD1_1_SG	QIAGEN	QT00060347
Glutamate ionotropic receptor NMDA type subunit 2A (*GRIN2A*)	Hs_GRIN2A_1_SG	QIAGEN	QT00050379
Integrin subunit beta 6 (*ITGB6*)	Hs_ITGB6_1_SG	QIAGEN	QT00082957
Ninein like (*NINL*)	Hs_NINL_1_SG	QIAGEN	QT00083034
Neuropilin 1 (*NRP1*)	Hs_NRP1_1_SG	QIAGEN	QT00023009
RNA binding protein, mRNA processing factor (*RBPMS*)	Hs_RBPMS_1_SG	QIAGEN	QT00042679
Receptor activity modifying protein 1 (*RAMP1*)	Hs_RAMP1_1_SG	QIAGEN	QT00230426
Paired like homeodomain 1 (*PITX1*)	Hs_PITX1_1_SG	QIAGEN	QT00014735
FYN binding protein 1 (*FYB*)	Hs_FYB_1_SG	QIAGEN	QT00045521
Nuclear factor I B (*NFIB*)	Hs_NFIB_1_SG	QIAGEN	QT00048139
EPH receptor B2 (*EPHB2*)	Hs_EPHB2_1_SG	QIAGEN	QT00089495
Fibroblast growth factor 7 (*FGF7*)	Hs_FGF7_1_SG	QIAGEN	QT00101850
Aminoadipate aminotransferase (AADAT)	RT²_qPCR_Primer_Assay_AADAT	QIAGEN	PPH14480A-200
Primer used in project III for *SLC6A4* 5-HTTLPR indel (rs1567826436) and rs25531 genotyping			
Solute carrier family 6 member 4 (Serotonin transporter, *SLC6A4*)	Fwd: GGCGTTGCCGCTCTGAATGC Rev: GAGGGACTGAGCTGGACAACCAC	Eurofins	n/a
Primer used in *SLC6A4* qPCR analysis			
Solute carrier family 6 member 4 (Serotonin transporter, *SLC6A4*)	Hs_SLC6A4_1_SG	QIAGEN	QT00058380

III.2. Methods

III.2.1. Working projects

This work was dedicated to identify rapidly determinable predictive biomarkers for the clinical outcome of antidepressant therapy and to provide insights in the molecular mechanisms underlying antidepressant effects. In analogy to the specific aims outlined in Chapter II, the work was set up to comprise the following three projects:

(I) Project I: Aim of project I was to probe associations between the expression of candidate genes and the response status of LCLs donors under naturalistic conditions. Donor patients were hence picked up from the naturalistic MARS study without prior stratification on their therapy history. Pre-selected genes were pertinent to the inflammatory and the

neuroplasticity hypotheses on depression etiology based on recent literature findings (Table 11). The experimental setup screened the effects of five antidepressants from different drug classes routinely employed in psychiatric clinical practice on these genes. Rapidly detectable associations with the response status of the donors i.e. differential expression between responders and non-responders were tested. This project will be henceforth referred to as the 'candidate genes approach'.

(II) Project II: Translating the experience gathered in Project I on *in vitro* incubation conditions with antidepressant agents, aim of this project was set to identify transcriptional predictive biomarkers in LCLs from tightly stratified SSRI-treated MDD patients at baseline and upon short-term incubation with the SSRI prototype drug citalopram. Putative genes were to be determined using whole-transcriptome analysis and differences in deregulated pathways and functional characteristics of asymmetrically expressed genes were to be identified using pathway enrichment analysis. A larger, less conservatively stratified MARS cohort of patients treated with serotonergic antidepressants was to be used for validation of the putative transcripts. Moreover, we wanted to test these putative transcripts for association with treatment resistance in an independent cohort of LCLs from response edge groups from the Sequenced Treatment Alternatives to Relieve Depression (STAR*D) study. Project II will be henceforth referred to as the 'genome-wide expression approach'.

(III) Project III: Aim of this approach was to conduct a systematic, four-level study of SERT molecular biology in LCLs from depression patient to investigate possible associations with clinical treatment outcomes. This project comprised study of *SLC6A4* genetic variants of 5-HTTLPR indel and rs25531 polymorphisms (level 1), gene transcription (level 2), and of protein total and surface expression (levels 3 and 4). At each level tests for association with clinical outcomes were conducted. Moreover, preliminary ubiquitination patterns of SERT were determined in LCLs from tightly stratified SSRI-treated MDD patients.

III.2.2. Study Populations

III.2.2.1. Munich Antidepressant Response Signature (MARS) study

MARS study was an observational, open-label clinical study with the aim to analyze pharmacogenetics of therapy response in patients with depressive episodes hospitalized in collaborating hospitals from South Bavaria and Switzerland[113]. Upon enrollment, patients were diagnosed according to the International Statistical Classification of Diseases, 10th version (ICD-10) and demographic data (gender, age) were collected. Depression severity was evaluated throughout the study period using the external-assessor-based 21-item Hamilton depression score - HAMD-21[8]. Patients were treated for 8 weeks according to the physician choice and were interviewed on weekly basis to document therapy and clinical progress. Clinical response was defined as ≥50% reduction in baseline HAMD score while clinical remission as a score <8. EDTA blood samples from 150 MARS patients were received from Max-Plank-Institute for Psychiatry (MPI) and were transformed with Epstein-Barr virus in BfArM laboratories to lymphoblastoid cell lines (LCLs) in line with MPI methodologies (see III.2.3.1). Transformation to LCLs was successful in 144/150 samples with success rate of 96%[196].

Cohorts of MARS study population used in this work

Being of an observational study design, the MARS study population contains heterogeneously treated depressive patients with diverse ICD-10 diagnoses. The current work made use of the naturalistic study setup so that different patient subgroups (cohorts) with distinct clinical characteristics were employed in addressing different research questions (see Chapter II for details on aims of this work):

1- For the candidate genes approach, a cohort of 21 cell lines (12 non-responders and 9 responders) representing patients treated with different antidepressant therapies was used (Table 8). Here, expression of the genes of interest was tested for rapidly detectable association with clinical response in non-stratified patients, resembling the observational design of MARS study. This cohort will henceforth be designated as the “naturalistic MARS cohort”.

2- In further analyses in projects II and III, patients were systematically stratified to investigate predictive biomarkers for treatment outcome after pharamcolgical therapy

with the serotonin-transporter-inhibiting antidepressant classes: selective serotonin reuptake inhibitors (SSRIs), serotonin norepinephrine reuptake inhibitors (SNRIs), and tricyclic antidepressants (TCAs). Here, donor patients were tightly stratified on their clinical diagnoses and documented therapy profiles. Bipolar disorder patients (n=13), patients with missing data at more than 2 visits (n=38) and cell lines with insufficient growth (n=9) were excluded. From the remaining patients, cell lines were included if donors were treated with serotonin-transporter-inhibiting antidepressants (SSRIs/SNRIs/TCAs) for ≥6 weeks. A cohort of n=69 patients: n=36 non-responders and n=33 responders, of which 16 were full remitters, emerged (Table 8, Supplementary table 1). These patients will be henceforth referred to as "MARS cohort". The MARS cohort was used in quantitative PCR validation of putative genes from microarray analyses (project II), in SERT total and surface expression, *SLC6A4* expression and genotyping (project III, see Figure 3).

3- Out of the MARS cohort, a subpopulation was further stratified on therapy profiles to achieve as much homogeneous cohort as possible. Here, patients were included only if proved as SSRI-responders or SSRI-non-responders. This is, responding patients were excluded if they had been treated with additional antidepressants besides SSRI for >2 weeks since clinical response in such cases could not be specifically attributed to SSRIs. The resulting cohort (n=17: n=9 responders, n=8 non-responders), henceforth designated the "exploratory cohort", was used for microarray genome-wide expression analyses (Figure 3, Table 8).

III.2.2.2. Response Edge Groups of Sequenced Treatment Alternatives to Relieve Depression (STAR*D) study

STAR*D was a multisite, randomized controlled trial on genetics of treatment response in major depression disorder (MDD) outpatients. Patients were treated according to a sequential 4-level-treatment protocol. At level 1 all patients were treated with citalopram. Patients without response or with severe treatment-intolerance in each level entered the next level where the therapy was switched or augmented with additional psychotropic drugs or with psychotherapy[197]. Disease severity was assessed using QIDS score along 14 weeks in 2 to 3-week intervals. Clinical

response was defined as ≥50% reduction in baseline score. In the current study samples from n=50 patients collected by G. Laje were purchased from NIMH Center for Collaborative Genetic Studies, Rodgers repository (Bethesda, MD, USA). Included cell lines were derived from response edge groups of the STAR*D patients with n=24 first-level responders and n=20 treatment-resistant patients (level-4-non-responders; Figure 3, Table 9, Supplementary table 2). STAR*D population was analyzed in an independent analysis to test association of genome-wide candidate genes and of SERT, *SLC6A4* expression with treatment resistance.

Table 8. Clinical characteristics of MARS cohorts used in this work. Differences were tested with Fisher test for gender and diagnosis and with t-test for age, depression scores and treatment duration ($p \leq 0.05$). Data are shown as mean ± SD. Table modified from Barakat *et al*.[196]

	MARS naturalistic cohort				**MARS exploratory cohort**				**MARS cohort**			
	Total (n=21)	**RESP (n=9)**	**NR (n=12)**	***p*-value**	**Total (n=17)**	**RESP (n=9)**	**NR (n=8)**	***p*-value**	**Total (n=69)**	**RESP (n=33)**	**NR (n=36)**	***p*-value**
Gender (females)	8	3	5	*N.S*	11	3	8	***0.01***	33	13	20	*N.S*
Age	52.0 ± 10.5	50.2 ± 11.9	53.3 ± 9.7	*N.S*	42.5 ± 12.4	38.1 ± 12.5	47.5 ± 11.02	*N.S*	47.5 ± 14.2	46.6 ± 15.2	47.4 ± 13.4	*N.S*
HAMD baseline	27.7 ± 6.0	27.1 ± 6.3	28.1 ± 6.0	*N.S*	24.1 ± 6.2	25.8 ± 6.8	22.2 ± 5.3	*N.S*	25.6 ± 6.4	26.2 ± 5.8	25.1 ± 6.9	*N.S*
HAMD 8 weeks	12.7 ± 7.2	6.0 ± 4.1	19.2 ± 4.3	***1.96E-5***	12.7 ± 7.2	8.1 ± 4.0	17.8 ± 6.5	***0.004***	13.1 ± 7.0	7.7 ± 4.5	18.0 ± 4.9	***9.35E-14***
Diagnosis												
Depressive episode (ICD10 code F32)	5	3	2	*N.S*	8	6	2	*N.S*	20	11	9	*N.S*
Recurrent depressive disorder (ICD10 code F33)	16	7	9		9	3	6		49	22	27	
Treatment duration (weeks)												
TCAs	2.6 ± 3.2	0.1 ± 0.3	4.8± 3.1	***0.0005***	0.4 ± 1.7	0.0± 0.0	0.9 ± 2.5	*N.S*	2.5 ± 3.4	2.1 ± 3.3	2.9 ± 3.6	*N.S*
SSRIs	2.4 ± 3.3	3.4 ± 3.7	1.5 ± 2.8	*N.S*	7.6 ± 0.7	7.8± 0.7	7.4 ± 0.7	*N.S*	2.9 ± 3.5	3.8 ± 3.8	2.1 ± 3.0	*0.05*
SNRIs	2.7 ± 3.3	1.9 ± 3.1	3.5 ± 3.4	*N.S*	0.6 ± 1.5	0.1± 0.3	1.1 ± 2.1	*N.S*	3.7 ± 3.7	3.2 ± 3.6	4.1 ± 3.7	*N.S*
NaSSAs	1.0 ± 2.4	2.2 ± 3.2	0.0 ± 0.0	***0.05***	1.1 ± 2.1	0.4 ± 0.9	1.8 ± 2.9	*N.S*	0.9 ± 2.1	1.4 ± 2.6	0.4 ± 1.5	*N.S*
NARIs	0.0 ± 0.0	0.0 ± 0.00	0.0 ± 0.0	*N.S*	0.1 ± 0.5	0.2 ± 0.7	0.0 ± 0.0	*N.S*	0.2 ± 1.1	0.1 ± 0.5	0.3 ± 1.4	*N.S*
SSRE	0.4 ± 1.6	0.9 ± 2.2	0.0 ± 0.0	*N.S*	0.0± 0.0	0.0± 0.0	0.0 ± 0.0	*N.S*	0.0 ± 0.0	0.0 ± 0.0	0.0 ± 0.0	*N.S*
other ADs	1.8 ± 2.9	0.8 ± 2.5	2.6 ± 3.1	*N.S*	0.2 ± 1.0	0.0± 0.0	0.5 ± 1.4	*N.S*	1.1 ± 2.3	1.0 ± 2.4	1.3 ± 2.2	*N.S*
Antipsychotics	3.9 ± 3.1	2.3 ± 2.6	5.4 ± 2.8	***0.02***	3.5 ± 3.4	3.4 ± 3.1	3.5 ± 3.9	*N.S*	4.2 ± 3.5	3.7 ± 3.6	4.7 ± 3.5	*N.S*
Mood stabilizers	4.3 ± 2.6	4.4 ± 2.2	4.2 ± 2.9	*N.S*	2.9 ± 3.0	2.6 ± 2.7	3.3 ± 3.5	*N.S*	2.8 ± 3.1	2.6 ± 2.9	3.0 ± 3.3	*N.S*
Benzodiazepines	4.0 ± 3.0	3.9 ± 3.2	4.2 ± 2.9	*N.S*	3.6 ± 3.0	2.9 ± 3.4	4.4 ± 2.5	*N.S*	3.4 ± 3.1	3.7± 3.2	3.0 ± 3.0	*N.S*
Sedatives	0.6 ± 1.0	0.4 ± 1.0	0.7 ± 1.1	*N.S*	1.3 ± 1.8	1.6± 2.2	1.0 ± 1.1	*N.S*	1.2 ± 1.7	1.1 ± 1.8	1.3 ± 1.7	*N.S*
Total treatment duration (weeks)	23.7 ± 7.3	20.3 ± 7.8	26.8 ± 5.5	*N.S*	21.2 ± 8.0	19.0± 7.5	23.8 ± 8.2	*N.S*	22.9 ± 7.7	22.6 ± 7.8	23.1 ± 7.8	*N.S*

RESP responding patients; NR non-responding patients.

Table 9. Clinical characteristics of STAR*D cohort. Differences were tested with Fisher test for gender and diagnosis and with t-test for age, depression scores ($p \leq 0.05$). Data are shown as mean ± SD. Table from Barakat *et al*.[196]

	Total (n=44)	Responders (n=24)	Treatment-resistant (n=20)	*p*-value
Anxious depression	27	14	13	*N.S*
Gender (Females)	23	14	9	*N.S*
Age	48.09 ± 12.1	47.54 ± 13.7	48.8 ± 10.3	*N.S*
QIDS 0	17.66 ± 3.1	16.92 ± 3.1	18.6 ± 2.9	*N.S*
QIDS end	7.95 ± 6.7	2.46 ± 1.9	14.6 ± 3.8	*3.7E-13*

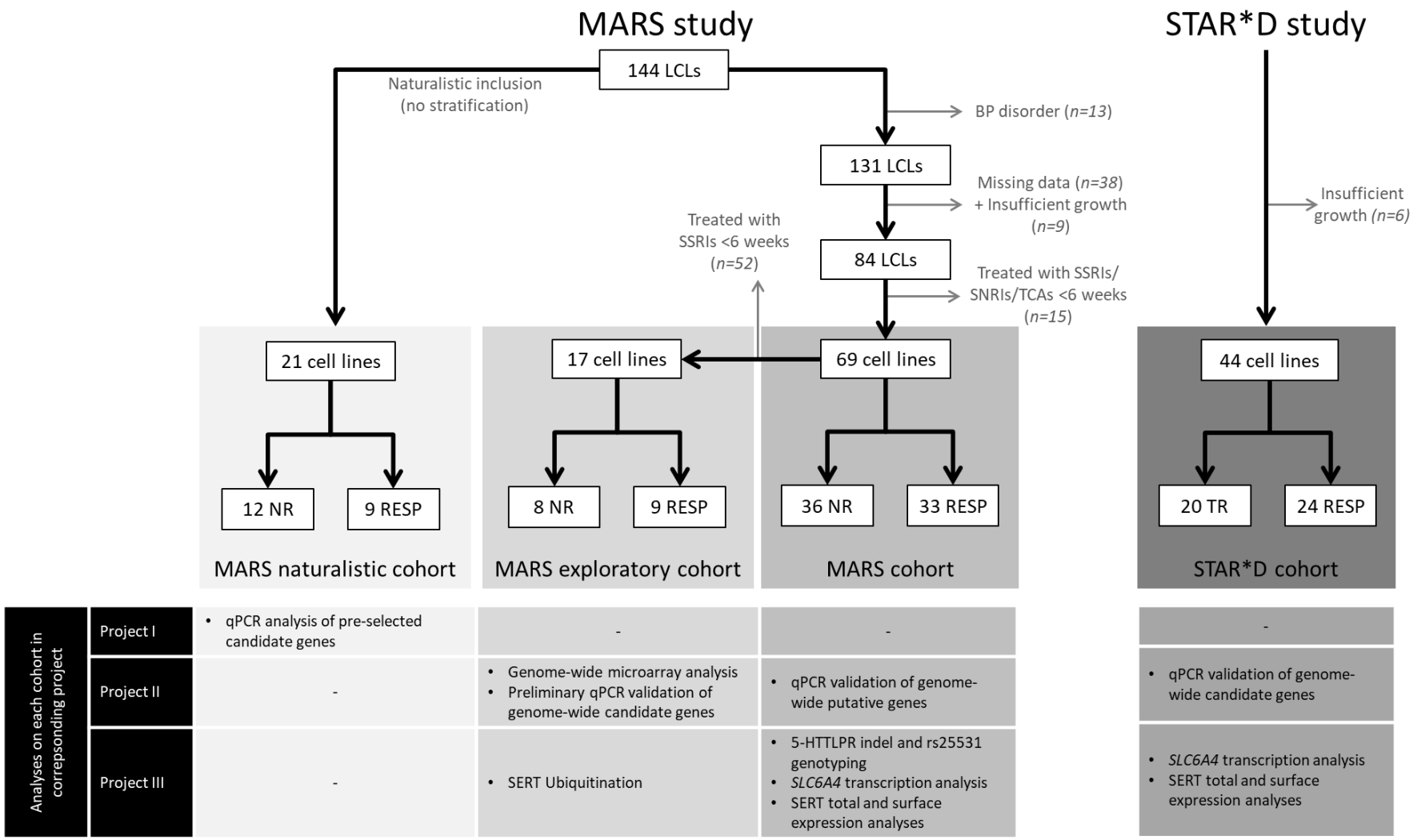

Figure 3. Cohorts of the lymphoblastoid cell lines (LCLs) used in this work. LCLs were derived from depression patients of the MARS and STAR*D studies populations. Cohorts from patients with distinct clinical characteristics were used to address different research questions. From the

observational MARS study three cohorts were employed. The “naturalistic cohort” retained the observational nature of MARS study and included LCLs from non-stratified patients i.e. treated with different antidepressant (ADs) treatments. Upon stratification by diagnosis and clinical outcome of donor patients, the SSRI-treated “exploratory cohort” and the “MARS cohort” of SSRI-, SNRI- and TCA-treated patients emerged. LCLs purchased from the STAR*D study were derived from 24 first-line-treatment responders and 20 treatment-resistant patients. Study setup is depicted as experimental steps done on each cohort as a whole. *5-HTTLPR serotonin transporter linked polymorphic region; BP bipolar disorder; FACS flow-cytometry-assisted cell sorting; LCLs lymphoblastoid cell lines; NR non-responders; qPCR quantitative polymerase chain reaction; RESP responders; SLC6A4 solute carrier 6A4 (serotonin transporter); SNRIs serotonin norepinephrine reuptake inhibitors; SSRIs selective serotonin reuptake inhibitors; TCAs tricyclic antidepressants; TR treatment-resistant patients; project I: transcriptional biomarker analysis using the candidate gene approach, project II: transcriptional biomarker analysis using the genome-wide-based approach; project III: SERT genotyping, transcription, total and surface expression in LCLs form MARS and STAR*D cohorts.* Figure modified from Barakat *et al*.[196]

III.2.3. Handling of Patients-Derived Lymphoblastoid Cell Lines (LCLs)

III.2.3.1. Generation of Lymphoblastoid Cell Lines

Human B-lymphocytes undergo transformation to the immortal lymphoblastoid cell lines (LCLs) upon infection with Epstein-Barr virus (EBV)[198]. Blood samples from 150 MARS patients were received from Max-Plank-Institute for Psychiatry (MPI) and were transformed with Epstein-Barr virus in BfArM laboratories to lymphoblastoid cell lines (LCLs) in line with MPI methodolgies. For the generation, peripheral blood mononuclear cells (PBMCs) were isolated from 9 ml EDTA whole blood by Ficoll density gradient. After centrifugation, PBMCs layer was aspirated, suspended in 800 µl EBV-supernatant from B95-8 cell culture and seeded in equal volumes in eight wells of a 48-well plate. Each well received 200 µl RPMI-1640 medium supplied with 20% fetal calf serum (FCS) and cells were incubated at 37°C, 5% CO_2. On day 5 after isolation cells were fed with 1 volume fresh RPMI-1640 medium and received cyclosporine A in final concentration of 1 µg/ml to eliminate remaining primary cells. On day 23 seeded wells from one sample were combined and further cultivated in a T25 flask. LCLs transformation was controlled by identifying existing leucocyte subpopulations using CD3-, CD19- and CD45-specific antibodies (Tritest™ Kit, BD Biosciences) as surface markers for T lymphocytes, B lymphocytes and leucocytes, respectively. Cell suspension was incubated with the antibody cocktail (10:1 volume ratio) for 30 min at 4°C. Samples were centrifuged (1500 *g*, 2 min) and cell pellet was washed with 1 ml 0.9% NaCl solution. Cells were afterward resuspended in 250 µl 0.9% NaCl solution and measured using FACSCalibur (BD Biosciences) flow-cytometer (Figure 4).

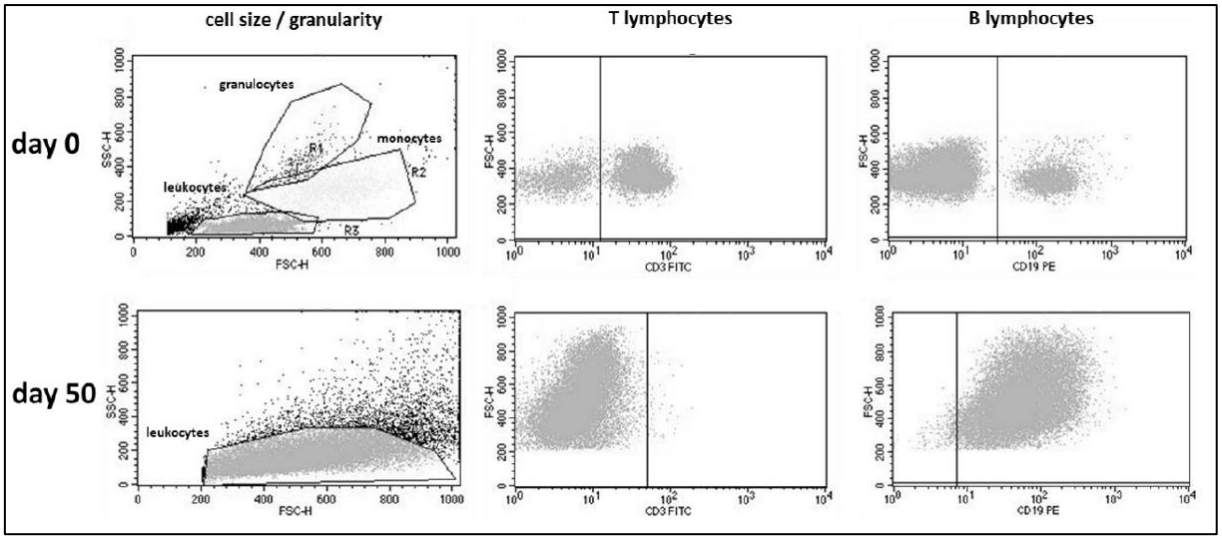

Figure 4. Cell identification before (day 0) and after (day 50) EBV transformation measured with flow cytometry using CD3-, CD19- and CD45-specific antibodies (TritestTM Kit). Cell population shift toward B lymphocytes is noticed through the increased fluorescence signal of CD19+ on account the decreasing T lymphocytes (decreased CD3+ fluorescence signal).

III.2.3.2. Long-term Storage of Lymphoblastoid Cell Lines

After achieving appropriate cell density and being controlled for mycoplasma contamination using MycoAlert™ Plus kit (Lonza Cologne GmbH), aliquots of 5-10 · 10^6 live cells were counted with trypan blue counting method in TC20™ cell counter. Cells were then resuspended in 1 ml FCS containing 10% DMSO in cryotubes. DMSO serves for reducing ice crystals formation during freezing and, hence, protects cell membranes. Aliquots were then transferred to CoolCell® freezing box and stored at -80°C for 24-48 hr. Subsequently, aliquots were transferred to liquid nitrogen tanks (-180 – -196°C) for long-term storage.

III.2.3.3. Cultivation and Incubation of Lymphoblastoid Cell Lines with Antidepressants

For culturing, a cryo-preserved aliquot was thawed in 37°C water bath. Cells were washed with 10 ml pre-warmed RPMI-1640 medium. Cell pellets were then resuspended in 10-20 ml RPMI-1640 medium supplied with 15% FCS, 2.00 mM L-glutamine, 100 µg/ml streptomycin sulfate and 100 U/ml penicillin (henceforth referred to as culture medium) and were transferred to T25 flasks in upright position. Cell cultures were fed three times a week by volume expansion with pre-warmed culture medium while maintaining live-cell count >2 · 10^5/ml. Larger cell culture volumes were held in T75 flasks. Cell lines were kept in culture for a maximum of 2 weeks before being incubated with antidepressants.

Experiments were conducted by incubating 1 · 10^7 LCLs cultivated in 20 ml medium with antidepressants in final concentrations as shown in Table 10. Drugs stock solutions were all

prepared in 96% ethanol. Final drug concentrations were in range of 10-fold of the therapeutic plasma concentration[199, 200], in line with earlier studies on short-term incubation of LCLs with antidepressants[201] and comparable with brain-blood ratios reported in rodents[202] and humans[203]. Controls received equal volume of ethanol achieving a final concentration of 0.03% v/v. At predetermined time-points (Table 10) aliquots were centrifuged and cell pellets were stored at -80°C for later nucleic acids and protein isolation. Flow cytometry experiment measuring SERT total and surface expression were conducted with aliquots freshly isolated from cell cultures as described in section III.2.5.4.

Table 10. Antidepressant concentrations (C_{test}) and incubation times with LCLs applied in the experiments of this work.

Drug	C_{test}	Incubation times (hr)
Candidate genes approach tests		
Imipramine HCl	10 µM	1, 6, 24
Paroxetine HCl	3 µM	1, 6, 24
Mirtazapine	3 µM	1, 6, 24
Citalopram HBr	3 µM	1, 6, 24
Fluoxetine HCl	8 µM	1, 6, 24
Ethanol (control)	0.03% v/v	1, 6, 24
Genome-wide expression analyses, SERT expression analyses		
Citalopram HBr	3 µM	24, 48
Ethanol (control)	0.03% v/v	24, 48

III.2.4. Identification of Transcriptional Biomarkers for Antidepressant Treatment Outcomes

III.2.4.1. RNA Isolation and Quality Control

i. RNA Isolation

For gene expression quantification RNA was extracted from LCLs using Nucleospin® RNA/Protein purification columns (Macherey Nagel). A cell pellet was lysed in 350 µl of the delivered lysis buffer containing 1% β-mercaptoethanol. After homogenization on the delivered homogenization column, cell homogenates were mixed with 1 volume ethanol 70% and RNA was bound by centrifuging the mixture through RNA-binding columns. The eluate was further used for ELISA analysis of total SERT (see III.2.5.3). DNA was digested by incubating

the membranes with rDNase for 15 min. Membranes were washed and RNA was eluted with RNase-free water. RNA concentrations and A260:280 ratios were determined using NanoDrop™ 1000 (Thermo Scientific). In this work all RNA samples had A260:280 ratios >1.9. Samples were stored at -80°C.

ii. Determination of RNA Integrity Number (RIN)

As reliability of gene expression results strongly depends on the integrity of nucleic acid samples used, RNA quality was controlled by calculating RNA integrity number (RIN) using 2100 BioAnalayzer (Agilent Technologies). In this method nucleic acid samples undergo micro-gel electrophoresis where the migrating molecules pass through a sensitive electrical resistance detector in a size-dependent temporal manner. Results are analyzed by generating electropherograms and gel-like images (Figure 5). Computing algorithm takes the entire electrophoretic trace, including the traditionally considered 18S and 28S bands, into account and, thus, allows for the classification of total RNA, based on a numbering system from 1 to 10, with 1 being the most degraded and 10 the most intact.

Procedure

Micro-gel solution was filtered to remove insoluble particles by centrifugation for 10 min at 1500 *g*. To 65 µl gel solution, 1 µl RNA 6000 Nano dye concentrate was added and the mixture was centrifuged for 10 min at 13000 *g*. Gel-dye mix (9 µl) was dispensed in the RNA chip using the Chip Prime Station. RNA 6000 Nano Marker (5 µl), RNA 6000 ladder (1 µl) and samples (1 µl) were pipetted in the corresponding wells. Assay was done using the Agilent 2100 Bioanalyzer instrument. Data were analyzed using Agilent 2100 Bioanalyzer Expert Software. In this work all RIN values were ≥9.6.

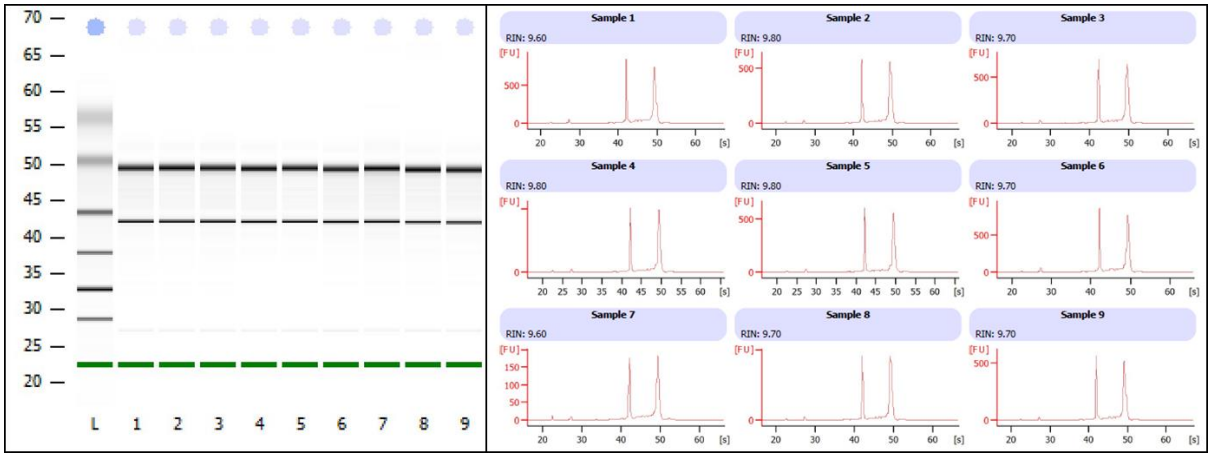

Figure 5. RNA integrity number (RIN) determination of 9 RNA samples using 2100 BioAnalyzer (Agilent). Shown are the generated gel-like image (left) and electropherograms (right) with visible 18S and 28S ribosomal RNA bands and lack of degraded RNA smears. RIN of further samples was >9.6 indicating good RNA integrity.

III.2.4.2. Complementary DNA Synthesis—Reverse Transcription PCR

RNA samples must be reverse transcribed into DNA prior to undergoing quantification via quantitative PCR (qPCR) reaction. RNA samples were reverse-transcribed to complementary DNA (cDNA) using Transcriptor First Strand cDNA Synthesis kit (Roche) according to the manufacturer's instructions. One microgram of total RNA from each sample was adjusted to 11 µl with RNase-free water and received 9 µl Mastermix (4 µl transcriptase buffer, 2 µl random hexamer primer, 2 µl dNTPs, 0.5 µl protector RNase inhibitor, 0.5 µl reverse transcriptase). Polymerase chain reactions (PCR) were carried out in 0.2 ml PCR-clean tubes. Reactions were held in *Mastercycler®gradient* (Eppendorf; 10 min at 25 °C, 30 min at 55 °C, 5 min at 85 °C). Resulting cDNA was diluted with PCR-clean water in ratio of 1:15.

III.2.4.3. Primers Design, Validation, and Efficiency Test

i. Candidate Genes Investigated in This Study

Table 11 lists the gene battery tested for gene expression following the candidate gene approach with literature on relevance to depression pathophysiology.

Table 11. The candidate genes battery tested for expression in a naturalistic LCLs cohort from responding (n=10) and non-responding (n=11) MARS patients.

	Gene	Function	Relevance
The Inflammatory Hypothesis of Depression	*IFNγ* (interferon gamma)	Pro-inflammatory cytokine	• Involved in anxiety and depression states modulation[204] • Reduced expression upon antidepressant treatment[205]
	TGFβ1, *TGFβR1* (TGFβ receptor 1)	Anti-inflammatory cytokine and its corresponding receptor	• Increased plasma levels of *TGFβ1* upon AD treatment in patients[80] • TGFβ pathway might be involved in antidepressants action[206]
	SMAD7 (Mothers against decapentaplegic homolog 7)	TGFβ receptor modulator	• Inhibits TGFβ actions possibly through ubiquitination of TGFβ1 receptor[207] • Lower baseline plasma levels in remitting patients[82]
	UCHL5 (Ubiquitin carboxyl-terminal hydrolase isozyme L5)	Ubiquitine hydrolase	• Modulator of SMAD7 function[83]
	Smurf1, *2* (E3 ubiquitin-protein ligases)	Ubiquitine ligases	• Modulators of SMAD7 function[83]
	SMPD1 (Acid sphingomyelinase)	Breakdown of sphingomyelin	• Overexpression in brain induces depressive-like symptoms[208] • AD treatment reduced levels in brain[209]
	FKBP5 (FK506 binding protein)	Co-chaperon of glucocorticoid receptors	• Genetic variants were associated with faster and better AD response, while others were associated with more depressive episodes[101]
The Neuroplasticity Hypothesis of Depression	*CREB1* (Cyclic AMP-responsive element-binding protein 1)	Transcription factor	• Plays a major role in neurogenesis and synaptic plasticity[210] • Decreased levels of CREB in the prefrontal cortex of depressed patients [211]
	CHL1 (Close homolog to L1)	Cell adhesion molecule	• Higher basal expression in early remitters • Genetic variants were associated with faster and better AD response[56]

BDNF (Brain-derived neurotrophic factor)	Neurtrophic factor	• Decreased serum levels in depression; increase upon treatment; association with improvement[212]
TET1 (Ten-eleven translocation 1)	DNA demethylase	• Knockout in nucleus accumbens of adult mice produced antidepressant-like effects[63] • Loss of the gene led to resistance to chronic stress in mice[64]

Abbreviations: AD antidepressant

ii. Primer Design

A specific and efficient amplification of gene transcripts during qPCR is critical for precise expression quantification. In this work, a number of qPCR primers were self-designed using publicly available *in-silico* tools and then validated for efficiency and specificity. The designing process involved in the first step retrieving mRNA sequences of the genes of interests from the Nucleotide database of the National Center for Biotechnology Information (NCBI). Sequences were then fed in NCBI-BLAST software and processed with primer design settings of the following:

- Amplicon size= 100-250 bp
- Primer melting point= 60±1°C.
- Forward and reverse primers must be separated by at least one intron to exclude confounding amplification of genomic DNA.

Returned primer pairs were then *in-silico* controlled for potential formation of secondary structures and gene specificity using OligoCalc and UCSC Genome Bioinformatics BLAT alignment tool, respectively. Selected primer sequences were ordered from Eurofins Genomics and dispersed in RNase-free water to achieve a concentration of 100 µM.

iii. Primer Validation: Specificity and Efficiency Tests

In polymerase chain reactions (PCR), a primer should specifically bind its complementary sequence (target sequence) and should not build primer dimers. Deviations from these prerequisites can be falsely interpreted as high expression of a gene and, in a worst case, as a false positive result. In this work, self-designed primers were tested for specificity using agarose gel electrophoresis. After a qPCR run was completed, nucleic acid products were run

on agarose gel (2%) electrophoresis for 80 min at 80 V. Detection was performed by including DNA Stain Clear G (SERVA) in the gel and later gel visualization using ChemiDoc™ Touch Imaging System (Biorad). Specificity was determined when only one fluorescence band was observed at the expected size of the amplicon. Primers with unspecific products, including primer dimers, were excluded. When different primer pairs that target the same gene were found specific, the primer pair with a band of higher intensity was chosen. For each of the target genes for candidate gene approach, at least one specific primer pair could be identified and was then further validated (Figure 6 Figure 8). A list of primers used in this work is provided in Table 7.

Moreover, a primer should exponentially amplify target sequences with each thermal cycle. Ideally, the number of the target sequence will double in each cycle, assuming the efficiency factor of a primer pair to equal 2. In practice, however, several biophysical factors may reduce primer efficiency resulting in erroneous results when the actual efficiency remains not determined. Amplification efficiency was tested by running qPCR tests with cDNA from 4 different samples, each with four serial-dilutions of factor 5 (1:15, 1:75, 1:375 and 1:1875). Crossing point (Cp) values were plotted against base-ten logarithm of the dilution and the slope of the resulting straight line was calculated. Efficiency was then calculated as $10^{(-1/\text{slope})}$. Efficiency factor was used as a quality control measure. Primer pairs with efficiency factors below 1.8 were excluded. Purchased, ready-to-use primers were used according to manufacturer's instructions. Amplification efficiency determinations showed that tested primers had an efficiency factor of >1.8 and were considered accepted (Table 12).

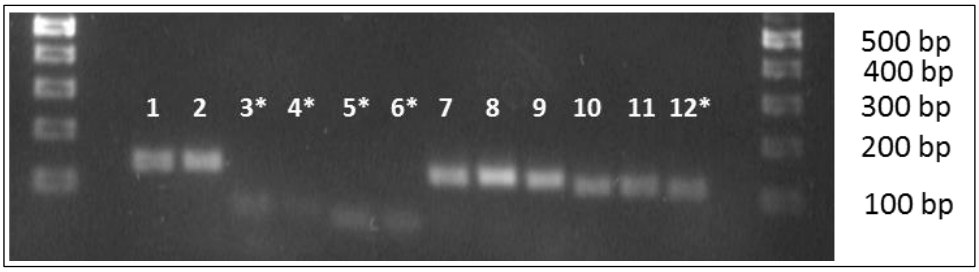

Figure 6. Primer specificity test: Visualization of PCR products on agarose gel for primers targeting IFN-γ (lanes 1, 2), IFN-γ (lanes 3, 4), TGFβ (lanes 5, 6), TGFβ (lanes 7, 8), TET1 (lane 9), TGFβ receptor (lanes 10, 11), TGFβ receptor (lane 12). Primers labelled with an asterisk were excluded from further experiments due to building of unspecific amplicons.

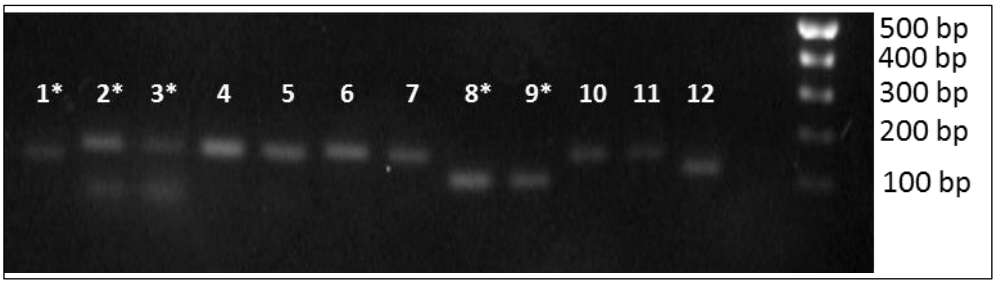

Figure 7. Primer specificity test: Visualization of PCR products on agarose gel for primers targeting TGFβ receptor (lane 1), UCHL5 (lanes 2, 3) UCHL5 (lanes 4, 5) Smurf1 (lanes 6, 7) Smurf1 (lanes 8, 9) Smurf2 (lanes10, 11) and FKBP5 (lane 12). Primers labelled with an asterisk were excluded from further experiments due to building of unspecific amplicons.

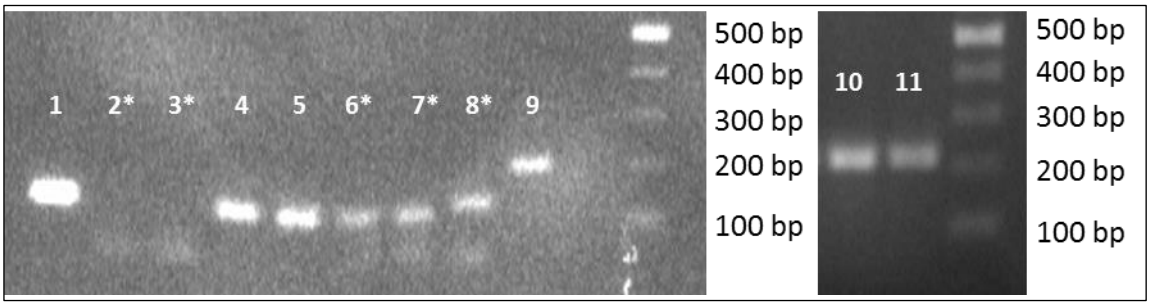

Figure 8. Primer specificity test: Visualization of PCR products on agarose gel for primers targeting FKBP5 (lane 1), FKBP5 (lanes 2, 3), SMPD1 (lanes 4, 5), SMPD1 (lanes 6, 7), SMAD7 (lane 8), CREB (lane 9), SMAD7 (lane 10, 11). Primers labelled with an asterisk were excluded from further experiments due to building of unspecific amplicons.

Table 12. Efficiency calculation for the self-designed primers.

Gene	Sample	Slope	R^2	Efficiency	Efficiency mean
TGFβ1	A	-4.551	0.997	1.659	1.80
	B	-3.777	0.998	1.840	
	C	-4.015	0.998	1.775	
	D	-3.571	0.998	1.906	
TGFβ_R1	A	-3.836	0.999	1.823	1.87
	B	-3.718	0.991	1.858	
	C	-3.499	0.992	1.931	
	D	-3.654	0.993	1.878	
UCHL5	A	-3.309	0.985	2.005	2.12
	B	-3.182	0.987	2.062	
	C	-2.654	0.992	2.381	
	D	-3.231	0.984	2.040	
Smurf1	A	-3.527	0.999	1.921	1.92
	B	-4.932	0.920	1.595	
	C	-3.281	0.941	2.018	
	D	-2.993	0.959	2.158	
Smurf2	A	-3.271	0.981	2.022	1.91
	B	-4.365	0.995	1.695	
	C	-3.764	0.980	1.844	
	D	-3.140	0.980	2.082	
FKBP5	A	-3.355	0.991	1.986	2.12

	B	-2.939	0.979	2.189	
	C	-2.806	0.996	2.272	
	D	-3.286	0.996	2.015	
SMPD1	A	-3.724	0.980	1.856	1.92
	B	-4.296	0.947	1.709	
	C	-3.082	0.982	2.111	
	D	-3.362	0.996	1.984	
TET1	A	-3.456	0.989	1.947	1.94
	B	-3.538	0.987	1.917	
	C	-4.047	0.993	1.766	
	D	-3.082	0.956	2.111	
CREB1	A	-3.235	0.987	2.038	2.06
	B	-3.778	0.999	1.839	
	C	-3.418	0.994	1.961	
	D	-2.653	0.961	2.382	
SMAD7	A	-3.4007	0.996	1.968	1.88
	B	-3.6654	0.992	1.874	
	C	-3.8886	0.997	1.808	
	D	-3.7198	0.996	1.857	
IFN γ	A	-4.069	0.980	1.761	1.90
	B	-3.256	0.995	2.028	
	C	-4.128	0.973	1.747	
	D	-3.223	0.988	2.043	

III.2.4.4. Identification of Optimal Reference Gene for Gene Expression Examinations

Normalization is indispensable for quantitative gene expression measurements. It controls for variations in RNA extraction, reverse transcription and pipetting procedure. Normalization must be done against a reference gene stably expressed throughout the diverse experimental conditions as feasible. To identify an appropriate reference gene, six genes commonly used as reference genes (also known as housekeeping genes) were tested. Expression levels of 18S ribosomal RNA (*18S rRNA*), β Actin (*ACTB*), Hypoxanthine-guanine phosphoribosyltransferase (*HPRT1*), Ribosomal Protein L13a (*RPL13A*), Glyceraldehyde 3-phosphate dehydrogenase (*GAPDH*) and TATA-box binding protein (*TBP*) were measured after 1, 6, 24 hours incubation of three different MARS cell lines with imipramine (10 µM), mirtazapine (3 µM), paroxetine (3 µM), fluoxetine (8 µM), citalopram (3 µM), and ethanol (0.03% v/v). Tests were carried out in two independent qPCR runs, each run with three technical replicates of each of the measured 54 samples. Stability of gene expression was determined through calculation of the coefficient of variation (CV%) of Cp value of each gene computed over all time points, drugs/ethanol

incubation and cell lines. The gene with the lowest CV% was used as a reference gene for gene expression normalization. CV% was lowest for TBP over all time points, drugs/ethanol incubations and cell lines (Table 13). Thus, TBP was used as a reference gene for normalization of all gene expression experiments in this work.

Table 13. Gene expression levels of six tested housekeeping genes averaged over incubation time points (1, 6, 24 hr) incubation drugs (imipramine, mirtazapine, paroxetine, fluoxetine, citalopram, and ethanol) and cell lines (n=3). The gene with the lowest Coefficient of variation (CV%) was considered for further gene expression normalization.

	18S rRNA	***ActinB***	***HPRT1***	***RPL13A***	***GAPDH***	***TBP***
Cp (Mean ± SD)	12.53 ± 2.38	18.91 ± 0.89	28.13 ± 0.96	22.84 ± 0.83	17.65 ± 0.65	25.03 ± 0.37
CV%	18.98	4.68	3.40	3.62	3.70	1.48

III.2.4.5. Quantitative Polymerase Chain Reaction (qPCR)

Quantitative polymerase chain reaction (qPCR) is the most used quantification method for gene expression. Similar to conventional PCR, polymerase enzyme amplifies the target sequence in each thermal cycle leading to exponential amplification of the nucleic acid molecules. Quantification of a target DNA occurs during the reaction i.e. real time using non-specific fluorescent dyes that intercalate with double-stranded DNA. Our experiments were carried out using QuantiTect SYBR Green PCR kit (QIAGEN) in LightCycler 480 II instrument (Roche). cDNA samples (already diluted 1:15) were pipetted in 5 µl volumes in 384-well plates in duplicates. Each well received 5 µl kit Mastermix and 1 µl gene-specific primer. A qPCR run consisted of 45 cycles (Table 14). Expression level of a gene was determined by the cycle at which the fluorescence of the sample significantly rose over background level (crossing point—Cp). Lower Cp values indicate, thus, higher expression levels of a gene. Mean Cp values of the duplicates were calculated and normalization was done using the ΔCp method using TBP as reference gene using the following formula

$$\Delta C_{p\ (gene\ X)} = C_{p\ (gene\ X)} - C_{p\ (TBP)}$$

Table 14. qPCR cycle conditions.

	Cycles	**Temperature**	**Held for(mm:ss)**	**Ramp rate (°C/sec)**
Pre-incubation	1	95°C	15:00	4.40
Amplification				
Denaturation	45	95°C	00:10	4.40
Annealing		55°C	00:15	2.20
Elongation		72°C	00:20	4.40
Melting Curves	1	95°C	00:05	4.40
		65°C	01:00	2.20

		97°C		0.06
Cooling	1	37°C	00:10	1.50

III.2.4.6. Whole-Genome Gene Expression Profiling

Microarray technology enables high-throughput screening of the whole-genome in short time and generates data of competitive quality. The analysis of the micro-array data is many-sided and a lot of information can be obtained using different analysis strategies. Whole-genome expression analyses were done using Agilent Single Color platform of 8 × 60K SurePrint microarrays containing probes for >56,000 genetic entities coding for >40,000 unique transcripts. Here, sample RNA is transcribed in two steps to fluorescence-labeled cRNA which hybridizes to the immobilized gene-specific oligonucleotide probes. Expression levels are determined measuring fluorescence intensity of each, now hybridized, spotted probe (genetic entity).

i. Procedure

RNA was extracted from the exploratory MARS cohort (n=17: n=9 non-responders, n=8 responders) after 24 and 48 hr incubation with citalopram (3 µM) or control (EtOH 0.03% v/v) as described above. 100 ng of total RNA were used for reverse transcription and labelling. cDNA was reversely transcribed with T7 promoter primers and AffinityScript reverse transcriptase by incubating the reaction mixture (10 µl) for 2 hr at 40°C followed by 15 min at 70°C. cRNA was then transcribed and, simultaneously, fluorescence-labeled by T7 RNA polymerase after addition of NTP mix and cyanin-3-cytidine triphosphate (Cy3). Cy3-labelled cRNA (specific activity >10.0 pmol Cy3/µg cRNA) was purified and 600 ng were fragmented at 60°C for 30 minutes in 1x Agilent fragmentation buffer and 2x Agilent blocking agent (25 µl). Afterward, the fragmentation mixture received 25 µl of 2x Agilent hybridization buffer and was hybridized to the microarray slides for 17 hours at 65°C. Microarrays were washed with GE Wash Buffer 1 (1 min, room temperature) and GE Wash buffer 2 (1 min, 37°C). Slides were immediately dried by centrifugation and fluorescence intensities were measured by SureScan Microarray Scanner (Figure 9).

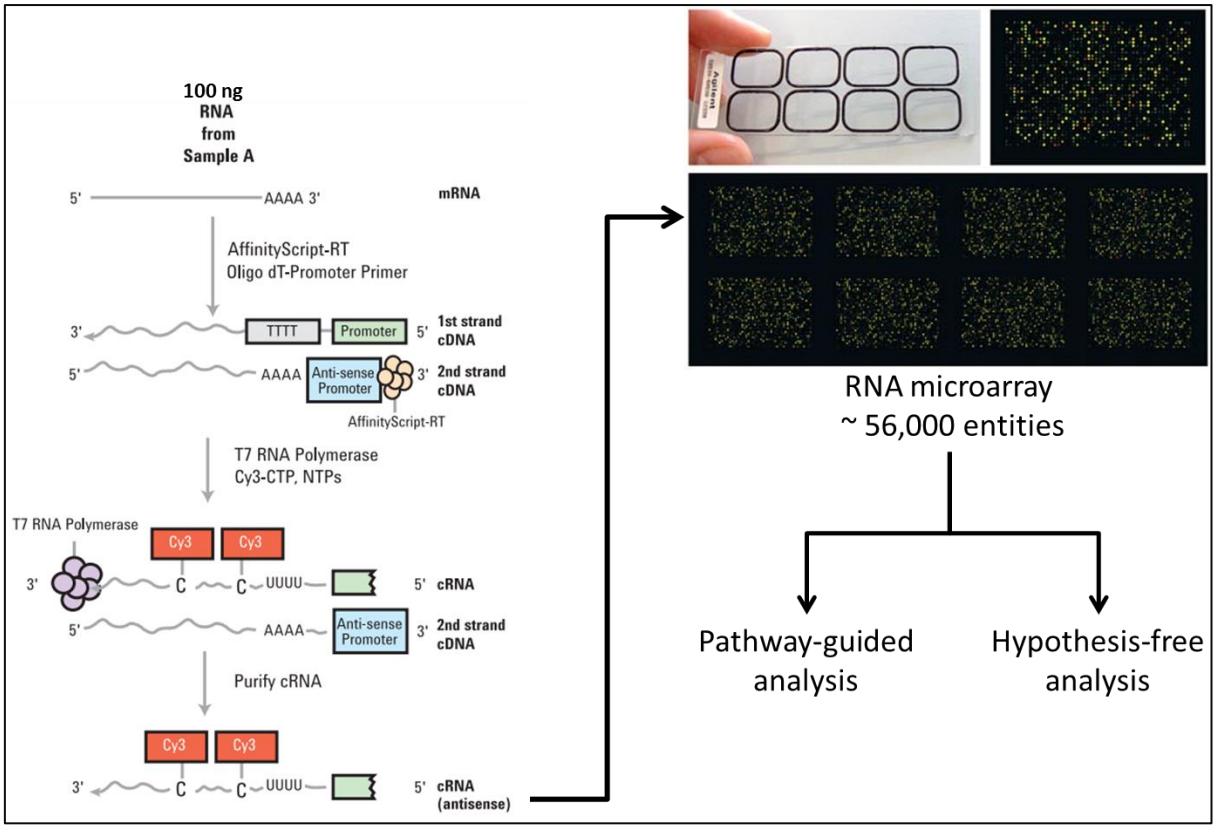

Figure 9. Workflow of whole-genome gene expression profiling using Agilent Single Color platform (8 x 60K) SurePrint microarrays. Isolated RNA was first reverse-transcribed to cDNA from which Cyanine-3-labelled cRNA was transcribed. The latter was then purified, fragmented and then hybridized on the RNA microarray. After 17 hr of hybridization, fluorescence intensities were measured by SureScan Microarray Scanner.

ii. Data Analysis

Quality control of measured microarrays was conducted using Feature Extraction Software v10. Parameters such as spot finding algorithms, spatial distribution of signals, spike-in and outlier signals were analyzed. Gene expression data were analyzed using GeneSpring (v.14.1.9, Agilent). After normalization through background subtraction, signal quality was categorized into flags. Signals of compromised fluorescence intensity (so called compromised flags) were removed from further analysis. Differential gene expression was calculated in fold-change (FC) in sets of pairs i.e. non-responders (NR) vs. responders (RESP) or citalopram-incubated (CTP) vs. control (ctrl). Pathway analysis was done in the pathway database of GenMAPP Pathway Markup Language[213].

Sixty-eight gene expression datasets generated from the exploratory MARS cohort (n=17: n=9 non-responders, n=8 responders) were analyzed using a hypothesis-free and a pathway-guided algorithm designed to detect cardinal and reactional transcriptomic differences, respectively, between the two response subgroups. In the hypothesis-free analysis, genetic

entities coding for autosomal genes and being differentially expressed in non-responders vs. responders (|FC|≥2, *p*-corr. ≤0.05) were determined at each time point, 24 and 48 hr. Cardinality was ensured by, firstly, selecting entities with consistently differential expression (|FC|≥2 NR/RESP) at both time points and, secondly, by computing a mean FC value (NR/RESP) over both incubations at both time points for each gene. Genetic features with the highest 10 mean |FC| values were further considered for qPCR validation.

Changes in gene expression in reaction to CTP incubation were analyzed using a pathway-guided algorithm. Genetic entities that reacted to CTP incubation with a |FC|≥2 (CTP/ctrl) in responders and non-responders groups were determined at each time point, 24 and 48 hr. These entities underwent pathway enrichment analysis ($p \leq 0.05$) to determine altered functions in each response group. Afterward, entities enriched in responders' pathways were identified and filtered on FC cutoff NR/RESP ≥2. Eight genes were functionally characterized based on published literature and were further considered for qPCR validation.

III.2.5. Serotonin Transporter Genotypes, Transcription, Total Expression and Surface Expression in LCLs from Patients With Different Antidepressant Treatment Outcomes

III.2.5.1. Genotyping of 5-HTTLPR indel and rs25531

In this set of experiments two polymorphisms, 5-HTTLPR indel (rs1567826436) and rs25531, were genotyped in MARS LCLs (but not STAR*D) through determination of PCR products upon gel electrophoresis followed by fluorescence visualization. The method was modified from Kraft *et al.*[214]. Determination of the haplotype was phase certain i.e. the method was able to determine whether indel and rs25531 detected genotypes are located on the same chromosome. Genomic DNA was extracted from MARS cell lines using AllPrep Mini kit (QIAGEN) according to the supplied manual. Amplification of the sequence spanning the 5-HTTLPR indel polymorphism and the SNP rs25531 was done using the forward primer 5'-GGCGTTGCCGCTCTGAATGC-3' and reverse primer 5'-GAGGGACTGAGCTGGACAACCAC-3' in LongRange PCR kit (QIAGEN) as detailed in Table 15 and Table 16. Genotyping of rs25531 G/A substitution alleles was done by digesting PCR products with MspI restriction enzyme. A volume of 21.5 µl from each sample received 0.6 µl MspI + 2.9 µl CutSmart™ buffer. Restriction mixture was incubated for 20 min at 37°C. Size of PCR products (L, S alleles) and restriction

products (G, A alleles) was determined by DNA electrophoresis on 2% agarose gels stained with DNA Stain clear G (SERVA). Gels were visualized using ChemiDoc™ Touch (Bio-Rad).

Table 15. Components of one PCR-reaction used for amplification of a DNA sequence spanning 5-HTTLPR indel polymorphism and rs25531.

Component	Volume (µl)
PCR buffer	5
dNTPs	2.5
FWD primer*	0.4
REV primer*	0.4
Q solution	10
Enzyme mix	0.4
DNA	equal to 150 ng
PCR-grade water	q.s. to 50

*Primers' final concentration was 0.8 µM.

Table 16. PCR-reaction conditions applied to amplify HTTLPR covering rs25531.

	Cycles	Temperature	Held for(mm:ss)
Pre-activation	1	93°C	03:00
Amplification			
Denaturation	35	93°C	00:15
Annealing + Elongation		68°C	04:00
Termination	1	68°C	30:00

Data interpretation

Long (L) and short (S) variants of 5-HTTLPR were determined by the existence of 529 and 486 bp bands, respectively. MspI endonuclease cuts the bond between two adjacent cytidine molecules only when flanked by two adjacent guanidine molecules (C|CGG). The presence of other nucleotides (adenosine in case of rs25531) flanking the cutting site prevents the restriction. Thus, G and A alleles of rs25531 were determined by the existence or the absence of digested fragments at the level of 166 bp, respectively. Phasing of haplotypes, i.e. identifying the alleles that are co-located on the same chromosome, was possible through observation of 340-bp and 297-bp bands, specific for L/A and S/A haplotypes, respectively (Table 17). Hardy-Weinberg equilibrium was tested for all alleles using Chi square–X^2 test.

To study gene effects on SLC6A4 transcription and clinical response, observed haplotypes were grouped in one of three functional tri-allelic groups [215] based on the apparent transcription behavior previously noticed [216]. The functional tri-allelic grouping system considers that the transcriptional activity of an L allele declines to that of an S allele in the

presence of the rs25531 G allele. According to this functional tri-allelic system the genotypes L*/L* (LA/LA), L*S* (LA/LG, LA/S) and S*S* (S/S, S/LG, LG/LG) result.

Table 17. Genotyping of 5-HTTLPR indel polymorphism and rs25531 through determination of PCR product sizes using DNA gel electrophoresis. Shown are the sizes of amplicons, restriction sties of MspI and DNA fragment sizes after restriction of each 5-HTTLPR/rs25531 haplotype.

Haplotype (5-HTTLPR in-del/rs22531)	Amplicon size (bp)	MspI restriction sites	Restricted fragments size (bp)
LA	529	340, 402	340, 62, 127
LG	529	166, 340, 402	166, 174, 62, 127
SA	486	297, 359	297, 62, 127
SG	486	166, 297, 359	166, 131, 62, 127

III.2.5.2. *SLC6A4* Transcription in Responding and Non-Responding Patients

Transcription of *SLC6A4* in LCLs from MARS and STAR*D studies was quantified under 3 µM CTP for 24 and 48 hr. One microgram total RNA was reverse-transcribed to cDNA as previously described (see III.2.4.2). *SLC6A4* expression was quantified using QuantiTect SYBR Green PCR kit (QIAGEN) in a LightCycler 480 II in technical triplicates. Gene expression was calculated by the ΔC_p method using TBP as reference gene (see III.2.4.4).

III.2.5.3. Enzyme-Linked Immunosorbent Assays (ELISA) of Serotonin Transporter Total Expression

An ELISA is an antibody-based detection assay for the quantitative measurement of a target substance. In this study, total SERT expression was determined using ELISA kit SEC890Hu (CloudClone) in LCLs from MARS and STAR*D study cohorts. This ELISA kit employs the quantitative sandwich immunoassay technique.

Sample preparation

Total protein from MARS and STAR*D samples was obtained by lysing cell pellets in 500 µl lysis buffer (0.1 mM EDTA, 0.1 Mm DTT, 100 mM Tris, 0.3 mM Triton X-100) containing cOmplete Ultra protease inhibitor cocktail (Roche). Samples were sonicated for 60 sec at 60% amplitude and 0.6 cycle in ice using Labsonic® (Sartorius AG). Cell lysates were centrifuged at 1500 *g* for 10 min. Total protein was quantified in the supernatant using the bicinchoninic acid (BCA) protein assay (Thermo Scientific).

ELISA assay *procedure*

ELISAs were conducted according to the manufacturer's instructions. Standard series of SERT, blank, quality controls and samples were added in volume of 100 µl each into the

corresponding wells of the 96-well ELISA plate. The plate was covered and incubated at 37°C for 1 hr. Supernatants were removed and 100 µl Detection Reagent A (containing a biotin-conjugated antibody to serotonin transporter) were added to each well. After 1 hr incubation at 37°C, supernatants were removed and wells were washed with 3 x 350 µl of Wash Solution per well. Afterwards, 100 µl of Detection Reagent B (containing avidin conjugated to horseradish peroxidase) were added to each well and the plate was incubated for 30 min at 37°C. After washing five times, each well received 90 µl of 3,3',5,5'-tetramethylbenzidine (TMB) and the plate was incubated for 15 min at 37°C. Upon addition of 50 µl of Stop Solution (H_2SO_4) the liquid in the wells turned yellow. Optical density was immediately measured at 450 nm using Spark® microplate reader (Tecan). After determination of total protein by the bicinchoninic acid (BCA) protein assay (Pierce), SERT content per mg total protein was calculated.

Analysis

A standard curve was inversely plotted with standard concentration on the y-axis and measured absorbance on the x-axis, as per manufacturer's instruction. A linear curve fit was drawn. The concentration of target protein within the samples could be calculated by inserting the measured absorbance values in the equation of the standard curve. The calculations were performed with the program XFluor4.

III.2.5.4. Determination of SERT Surface Expression using Flow Cytometry

Surface expression levels of serotonin transporter (SERT) in LCLs were determined via flow cytometry using a monoclonal SERT mouse anti-human antibody conjugated to Alexa-Flour-488. The antibody is raised against an epitope located on the extracellular loop between TMDs vii and viii of the transporter. Hence, staining of intact cells will label transporter molecules located on the cell surface. Antibody labelling of cells was conducted according to a standard in-house method developed by the Flow Cytometry Core Facility (FCCF) of the Institute of Molecular Medicine at University Clinics Bonn. To exclude erroneous measurement of dead cells, cellular viability was determined by simultaneous co-staining with a nucleus stain (SYTO61).

Samples *preparation*

LCLs were incubated with CTP (3 µM) and ethanol (0.03% v/v) for 24 and 48 hours as described in III.2.3.3. After incubation, $2 \cdot 10^6$ cells were centrifuged and washed with ice-cold PBS.

Samples were afterward fixed in methanol-free 2% formaldehyde for 10 minutes on ice. Each sample was incubated with the staining buffer (2 mM EDTA, 0.5% bovine serum albumin, 0.1% sodium azide) containing 5 µg/ml Alexa-Fluor488-conjugated anti-SERT antibody (FL-N40, Advanced Targeting Systems) and 10 µM of the nuclear fluorescent stain SYTO®61 (Thermo Fisher, Darmstadt, Germany). Samples were stained for 1 hr in the dark and were occasionally stirred. Afterward, cells were washed, centrifuged, resuspended in 400 µl buffer and were measured using FACSCalibur™.

Measurement protocol

Each sample was shortly stirred to break possible cell aggregates before measurement. Detectors were set to a parameters' combination enabling collecting data on all passing cells (Table 18). These parameters were held unchanged throughout the experiment. Collected data on cell size and granularity (forward and side scatter, respectively) were visualized in dot plot. Single-cells population was gated to rule out confounding measurement of cell debris and cell aggregates.

Prior to quantification of the fluorescence intensity of cells labeled for SERT, target cell population on forward scatter/side scatter (FSC/SSC) dot-plot was to be determined. For this purpose, cells that had a fluorescence intensity for CD19 (FL2-PE channel) and CD45 (FL3-PerCP channel) exceeding $1 \cdot 10^1$ were considered to be non-aberrant LCLs and their location on the FSC/SSC was determined through reverse gating. A panel was created in which the determined location for mature LCLs was gated. This panel was used for subsequent surface SERT quantification (Figure 10).

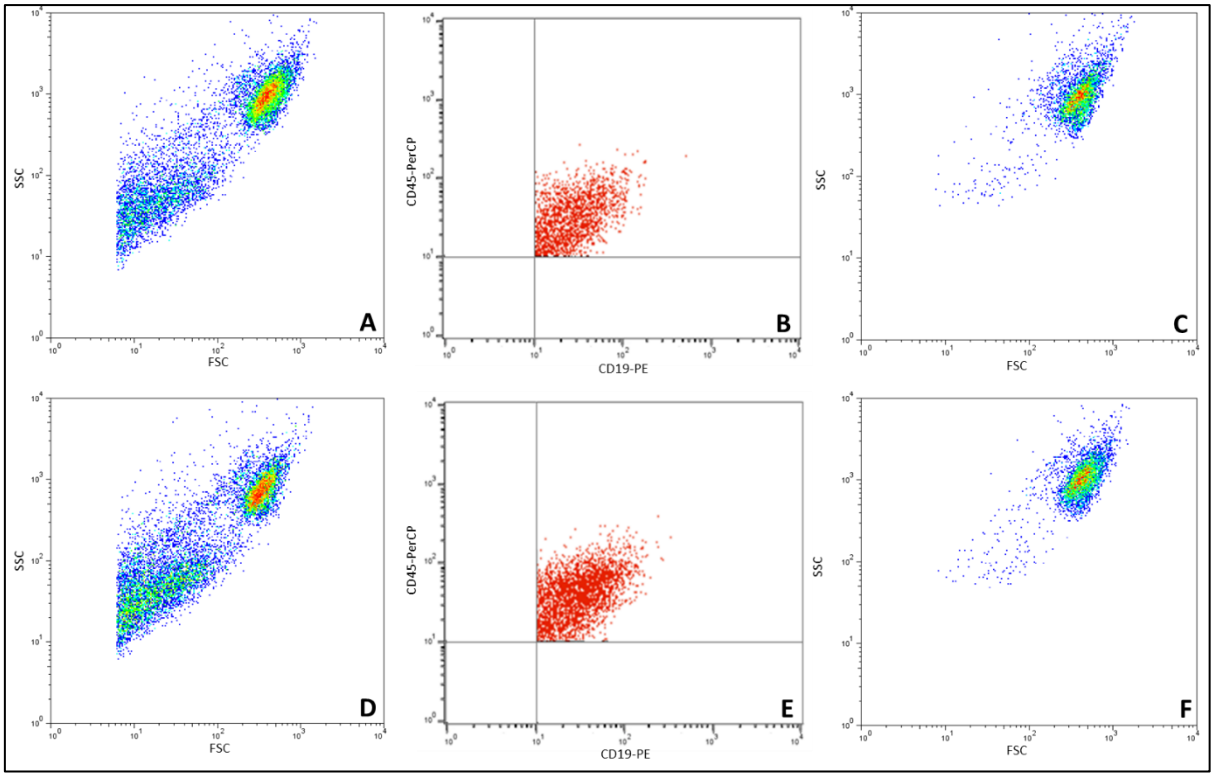

Figure 10. Determination of the target cell population on FSC/SSC dot plot, exemplary in two LCL samples. A, D: FSC/SSC dot plot of cells showing two distinct population of cells. B, E: Upon labelling for CD19 and CD45 using TriTest™, cells that showed fluorescence intensity above $1 \cdot 10^1$ were gated. C, F: A subsequent measurement for the gated population enabled determination of the target cell population on FSC/SSC plot. A corresponding measurement panel specific for the target cell population was created and used for subsequent surface SERT quantification. *FSC forward scatter; SSC side scatter*.

Measurements were performed until 10,000 events were reported inside the FSC/SSC gate. The fraction of cells that had a SYTO®61 fluorescence above $1 \cdot 10^1$ (FL4/APC channel) and FL-N40 fluorescence above $2 \cdot 10^1$ (FL1/FITC channel) was considered as positive and was used for further analyses. Negative controls of non-labeled cells were run in parallel in each measurement.

Table 18. FACS detection channel parameters used for SERT total and expression quantification.

Channel	Voltage	AmpGain	Mode
Forward scatter	E-1	1.37	Log
Side scatter	304	1	Log
FL1/FITC	498	1	Log
FL4/APC	328	1	Log

III.2.5.5. Ubiquitination of Serotonin Transporter in Responders and Non-Responders LCLs[1]

Ubiquitin is a small regulatory protein that covalently binds to proteins to signal several processes such as intracellular trafficking and proteasomal degradation. Determination of ubiquitinated proportions of SERT was studied in MARS exploratory cohort (n=17, 9 responders; 8 non-responders; see Table 8) upon incubation with CTP for 24 hours. Isolation of ubiquitinated proteins was conducted using immunoprecipitation (IP), a protein purification technique that involves binding target protein using a protein-specific antibody. The resulting antibody-antigen complex is then pulled down by being adsorbed to solid matrix e.g. agarose or magnetized beads. The isolated protein is then analyzed by Western blot (WB). In this project, the first step of IP involved binding/co-precipitating of all ubiquitinated proteins using anti-ubiquitin antibodies in combination with protein A agarose beads. In the second step, ubiquitinated and non-ubiquitinated SERT was detected and quantified via Western Blotting of IP bound and unbound fractions, respectively. In a pre-experiment series, IP conditions including time of antibody and beads incubation and rotation pattern were optimized until no ubiquitin signals could be detected in the unbound fraction, confirming a complete binding of ubiquitinated proteins. A negative control of non-ubiquitinated protein (E.coli-recombinant CYP2D6) was used to exclude unspecific precipitation of non-ubiquitinated proteins. Changes in SERT ubiquitination levels upon incubation with CTP and differences between responders and non-responders LCLs were studied by analyzing chemiluminescence intensity of SERT signals on WB using Image Lab Software v.5.2.1 (Bio-rad). Total β actin was used for signal normalization.

Procedure

Protocol was adopted from CST Guide[217] with modifications. Cells were lyzed using 1x cell lysis buffer (CST) containing cOmplete protease inhibitor (Roche). Equal protein amounts were adjusted with lysis buffer to 200 µl and then received 1 volume denaturing buffer (50 mM Tris, pH 7.5 + 70 mM β-mercaptoethanol). The mixture was boiled for 10 min, chilled on ice, centrifuged and 200 µl supernatant was used for immunoprecipitation. Samples received 2.5 µl anti-ubiquitin (Cell Signaling Technologies CST) and were shaken overnight at 4°C.

[1] Disclaimer: This set of experiments and the resulting Western blots have been part of the Master thesis "Ubiquitination of Serotonin Transporter in Lymphoblastoid Cell Lines" submitted to Bonn-Rhine-Sieg University of Applied Sciences in 2018 by Ms. Ilina Mansour. The experiments were designed and conducted under direct lab supervision of Abdul Karim Barakat, author of the current work. All relevant figures, analyses and discussion presented in this thesis were drafted and formulated by the current author himself.

Precipitation of the resulting immune complexes was done by adding 20 µl of protein A agarose beads (50% slurry, CST) to each sample and following shaking for 3 hr. Samples were then centrifuged for 30 sec at 4000 *g.* The supernatant containing the unbound fraction (UF, non-ubiquitinated proteins) was aspirated and appropriately labelled. Beads were washed 5 times with 500 µl 1 x lysis buffer and were then resuspended with 20 µl 3 x loading buffer, and vortexed. Samples were heated to 95°C for 5 min, centrifuged and 20 µl of each sample was loaded on SDS-PAGE (Bio-Rad). After electrophoresis, gels were blotted on PVDF membranes. The blots were blocked with 5% skimmed milk and incubated with antibodies (anti-SERT, anti-ubiquitin, anti-β actin). Detection was done using the corresponding, HRP-conjugated secondary antibodies followed by adding ECL substrate (Thermo Scientific). Images were taken using ChemiDoc™ Touch Imaging system (Bio-Rad).

III.2.6. Statistics

Descriptive analysis of the study cohorts was done using Fisher exact test and Student's t-test. Gene expression of the candidate genes was tested for association with clinical response using unpaired Welch's t-tests ($p \leq 0.05$).

Gene expression data obtained from microarray experiments were analyzed using the statistical tools in GeneSpring software. Here, differences in gene expression were tested for significance using two-way ANOVA test adjusted for multiple testing using Benjamini-Hochberg FDR (p-corr. ≤0.05).

qPCR validation results were tested for association with clinical response and remission in MARS population and with treatment-resistance in the independent STAR*D cohort using unpaired Welch's t-tests ($p \leq 0.05$). Furthermore, ΔCp values were tested for correlations with clinical improvement, calculated as $HAMD_{8w}/HAMD_{baseline}$ and $QIDS_{end}/QIDS_{baseline}$, using Pearson's correlation test. To analyze the effects of the response and remission status of the donors on the gene expression levels in more detail, linear mixed effects models were conducted with respect to the replicated block design of the experiment. The continuous gene expression levels were modelled as a combination of fixed and random effects thereby adjusting for possible confounders. Age, gender, depression baseline score (Hamilton score in case of MARS, QIDS baseline score in case of STARD) and the response and the remission status were treated as fixed effects for the cell lines whereas the experimental units, treatment (two factors levels: control, CTP) and time of measurement (two times: 24 hours,

48 hours) were included as nested random effects. The random effects were modelled with variable intercept but without variable interaction effects for the experimental factors treatment and time of measurement to avoid an increase of parameters. Confirmation of model design were made by visual inspection of the trellis plots of the gene expression levels and by AIC criterion indicating no benefits in case of modeling additionally the slope of the experimental factors. It might be noted that both experimental factors could also be handled as fixed effect, but, as our primary interest was only on the effect of the response respectively the remission status, taking into account the nested within-group variance of the experimental units suffices to comply with the grouped structure of the experimental design. Hardy-Weinberg equilibrium of 5-HTTLPR indel and rs25531 alleles were tested with Chi square–X^2 test. *SLC6A4* transcription, SERT surface and total expression results were tested for association with clinical response and remission in MARS population and with treatment-resistance in the independent STAR*D cohort using unpaired Welch's t-tests ($p \leq 0.05$). Correlation between SERT protein and gene expression was tested with Pearson's correlation. Tests were performed with R v3.5.1 including the libraries coin v1.1-2 and survival 2.39-5 (R Foundation for Statistical Computing, Vienna, Austria) and with MS-Excel. Data are presented as mean ± SEM unless otherwise indicated.

Chapter IV Results

Prediction of treatment outcome is a persistent, unmet need in the psychiatric clinical practice. Lymphoblastoid cell lines (LCLs) have been successfully employed as models in neuropsychiatric biomarker research. In search for rapidly determinable predictors for antidepressant outcome, this work was dedicated to identify predictive biomarkers using LCLs form depression patients previously characterized for clinical therapy outcome. Efforts were focused on whole-transcriptome profiling and on studying serotonin transporter (SERT) at the four levels of genetics and transcription, as well as total and surface protein expression. A candidate-gene approach preceded the transcriptome-wide analysis probing associations with clinical response in a naturalistic setup and screening antidepressant effects and incubation conditions.

IV.1. The Candidate Gene Approach in LCLs from the Naturalistic MARS cohort

Imipramine (TCA), mirtazapine (NaSSA), paroxetine, fluoxetine and citalopram (all SSRIs) were screened for effects on gene expression upon incubation of lymphoblastoid cell lines from 21 MARS patients (n=9 responders, n=12 non-responders). The cohort consisted of non-stratified patients maintaining the observational design of MARS study. The investigated genes were pre-selected following the candidate genes strategy to be pertinent to the inflammatory and the neuroplasticity hypothesis of depression based on current literature relevance. For each incubation (5 antidepressants + 1 control), expression of 11 genes were probed at 3 time points, 1, 6 and 24 hours. Expression of all 11 genes could be detected in LCLs as evidenced by Cp values below 40. Out of the 198 conducted tests for the 11 genes, only two tests for *TGFβ1* showed significant differential expression between the two response groups. After 24 hours of incubation with imipramine and citalopram, expression was lower in responders LCLs than in non-responders' (p=0.037 and 0.012, respectively). Although similar trends were observed under mirtazapine, paroxetine, fluoxetine and control at the same time point, the results have marginally failed to achieve the significance threshold (p=0.134, 0.066, 0.073 and 0.086 respectively; Figure 11C). *TGFβ1* expression at 1 and 6 hr was not significantly different between responders and non-responders (Figure 11A, B). No influence of antidepressants on gene expression was noticed. No significant differences in the expression of TGFβ receptor1 gene (*TGFβR1*) were noticed. *SMAD7*, an inhibitory SMAD of TGFβ1 actions as well as its

function-modulating proteins *Smurf1, Smurf2* and *UCHL5* did not show differential expression between responders and non-responders.

Expression of *BDNF*, CREB, *IFNγ, FKBP5, SMPD1, TET1* and *CHL1* were not significantly different between responders and non-responders.

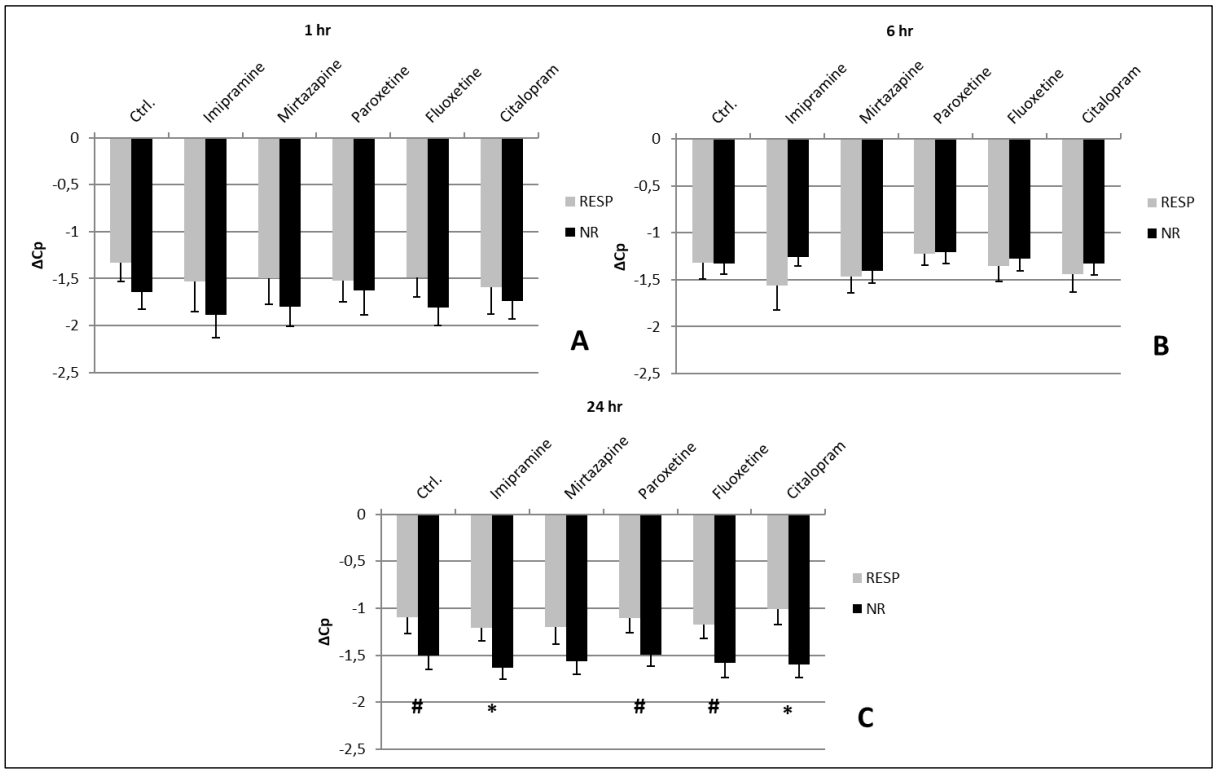

Figure 11. *TGFβ1* expression in responders (n=9) and non-responders (n=12) LCLs from the naturalistic MARS cohort after incubation for 1 (A), 6 (B) and 24 (C) hours with antidepressants or control. Expression values are given as ΔCp (mean ±SEM) after normalization to the reference gene, *TBP*. *NB* higher ΔCp values indicate lower expression. **p≤0.05, #p≤0.1, RESP: responding patients, NR: non-responding patients*.

IV.2. Variability in Genome-Wide Gene Expression Profiling in LCLs of Clinical Responders and Non-Responders after Incubation with Citalopram: The Exploratory MARS Cohort

Unlike the setup of the candidate gene approach, several measures were pre-considered for the experimental design of project II. First, stratification of the exploratory cohort based on diagnosis and clinical medications was carried out in an approach to minimize variabilities accompanying naturalistic studies. Secondly, taking into account the negative results at 1 and 6 hours as well as the longer times usually needed to observe clinical effects, incubation times were shifted to 24 and 48 hours. Lastly, based on its wide clinical use and high selectivity to serotonin transporter, citalopram was employed in subsequent analyses. The whole-transcriptome was studied in an exploratory MARS cohort consisting of SSRI-treated patients

who were clinically characterized as responders (≥50% decrease in HAMD score), and non-responders (<50% decrease in HAMD score) after 8-week SSRI-treatment (n=17; 9 responders, 8 non-responders). Details on patients' characteristics are given in Table 8. For biomarker analyses, LCLs from patients were cultivated and gene expression profiles were measured at baseline and after incubation with CTP for 24 and 48 hr. Data were analyzed using a hypothesis-free and a pathway-guided algorithm designed to detect cardinal and reactional transcriptomic differences, respectively, between the two response subgroups.

IV.2.1. Hypothesis-Free Analysis in the Exploratory MARS Cohort

Results from the hypothesis-free algorithm revealed 55 and 28 genetic features that were significantly differentially expressed between responders vs. non-responders after 24 and 48 hours, respectively (|FC|≥2, *p-corr.* ≤0.05; Supplementary table 3). Twenty-one features were consistently differentially expressed (|FC|≥2, NR/RESP) over both time points. Cardinality was further ensured by computing a mean FC value averaged over incubations and time points for each gene. After ranking for calculated mean FC values, top ten genetic features, coding for nine genes, were considered for qPCR validation (Figure 12, Table 19)[196].

IV.2.2. Pathway-Guided Analysis in the Exploratory MARS Cohort

CTP effects on gene expression were analyzed using the pathway-guided algorithm. After 24 hr, CTP altered the expression of 94 and 185 and after 48 hr of 1198 and 158 features in non-responders and responders, respectively (Supplementary table 4, Supplementary table 5). Pathway-enrichment analysis revealed 25 different enriched pathways (*p-corr.* ≤0.05) in each response group after 24 hr incubation, while after 48 hr 139 and 14 pathways were enriched in non-responders and responders, respectively (Supplementary table 6). The top 10 significant enriched pathways altered in responders were mainly involved in neurotransmitter metabolism, drug addiction, Parkinson's disease, neuroprotection, and serotonin receptor signaling. On the other hand, the most significant pathways in non-responders were involved in cellular adhesion and junction and integrin interactions, in addition to immunological pathways like signaling through T-cell receptor, B-cell receptor, IFNγ, CD28 co-stimulation and MHC-II antigen presentation (Table 20). For putative gene selection, 40 genetic features enriched in pathways deregulated in responders ($p \leq 0.05$) were considered. Features were then filtered on differential expression in response groups (|FC|≥2 NR/RESP). Out of the resulting 14 features, 8 genes with functional relevance were considered for further qPCR

validation (Figure 12; Table 19). Interestingly one gene, *GAD1*, emerged as a hit in both the hypothesis-free and the pathway-guided algorithms[196].

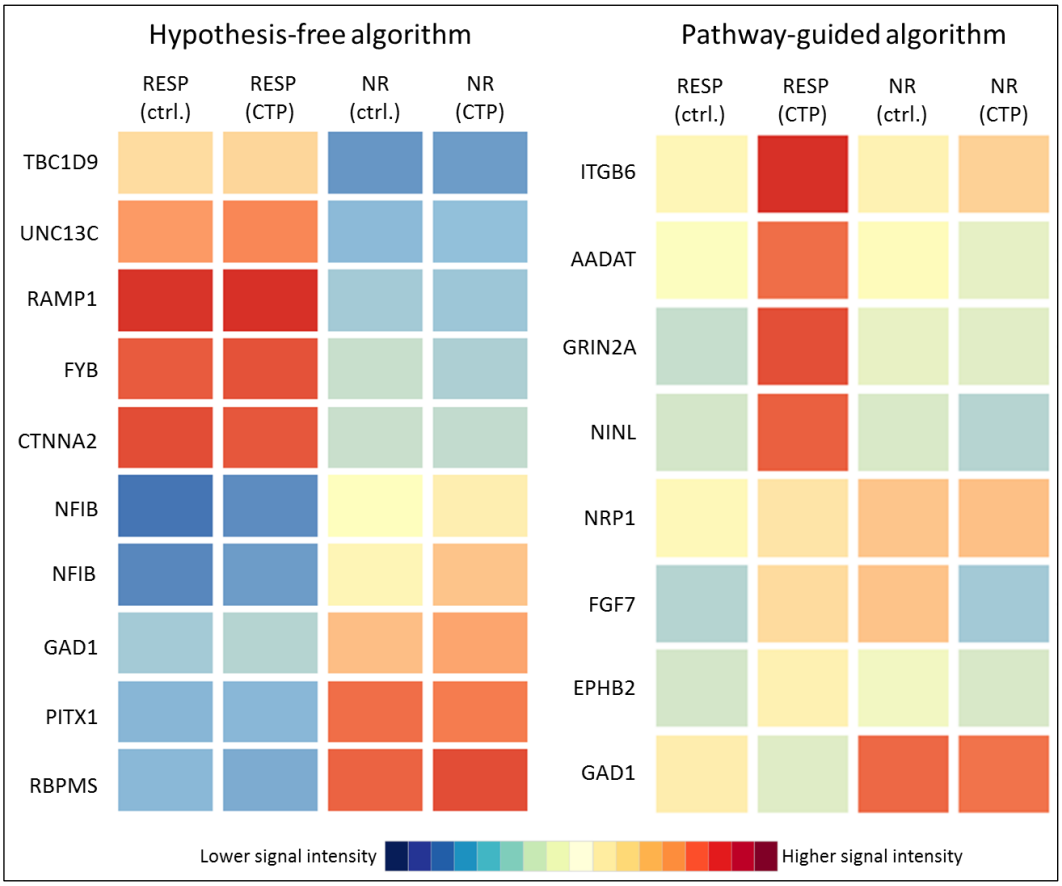

Figure 12. Expression of the candidate genes resulted from the whole-genome expression analysis shown as heat-map of the microarray data (blue-red color scale indicates lower-higher expression, respectively). Figure from Barakat *et al*.[196]

Table 19. Cardinal and reactional candidate genes obtained from whole-transcriptome profiling using hypothesis free and pathway-guided algorithms. Fold-change differential expression in the response groups and functional relevance of each gene are shown. Table from Barakat *et al*.[196]

Hypothesis-free algorithm			
Gene	**Averaged FC (NR/ RESP)**	***p*-corr. value**	**Functional relevance**
TBC1D9	-3.59	0.043	linked to ADHD[218]
UNC13C	-4.07	0.049	might be involved in PTSD[219]
RAMP1	-4.63	0.043	activity modifying protein for CGRP-receptor CGRP has been linked in depression patients CSF and plasma [220 221]
FYB	-3.49	0.043	adapter for FYN, which in turn was associated with long term potentiation[222]
CTNNA2	-3.55	0.043	found related to bipolar disorder[223]

NFIB	+3.75	0.049	Found involved in depression and antidepressant effects in animal models[224]
GAD1	+3.10	0.020	linked to depression and antidepressant response[225, 226]
PITX1	+4.12	0.049	SNPs were associated with autism[227]
RBPMS	+6.47	0.047	loss of function leads to decreased arborization of axons[228]
Pathway-guided algorithm			
Gene	**Averaged FC (NR/ RESP)**	***p*-corr. value**	**Functional relevance**
NRP1	+2.75	0.046	upregulated in postmortem brains from depressed patients[229]
FGF7	-2.10	0.013	involved in inhibitory synapse formation[230]
EPHB2	+2.36	0.018	linked to depression-like behaviors in animal models[231]
ITGB6	-2.40	4.66E-03	linked to antidepressant response in MARS cohort[56]
AADAT	+2.60	9.44E-03	polymorphism was found to modulate SSRI response [232]
GRIN2A	-2.69	3.05E-04	found to be hypermethylated in the hippocampus of MDD patients[233]
NINL	-2.75	0.031	quantitative traits-associated susceptibility loci for brain development[234]
GAD1	+3.10	0.043	expression and variants were linked to depression and antidepressant response[225, 226]

ADHD Attention Deficit Hyperactivity Disorder; PTSD post-traumatic stress disorder.

Table 20. Ten most significantly deregulated pathways in responders (n=9) and non-responders (n=8) LCLs from the exploratory SSRI-treated patients after incubation with CTP.

Deregulated pathways in RESP	***p-corr.***	**Deregulated pathways in NR**	***p-corr.***
Role of Osterix and miRNAs in tooth development (WP3971_91525)	1.17E-03	Focal Adhesion (WP306 94849)	3.60E-10
Elastic fibre formation (WP2666 76849)	0.005	Integrin cell surface interactions (WP1833_77019)	6.68E-10
Hypothetical Network for Drug Addiction (WP666_68893)	0.005	Vitamin D Receptor Pathway (WP2877_94793)	8.02E-10
Melatonin metabolism and effects (WP3298_91618)	0.005	MHC class II antigen presentation (WP2679_76872)	1.38E-09
Neurotransmitter Receptor Binding And Downstream Transmission In The Postsynaptic Cell (WP2754_77001)	0.007	TCR signaling (WP1927_76950)	1.41E-09
Parkinsons Disease Pathway (WP2371_87374)	0.007	TYROBP Causal Network (WP3945_90843)	3.45E-09
NO-cGMP-PKG mediated Neuroprotection (WP4008_92677)	0.009	Interferon gamma signaling (WP1836_77096)	3.96E-09
Tryptophan metabolism (WP465_94086)	0.009	Cell junction organization (WP1793_77057)	4.23E-09
Serotonin Receptor 2 and STAT3 Signaling (WP733_74441)	0.013	Costimulation by the CD28 family (WP1799_77064)	4.84E-09
Lung fibrosis (WP3624_92327)	0.013	B Cell Receptor Signaling Pathway (WP23_92558)	5.00E-09

IV.2.3. qPCR Validation of the Putative Genes in MARS Cohort (n=69)

After establishing the microarray results, the resulting putative genes were validated via qPCR, firstly in the exploratory MARS cohort. Out of the 16 putative transcripts (from 17 features), four showed a different expression ($p \leq 0.05$) between the response groups at least under one of the incubation conditions: Glutamate Decarboxylase 1 (GAD1), FYN binding protein (FYB), Receptor Activity Modifying Protein 1 (RAMP1), TBC1 Domain Family Member 9 (TBC1D9). Further four genes showed a trend ($p \leq 0.2$): Paired like homeodomain 1 (PITX1), Nuclear factor I B (NFIB), Glutamate ionotropic receptor NMDA type subunit 2A (GRIN2A), Aminoadipate aminotransferase (AADAT) (Figure 13, Supplementary table 7). Expression of RNA-binding protein with multiple splicing (RBPMS) and catenin alpha-2 (CTNNA2) was below the detection limit (Cp values >40)[196].

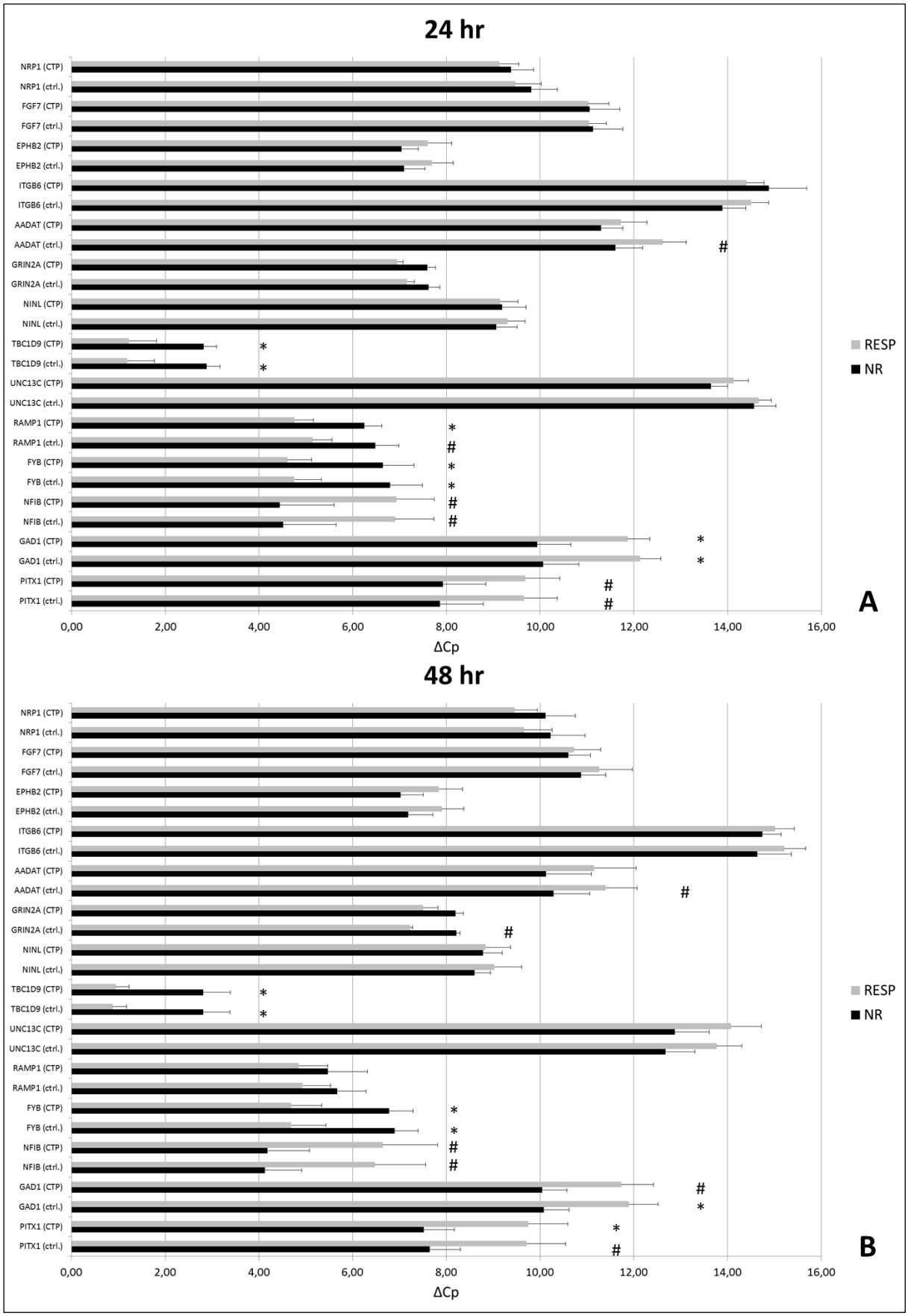

Figure 13. Validation of the putative genes using qPCR in the exploratory MARS cohort (n=17; 9 responders, 8 non-responders) shown as ΔCp values ($Cp_{target\ gene}$–$Cp_{reference\ gene}$; mean±SEM)

after 24 (A) and 48 (B) hours of incubation with CTP. *RBPMS* and *CTNNA2* levels were below the detection limit of qPCR. Eight genes showed either a significant, or a tendency toward an association with response status and were further eligible for validation in the MARS cohort (n=69). *NB lower ΔCp indicates higher expression; * p≤0.05, # p≤0.2. CTP citalopram; ctrl control; NR non-responders; RESP responders.* Figure from Barakat *et al*.[196]

Expression of the resulting 8 putative genes was further investigated in LCLs from MARS cohort of depression patients characterized for response upon treatment with a serotonin-transporter-inhibiting antidepressant of the classes SSRIs, SNRIs and TCAs (n=69; 33 responders, 36 non-responders). Bivariate statistics (Welch's test) showed a marginal to significant association of *GAD1* with response status (p=0.038 – 0.069; Figure 14) while *TBC1D9* expression demonstrated association with remission status that was persistent over both time points and at CTP and baseline incubation (p=0.014 – 0.021; Figure 15). Pearson's analyses showed significant correlations between *NFIB* expression levels and clinical improvement (p=0.015 – 0.025, r=-0.123 – -0.295; Figure 16).

Due to the interference of several complex variables in the measurements, an additional linear mixed-effects (LME) model was developed to test the effects of clinical response and remission on gene expression. Baseline depression severity (baseline HAMD score), gender, age, incubation and incubation time were corrected for as covariates. Thereof, the analysis showed an association of *GAD1* expression with response status (p=0.045) but only a tendency toward association with remission status (p=0.088). Expression of *TBC1D9* and *NFIB* could not reach significance for association with response (p=0.63 and 0.53, respectively) nor with remission (p=0.29 and 0.181, respectively)[196].

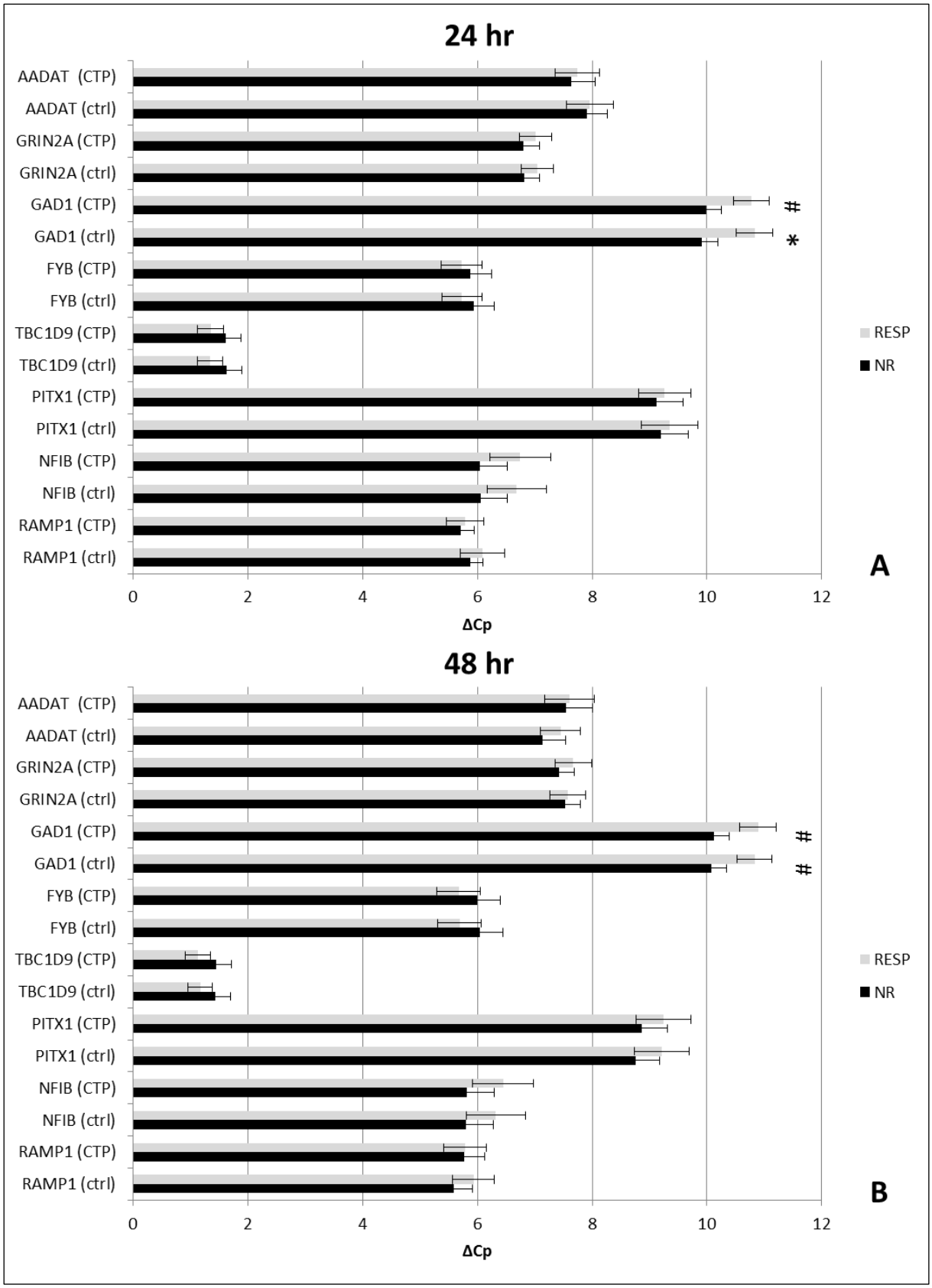

Figure 14. Expression of 8 putative genes in LCLs from responders and non-responders of the MARS cohort (n=69). Glutamate Decarboxylase 1 (*GAD1*) demonstrated higher expression in non-responders LCLs after 24 hr at baseline (p=0.038; A). Similar trends were noticed after 48

hr (p=0.063 – 0.069; B). *NB lower ΔCp indicates higher expression; * p≤0.05, # p≤0.10. CTP citalopram; ctrl control; NR non-responders; RESP responders.*

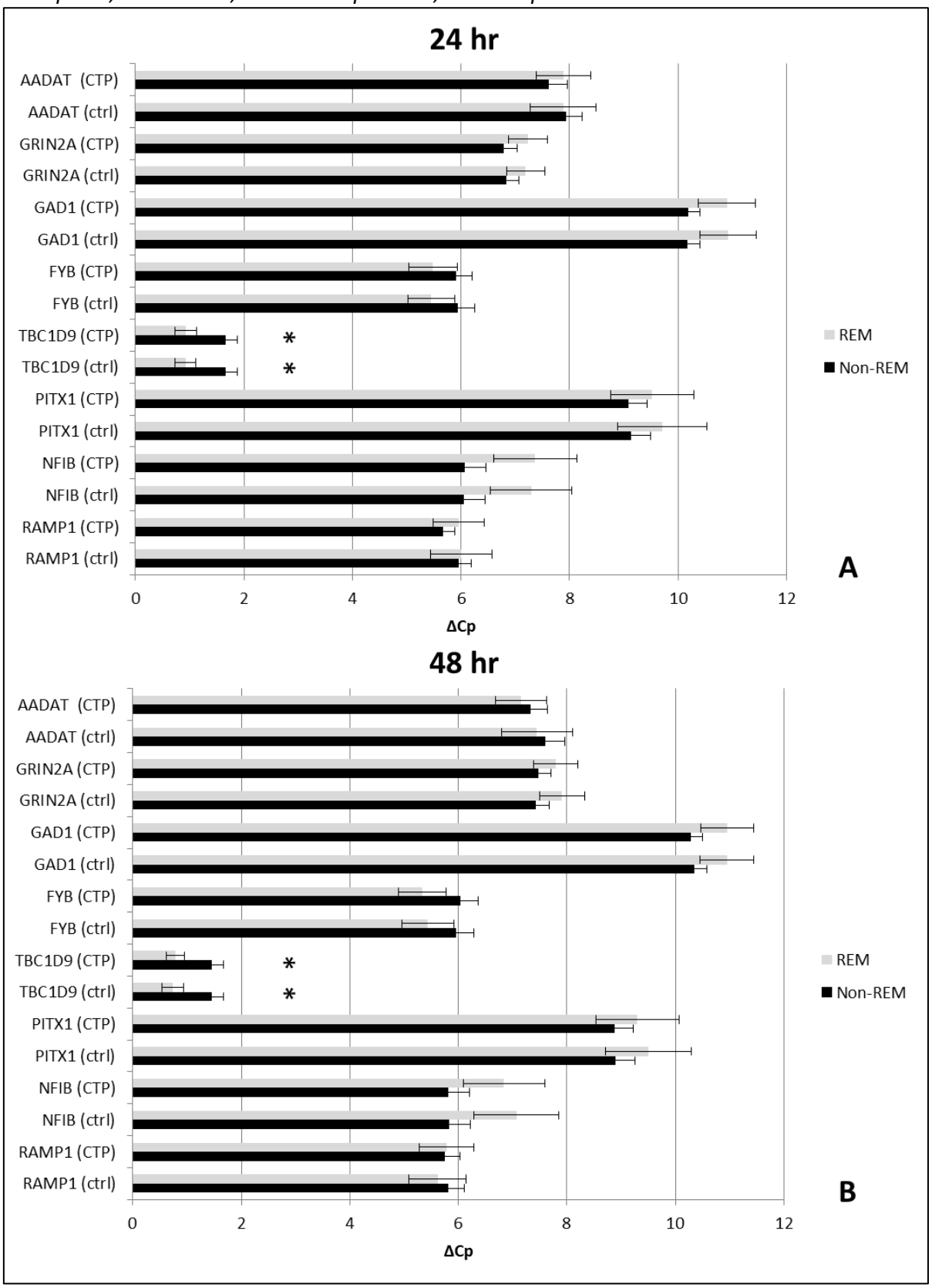

Figure 15. Expression of 8 putative genes in LCLs from remitters and non-remitters of the MARS cohort (n=69). TBC1 Domain Family Member 9 (*TBC1D9*) demonstrated higher expression in remitters' LCLs that was persistent over both time points and at CTP and baseline

incubation (p=0.014 – 0.021). *NB lower ΔCp indicates higher expression; * p≤0.05, # p*≤0.10. *CTP citalopram; ctrl control; Non-REM non-remitters; REM remitters.*

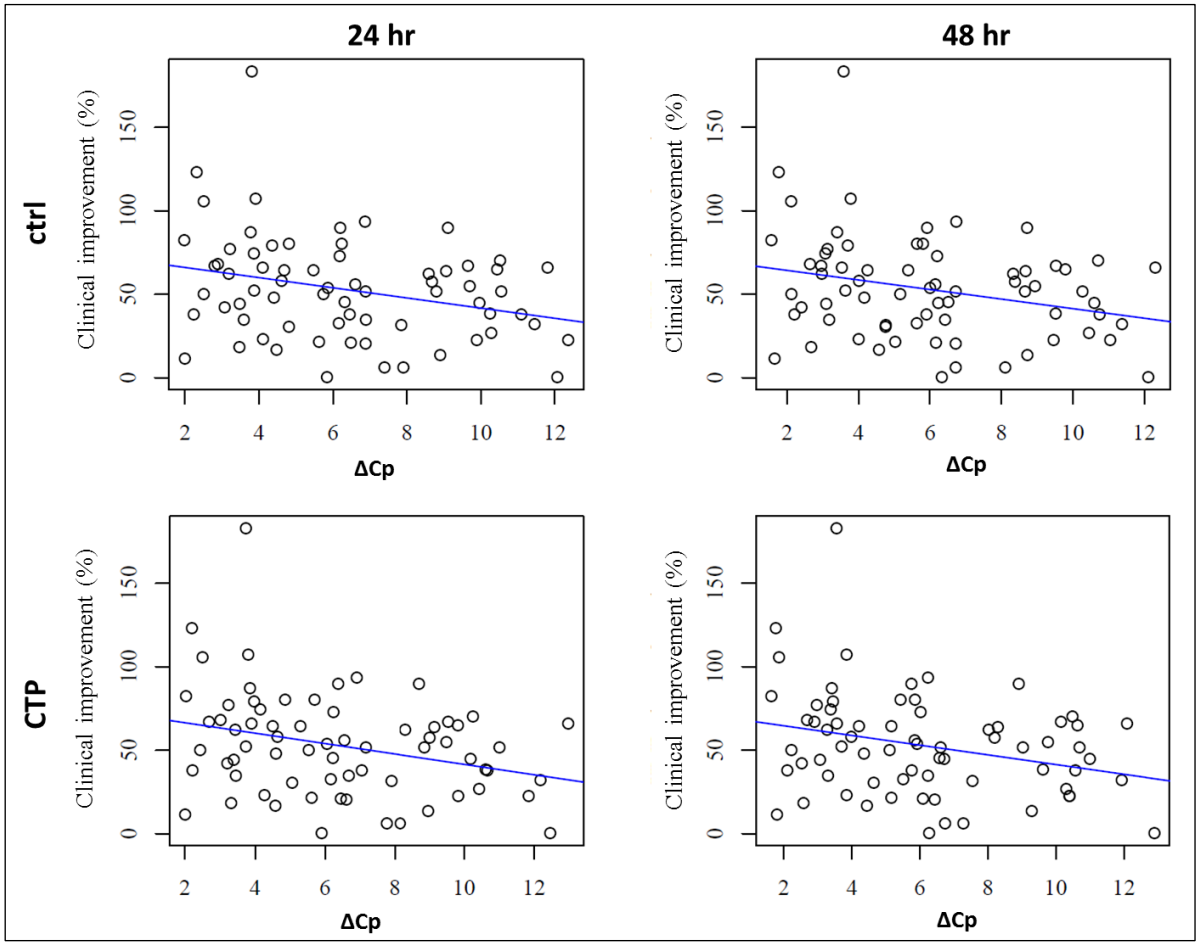

Figure 16. Correlation between gene expression of Nuclear Factor I B (*NFIB*) in MARS LCLs with clinical improvement measured as $HAMD_{end}/HAMD_{baseline}$% of donor patients. *NFIB* transcription levels showed correlation with clinical improvement that was stable through 24 and 48 hr incubation with CTP and at baseline (p=0.015 – 0.025, r=-0.271 – -0.295). *NB higher ΔCp values indicate lower expression.*

IV.2.4. Expression of the Putative Genes in Response Edge Groups from the STAR*D Study

Expression of *GAD1, FYB, RAMP1, TBC1D9, PITX1, NFIB, GRIN2A* and *AADAT* was tested in LCLs from 24 first-line-treatment responders and 20 treatment-resistant patients from the STAR*D cohort following the same experimental setup applied on MARS LCLs. Bivariate tests could not detect associations with clinical outcomes (Figure 17). Multivariate analysis showed only a remarkable tendency toward association with the expression of *NFIB* (p=0.068). *TBC1D9* and *GAD1* expression showed no association with treatment resistance (p=0.27 and 0.23, respectively)[196].

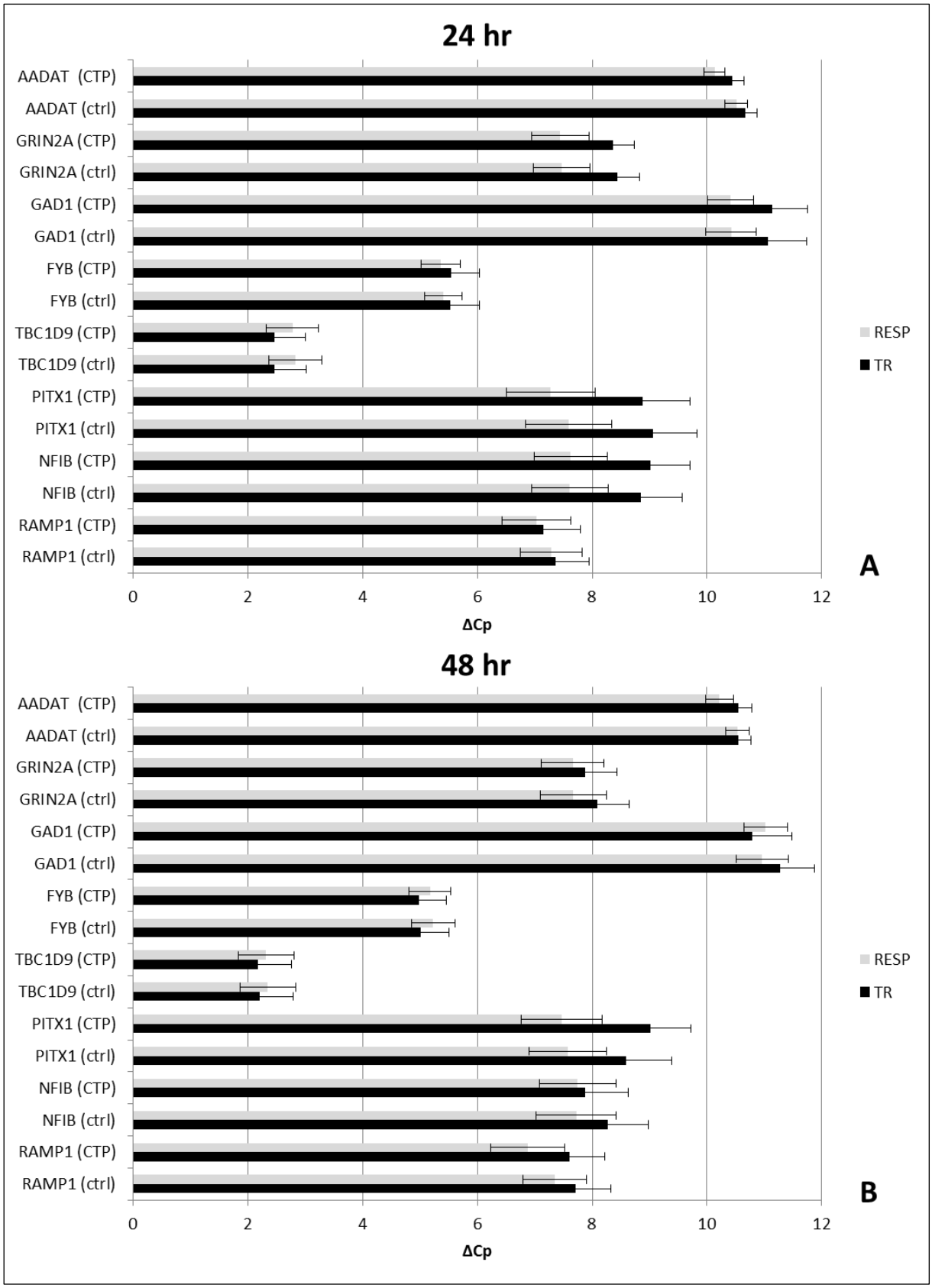

Figure 17. Expression of 8 putative genes in LCLs from responders (n=24) and treatment-resistant patients (n=20) from the STAR*D cohort. No associations with clinical outcome could be detected. *CTP citalopram; ctrl control; RESP responders; TR treatment-resistant patients.*

IV.3. Serotonin transporter Genotypes, Transcription, Total and Surface Expression in LCLs from Patients with Different Antidepressant Treatment Outcomes

IV.3.1. 5-HTTLPR indel/rs25531 Polymorphisms and Clinical Response in MARS Cohort

5-HTTLPR indel/rs25531 hyplotyping was carried out in the LCLs from the MARS cohort of 69 patients stratified on therapy history with serotonin-transporter-inhibiting antidepressants. Genotyping was carried out through PCR product sizing using DNA gel electrophoresis. The long (L) and the short (S) alleles could be identified through the observation of 529 and 486 bp bands (Figure 18 A). rs25531 G and A alleles were identified following restriction with MspI endonuclease through the existence or absence of a 166 bp band, respectively (Figure 18 B). 5-HTTLPR L and S alleles showed frequencies of 0.59 and 0.41 wherease frequencies of 0.93 and 0.07 were noticed for the rs25531 A and G alleles, respectively. Accordingly, haplotypes LA, LG, SA and SG had frequencies of 0.53, 0.07, 0.41 and 0.00, respectively (Table 21). Observed frequencies of genotypes and haplotypes were comparable to previously reported frequencies[162, 235]. Hardy-Weinberg equilibrium test revealed X^2 values below the corresponding critical value for each X^2 test at significance level α=0.05 indicating that genotypes and haplotypes of the tested sample were in equilibrium (Table 22).

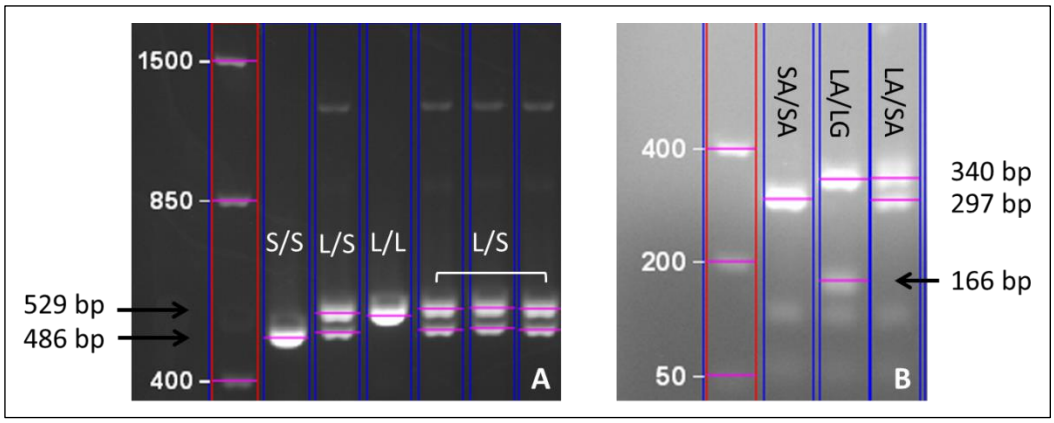

Figure 18. Genotyping of 5-HTTLPR indel L, S alleles (5 samples; A) and rs25531 A and G alleles (3 samples; B): Visualization of PCR products with and without restriction with MspI (different samples shown for each test). L and S alleles were determined through the observation of 529 and 486 bp bands, respectively (A), while rs25531 G and A alleles through the existence or absence of a 166 bp band following restriction, respectively (B).

Upon investigation of association of genotype with response status of donor patients, no genotype effects were noticed. The functional tri-allelic groups S*/S*, L*/S* and L*/L* (see III.2.5.1 for details) did not differ significantly between responders/non-responders nor remitters/non-remitter (p=0.214, 0.418, respectively; Figure 19).

Table 21. Allele events and frequency of 5-HTTLPR indel and rs25531 polymorphisms in MARS cohort (n=69).

Allele	Events	Observed frequency	Previously reported frequency*
5-HTTLPR indel			
L	82	0.59	0.57
S	56	0.41	0.43
rs25531			
A	129	0.93	0.925
G	9	0.07	0.075
Indel/rs25531			
LA	73	0.53	0.500
LG	9	0.07	0.065
SA	56	0.41	0.432
SG	0	0.00	0.003

** As reported by Wendland et al. 2006 and Odgerel et al. 2013 [162, 235].*

Table 22. Observed and expected frequency of 5-HTTLPR and rs25531 genotypes/haplotypes in MARS cohort. Hardy-Weinberg equilibrium was measured using X^2 statistics. i.e. when X^2 below the critical value, polymorphisms are in Hardy–Weinberg equilibrium.

Genotype/Haplotype	Observed freq.	Expected freq.	X^2	Critical X^2 value
5-HTTLPR indel				
L/L	0.35	0.35	0.04	3.84
S/S	0.16	0.16		
L/S	0.49	0.48		
rs25531				
A/A	0.87	0.87	0.33	3.84
G/G	0.00	0.00		
A/G	0.13	0.12		
Indel/rs25531				
LA/LA	0.29	0.28	0.66	7.81
LA/LG	0.06	0.07		
LA/SA	0.42	0.43		
LA/SG	0	0		
LG/LG	0	0		
LG/SA	0.07	0.05		
LG/SG	0	0		
SA/SA	0.16	0.16		
SA/SG	0	0		
SG/SG	0	0		

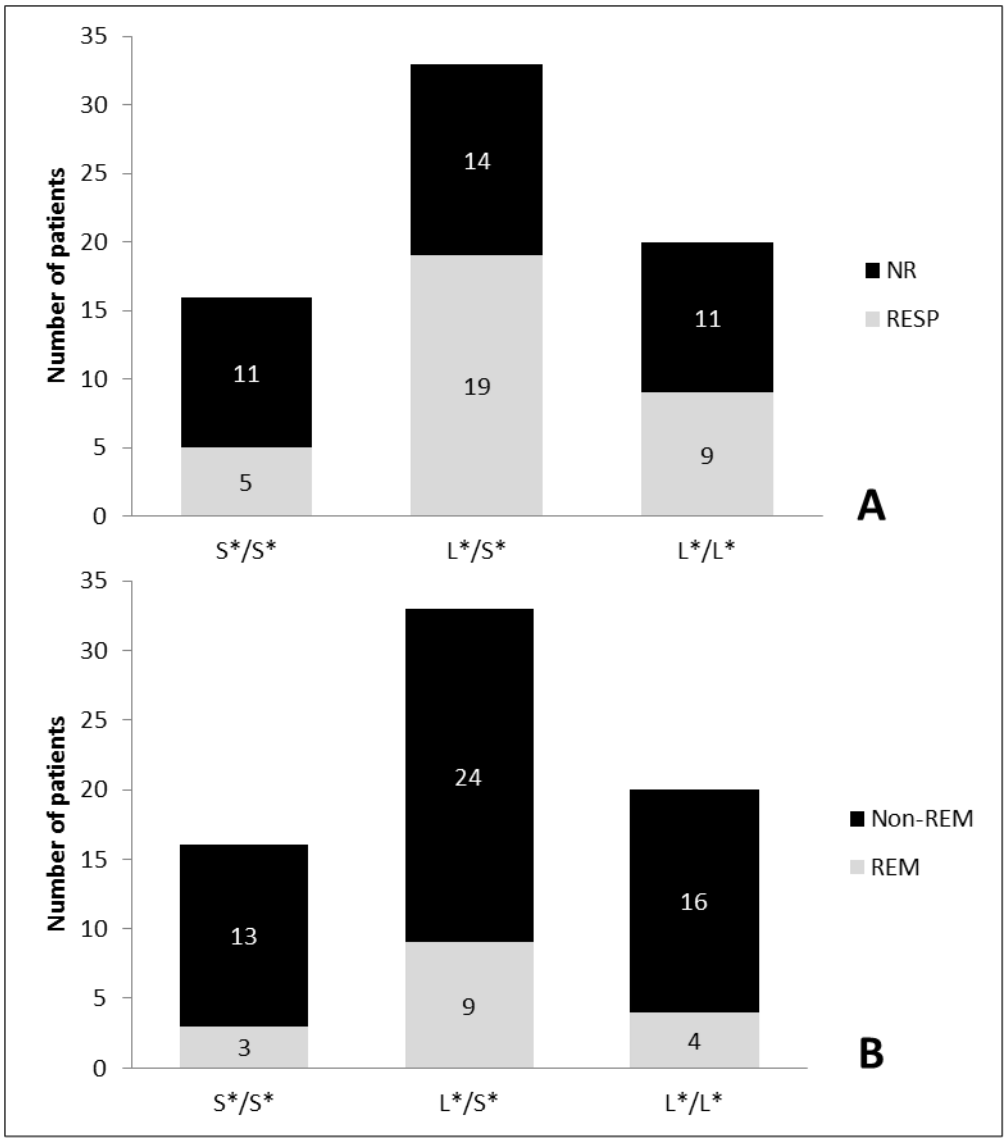

Figure 19. 5-HTTLPR indel/rs25531 haplotypes in MARS cohort. Variants' effects on treatment outcome were studied through grouping of the observed haplotypes in one of three functional tri-allelic groups considering that the transcriptional activity of an L allele declines to that of an S allele in the presence of the rs25531 G allele. Accordingly, the following functional genotypes result: L*/L* (LA/LA), L*S* (LA/LG, LA/S) and S*S* (S/S, S/LG, LG/LG). No genotype effects were noticed on response (p=0.214, A) or on remission (p=0.438; B). *RESP responders; NR non-responders; REM remitters; Non-REM non-remitters.*

IV.3.2. Serotonin Transporter (*SLC6A4*) Transcription in MARS and STAR*D LCLs

SLC6A4 expression was investigated in LCLs from MARS and STAR*D cohorts for correlation with therapy outcome and for changes upon incubation with CTP. Upon normalization to the reference gene TBP, ΔCp values did not show significant changes upon CTP incubation after 24 and 48 hr, nor were there association with response, remission or treatment resistance identified in MARS and STAR*D cohorts, respectively (Figure 20). STAR*D cells were noticed to generally demonstrate lower *SLC6A4* transcription (higher ΔCp values) than MARS cells.

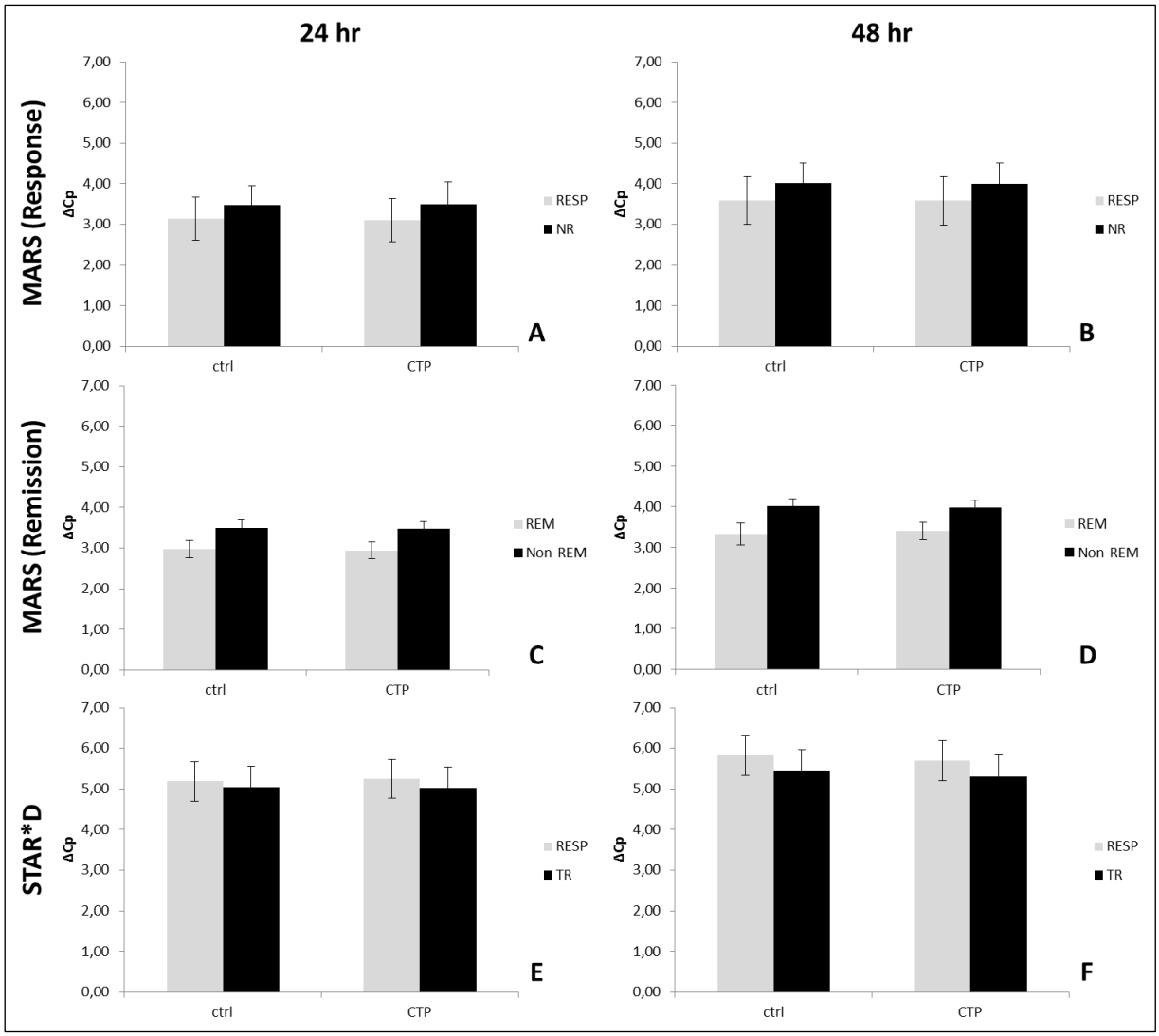

Figure 20. Expression of serotonin transporter gene, *SLC6A4*, in MARS (A-D) and STAR*D (E, F) LCLs. Transcription levels are shown as ΔCp values (mean±SEM) after normalization to *TBP* after 24 (A, C, E) and 48 (B, D, F) hr of incubation with citalopram (CTP). Results from MARS cohort are depicted for responders vs non-responders (A, B) and for remitter vs non-remitters (C, D). No significant changes upon CTP incubation nor association with response, remission or treatment resistance could be identified. *CTP citalopram*, *ctrl control, RESP responders; NR non-responders; REM remitters; Non-REM non-remitters; TR treatment resistant patients.*

Moreover, in MARS cohort, effects of 5-HTTLPR indel/rs25531 functional tri-allelic groups on *SLC6A4* transcription were investigated. The functional genotypes L*/L*, L*/S*, and S*/S* did not significantly differ in means of *SLC6A4* transcription after 24 and 48 hr of incubation with CTP or control (p=0.608-0.930, Figure 21).

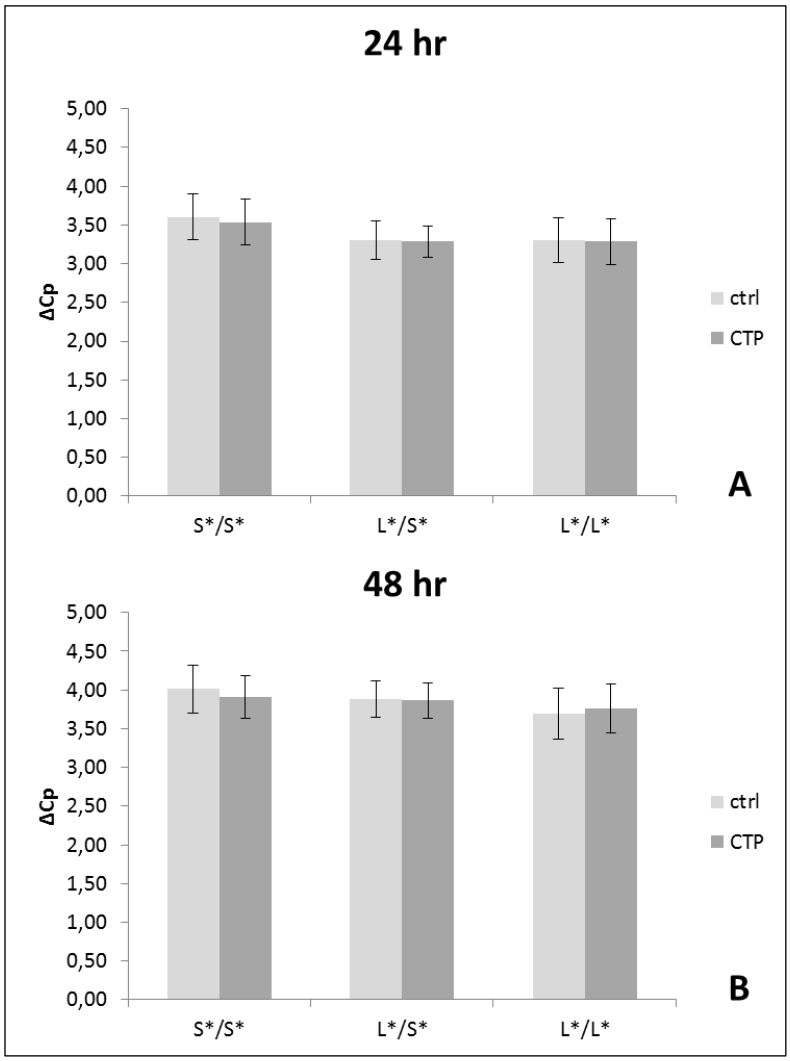

Figure 21. *SLC6A4* transcription in the 5-HTTLPR/rs25531 tri-allelic functional groups S*/S*, L*/S* and L*/L* in MARS cohort. Transcription levels are shown as ΔCp values (mean±SEM) normalized to *TBP*. No genotype effects were noticed on *SLC6A4* transcription after 24 hr (p=0.73, 0.76 for ctrl and CTP, respectively; figure A) nor after 48 hr (p=0.77, 0.93 for ctrl and CTP, respectively figure B). *CTP citalopram; ctrl control.*

IV.3.3. Serotonin Transporter Total Protein Expression in MARS and STAR*D LCLs

Quantification of total SERT in MARS and STAR*D LCLs was carried out using specific ELISA assay. In MARS cohort, CTP did not affect SERT levels in responders (p=0.39, 0.55) nor in non-responders cells (p=0.36, 0.23) after 24 and 48 hr incubation, respectively (Figure 22 A, B). Although SERT expression was apparently higher in responders after 24 hr incubation compared to non-responders, the difference between the two response groups did not reach

significance (p=0.12, 0.49 for ctrl, CTP respectively; Figure 22 A). Likewise, no difference in SERT expression between responders and non-responders was noticed after 48 hr incubation (p=0.94, 0.37 for ctrl, CTP respectively, Figure 22 B). Similar insignificant results were observed for associations with remission (Figure 22 C, D). In STAR*D cohort, SERT expression did not demonstrate changes upon incubation with CTP, either, nor differences between responders and treatment-resistant patients at both time points (p range 0.28–0.60 (Figure 22 E, F). In line with the findings on low *SLC6A4* transcription levels in STAR*D LCLs, these cell lines showed also lower SERT total expression than MARS LCLs (Figure 22 E, F).

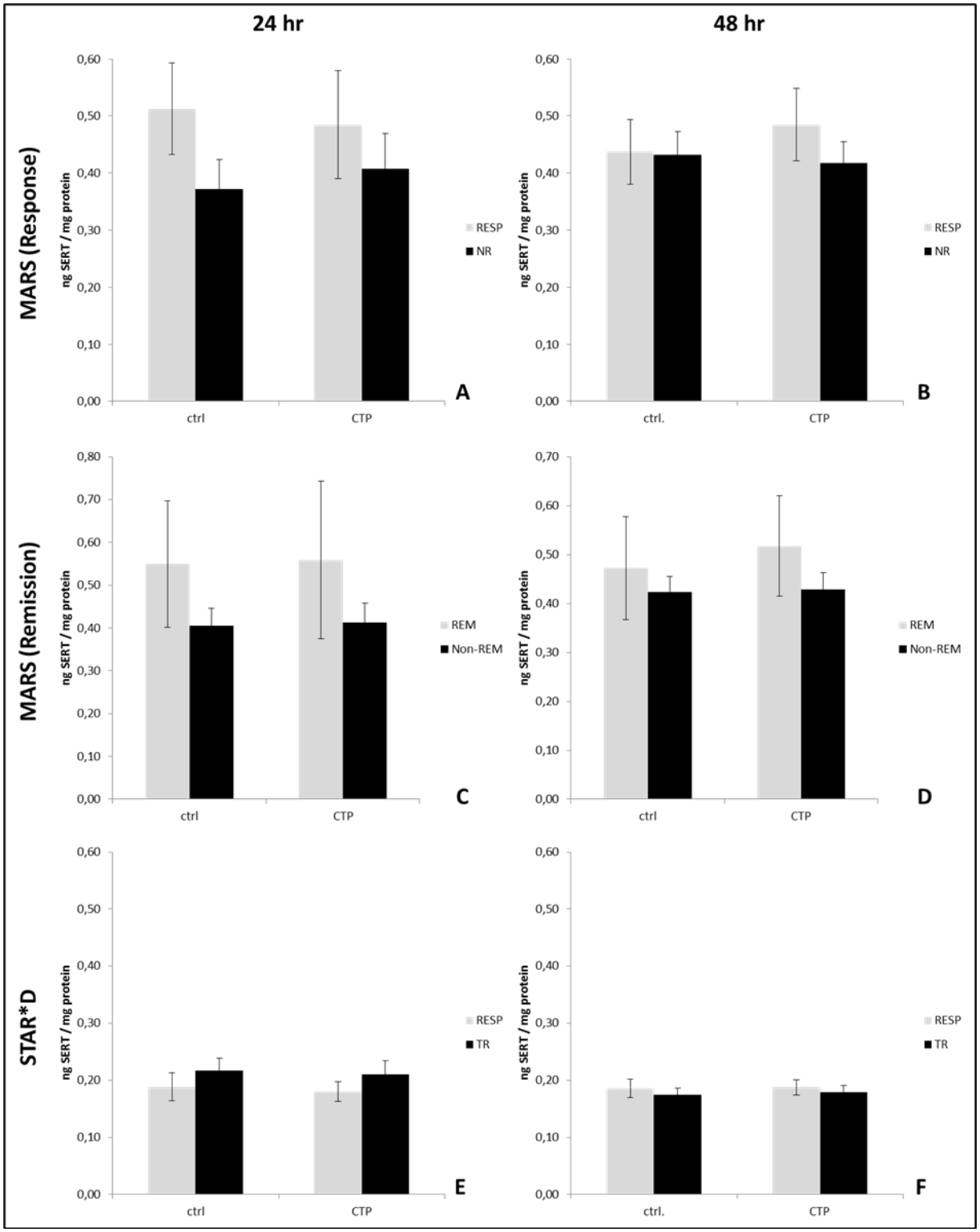

Figure 22. Total SERT expression in LCLs in MARS (A-D) and STAR*D (E, F) LCLs. Quantifiaction was carried out using ELISA assay, SERT levels are shown in ng SERT/mg total protein. Results from MARS cohort are depicted for responders vs non-responders (A, B) and for remitter vs non-remitters (C, D). No significant changes upon CTP incubation nor association with response, remission or treatment resistance could be identified. *RESP responders; NR non-responders; REM remitters; Non-REM non-remitters; TR treatment resistant patients.*

Total SERT expression levels were also tested for correlation with the gene expression (i.e. *SLC6A4* transcription) as determined per qPCR. Pearson's correlation tests could not identify meaningful correlations between ΔCp values and SERT amounts quantified by ELISA (r=-0.03 – -0.25, p=0.11 – 0.81; Figure 23).

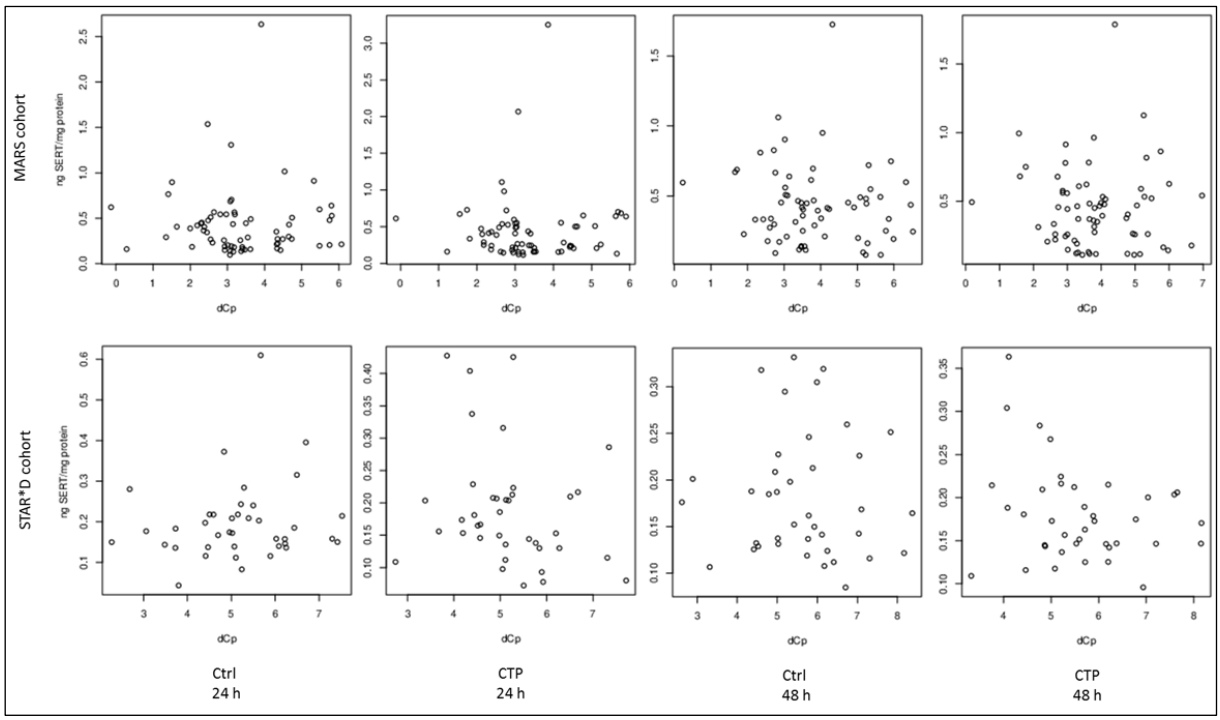

Figure 23. Correlation between SERT gene expression and protein expression was tested using Pearson´s compound moment correlation. Transcription of SERT (*SLC6A4*) was not correlated with its total protein expression measured per ELISA in MARS (r=-0.02 – -0.12, p=0.38 – 0.89) nor in STAR*D LCLs (r=-0.03 – -0.25, p=0.11 – 0.81).

IV.3.4. Serotonin Transporter Surface Expression in MARS and STAR*D LCLs

After determination of mRNA and total protein expression, expression of SERT at its functional location at the cell surface was determined. To this end, a flow cytometry method was employed in which SERT molecules located at the cell surface were labeled using a monoclonal antibody raised against an extracellular epitope. In MARS cohort, responders and non-responders LCLs as well as LCLs from remitters and non-remitter did not differ in surface SERT levels at both time points and under CTP and control incubation (p=0.22-0.65; Figure 24 A-D). On the other hand, surface SERT in STAR*D LCLs showed a stable association with clinical treatment outcome of donor patients regardless of incubation or time. Thereof, after 24 hr responders LCLs had lower surface SERT than treatment-resistant cells (TR) under CTP (16.4% vs. 22.2%; p=0.02) and control (16.4% vs. 21.4%; p=0.04), not substantially different from the

values after 48 hr under CTP (15.1% vs. 19.9%; *p*=0.05) and control (15.0% vs. 20.2%; *p*=0.03; Figure 24 E, F), respectively.

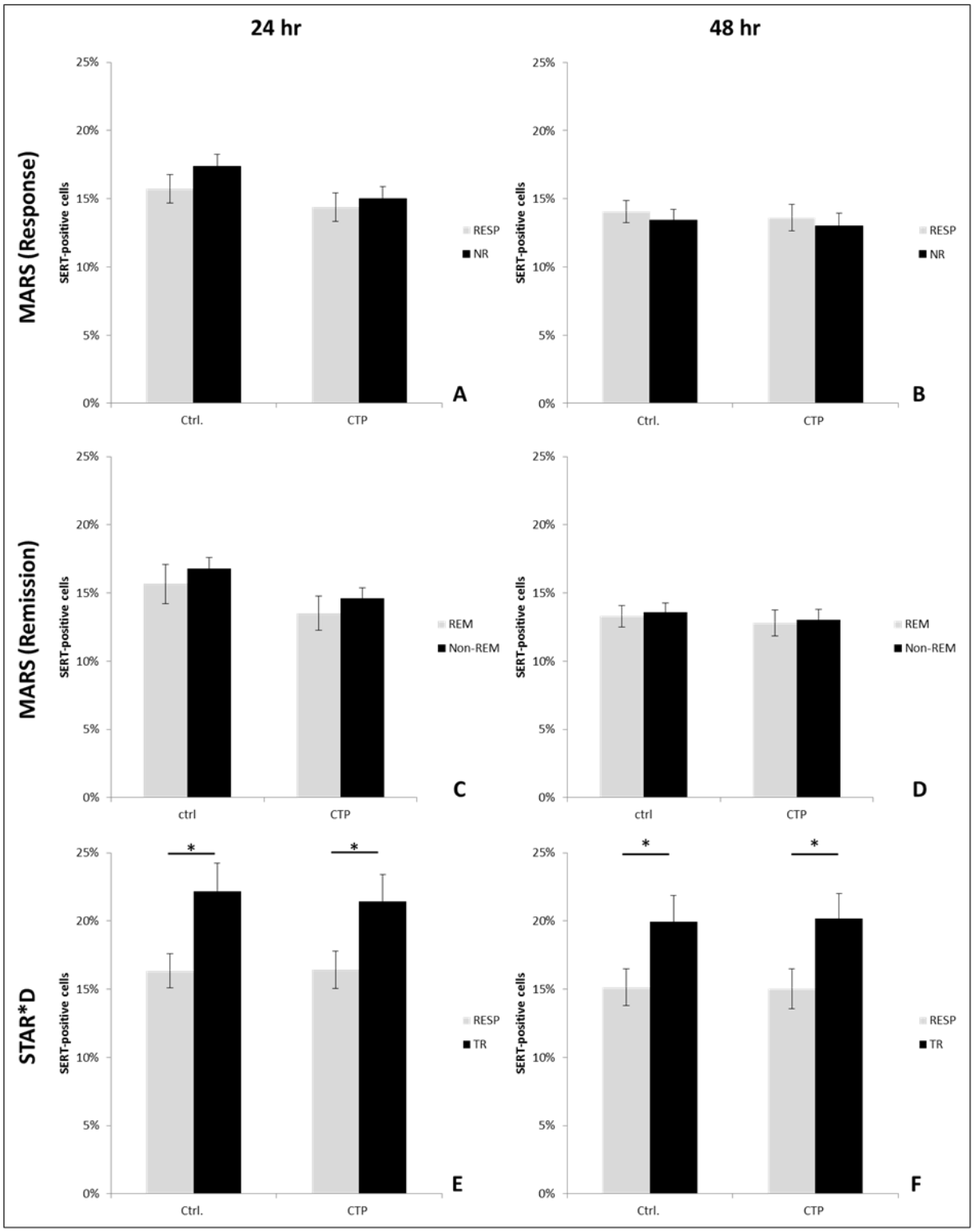

Figure 24. Surface SERT expression in MARS (A-D) and STAR*D (E, F) LCLs. Determination was done via flow cytometry using a monoclonal antibody against an extracellular loop in SERT after 24 (A, C, E) and 48 (B, D, F) hr of incubation with CTP. Results from MARS cohort are depicted for responders vs non-responders (A, B) and for remitter vs non-remitters (C, D). Results are shown as fluorescent-positive cell fractions exceeding a predetermined threshold

of $2.0 \cdot 10^1$. No significant changes upon CTP incubation nor association with response (A, B) or remission (C, D) could be identified in MARS cohort. In STAR*D cohort, responders LCLs had lower surface SERT than treatment-resistant cells (TR) under CTP and at baseline (p=0.02, 0.04 respectively; figure E) as well as after 48 hr (p=0.05, 0.03 for CTP and control, respectively, figure F). *RESP responders; NR non-responders; REM remitters; Non-REM non-remitters; TR treatment resistant patients.*

IV.3.5. Ubiquitination of Serotonin Transporter in Responders and Non-Responders LCLs[2]

Ubiquitinated proportions of SERT were determined in MARS exploratory cohort (n=17, 9 responders; 8 non-responders, see Table 8) upon incubation with CTP for 24 hr via immunoprecipitation. WB analysis with anti-ubiquitin revealed patterns of ubiquitinated proteins in IP bound fractions that relatively homogenously distributed along the different MW ranges. Since the same antibody was employed for IP and WB, heavy and light IgG chains expectedly appeared at 50 and 25 kDa, respectively. No specific signals could be detected in the unbound fractions, indicating complete precipitation of ubiquitinated proteins (Figure 25). Upon immune-labelling with anti-SERT antibody, double bands with MW range of 60-64 kDa were observed, matching the expected molecular weight by the manufacturer. Interestingly, unbound fractions revealed no signals for SERT (Figure 26), a result that called up to exclude unspecific precipitation of non-ubiquitinated proteins. To address this suspicion, an IP was run with a recombinant CYP2D6 protein produced in E.coli, since prokaryotes are known not to possess the ubiquitination machinery. On WB, for the bound fraction a faint signal for CYP2D6 could be visually observed. Signal intensity analysis quantified the signal to be 16.0% of the total loaded, non-ubiquitinated protein (Figure 26).

[2] Disclaimer: This set of experiments and the resulting Western blots have been part of the Master thesis "Ubiquitination of Serotonin Transporter in Lymphoblastoid Cell Lines" submitted to Bonn-Rhine-Sieg University of Applied Sciences in 2018 by Ms. Ilina Mansour. The experiments were designed and conducted under direct lab supervision of Abdul Karim Barakat, author of the current work. All relevant figures, analyses and discussion presented in this thesis were drafted and formulated by the current author himself.

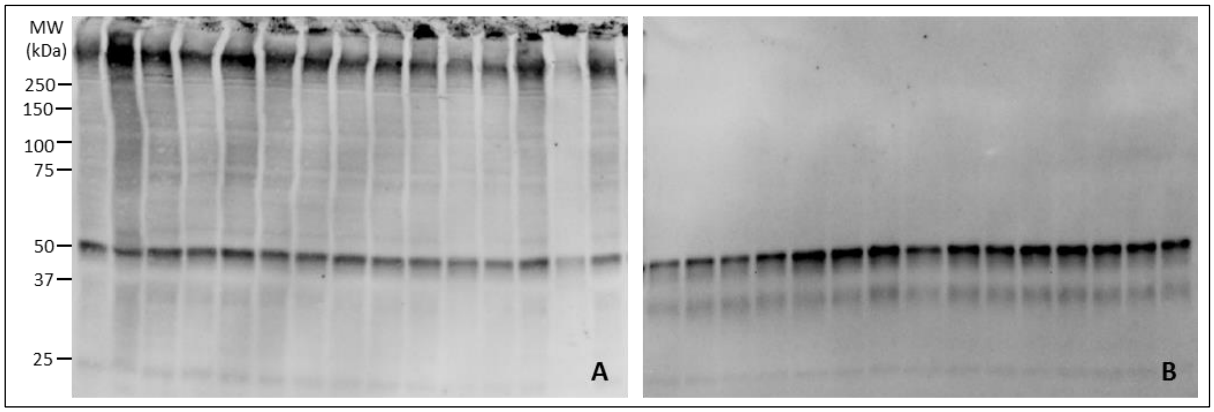

Figure 25. Detection of ubiquitinated proteins via Western blot in bound (A) and unbound (B) fractions upon immunoprecipitation of cell lysates from MARS LCLs with anti-ubiquitin. Complete precipitation of ubiquitinated proteins was determined through absence of ubiquitin signals/pattern in unbound fractions. Heavy and light IgG chains expectedly appear at 50 and 25 kDa.

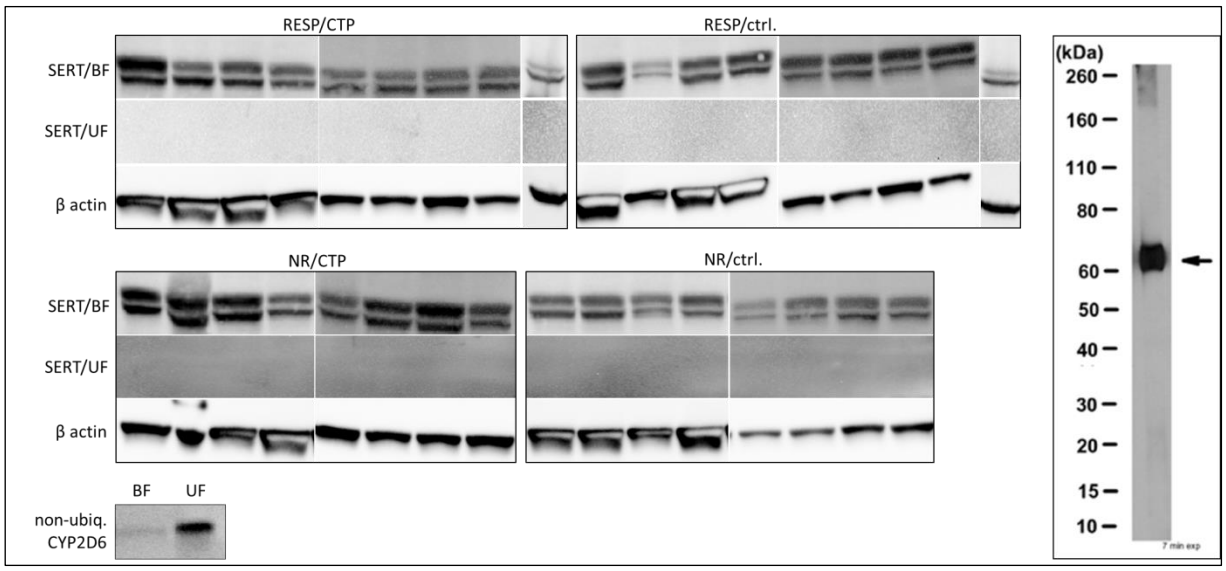

Figure 26. Detection of SERT in bound (BF) and unbound (UF) fractions upon immunoprecipitation of cell lysates from the exploratory MARS cohort (n=17; 9 responders, 8 non-responders) after incubation with citalopram. In BF, SERT labelled as double bands at 61-63 kDa (SERT/BF captures) in match to the expected signal by the manufacturer (right capture). Unbound fractions did not show SERT signals (SERT/UF captures). To exclude unspecific precipitation of non-ubiquitinated proteins, an E.coli-recombinant CYP2D6 underwent IP under identical conditions. IP bound fraction showed only a weak signal for CYP2D6 which was found to make up 16.0% of the total loaded protein. *CTP citalopram; ctrl control; RESP responders; NR non-responders; BF bound fraction of immunoprecipitation; UF unbound fraction of immunoprecipitation.*

After normalization to total β actin, ubiquitinated SERT did not show significant differences between responders and non-responders under ctrl (p=0.55) nor under CTP incubation (p=0.11). Compared to control conditions, CTP only insignificantly increased ubiquitinated

SERT in non-responders (p=0.07) whereas no effect could be observed in responders LCLs (p=0.65, Figure 27).

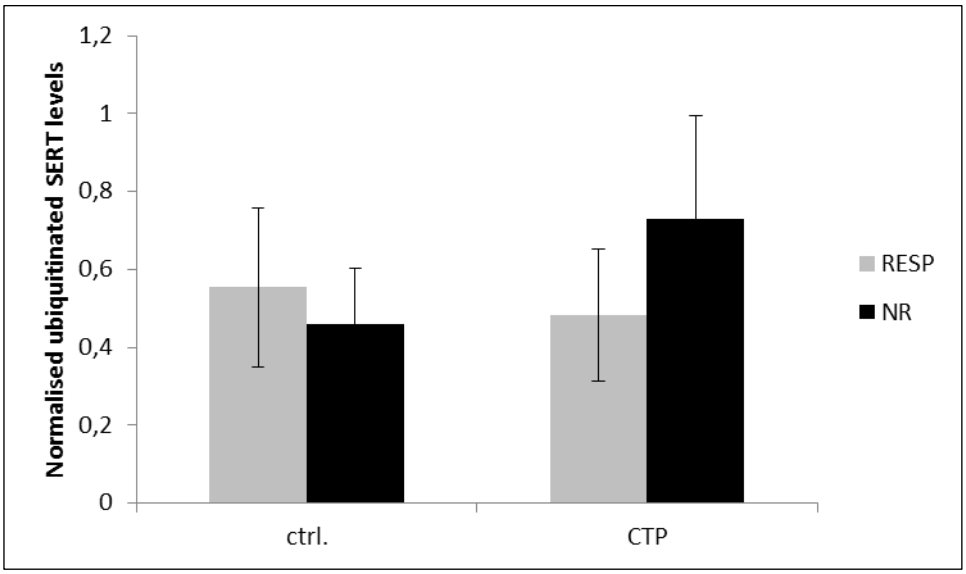

Figure 27. Ubiquitination of SERT in LCLs from MARS exploratory cohort (n=17; 9 responders, 8 non-responders) upon 24 hr incubation with CTP. Changes in SERT ubiquitination levels upon incubation with CTP and differences between responders and non-responders LCLs were studied by analyzing chemiluminescence intensity of SERT signals on Western Blot. β actin was used for signal normalization. No differences between responders and non-responders could be identified. CTP only insignificantly increased ubiquitination in non-responders LCLs (p=0.07) but not in responders (p=0.65). *CTP citalopram; ctrl control; RESP responders; NR non-responders.*

Chapter V Discussion

V.1. The Candidate Gene Approach in LCLs from the Naturalistic MARS Cohort

Aim of the candidate gene approach was to probe the association between the expression of candidate genes and treatment outcome of antidepressant pharmacological therapy while maintaining the naturalistic setup of the MARS study. Genes were pre-selected to be pertinent to the inflammatory and the neuroplasticity hypothesis of depression based on current literature. Being picked up with prior stratification on clinical treatment of donor patients, this cohort should have retained the naturalistic setup of the MARS study. Hence, predictors resulting from this approach were intended to be future candidates as global biomarkers for antidepressant response. Five antidepressants from different classes routinely used in clinical practice were screened for possible effects on expression of the candidate genes. By this means, out of 198 tested sets, only *TGFβ1* expression showed potential to be a candidate predictive biomarker as significantly higher levels were observed in responders LCLs under the effect of imipramine, a TCA, and citalopram, a SSRI. The noticeable, however insignificant, trend in the same direction observed under mirtazapine, a NaSSA, and the SSRIs fluoxetine and paroxetine may further underscore the clinical potential of this result. Since antidepressants did not radically affect the gene expression levels, as noticed by the close pre- and post-incubation ΔCp values, it might be expected that determination of *TGFβ1* levels already at baseline could have response-predicting potential. However, these assumptions must be taken with caution due to the small sample size and the *in vitro* setup of our investigations.

TGFβ1 is a prototypical member of a larger cytokine family that exert a broad range of effects including regulating cell growth, differentiation, apoptosis and pro-/anti-inflammatory cytokines balance[236]. As reviewed in 2012, three isoforms of TGFβ are known (TGFβ1, TGFβ2 and TGFβ3) out of which TGFβ1 is the most abundant and ubiquitously expressed isoform. All isoforms exert their function through the same receptor signalling pathways[237]. TGFβ expression has been identified in several tissues including the central nervous system and adrenal cortex[238], suggesting a tight implication in the regulation of the HPA axis. Accordingly, studies on TGFβ expression variability in depression repeatedly suggest a role in the psychoimmunology of the disease, but still do not clearly draw the features of this involvement. While some studies indicated decreased expression in the blood of depressed

patients[239], some found no difference[240], and others indicated an increased expression[241]. In two studies on depression therapy, TGFβ increased after 6 and 8 weeks of antidepressant treatment. While a correlation with initial HAMD scores was observed, both studies reported no correlations between TGFβ levels and changes in HAMD scores along the treatment course[80, 242]. Interestingly, in the only report on short-term effects of antidepressants we have been aware of, a decreased expression of *TGFβ* was observed in the microglia from healthy donors[243]. We could not locate data on TGFβ short-term expression in association with clinical response. Our results of lower expression in responders might be, thus, in line with the latter data on short-time incubation of healthy microglia with antidepressants, assuming responders as a clinical phenotype are closer to healthy individuals than non-responders.

The absence of significant findings on the remaining ten candidate genes could be attributed to several factors, mainly related to differences in experimental settings between our study and literature. Thereof, the short cultivation/incubation time under which we observed the gene expression might be a pivotal difference. This is due to the fact that most studies set longer cultivation times to simulate the usual 3- to 8-week lag time needed for observing the clinical antidepressant effect. Further key factors that could have resulted in non-reproducibility of earlier findings include different cell types employed, the absence of *in vitro/in vivo* correlations and clinical distinctions of the donor individuals.

V.2. The Candidate Genes Approach: Pros and Cons

Genomics of complex and quantitative traits can be investigated using one of two widespread methodologies: the candidate genes approach and the less selective genome-wide analysis, with each having specific advantages and disadvantages. Genome-wide technologies are considered high throughput technologies that enable scanning of tens of thousands of genomic features in very short time with acceptable reproducibility and sensitivity. The analyses usually proceed without preconception with respect to the functional relevance of the investigated features. However, besides being expensive and resource-intensive, genome-wide analyses only locate the glancing chromosomal regions under population-based experimental designs, which usually embed a large number of candidate genes, often resulting in detection of correlation rather than causation[244]. On the other hand, candidate-gene studies typically investigate a smaller number of genes that have been pre-selected based on a presumed relevance to a suggested biological mechanism. Clearly enough, the focus of a candidate study is on specific biological paths or processes, i.e. causation, rather than on

detection of all possible associated genomic features. The applicability of the candidate gene approach in psychiatric research has been limited by the insufficient knowledge of the exact pathophysiology of the most psychiatric disorders beside the usually unfeasible accessibility to relevant organ tissues. Nevertheless, even in the era of genome-wide association technology, some of the most commonly studied genes were detected through candidate gene approaches. Prime examples from depression research are HTTLPR and FKBP5, both of which originated via a candidate gene approach. In this work, 11 genes functionally mapping to the neuroplasticity and the inflammatory hypotheses of depression pathogenesis were investigated for association with antidepressant response using the candidate gene approach. Expression of all 11 genes could be detected in LCLs as evidenced with Cp value below 40. However, only *TGFβ1* could show significant findings. This low rate of significant findings could be principally attributed to the investagtional (trial and error) nature of the candidate gene approach (despite careful review of pathophysiological contexts), beside the factors discussed at the end of the previous section (V.1). Subsequent to project I, further gene expression analyses were carried out throughout project II in an endeavor to bundle the strengths of both the candidate gene and the genome-wide approaches in one work.

V.3. Whole-Genome Expression Analysis

V.3.1. Experimental Setup

A tight stratification resulting in an exploratory cohort of 17 MARS LCLs representing SSRI-responders and SSRI-non-responders was considered in order to reduce variabilities usually accompanying observational studies. The secondary, less conservative stratification included patients treated with serotonin-transporter-inhibiting antidepressants and resulted in a validation cohort of 69 LCLs. Citalopram (CTP) was chosen over imipramine and other antidepressants as previous studies showed citalopram having the highest serotonin transporter/norepinephrine transporter selectivity[245]. Moreover, studies on drug utilization also showed that CTP is the most widely prescribed antidepressant in Germany[246], conferring our results further clinical and real-life practice relevance. LCLs have been previously successfully employed in investigation of transcriptomic biomarkers for antidepressant response prediction. However, in contrast to earlier works which mostly looked for long-term changes[129, 134, 135], this work focused on studying pragmatic, short-term transcriptional changes occurring after 24 and 48 hours of *in-vitro* incubation with CTP. Differential

expression regulation persistent through both-time points should indicate higher robustness of identified candidate genes. CTP concentration used (3 µM) was 10-fold higher than therapeutic plasma concentration[200]. However, being a racemic mixture of the active S- and inactive R-enantiomers, CTP concentration employed is comparable to brain-blood ratios reported in rodents[202] and humans[203]. Whole-transcriptome data were analyzed using a hypothesis-free and a pathway-guided algorithm designed to detect cardinal and reactional transcriptomic differences, respectively, between the responding and non-responding patients-derived LCLs[196].

V.3.2. Identification of Transcriptional Antidepressant Response Biomarkers

Determination of cardinal and reactional transcriptomic differences between the responders and non-responders of the MARS exploratory cohort idenitifed 16 putative genes. Upon 2-step validation in cell lines from 69 MARS patients, *GAD1*, *TBC1D9* and *NFIB* were found potential biomarkers for response, remission and clinical improvement, respectively.

V.3.2.1. *GAD1* Expression as a Predictive Biomarker for Antidepressant Response

The emergence of *GAD1* as a hit in both the cardinal and the pathway-guided algorithms implies a significant role in the static and the reactional response physiology. This suggestion was initially only partially substantiated through the bivariate statistics. However, upon correction for age, gender and baseline depression scores, the regression analysis highlighted the predictive potential of *GAD1* for treatment response, whereas association with remission status marginally missed the significant threshold.

GAD1 encodes glutamate decarboxylase 1, an enzyme responsible for the last and rate-limiting step in the synthesis of the inhibitory neurotransmitter GABA from the excitatory glutamate[247]. Thus, *GAD1* acts as a link between the two opposing circuits in the brain. The dominance of GABA and glutamate on the inhibitory and excitatory signaling, respectively, underlines their roles in emotional stability and the pathophysiology of mood disorders[248]. Moreover, the hypothalamic-pituitary-adrenal (HPA) axis and, consequently, the body's neuroendocrine response to stress is subject to tight control by the GABAergic signaling[249]. There is growing evidence that GABAergic imbalance exacerbates stress impact in depression. An earlier work revealed gene variants interactions between *GAD1* and corticotrophin-releasing-hormone-receptor 1 *CRHR1* in a group of depression patients[250]. Interestingly, earlier results from the MARS study identified five SNPs in the other enzyme isoform, *GAD2*,

as predicative for unipolar depression and anxiety disorder [103]. The antidepressant response has also been found to correlate with *GAD1* genetic variants as a SNP in *GAD1*, rs11542313, was found to co-modulate antidepressant therapeutic response[226].

Earlier expression studies found reduced *GAD1* levels in brain samples from depression patients[225]. However, *GAD1* expression in blood showed an opposite regulation to that in the brain. Lin *et al.* found increased GAD1 in drug-naïve patients than in medicated patients and healthy individuals[251]. Suitably, our results of higher expression of GAD1 in non-responders LCLs are in a better accordance with results from peripheral lymphocytes than with those from brain samples. Our findings are indicative for the potential *GAD1* expression bears as a rapidly detectable, predictive biomarker for antidepressant treatment outcome[196].

V.3.2.2. *TBC1D9* Expression as a Predictive Biomarker for Remission

Remission (defined as the virtual absence of depressive symptoms) is assumed to be the more stable outcome phenotype compared to response (defined as a 50%-reduction of symptomatology)[252]. *TBC1D9* levels were consistently higher in MARS remitters cells than in non-remitters over both time points and at baseline as well as CTP incubation. TBC1D9 belongs to the Tre-2/Bub2/Cdc16 (TBC) domain-containing protein family. Members of this family possess a GTPase-activating activity with affinity to the Rab family, the largest intracellular membrane trafficking protein family in eukaryotes[253]. Evidence on TBC1D9 function is sparse. Relation to neuropsychiatric disorders emerged as a missense mutation (His1179Tyr) in TBC1D9 was observed in individuals with *de novo* ADHD i.e. with no family history[218]. Further members of TBC family were repeatedly found to be involved in intraneuronal vesicle trafficking and, hence, in neuropsychiatric disorders. TBC1D12, for example, was found to modulate neuron morphology by stimulating neurite formation[254]. Links to depression have also been previously reported. Expression of TBC1D10C and TBC1D5 in blood has been found elevated in mice models[255] and patients[124] respectively. Our findings on the consistent association of *TBC1D9* expression with remission status requires further validation since our cohort included only 16 remitters, an issue that hampers generalizability of our results in the current time[196].

V.3.2.3. *NFIB* Expression as a Predictive Biomarker for Clinical Improvement

Unlike the binary categorization of treatment outcome, according to which individuals are seen as responders and non-responders (or remitters and non-remitters), the concept of the

parameter 'clinical improvement' considers depression symptoms to exist, elevate and dim along a continuum of severity[256-258]. This is in line with the fact that biomarkers associated with depression often show distributions, rather than binary conditions where a biomarker is either present or absent[259]. Growing research considers that treatment outcome phenotypes also manifest in a continuum of gradually decreasing symptoms[260-262]. Predicting non-binary clinical improvement may thus help health care practitioners in decision making on antidepressant prescription for patients with mild-to-moderate depression since antidepressants have been shown less effective in this population and binary categorization is less applicable[263]. *NFIB* expression levels were significantly correlated with clinical improvement in an inversely proportional manner i.e. lower *NFIB* expression correlated with better clinical improvement. *NFIB* belongs to the nuclear factor one (NFI) transcription factor family which are considered essential for normal development of the central nervous structures including the spinal cord cerebellum and hippocampus[264-266]. NFIB namely coordinates gliogenesis in embryos and is involved in the differentiation of astrocytes and oligodendrocytes[264, 267, 268]. Implication of glial cells in MDD has raised from observations of their decreased numbers in hippocampus and prefrontal cortex (PFC) in post-mortem samples taken from depressed patients[269, 270]. *NFIB* expression has also been related to the HPA axis functioning as animal studies identified increased expression in the frontal cortex in rats and in the PFC and amygdala in mice subject to chronic mild stress. These increments were normalized through pharmacological treatment[224, 271, 272]. Moreover, NFIB expression was found to be responsive to changes in plasma cortisol concentration[273]. Although Pearson's analyses reported significant correlations between *NFIB* and clinical improvement, caution should be practiced in interpreting the results due to the absence of positive findings from the regression analyses upon correction for confounders[196].

V.3.2.4. Validation in Treatment-Resistance Depression LCLs from the STAR*D study

Potential treatment-resistance-related molecular profiles were investigated by analyzing an independent cohort of cells derived from the extreme clinical outcome phenotypes i.e. first line responders and treatment-resistant patients from the STAR*D study. The latter group consisted of patients who did not respond to all 4 treatment phases set in the study protocol. Analyzing putative genes in this cohort showed solely a tendency toward an association of *NFIB* expression with treatment resistance. Associations with *GAD1* and *TBC1D9* were not

replicated in the STAR*D cohort. Although initially surprising, these findings are in line with the growing evidence on absence of, or merely partial overlap between biomarkers for different clinical outcome phenotypes. Earlier reports using cell models from depression patients detected a predictive association between cell proliferation rates with treatment-resistance, but not with non-response status. Moreover, transcriptome-wide analyses identified biomarkers for treatment resistance that only partially overlapped with non-response. Whereas *WNT2B, ABCB1* and *FZD7* expression correlated with treatment-resistance status, expression of *WNT2B, SULT4A* correlated with response status, suggesting only *WNT2B* as a common predictor[134, 135]. A similar course could be drawn up by the few available results from genetic studies. The European Group for the Study of Resistant Depression (GSRD) correlated specific variants of *BDNF's* rs6265 and rs10501087 to non-response, while *5HTR2A's* rs7997012 and *CREB1's* rs7569963 were found to correlate with treatment resistance (reviewed by Schosser *et al*.[274]). Similarly, a prospective clinical study with 220 depression patients characterized for response, remission, non-response, non-remission and treatment resistance identified different genetic variants for each phenotype of treatment outcome. Only *MAPK1* rs6928 G/GG-alleles could be associated with better treatment outcomes, response and remission, respectively[58]. A later meta-analysis of three independent samples (n_{total}=3225) found two gene-sets (GO:0000183 chromatin silencing and GO:0043949 regulation of cAMP-mediated signaling) to be enriched in treatment resistance versus the compiled group of responders and non-responders[275]. Taken together with earlier findings, our results suggest the existence of distinct neurobiological etiologies of different treatment outcomes.

Noteworthy is the absence of findings from earlier research from our working group in the hits from the current transcriptome-wide analysis[56, 134, 135]. This absence might be attributed to several aspects that mark up the present study. First, earlier findings were largely driven by the proliferation rate of LCLs as a surrogate *ex-vivo* biomarker for neuroplasticity, while the current study employed LCLs fully irrespective of their proliferation rate. Moreover, the current work stratified donor patients on diagnostic (only unipolar depression) and therapeutic (SERT-inhibiting antidepressants) profiles to obtain a cohort as homogeneous as feasible. Lastly, the incubation time in earlier studies was 3 weeks, resembling the usual time needed for reliable evaluation of treatment efficacy whereas in this study cell lines were incubated for 24 and 48 hours in an approach closer to real-life biomarker applicability[196, 276].

V.3.3. Pathway Analysis of Citalopram-Deregulated Features in LCLs from Responders and Non-Responders

The pathway analyses revealed a transcriptional reaction to short-time incubation with CTP that was markedly response-status-dependent. While the deregulated pathways in responders' cells highlighted involvement of neurotransmitters metabolism, serotonin receptor and other neurological and neuropathological events, non-responders cells showed less neural-specific reaction with most significant pathways being involved in cell adhesion and immune response. Unlike the hypothesis-free analysis in which straight comparisons between gene expression levels in the two response groups (RESP/NR) were drawn, the pathway analysis focused on genes that were deregulated by CTP incubation in each response group (CTP/ctrl). Pathway analysis have been suggested to increase power in detecting associations with antidepressant response in comparison to approaches studying single genetic signatures[277, 278]. However, lack of solid findings in antidepressant pharmacogenetic studies might have led to fewer reports on pathways associated with antidepressant response[116]. Additionally, very few studies investigated the pathway regulation elicited by antidepressants in association with the clinical outcome. In an earlier proteomic analysis of mononuclear cells in depression patients before and after 6-week antidepressant treatment, de Souza *et al.* suggested that antidepressant medication affects similar biological pathways in responders and non-responders but in different direction[279]. This seems to come in conflict with our results of responders and non-responders deregulating different pathways in reaction to CTP. Several technical differences can explain the discrepancy in results. While our study focused on identifying applicable, short-term biomarkers in homogenous cell lines derived from one leucocyte subtype, the B lymphocytes, de Souza *et al.* investigated mononuclear cell populations after a long-term 6-week antidepressant therapy. Additionally, our study did not consider post-transcriptional events, including the proteome, which was in focus of de Souza's study.

The findings of neurotransmitters metabolism pathways (dopamine, serotonin and other biogenic amines) recall the conventional hypothesis on involvement of neurotransmitter imbalance as an underlying biological mechanism of depression[17]. In line with our results, a previous pharmacometabolomic study reported involvement of neurotransmitter metabolic pathways in response to the SSRI sertraline. Peripheral baseline levels of dihydroxyphenylacetic acid (DOPAC), a metabolite of dopamine, and serotonin, seen as a

metabolite of tryptophan, were found among other metabolites with a binary response-discriminant ability[280]. Further studies identified alterations in expression of serotonin biosynthesis pathway genes to correlate with SSRI response and decreased metabolism of tryptophan to be associated with response to ketamine[281, 282].

There is growing evidence that the immune system plays a major role in depression pathophysiology and therapy response which resulted in the emergence of the immunological hypothesis of depression[283]. Genetic variants and expression of inflammatory blood markers including chemokines, cytokines and acute phase proteins were associated with depression and/or poor therapy response[284]. In this context, our results come in analogy with previous findings of B cell receptor signaling pathway being associated with clinical outcome in two independent cohorts of depression patients[285]. Further studies reported increased soluble IL-2 receptor, a T cells activity marker, in peripheral blood in depression patients[286]. Treatment with interferons, on the other hand, was repeatedly found to induce depressive episodes[287-289].

Cellular adhesion molecules (CAMs) are cell surface proteins involved in cell-cell or cell-extracellular matrix binding, a process important for immune response, inflammation and neurogenesis[290]. Polymorphisms and expression of several CAMs were linked to autistic spectrum disorders, schizophrenia and depression[291, 292]. In a large-scale GWAS (n=3394) investigating molecular mechanisms involved in depression etiology, cell adhesion molecules and focal adhesion pathways were found to be among the top 5 enriched pathways. Further pathways were found related to neurotransmitters and the immune system[293]. Lately, two CAMs, CHL1 and ITGB3, were repeatedly reported to be putative predictors of antidepressant response. Associations between SNPs rs4003413 (CHL1) and rs3809865 (ITGB3) with response could be significantly replicated in two independent depression samples, while expression data found associations with early remission[56, 57].

Results from animal studies on pathway regulation in response models are spars. In a study in rats, animals that responded to escitalopram treatment after chronic mild stress showed differential expression to non-responding littermates in genes related to apoptosis, hippocampal neurotransmission and TNF signaling, coming in good accordance with our enriched pathways[294].

Thus, our findings show that deregulated pathways underline a molecular profile of antidepressant drug effects that differs between responders and non-responders (Top 10

significantly enriched pathways in responders LCLs involved in neurotransmitter metabolism, drug addiction, Parkinson's disease, neuroprotection, and serotonin receptor signaling, while in non-responders most significant pathways involved in cellular adhesion, integrin interactions, in addition to immunological pathways). Although altered pathways in both response groups are known to be involved in depression biology and/or antidepressant response mechanism, the complex, less specific reaction seen in non-responders could either imply a more complicated underlying molecular pathophysiology in these patients or an indefinite reaction to antidepressant therapy in which some pathways oppose the sought healing effects provoked by the others.

It should be noticed, however, that unlike the expression of the putative genes which was validated in a larger sample size using a distinct technical methodology and multi-variate statistical analyses corrected for, among others, age and gender, data from the pathway analysis were based on a limited sample size which was unbalanced for gender[196].

V.4. SERT Genotypes, Transcription, Expression and Antidepressant Clinical Outcome

V.4.1. Association of 5-HTTLPR indel and rs25531 Polymorphisms with Response and Serotonin Transporter Expression in MRAS cohort

Previous work on genetic effects of HTTLPR indel and rs25531 polymorphisms had shown inconsistent results[295]. Stratifications by ethnicity and by antidepressant treatment were suggested to omit bias during the statistical detection of allele effect[172]. This work bundled efforts to address knowledge gaps in this context. Donor MARS patients were stratified on administered pharmacological treatment; as such, only patients treated with SERT-inhibiting antidepressants were included. Nevertheless, no allelic effects on response could be detected. It could be argued that further stratification down to antidepressant class and/or larger samples might have been needed. Such stratification for the MARS cohort would result in too small, underpowered samples as the majority of patients were treated with combination therapies due to the observational nature of the study. Assuming it were feasible, possibility of detecting positive findings would remain questionable. In a STAR*D sample of 1914 subjects, Kraft and colleagues failed to detect association of ten SNPs in the *SLC6A4* gene (including rs25531) with the treatment response to citalopram[296]. A separate analysis of 5-HTTLPR indel by the same group also ended negative[170]. On the other hand, reports on positive associations with treatment outcome have been inconsistent. Whereas a meta-analysis observed a

significant association of the S carriers with higher remission and response rates, other studies including a meta-analysis associated the better clinical outcomes to L carriers [171, 297, 298]. Moreover, and in contrast to the findings in Caucasians, a recent study on Korean population demonstrated effects of SS and G genotypes on better clinical outcome but negated an interaction between 5-HTTLPR indel and rs25531[299]. Oddly enough, a re-analysis of the 1914 STAR*D patients originally analyzed by Kraft *et al.* did establish a positive association between the indel polymorphism and remission[296, 300]. The authors attributed the later opposite findings to inclusion of patients whose clinical outcome was previously categorized as undetermined. The largest meta-analysis conducted so far with 5408 patients found no statistically significant effect on antidepressant response or remission[172]. Thus, it is made clear that heterogeneity in methodologies, sample size, outcome measures, ethnicities, analytical approaches and medications across studies, although the majority of which were controlled and interventional, is the main source of result inconsistencies. Being of observational design, the MARS study has the strength of reflecting how depressive disorder is managed in real-world practice, that is, patients are often subject to combinations of antidepressants, combinations with other psychoactive drugs and/or combinations with psychotherapies. Hence, the predictive power of HTTLPR variants testing in such complex therapeutic maneuvers remains to be realized.

V.4.2. Serotonin Transporter Transcription, Expression and Surface Expression as Biomarkers For Antidepressant Treatment Outcome

Efforts on characterization of SERT expression regulators have been running since the complete delineation of SERT gene locus in 1998[301]. SERT transcription process largely depends on cAMP signaling through transcription factors able to bind the cAMP Response Element (CRE) which is contained in SERT promoter[302]. Upon translation of mRNA to proteins, SERT becomes subject to heavy post-translational modifications that regulate multiple biological processes such as folding and insertion at the plasma membrane, protecting 5-HTT against degradation and trafficking[303].

Our work showed that MARS as well as STRA*D LCLs from responders, non-responders and treatment-resistant patients did not show static differences nor reactional i.e. antidepressant-dependent changes in SERT expression, both at mRNA and total protein levels. Low SERT availability levels in the CNS have been brought to associations with several disorders known

to influence affection including anxiety, OCD and MDD[174, 175, 304]. These decreases were confirmed through a meta-analysis of studies on depression patients showing reduced SERT binding sites in key elements of the limbic system including the striatum and the amygdala[305]. SERT is known to be expressed in different cell types outside the CNS including placental cells, platelets and lymphocytes[306]. Peripheral and central SERT were found to be highly comparable with regard to pharmacological properties including 5-HT uptake, sensitivity to antidepressants and expression. Thus, peripheral SERT has been repeatedly employed as a surrogate indicator in respective pathological studies[176]. Indeed, previous works on SERT content in blood also showed a decreased expression in platelets, monocytes and lymphocytes from depression patients[178, 307-309]. These pathological reductions could be restored following antidepressant treatment for 6-8 weeks[178, 307]. Interestingly, mRNA showed opposite expression patterns to those of the protein. Depression patients had higher *SLC6A4* blood levels in comparison to healthy controls which recovered upon adequate antidepressant therapy course of 8 weeks[310-312]. Evidence on association between SERT expression with treatment outcome remains sparse. Belzeaux *et al.* followed 13 depression patients for 30 weeks and reported lower gene expression in responders blood samples compared to non-responders[185]. These dynamic expression patterns were not observed in our results, most likely due to the much shorter observation time courses (24-48 hours) applied in our pragmatic biomarker-seeking work. Data on short-term effects of antidepressant on SERT expression are scarce. A three to four-day fluoxetine treatment was reported to decrease *SLC6A4* expression in some subdivisions of the dorsal raphe nucleus (DRN) in rat brains[313]. However, inconsistencies between animal and human studies on SERT determinations have been repeatedly documented e.g. rat models showed increased (vs. decreased in human) SERT binding sites in several brain regions which decreased consequent to antidepressant treatment[314].

SERT total protein expression did not show significant correlation with gene expression. In a previous investigation on combined data from post-mortem brains (n=112) and Allen Human Brain Atlas, strong linear relationship between gene and protein expression for both the 5-HT_{1A} and the 5-HT_{2A} receptors but not for SERT could be noticed. The data indicated that transcription-translation correlation might be protein-specific rather than cell-type specific[314]. A possible reason for the mRNA/protein levels dissociation might be the fact that SERT is subject to heavy epigenetic regulation. Beside DNA methylation covered above (see V.4.1)

micro-RNA represent another layer of epigenetic regulation of SERT expression. Micro-RNAs (miRNA) are small non-coding RNA sequences occurring naturally in eukaryotes and are able to interact with the 3´ untranslated region (3´UTR) of the messenger RNA of target genes i.e. complementary RNAs. This RNA-RNA interaction results in translation suppression and/or mRNA degradation[315]. Several microRNAs were shown to modulate *SLC6A4* mRNA expression including miR-15, miR-15a, miR-16, miR-24, miR-195, miR-135a and miR-322 (reviewed by Baudry *et al.* 2019[316]). Nevertheless, the trend of lower transcription levels in STAR*D cohort compared to MARS cohort was maintained in ELISA results.

Unlike gene and total protein expression, surface SERT demonstrated a stably higher expression in LCLs from treatment-resistant patients than in those from first-line responding patients. Regulation of membrane localization of monoamine transporters is subject to several protein kinases which exert distinct effects. SERT surface expression increases upon chronic activation of the stress kinase, p38 MAPK, and protein kinase G (PKG) while it decreases upon activation of protein kinase C[181, 182, 317]. Interestingly, molecular mechanisms assumed to underlie antidepressant effects in mice have been shown to increase expression of a phosphorylated PKC isoform, PKCζ, together with an increase in BDNF and hippocampal neurogenesis. The latter was inhibited upon parallel administration of PKCζ inhibitors[318]. The quest of whether antidepressant clinical response might be related to variabilities in protein kinases remains to be resolved. Only recently a protocol of a relevant clinical study has been published[319]. On the other hand, and in line with the monoaminergic hypothesis, increased SERT surface expression has previously been suggested as the functional mechanism responsible for affective disorders. A study simulating the HPA axis dysregulation, regularly noticed in depression, demonstrated that agonizing the glucocorticoid receptor using dexamethasone resulted in increment of SERT surface expression in serotonergic neurons. The effect was not due to increased SERT translation and abated through the inhibition of the glucocorticoid receptor[320]. Moreover, platelets from depressive patients showed increased 5-HT uptake (V_{max}) without changes in SERT affinity (K_m), indicating higher SERT surface expression[321]. In the only approach we could identify on association between surface expression, depression diagnosis and treatment outcome, Rivera-Baltanas *et al.* employed confocal laser microscopy to study the size of SERT clusters on lymphocyte surfaces from depression patients and controls. SERT cluster size, but not number, was greater in patients than in control lymphocytes, thus replicating previous findings indicative for higher SERT

surface expression in depression patients. On the other hand, lower HDRS scores after treatment were associated with fewer but larger surface SERT clusters at the baseline which increased in number but not in size after 8-week treatment[188]. However, the study setup was distinct to ours. Beside principal differences in treatment duration and in methodological platforms employed, the group studied HDRS scores before and after treatment without setting categories for response and non-response, making direct comparison to our findings unfeasible. Moreover, SERT surface expression as an independent parameter was not quantified.

Our findings showed that CTP did not affect SERT surface expression. Previous efforts established apparently opposite findings. In a study employing confocal laser microscopy in HEK cells transfected with human *SLC6A4* and in serotonergic neurons, Lau *et al*. showed that citalopram resulted in complete internalization of SERT already after 1 hour incubation which persisted up to 24 hours[187]. The current work initially aimed to study whether similar findings could be replicated in LCLs and whether differences exist between responders and non-responders LCLs. The methodological distinctions between the two works may explain to some extent the apparently opposite findings. The authors noted in their work that under different, suboptimal technical conditions, SERT signals could be observed in samples presented as absent of SERT surface expression.

It could be noticed that SERT gene and total protein expression in MARS LCLs were almost 2-fold-higher than those in STAR*D LCLs. The two studies do have inherent dissimilarities including STAR*D was designed as an interventional study conducted on major depressive disorder (MDD) outpatients of any ethnicity who later underwent four sequenced treatment levels. Diagnosis of psychotic symptoms or history of bipolar disorder was set as exclusion criteria[197]. Depression severity was measured with the self-reported Quick Inventory of Depressive Symptomatology (QIDS)[9]. On the other hand, MARS was designed as an observational study conducted on hospitalized Caucasian patients broadly diagnosed with affective disorders including bipolar disorder (BP) and MDD with or without psychotic symptoms (BP patients were excluded in our work). The clinician-rated HAMD-21 was used to assess depression severity[113]. Although the correlation between the self-reported QIDS scale and HAMD was found to be high in a meta-analysis of seven studies on patients diagnosed with depression, the presence of treatment resistance in one study population may compromise the correlation magnitude[322, 323]. This may produce bias in outcome-phenotype

interpretations since the STAR*D cohort mainly concerns treatment resistance in comparison to first line responders. Being of different setups and designs, STAR*D and MARS might have recruited patients with distinct pathological and demographical background that might generate SERT expression variabilities. However, as we are not aware of the generation protocol and passage number of the purchased STAR*D cells, model-dependent causes cannot be entirely ruled out.

V.4.3. Ubiquitination of Serotonin Transporter in Responders and Non-Responders LCLs

According to our ubiquitination analysis, SERT could be detected in the ubiquitinated but not in the non-ubiquitinated fractions, indicating that the major, if not the entire, part of the protein is ubiquitinated in our model. A nonspecific precipitation of non-ubiquitinated proteins could not be completely ruled out as a proportion of 16% of non-ubiquitinated (E.coli-recombinant) CYP2D6 co-precipitated with anti-ubiquitin beads. However, in light of complete visible absence of SERT signals in unbound fractions, this finding is not expected to meaningfully influence the validity of the results. Beside phosphorylation, which modulates SERT subcellular localization as discussed above, ubiquitination was also found to control protein trafficking, fates and functionality in a ubiquitination-pattern-dependent matter. Hence, multi-ubiquitination (ubiquitination on several lysine residues) was found to regulate internalization of surface proteins, while poly-ubiquitination (serial addition on previously attached ubiquitin through ubiquitin lysine residues) targets proteins for proteasomal degradation[191-193]. Ubiquitin signals may also modulate protein activity e.g. kinase activation, signal transduction, endocytosis and DNA damage tolerance[194]. However, the widely spread commercial antibody-based methods, including immunoprecipitation, are not specific to monovalent or polyvalent protein bindings. It is thus not possible to reveal the ubiquitination pattern of SERT, which led to the complete co-precipitation in the ubiquitinated fractions in our hands.

SERT bands detected using WB were in range of 60-64 kDa, lying slightly lower than the expected molecular weight by the manufacturer (70 kDa). However, ubiquitination should be expected to increase the MW of the detected bands. Human SERT is known to be expressed in a wide, tissue-dependent, molecular weights range between 65–100 kDa. Irrespective of ubiquitination status, SERT was detected at 65 kDa in lymphoid cells when using the same antibody employed in this study, thus lying in good match to our results[306]. In absence of

further investigations, the low molecular weight observed in this work remains to be elucidated. In a previous study, Mouri *et al.* showed that LCLs from fluvoxamine-resistant MDD patients had higher SERT expression accompanied with lower ubiquitinated protein in comparison with sensitive patients[195]. Effects of *in vitro* antidepressants on ubiquitination levels and non-ubiquitinated fractions were not explored. Although not immediately comparable, animal studies showed that total ubiquitination activity was higher in responding mice than in their non-responding littermates[324]. In a better match to the human study, the current work showed higher SERT expression in resistant LCLs (STAR*D) and lower ubiquitinated levels in non-responders LCLs (MARS), both, however, did not reach significance. CTP incubation only insignificantly increased SERT ubiquitination in LCLs from non-responders. Earlier works showed that antidepressants do influence elements of the ubiquitination system[325, 326]. Moreover, tianeptine, an atypical antidepressant, increased ubiquitination of the glutamate receptor subunit GluA2[327]. Findings on antidepressants effects on monoamine transporters ubiquitination, and much less on association with treatment outcomes, could not be retrieved from the current literature.

V.5. Limitations

Having investigated biomarkers across the two independent MARS and STAR*D trials, the current work has several strengths, but also carries the limitations of the source studies. These have been reviewed in details elsewhere[78, 296, 328]. Nevertheless, some relevant limitations should be briefly addressed. The first limitation that should be seriously considered is the heterogeneity between MARS and STAR*D trials in setup and design. Whereas STAR*D had an interventional study design recruiting outpatients, MARS was an observational study on stationary inpatients. This key difference is expected to result in heterogeneity in response and remission rates as such a closely monitored inpatient might have not responded if were to be treated in outpatient settings. Secondly, the self-reported Quick Inventory of Depressive Symptomatology (QIDS) scale was used in STAR*D study whereas the clinician-rated HAMD-21 was employed in MARS[113]. Although the correlation between the self-reported QIDS scale and HAMD was found to be high in a meta-analysis, the presence of treatment resistance in one study population may compromise the correlation magnitude[322, 323]. This may produce bias in outcome-phenotype interpretations since the STAR*D cohort mainly concerns treatment resistance in comparison to first line responders. Moreover, the treatment duration adopted to designate response as an endpoint was uniformly set to 8 weeks in the MARS study, while it ranged from 6 to 14 weeks in the STAR*D cohort. This might have led to some findings being overlooked due to inconsistent treatment timeframes. However, these inter- and intra-study heterogeneities can be seen as an advantage to test validity and generalizability of candidate biomarkers across clinical outcome-phenotypes, and also across outcome endurances. Another limitation is that both studies did not include a placebo group, an issue that hampered a thorough evaluation of response to treatment against to placebo and prevented making sure that responding patients truly responded because of the medication. This, however, is a disadvantage shared with the majority of treatment studies in depression attempting to discover outcome predictors. Thus, in absence of placebo, it cannot be ruled out that it is not drug response per se that is being measured, but that observations may actually relate to the speed of recovery or the placebo effect. Also the inter-individual heterogeneity within the MARS cohort which results from its observational character should be considered. This concerns in the first place the different polypharmacy of individual patients which may mask a non-response, if those patients were to be managed with monotherapy; as well as the distinct diagnoses. Although we tried to address this problem

with a tight stratification before gene expression profiling, we cannot rule out that effects in gene expression might have been overlooked due to this fact. Despite our study design to investigate biomarkers for serotonin-transporter-inhibiting antidepressants through investigating LCLs from stratified patients treated with such, we cannot rule out that our findings might be specific to citalopram, the only employed antidepressant in the study, and may not be the same for other SSRIs or other classes of antidepressant medications due to slight differences in each drug chemical structure, transporter affinity, selectivity, and receptor binding profile. Moreover, our biomarker profiling was conducted in a homogenous *in-vitro* model based on LCLs derived from B-lymphocytes collected from depression patients. Thus, results *in vitro* in other leukocytes subpopulations e.g. primary PBMCs, or *in vivo* in patients whole blood specimens might deviate from that observed in our cell models.

V.6. Summary

Personalization of antidepressant treatment can be realized by identification of biomarkers that can be employed in clinical practice for the prediction of patients' response. In this work, efforts were compiled to identify peripheral biomarkers predictive for clinical outcome using lymphoblastoid cell lines (LCLs) derived from depression patients recruited in large depression trials (MARS and STAR*D) with monitored treatment outcomes as *in vitro* model. LCLs have been successfully employed as models in neuropsychiatric biomarker research as they can be easily prepared for large population samples and reliably maintain inter-individual variation in gene-expression levels. Based on whole-transcriptome investigations, our pathway analyses suggest that biological pathways reacting to short-term citalopram incubation are largely distinct between responding and non-responding patients LCLs. Whereas in clinical responders neural function pathways were primarily deregulated, citalopram mainly affected pathways involved in cell adhesion and immune response in non-responders LCLs. Transcriptional biomarker analyses showed associations between *GAD1, NFIB, and TBC1D9* transcript levels with response status, remission status, and improvement in depression scale, respectively, but not with treatment resistance. Moreover, the current work systemically investigated serotonin transporter (SERT) variants, transcription, and total and surface protein expression for associations with clinical outcome. Genetic investigations of the SERT-coding gene (*SLC6A4*) polymorphisms 5-HTTLPR and rs25531 did not reveal associations with the clinical outcome of the donor patients. *SLC6A4* transcription and total protein analysis did not show static or reactional (i.e. upon antidepressant incubation) differences in SERT expression

between responders and non-responders LCLs. However, surface SERT demonstrated a stably higher expression in LCLs from treatment-resistant patients than in those from responding patients. Our whole-transcriptome results propose the existence of distinct pathway regulation mechanisms in responders vs. non-responders and suggest *GAD1*, *TBC1D9*, and *NFIB* as tentative predictors for clinical response, full remission, and improvement in depression scale, respectively, with only a weak overlap in predictors of different therapy outcome phenotypes. Whereas no transcriptional biomarker for treatment-resistance could be identified, our SERT analyses suggest an association of this clinical phenotype with higher cell surface expression of SERT.

Chapter VI Outlook

Depressive disorders already make up the largest share of the mental disorders on the globe. Future prognoses prophesy increasing rates of depression. The rapid population growth along the improvement of medicine practice in today's developing countries should lead to more precise diagnosis of cases and will contribute to the increment in under-reported morbidities prevalence. Another rate-steering factor is the quick municipality urbanization, which is often experienced with social isolation, chronic stress and anxiety[329]. The effects of the climate change and the accompanying natural and public health catastrophes are expected to play growingly malicious roles on the human psyche[330]. A current example is the COVID-19 pandemic which triggered 25% increase in anxiety and depression prevalence worldwide[331]. Hence, the need for novel, more and rapidly effective antidepressant therapies is immense. The search for therapeutic agents outside the monoaminergic circuit has already delivered its first fruit. Esketamine, an NMDA antagonist with modulating effects on the glutamatergic system, has been approved by the U.S. FDA as well as by the European Medicines Agency for the treatment of depression. Further illicit drugs and/or their derivatives are being investigated for potential therapeutic applications in depressive disorders like LSD (ClinicalTrials.gov ID: NCT03866252) and cannabidiol (ClinicalTrials.gov ID NCT04732169). Another candidate approach for research on novel antidepressant class should be steered toward the imbalance between pro- and anti-inflammatory cytokines, as the immune system has frequently been found involved in depressive disorders. However, with the development of new antidepressants, we ought to expect the immergence of the need for corresponding, novel, predictive biomarkers. Investigations in this field turned out to be a challenging duty due to the high ambiguity and individuality of depression. Consequently, determination of standardizable parameters to predict individual treatment outcome seems for the mean time unrealizable. The approach of setting up combined panels of validated DNA, RNA and protein biomarker signatures might be the future of personalized medicine in depression. This is attributed to the fact that depression is highly multifaceted with indications of genetic and post-genetic implications. The development of rapid and easy to handle sets covering such biomarker signatures is a promising candidate solution to further progress in the field. Examples of such companion diagnostic panels applied today in clinical practice are found mainly in oncology. *GAD1, TBC1D9* and *NFIB* reported here as candidate biomarkers, side by

side with the SERT surface expression, could be a part of such combined biomarker panels. However, these signatures should be first further validated on the molecular, clinical and pharmacogenetic levels. Immunological methods like ELISAs and Western Blots can be employed for further characterization of these genes by detecting their protein products. The pharmacogenetic validity can be checked using knockdown or miRNA silencing in *in vitro* models like LCLs or neuronal cell lines (e.g. neuroblastoma cell line SH-SY5Y or cortical neuron cell line HCN-2) or *in vivo* in depression animal models. For the determination of biomarkers, the ease of tissue accession and sample collection should be granted. Phlebotomy and a subsequent isolation of lymphocytes can be feasibly established in clinical routine using affordable equipment if the previous data on our candidate biomarkers were to be confirmed in further studies and transferred to patient lymphocytes. Eventually, however, the economic aspects should also be taken into account, such as a positive cost-benefit ratio or the duration of the test procedure[332]. Should our findings be replicated by independent investigation in near future, this would be a step forward in establishing predictive biomarkers for antidepressant treatment outcome.

Chapter VII Supplementary Materials

Supplementary table 1. Clinical data overview of MARS responding (n=33, light shade) and non-responding (n=36, dark shade) donor patients stratified on clinical diagnosis and documented therapy profiles. Listed cell lines were used in qPCR valdiation of candidate genes from microarray analyses, in *SLC6A4* transcription and genotyping and in SERT total and surface expression. SSRI-treated exploratory cohort is shown in bold. The latter cell lines were used in whole-transcriptome microarray analyses.

				HAMD-21 score		Treatment duration (weeks)										
Cell line	Age	Sex	ICD10	week 0	week 8	TCA	SSRI	SNRI	NaSSA	NARI	SSRE	OTH	AP	MS	BZD	SED
K1124	48	M	F33.2	20	9	8	0	0	0	0	0	0	0	3	0	0
K1112	50	M	F33.2	25	5	0	0	8	0	0	0	0	0	3	0	0
K0171	48	F	F33.1	24	10	4	8	0	0	0	0	0	0	0	0	0
K0429	52	M	F33.3	35	17	7	0	4	4	0	0	0	0	0	3	0
K1114	22	M	F33.2	29	6	0	4	7	0	0	0	0	8	0	0	0
K1113	74	F	F33.2	16	5	0	2	7	6	2	0	1	1	0	0	2
K1123	21	F	F32.2	24	12	8	0	3	0	0	0	4	1	2	0	3
K1106	58	F	F32.2	30	4	0	0	8	0	0	0	0	8	0	6	0
K0738	58	M	F33.2	35	4	0	0	7	7	0	0	0	0	3	6	0
K1108	46	F	F32.2	26	9	8	0	0	0	0	0	1	8	0	6	0
K1130	62	M	F33.2	18	3	8	0	0	0	0	0	0	0	8	4	5
K1149	78	F	F33.2	17	1	8	8	0	0	0	0	0	0	5	1	4
K1125	44	F	F33.2	21	10	0	0	8	0	0	0	8	8	0	2	0
K1122	44	M	F33.2	29	11	4	0	8	0	0	0	0	8	0	7	0
K0446	44	F	F33.3	33	10	0	8	0	8	0	0	0	7	0	7	0
K1120	77	M	F32.2	21	8	0	8	0	8	0	0	0	7	0	7	0
K0739	54	M	F33.2	29	13	0	3	7	0	0	0	0	5	8	7	0
K0872	53	M	F33.2	30	8	0	0	8	0	0	0	8	0	8	7	0
IN0108	41	F	F33.3	34	2	0	0	8	0	0	0	0	8	8	8	0
K1081	53	M	F33.2	31	14	8	8	0	0	0	0	0	8	1	7	3
K1091	65	M	F32.2	28	14	0	0	3	8	0	0	8	8	2	7	0
K0734	43	M	F33.2	27	0	0	6	0	6	0	0	0	0	5	5	0
K0732	30	M	F33.2	24	0	0	0	0	7	0	0	0	0	4	0	0
IN0012	61	F	F33.2	27	6	5	0	6	0	0	0	3	7	2	6	4
K0728	38	M	F33.2	40	15	0	8	0	2	0	0	0	6	7	7	0
K0095	25	M	F32.2	22	7	0	8	0	0	0	0	0	0	0	0	0
K0437	19	F	F33.2	25	11	0	8	0	0	2	0	0	0	0	0	4
K0751	45	F	F32.2	31	10	0	8	0	0	0	0	0	3	3	7	3
K1062	62	M	F32.2	18	4	0	8	0	0	0	0	0	3	4	6	0
K1069	32	M	F32.1	28	5	0	6	0	0	0	0	0	4	3	0	1
K1077	42	M	F32.2	19	4	0	8	0	0	0	0	0	7	0	0	0
K1118	36	M	F32.2	27	12	0	8	0	0	0	0	0	8	0	0	0
K1144	44	F	F33.2	22	5	0	8	1	2	0	0	0	0	6	6	6
K1060	24	F	F32.2	15	14	0	0	8	0	0	0	0	0	0	0	0
K1088	50	M	F32.1	36	23	8	2	0	0	0	0	0	0	0	0	1

K1129	49	F	F32.2	19	17	8	0	0	0	0	0	1	1	0	2	2
K0881	48	M	F33.2	29	19	0	0	6	0	0	0	3	2	7	0	0
K1115	56	M	F33.2	14	8	0	1	8	0	0	0	0	8	0	1	0
K0184	41	F	F33.2	36	24	8	0	0	0	3	0	0	0	0	8	0
K1084	24	M	F33.2	33	17	0	0	8	0	0	0	0	8	0	3	0
K1089	53	M	F33.2	32	21	0	0	8	0	0	0	2	8	0	0	1
K1054	28	M	F32.2	20	16	0	3	8	0	0	0	0	3	0	0	5
K1080	71	F	F32.2	18	10	0	3	8	0	0	0	0	8	0	0	0
K1087	21	M	F33.2	22	16	1	1	8	0	0	0	1	1	0	3	5
K1107	78	F	F33.2	34	22	8	2	0	0	0	0	1	6	0	0	4
K1104	50	M	F33.2	33	17	0	0	8	0	0	0	0	8	0	6	0
K0912	56	F	F33.2	28	23	8	0	0	0	0	0	0	7	1	7	0
K0455	42	F	F33.2	28	19	0	1	8	2	0	0	0	8	6	0	1
K1119	52	F	F32.2	15	10	8	0	0	0	0	0	8	7	3	0	0
K0792	62	M	F33.3	30	21	8	0	0	0	0	0	0	8	4	7	0
K0744	56	M	F33.2	21	13	6	0	8	0	0	0	2	4	7	0	0
K1057	35	M	F32.2	26	20	0	0	7	0	0	0	0	7	8	5	0
K1110	43	F	F33.2	25	20	6	0	4	0	0	0	0	8	3	6	2
K0740	41	M	F33.3	36	22	0	1	7	0	0	0	8	8	0	7	0
K1083	48	M	F33.2	24	19	0	0	8	0	0	0	0	8	8	7	0
K0135	44	M	F33.1	12	22	8	3	0	0	8	0	0	0	8	0	5
K0805	75	F	F33.2	29	26	7	0	8	0	0	0	4	8	6	1	2
K1090	32	M	F33.2	27	20	3	0	8	0	0	0	4	8	8	5	5
K0882	49	M	F33.3	31	16	6	0	1	0	0	0	4	6	6	6	2
K0138	48	F	F33.2	30	16	0	0	0	6	0	0	0	0	6	0	3
K1075	50	F	F33.2	22	14	6	0	3	0	0	0	3	1	0	0	0
K0054	53	F	F32.2	14	15	0	7	0	0	0	0	0	0	0	0	0
K0124	22	F	F33.2	31	27	0	8	5	0	0	0	0	8	0	7	1
K0398	48	F	F33.2	22	27	0	8	0	8	0	0	0	0	8	4	0
K0719	51	F	F32.2	23	12	7	8	0	0	0	0	0	0	8	5	1
K1049	59	F	F33.2	19	20	0	6	4	0	0	0	0	8	5	2	0
K1072	52	F	F33.2	19	11	0	8	0	3	0	0	0	7	4	7	3
K1085	49	F	F33.2	22	12	0	7	0	0	0	0	4	0	0	4	2
K1143	46	F	F33.2	28	18	0	7	0	3	0	0	0	5	1	6	1

Abbreviations:

TCA tricyclic antidepressants
SSRI selective serotonin reuptake inhibitors
SNRI serotonin norepinephrine reuptake inhibitors
NASSA Noradrenergic and Specific Serotonergic Antidepressant
NARI Noradrenergic reuptake inhibitors
SSRE selective serotonin reuptake enhancer
OTH other antidepressants
AP antipsychotics
MS mood stabilizers
BZD benzodiazepines
SED sedatives
HAMD Hamilton's depression score
ICD10 diagnosis according to International Classification of Diseases version 10

Supplementary table 2. Clinical data overview of included first-line responding (n=24, light shade), and treatment-resistant (n=20, dark shade) STAR*D patients.

	Anxious			Quick inventory depression Symptomatology (QIDS) score						
Cell line	depression	Sex	Age	week 0	week 2	week 4	week 6	week 9	week 12	week 14
14132	No	M	28	16	3	6	2	1	2	
14267	Yes	F	53	16	13	9	1	2	0	
14451	Yes	F	26	12	11	8	6	2	1	
755591	Yes	F	54	21	19	14	2	2	15	1
16718	Yes	F	38	20	12	9	6	4	2	
17563	No	M	53	13	11	13	13	10		6
17827	Yes	M	55	13		8		4	6	
17853	Yes	M	32	20	9	6	9	7	2	
234078	Yes	F	48	17	12	6	3	3		
311634	No	M	70	15	8	5	2			
323701	No	M	28	16	8	9	7	4	4	
330833	No	M	44	15	16	3	3	4	0	
352423	No	F	48	17	8		3	3		1
362372	No	F	42	17	6	10	11		1	
367664	Yes	F	27	19	17	13	6	0	0	
375024	Yes	M	53	15	14	17	9	7	4	
400643	No	F	35	15	12	10	4	3	4	
409700	No	F	65	12	8	5	5	2	1	
411724	Yes	M	69	19	13	6	7	4	5	
443508	Yes	M	42	23	22	12	6	5		2
466830	No	F	68	16	9	7	5	2	1	
510496	Yes	F	60	18	19	9	8	4		
546797	Yes	F	49	18	14	9	11	8	3	
550878	Yes	F	54	23	21	16	7	5	3	
566271	No	F	38	16	13	15	11	13		
572045	Yes	M	57	20	13	15	8	13		
578879	Yes	F	60	22	14	13	14	14		
592780	Yes	M	55	16	13	14	14		16	
613529	Yes	F	52	19	19	19	19	19		
635406	Yes	M	56	21	19	7	14			
301611	No	F	52	14	18	17	12			
14754	No	F	49	23	11	13	13	5	8	
14951	Yes	M	53	19	15	19		10	14	
15100	No	M	38	17	15	14	10		10	
15920	Yes	M	61	22	19	21	18	19	18	
17326	Yes	M	43	21	11	11	8			
18132	No	M	32	15	17	17	17			
232816	Yes	M	63	17	16	14	18	19	21	
521742	Yes	F	42	18		18	6	16	10	
396613	Yes	F	47	21	13	13	16			
402264	Yes	F	24	22	17	19				

407004	Yes	M	56	14	13	15	15			
478406	No	F	55	18	12	15	17			
437434	No	M	42	16	17	15	18			

Supplementary table 3: Genetic entities coding for autosomal genes with differential expression in non-responders vs. responders (|FC|≥2, p-corr. ≤0.05) after 24 and 48 hours.

				24 hr		
Probe Name	**p - corr.**	**FC NR/RESP (CTP)**	**FC NR/RESP (ctrl.)**	**Gene Symbol**	**Gene Name**	**Entrez Gene ID**
A_23_P156826	0.02	-3.23	-2.49	ADTRP	androgen-dependent TFPI-regulating protein	84830
A_33_P3419790	0.03	-2.86	-2.54	ADTRP	androgen-dependent TFPI-regulating protein	84830
A_23_P214627	0.05	-2.13	-2.12	AIF1	allograft inflammatory factor 1	199
A_23_P94501	0.02	-2.80	-2.55	ANXA1	annexin A1	301
A_33_P3323722	0.03	-2.76	-2.95	ARL4C	ADP-ribosylation factor-like 4C	10123
A_23_P412562	0.03	-2.51	-2.58	C1orf162	chromosome 1 open reading frame 162	128346
A_32_P453321	0.02	-2.45	-2.62	C1orf228	chromosome 1 open reading frame 228	339541
A_33_P3249936	0.04	1.94	2.21	C3orf67	chromosome 3 open reading frame 67	200844
A_23_P84736	0.04	-3.09	-3.09	CTNNA2	catenin (cadherin-associated protein), alpha 2	1496
A_23_P411761	0.05	2.06	1.69	CABP1	calcium binding protein 1	9478
A_23_P326893	0.04	2.15	2.10	CCDC151	coiled-coil domain containing 151	115948
A_32_P167471	0.04	-2.46	-2.30	CLMN	calmin (calponin-like, transmembrane)	79789
A_33_P3344477	0.04	-2.42	-1.89	FERMT2	fermitin family member 2	10979
A_33_P3805090	0.04	2.48	2.92	FNIP2	folliculin interacting protein 2	57600
A_24_P393740	0.02	-3.64	-2.90	FYB	FYN binding protein	2533
A_33_P3365142	0.02	2.32	2.36	GAD1	glutamate decarboxylase 1 (brain, 67kDa)	2571
A_33_P3282489	0.04	-3.14	-2.43	GCNT1	glucosaminyl (N-acetyl) transferase 1, core 2	2650
A_23_P254944	0.05	-4.56	-5.23	GSTT1	glutathione S-transferase theta 1	2952
A_23_P128993	0.05	-2.17	-2.62	GZMH	granzyme H (cathepsin G-like 2, protein h-CCPX)	2999
A_33_P3342628	0.04	2.13	2.40	HES4	hes family bHLH transcription factor 4	57801
A_32_P505730	0.03	-2.66	-2.80	HLA-DPB2	major histocompatibility complex, class II, DP beta 2 (pseudogene)	3116
A_23_P162300	0.02	-2.41	-2.30	IRAK3	interleukin-1 receptor-associated kinase 3	11213
A_23_P312132	0.05	-2.38	-2.39	ITGAX	integrin, alpha X (complement component 3 receptor 4 subunit)	3687
A_33_P3267799	0.02	-2.63	-2.30	LILRB4	leukocyte immunoglobulin-like receptor, subfamily B (with TM and ITIM domains), member 4	11006
A_21_P0003637	0.01	2.34	2.45	lnc-ALPK1-1	lnc-ALPK1-1:3	
A_32_P169406	0.02	2.46	2.19	LOC400043	uncharacterized LOC400043	400043
A_32_P89352	0.04	2.83	3.17	MACROD2	MACRO domain containing 2	140733
A_24_P854913	0.02	3.36	3.95	METTL21A	methyltransferase like 21A	151194
A_32_P438767	0.03	2.74	2.88	NEUROG2	neurogenin 2	63973
A_23_P216448	0.02	3.61	3.64	NFIB	nuclear factor I/B	4781
A_24_P658427	0.02	3.55	4.23	NFIB	nuclear factor I/B	4781

A_33_P3241428	0.05	1.86	2.62	OBSL1	obscurin-like 1	23363
A_33_P3240328	0.05	3.81	4.11	PITX1	paired-like homeodomain 1	5307
A_24_P921321	0.03	-3.48	-3.33	PTPRJ	protein tyrosine phosphatase, receptor type, J	5795
A_23_P50946	0.02	-4.77	-4.49	RAMP1	receptor (G protein-coupled) activity modifying protein 1	10267
A_23_P71316	0.05	5.38	4.25	RBPMS	RNA binding protein with multiple splicing	11030
A_23_P94819	0.04	2.07	2.25	RPH3AL	rabphilin 3A-like (without C2 domains)	9501
A_24_P96403	0.02	-2.75	-2.73	RUNX1	runt-related transcription factor 1	861
A_33_P3211804	0.03	-2.32	-2.22	RUNX1	runt-related transcription factor 1	861
A_33_P3303136	0.01	-2.07	-2.48	SERPINB6	serpin peptidase inhibitor, clade B (ovalbumin), member 6	5269
A_23_P210708	0.04	-2.75	-2.64	SIRPA	signal-regulatory protein alpha	140885
A_23_P307382	0.02	-2.54	-2.20	SLC32A1	solute carrier family 32 (GABA vesicular transporter), member 1	140679
A_33_P3283824	0.02	2.02	1.95	SLC39A8	solute carrier family 39 (zinc transporter), member 8	64116
A_23_P41487	0.02	-3.39	-3.50	TBC1D9	TBC1 domain family, member 9 (with GRAM domain)	23158
A_33_P3387696	0.01	-2.64	-2.12	TMBIM4	transmembrane BAX inhibitor motif containing 4	51643
A_33_P3363560	0.04	-2.09	-2.06	TMEM51	transmembrane protein 51	55092
A_33_P3494748	0.01	2.57	2.42	TMEM65	transmembrane protein 65	157378
A_33_P3423585	0.04	-3.31	-3.22	UNC13C	unc-13 homolog C (C, elegans)	440279
A_23_P34345	0.02	-2.98	-3.03	VCAM1	vascular cell adhesion molecule 1	7412
A_33_P3299254	0.04	-2.19	-2.30	VPREB3	pre-B lymphocyte 3	29802
A_33_P3401990	0.04	-2.03	-2.43	VPREB3	pre-B lymphocyte 3	29802
A_23_P29769	0.03	2.06	1.55	WWTR1	WW domain containing transcription regulator 1	25937
A_33_P3257165	0.03	-1.58	-2.34	YPEL1	yippee-like 1 (Drosophila)	29799
A_21_P0007166	0.04	-2.56	-2.17			
A_21_P0003917	0.05	-2.05	-2.10			

48 hr

ProbeName	p - corr.	FC NR/RESP (CTP)	FC NR/RESP (ctrl.)	GeneSymbol	Gene Name	Entrez Gene ID
A_23_P156826	0.04	-2.18	-3.59	ADTRP	androgen-dependent TFPI-regulating protein	84830
A_23_P412562	0.04	-3.73	-2.62	C1orf162	chromosome 1 open reading frame 162	128346
A_32_P453321	0.04	-4.03	-2.37	C1orf228	chromosome 1 open reading frame 228	339541
A_24_P944299	0.05	4.71	3.17	CDC42BPA	CDC42 binding protein kinase alpha (DMPK-like)	8476
A_24_P393740	0.04	-2.95	-4.47	FYB	FYN binding protein	2533
A_33_P3365142	0.04	4.68	3.04	GAD1	glutamate decarboxylase 1 (brain, 67kDa)	2571
A_33_P3282489	0.05	-2.06	-3.83	GCNT1	glucosaminyl (N-acetyl) transferase 1, core 2	2650
A_23_P128993	0.04	-3.92	-2.89	GZMH	granzyme H (cathepsin G-like 2, protein h-CCPX)	2999
A_32_P505730	0.04	-3.52	-3.11	HLA-DPB2	major histocompatibility complex, class II, DP beta 2 (pseudogene)	3116
A_23_P162300	0.04	-3.30	-2.65	IRAK3	interleukin-1 receptor-associated kinase 3	11213
A_23_P84736	0.04	-4.12	-3.91	CTNNA2	catenin (cadherin-associated protein), alpha 2	1496

A_32_P217140	0.05	-3.52	-3.83	ISX	intestine-specific homeobox	91464
A_33_P3267799	0.05	-4.46	-2.57	LILRB4	leukocyte immunoglobulin-like receptor, subfamily B (with TM and ITIM domains), member 4	11006
A_21_P0010261	0.05	-3.55	-1.96	LOC102725378	uncharacterized LOC102725378	102725378
A_24_P658427	0.04	6.46	3.21	NFIB	nuclear factor I/B	4781
A_23_P216448	0.05	4.28	2.95	NFIB	nuclear factor I/B	4781
A_24_P213161	0.05	3.33	3.61	NLRP2	NLR family, pyrin domain containing 2	55655
A_33_P3240328	0.05	4.60	3.97	PITX1	paired-like homeodomain 1	5307
A_23_P50946	0.04	-4.81	-4.45	RAMP1	receptor (G protein-coupled) activity modifying protein 1	10267
A_23_P71316	0.04	12.11	4.12	RBPMS	RNA binding protein with multiple splicing	11030
A_23_P41487	0.04	-2.80	-4.68	TBC1D9	TBC1 domain family, member 9 (with GRAM domain)	23158
A_33_P3423585	0.05	-6.27	-3.49	UNC13C	unc-13 homolog C (C, elegans)	440279
A_23_P34345	0.05	-3.29	-2.17	VCAM1	vascular cell adhesion molecule 1	7412
A_21_P0011045	0.05	-4.01	-2.19	XLOC_l2_002952		
A_21_P0011653	0.05	-5.49	-3.42	XLOC_l2_006399		
A_21_P0006615	0.05	-4.10	-2.68			
A_21_P0007166	0.04	-4.96	-2.42			
A_21_P0003917	0.04	-3.20	-2.56			

Supplementary table 4. Genetic entities that reacted with a deregulation fold-change ≥ 2 (CTP/Ctrl.) after 24 and 48 hr of incubation with CTP in LCLs from responding patients.

			24 hr	
Probe Name	**FC (CTP/Ctrl.)**	**Gene Symbol**	**Gene Name**	**Entrez Gene ID**
A_23_P14986	-2.79	HSD11B2	hydroxysteroid (11-beta) dehydrogenase 2	3291
A_21_P0013150	-2.64	LOC100422737	uncharacterized LOC100422737	100422737
A_21_P0011442	-2.56	XLOC_l2_005245		
A_21_P0005535	-2.51			
A_21_P0009662	-2.39	lnc-ZNF507-4	lnc-ZNF507-4:2	
A_33_P3267463	-2.11	RFX3	regulatory factor X, 3 (influences HLA class II expression)	5991
A_33_P3270926	-2.11			
A_33_P3309656	-2.10			
A_21_P0013893	-2.10			
A_33_P3383975	-2.07			
A_21_P0007020	-2.05	MIR3663HG	MIR3663 host gene (non-protein coding)	101927704
A_33_P3420380	-2.05	ITIH5	inter-alpha-trypsin inhibitor heavy chain family, member 5	80760
A_21_P0009031	-2.04	lnc-TOX3-3	lnc-TOX3-3:1	
A_23_P419786	-2.03	ZNF781	zinc finger protein 781	163115
A_33_P3373009	-2.03			
A_33_P3249046	-2.00	CLDN2	claudin 2	9075
A_21_P0013119	2.01	XLOC_l2_013233		
A_24_P85557	2.01	GPR37	G protein-coupled receptor 37 (endothelin receptor type B-like)	2861

A_24_P353619	2.01	ALPL	alkaline phosphatase, liver/bone/kidney	249
A_23_P215828	2.01	CYP3A43	cytochrome P450, family 3, subfamily A, polypeptide 43	64816
A_33_P3264416	2.01			
A_21_P0011803	2.02	XLOC_l2_007315		
A_23_P151361	2.02	SMIM2	small integral membrane protein 2	79024
A_21_P0000418	2.02	SNORD114-21	small nucleolar RNA, C/D box 114-21	767599
A_23_P353149	2.03	TEX33	testis expressed 33	339669
A_21_P0001984	2.03	lnc-CXXC11-1	lnc-CXXC11-1:1	
A_21_P0003590	2.04	lnc-STIM2-3	lnc-STIM2-3:1	
A_32_P68097	2.04	FAM135B	family with sequence similarity 135, member B	51059
A_21_P0014278	2.04	CLIP1-AS1	CLIP1 antisense RNA 1	100507066
A_23_P326020	2.04	CSMD3	CUB and Sushi multiple domains 3	114788
A_21_P0005398	2.04	lnc-FZD1-1	lnc-FZD1-1:1	
A_33_P3380252	2.04			
A_33_P3235761	2.05	LOC284023	uncharacterized LOC284023	284023
A_33_P3243008	2.05	KCNU1	potassium channel, subfamily U, member 1	157855
A_23_P378427	2.05	STARD6	StAR-related lipid transfer (START) domain containing 6	147323
A_21_P0013718	2.05			
A_33_P3305710	2.05			
A_33_P3365978	2.06	ST7-AS2	ST7 antisense RNA 2	93654
A_21_P0003874	2.06	lnc-ZFP42-2	lnc-ZFP42-2:6	
A_21_P0006773	2.06			
A_21_P0004604	2.06	LOC100507477	uncharacterized LOC100507477	100507477
A_23_P351328	2.06	PRR30	proline rich 30	339779
A_21_P0011737	2.06	XLOC_l2_006996		
A_33_P3377100	2.06	GHRH	growth hormone releasing hormone	2691
A_21_P0008242	2.06	lnc-GPC5-2	lnc-GPC5-2:1	
A_23_P216579	2.07	PALM2	paralemmin 2	114299
A_21_P0008812	2.07	lnc-C15orf2-8	lnc-C15orf2-8:3	
A_21_P0008898	2.07			
A_33_P3256972	2.07	ACTL7B	actin-like 7B	10880
A_21_P0001313	2.07	lnc-NFIA-1	lnc-NFIA-1:1	
A_21_P0001264	2.08	lnc-PRDM2-1	lnc-PRDM2-1:1	
A_21_P0011976	2.08			
A_24_P929565	2.08	LINC01121	long intergenic non-protein coding RNA 1121	400952
A_21_P0005081	2.08	lnc-AL078585,1-3	lnc-AL078585,1-3:1	
A_24_P555066	2.08	SMTNL2	smoothelin-like 2	342527
A_33_P3357853	2.08	SLC25A48	solute carrier family 25, member 48	153328
A_19_P00316544	2.08	LOC102467213	uncharacterized LOC102467213	102467213
A_33_P3227842	2.08	EPB41	erythrocyte membrane protein band 4,1	2035
A_21_P0013634	2.09	GPR116	G protein-coupled receptor 116	221395
A_33_P3497352	2.09	GRIA4	glutamate receptor, ionotropic, AMPA 4	2893
A_33_P3264569	2.09			

A_21_P0004453	2.09	lnc-PRELID2-2	lnc-PRELID2-2:1	
A_21_P0009683	2.09	lnc-ZNF333-3	lnc-ZNF333-3:1	
A_33_P3294645	2.09	DUSP27	dual specificity phosphatase 27 (putative)	92235
A_33_P3274647	2.09	CAMK2A	calcium/calmodulin-dependent protein kinase II alpha	815
A_23_P253484	2.10	AADAT	aminoadipate aminotransferase	51166
A_21_P0011596	2.10	XLOC_l2_006138		
A_21_P0007069	2.10	lnc-KIF20B-4	lnc-KIF20B-4:5	
A_21_P0005039	2.10	lnc-SYNCRIP-1	lnc-SYNCRIP-1:1	
A_33_P3485976	2.10	LOC283177	uncharacterized LOC283177	283177
A_23_P52227	2.11	GDF10	growth differentiation factor 10	2662
A_21_P0006155	2.11	lnc-RORB-2	lnc-RORB-2:3	
A_33_P3279426	2.11	GIGYF2	GRB10 interacting GYF protein 2	26058
A_21_P0002792	2.11			
A_21_P0001526	2.11	LOC101927656	uncharacterized LOC101927656	101927656
A_33_P3355004	2.12	DDC	dopa decarboxylase (aromatic L-amino acid decarboxylase)	1644
A_33_P3376976	2.12	LOC646813	DEAH (Asp-Glu-Ala-His) box helicase 9 pseudogene	646813
A_21_P0001133	2.12	lnc-FAM151A-3	lnc-FAM151A-3:1	
A_23_P301886	2.13	SIM2	single-minded family bHLH transcription factor 2	6493
A_21_P0007751	2.13	lnc-C12orf42-1	lnc-C12orf42-1:1	
A_24_P275199	2.13	KCNC1	potassium channel, voltage gated Shaw related subfamily C, member 1	3746
A_33_P3365441	2.14			
A_24_P355967	2.14	HTR2A	5-hydroxytryptamine (serotonin) receptor 2A, G protein-coupled	3356
A_21_P0012394	2.14	XLOC_l2_009886		
A_33_P3337617	2.14			
A_21_P0014840	2.14	LOC100507630	uncharacterized LOC100507630	100507630
A_33_P3228455	2.14	FXYD3	FXYD domain containing ion transport regulator 3	5349
A_33_P3395206	2.14			
A_33_P3313695	2.14			
A_21_P0006642	2.16			
A_21_P0005624	2.17	LINC01301	long intergenic non-protein coding RNA 1301	100505532
A_21_P0014160	2.17	LOC102725454	uncharacterized LOC102725454	102725454
A_21_P0005743	2.18	lnc-GRHL2-7	lnc-GRHL2-7:3	
A_21_P0004851	2.18	lnc-HDGFL1-2	lnc-HDGFL1-2:1	
A_33_P3764663	2.18	MKRN9P	makorin ring finger protein 9, pseudogene	400058
A_23_P86411	2.19	MYO3A	myosin IIIA	53904
A_21_P0013276	2.19	XLOC_l2_013645		
A_21_P0010427	2.20	lnc-FAM19A5-1	lnc-FAM19A5-1:1	
A_24_P127691	2.20	DNAH14	dynein, axonemal, heavy chain 14	127602
A_21_P0004065	2.20			
A_33_P3277173	2.21	SSPO	SCO-spondin	23145
A_21_P0011987	2.21	XLOC_l2_008409		
A_23_P89334	2.21	MYH13	myosin, heavy chain 13, skeletal muscle	8735

A_21_P0008182	2.22	LINC01069	long intergenic non-protein coding RNA 1069	101927176
A_21_P0011687	2.22	XLOC_l2_006670		
A_23_P154643	2.22	BMP7	bone morphogenetic protein 7	655
A_21_P0002911	2.22	LOC102724604	uncharacterized LOC102724604	102724604
A_21_P0002945	2.23	lnc-TTC21A-2	lnc-TTC21A-2:1	
A_24_P126892	2.24			
A_21_P0012525	2.24	lnc-MUC20-2	lnc-MUC20-2:1	
A_21_P0006621	2.25	CALML3-AS1	CALML3 antisense RNA 1	100132159
A_21_P0011628	2.25	LINC01497	long intergenic non-protein coding RNA 1497	102723487
A_23_P91081	2.25	EPCAM	epithelial cell adhesion molecule	4072
A_21_P0013603	2.25	lnc-METTL11A-2	lnc-METTL11A-2:1	
A_23_P217755	2.25	SHROOM2	shroom family member 2	357
A_21_P0005086	2.26	lnc-T-1	lnc-T-1:1	
A_23_P344578	2.26	FAM154A	family with sequence similarity 154, member A	158297
A_33_P3382229	2.26	TNNT3	troponin T type 3 (skeletal, fast)	7140
A_23_P203773	2.27	CCDC34	coiled-coil domain containing 34	91057
A_23_P402187	2.27	PKHD1	polycystic kidney and hepatic disease 1 (autosomal recessive)	5314
A_21_P0008970	2.27	lnc-AC009120,10,1-2	lnc-AC009120,10,1-2:1	
A_33_P3360412	2.28	PIGQ	phosphatidylinositol glycan anchor biosynthesis, class Q	9091
A_21_P0010839	2.28	XLOC_l2_001683		
A_21_P0007306	2.29	lnc-GLB1L2-1	lnc-GLB1L2-1:8	
A_19_P00317277	2.29	LINC01127	long intergenic non-protein coding RNA 1127	100506328
A_23_P214079	2.30	SPINK1	serine peptidase inhibitor, Kazal type 1	6690
A_19_P00322837	2.31	LINC01470	long intergenic non-protein coding RNA 1470	101927134
A_21_P0011070	2.31	LOC100506691	uncharacterized LOC100506691	100506691
A_21_P0012449	2.31	LINC00971	long intergenic non-protein coding RNA 971	440970
A_21_P0009970	2.31	lnc-DDX27-4	lnc-DDX27-4:1	
A_33_P3418005	2.32	CCDC160	coiled-coil domain containing 160	347475
A_21_P0006843	2.33	lnc-MYO3A-2	lnc-MYO3A-2:1	
A_21_P0008572	2.34	lnc-LOXL1-1	lnc-LOXL1-1:1	
A_21_P0008969	2.34			
A_21_P0013488	2.34	XLOC_l2_014217		
A_21_P0004150	2.34			
A_19_P00317945	2.34			
A_21_P0002955	2.35	lnc-LARS2-1	lnc-LARS2-1:1	
A_24_P283591	2.35	OR1Q1	olfactory receptor, family 1, subfamily Q, member 1	158131
A_21_P0012565	2.35			
A_21_P0012817	2.36	LOC100506272	uncharacterized LOC100506272	100506272
A_33_P3281250	2.38			
A_21_P0006540	2.41	lnc-MAGEE2-1	lnc-MAGEE2-1:1	
A_21_P0006918	2.42	lnc-ADRB1-1	lnc-ADRB1-1:1	

A_33_P3294921	2.42	PRUNE2	prune homolog 2 (Drosophila)	158471
A_33_P3239594	2.42	SLITRK5	SLIT and NTRK-like family, member 5	26050
A_33_P3277913	2.43	MAP2	microtubule-associated protein 2	4133
A_21_P0006563	2.43	ZC3H12B	zinc finger CCCH-type containing 12B	340554
A_23_P163216	2.45	ATP8B4	ATPase, class I, type 8B, member 4	79895
A_21_P0013734	2.45	LOC101927993	uncharacterized LOC101927993	101927993
A_23_P204208	2.46	KLRD1	killer cell lectin-like receptor subfamily D, member 1	3824
A_33_P3331731	2.47			
A_21_P0002098	2.48			
A_33_P3310649	2.48	lnc-KLF7-1	lnc-KLF7-1:3	
A_21_P0007815	2.49	lnc-RAD51AP1-1	lnc-RAD51AP1-1:1	
A_21_P0008183	2.49	lnc-RNF219-1	lnc-RNF219-1:2	
A_21_P0002773	2.50			
A_21_P0009017	2.50	lnc-UMOD-1	lnc-UMOD-1:1	
A_21_P0006716	2.52			
A_23_P36825	2.52	GPRC5A	G protein-coupled receptor, class C, group 5, member A	9052
A_33_P3305731	2.54	NINL	ninein-like	22981
A_21_P0012665	2.59			
A_21_P0009090	2.59	lnc-CA5A-3	lnc-CA5A-3:1	
A_23_P138910	2.59	DDX25	DEAD (Asp-Glu-Ala-Asp) box helicase 25	29118
A_23_P252981	2.61	ACE2	angiotensin I converting enzyme 2	59272
A_21_P0009691	2.63			
A_21_P0001968	2.66			
A_33_P3272260	2.69	SIRPB2	signal-regulatory protein beta 2	284759
A_23_P35293	2.70	GJB5	gap junction protein, beta 5, 31,1kDa	2709
A_33_P3404804	2.72			
A_19_P00322576	2.74			
A_21_P0001906	2.76	FAM138D	family with sequence similarity 138, member D	677784
A_33_P3280237	2.83			
A_21_P0006967	2.86	lnc-C10orf31-7	lnc-C10orf31-7:6	
A_21_P0007102	2.86	lnc-MBL2-2	lnc-MBL2-2:3	
A_23_P154217	2.88	ITGB6	integrin, beta 6	3694
A_24_P381844	2.89	GRIN2A	glutamate receptor, ionotropic, N-methyl D-aspartate 2A	2903
A_33_P3395472	3.05			
A_21_P0013645	3.06			
A_33_P3383044	3.09	B9D1	B9 protein domain 1	27077
A_33_P3239794	3.11			
A_33_P3367731	3.23	SLC24A2	solute carrier family 24 (sodium/potassium/calcium exchanger), member 2	25769
A_21_P0014451	3.59			
A_33_P3283718	3.94	lnc-MYO10-1	lnc-MYO10-1:1	
A_33_P3533325	3.99	ASXL3	additional sex combs like transcriptional regulator 3	80816
48 hr				

Probe Name	FC (CTP/Ctrl.)	Gene Symbol	Gene Name	Entrez Gene ID
A_21_P0013635	-4.83	XLOC_l2_015177		
A_23_P31996	-3.79	SLC46A2	solute carrier family 46, member 2	57864
A_21_P0005310	-3.76			
A_21_P0014901	-3.76			
A_21_P0007065	-3.76	LINC01515	long intergenic non-protein coding RNA 1515	101928913
A_19_P00321096	-3.60			
A_21_P0012215	-3.20			
A_33_P3312774	-3.03			
A_21_P0014555	-3.00	LOC100506446	uncharacterized LOC100506446	100506446
A_33_P3309289	-2.98	ST3GAL4	ST3 beta-galactoside alpha-2,3-sialyltransferase 4	6484
A_21_P0011886	-2.98	LOC728763	rootletin-like	728763
A_33_P3408569	-2.96	lnc-KHDRBS2-1	lnc-KHDRBS2-1:1	
A_21_P0012844	-2.94	LINC00992	long intergenic non-protein coding RNA 992	728342
A_33_P3288574	-2.92	KRTAP10-11	keratin associated protein 10-11	386678
A_33_P3290714	-2.89	HS6ST2	heparan sulfate 6-O-sulfotransferase 2	90161
A_23_P374689	-2.85	GAD1	glutamate decarboxylase 1 (brain, 67kDa)	2571
A_33_P3533325	-2.84	ASXL3	additional sex combs like transcriptional regulator 3	80816
A_33_P3233645	-2.76	MT1G	metallothionein 1G	4495
A_21_P0006113	-2.75	lnc-C9orf104-2	lnc-C9orf104-2:1	
A_21_P0001607	-2.75	lnc-UCHL5-1	lnc-UCHL5-1:1	
A_33_P3352382	-2.74	ARG1	arginase 1	383
A_24_P289299	-2.73	ARHGEF25	Rho guanine nucleotide exchange factor (GEF) 25	115557
A_21_P0006262	-2.73	DNAJB5-AS1	DNAJB5 antisense RNA 1 (head to head)	101926900
A_33_P3242693	-2.72	SLC22A11	solute carrier family 22 (organic anion/urate transporter), member 11	55867
A_24_P221235	-2.71			
A_21_P0004440	-2.69	lnc-C5orf63-1	lnc-C5orf63-1:3	
A_33_P3251841	-2.66	DSEL	dermatan sulfate epimerase-like	92126
A_33_P3229301	-2.65	DKFZp434J0226	uncharacterized LOC93429	93429
A_33_P3352906	-2.62	KCNIP4-IT1	KCNIP4 intronic transcript 1 (non-protein coding)	359822
A_21_P0003178	-2.61	lnc-KY-1	lnc-KY-1:1	
A_23_P372946	-2.60	TM4SF19	transmembrane 4 L six family member 19	116211
A_24_P42039	-2.59			
A_21_P0013853	-2.58	lnc-XIAP-1	lnc-XIAP-1:1	
A_21_P0007434	-2.57			
A_33_P3276630	-2.54	DYNLRB2	dynein, light chain, roadblock-type 2	83657
A_21_P0013025	-2.54	LOC101927020	uncharacterized LOC101927020	101927020
A_24_P555066	-2.53	SMTNL2	smoothelin-like 2	342527
A_21_P0007082	-2.53			
A_21_P0003221	-2.51	lnc-OXNAD1-2	lnc-OXNAD1-2:3	

A_21_P0011222	-2.50	LINC00463	long intergenic non-protein coding RNA 463	101928922
A_33_P3366156	-2.50	SPATA9	spermatogenesis associated 9	83890
A_23_P155487	-2.49	SLC38A3	solute carrier family 38, member 3	10991
A_21_P0003975	-2.45	LOC102723526	uncharacterized LOC102723526	102723526
A_21_P0006184	-2.44	LOC102724478	uncharacterized LOC102724478	102724478
A_23_P80718	-2.43	SYNPR	synaptoporin	132204
A_21_P0014302	-2.39			
A_33_P3307402	-2.39			
A_33_P3313640	-2.38			
A_23_P217755	-2.38	SHROOM2	shroom family member 2	357
A_32_P196021	-2.37	FGF7	fibroblast growth factor 7	2252
A_21_P0006821	-2.37	lnc-PFKFB3-1	lnc-PFKFB3-1:1	
A_33_P3333342	-2.37	FLJ46552	FLJ46552 protein	401230
A_33_P3230841	-2.34	DUPD1	dual specificity phosphatase and pro isomerase domain containing 1	338599
A_23_P124946	-2.33	CMYA5	cardiomyopathy associated 5	202333
A_21_P0008572	-2.32	lnc-LOXL1-1	lnc-LOXL1-1:1	
A_21_P0005595	-2.30	lnc-AC091801,1,1-5	lnc-AC091801,1,1-5:2	
A_33_P3415596	-2.29			
A_33_P3291244	-2.28	CCDC60	coiled-coil domain containing 60	160777
A_33_P3237135	-2.28	MMP2	matrix metallopeptidase 2 (gelatinase A, 72kDa gelatinase, 72kDa type IV collagenase)	4313
A_21_P0012142	-2.28	ZNF663P	zinc finger protein 663, pseudogene	100130934
A_33_P3359864	-2.26			
A_33_P3808435	-2.25			
A_21_P0004547	-2.25	lnc-HNRNPAB-2	lnc-HNRNPAB-2:1	
A_21_P0009254	-2.24	lnc-ABI3-2	lnc-ABI3-2:4	
A_21_P0013698	-2.24			
A_21_P0013368	-2.24	LOC102659288	uncharacterized LOC102659288	102659288
A_21_P0011871	-2.23	LOC100996693	CAVP-target protein-like	100996693
A_21_P0008373	-2.23	lnc-GPR65-2	lnc-GPR65-2:1	
A_33_P3418686	-2.22	HCN4	hyperpolarization activated cyclic nucleotide gated potassium channel 4	10021
A_33_P3349661	-2.21	PCDH9	protocadherin 9	5101
A_21_P0001437	-2.21	lnc-KIAA1383-2	lnc-KIAA1383-2:2	
A_21_P0014359	-2.21			
A_21_P0003752	-2.20	lnc-TSPAN5-1	lnc-TSPAN5-1:1	
A_23_P95930	-2.20	HMGA2	high mobility group AT-hook 2	8091
A_33_P3859897	-2.20	lnc-KBTBD5-2	lnc-KBTBD5-2:2	
A_24_P400324	-2.20	THSD7A	thrombospondin, type I, domain containing 7A	221981
A_33_P3423626	-2.19	LOC151121	uncharacterized LOC151121	151121
A_21_P0005755	-2.19	lnc-UTP23-1	lnc-UTP23-1:2	
A_24_P928052	-2.18	NRP1	neuropilin 1	8829
A_33_P3408320	-2.17	CERS1	ceramide synthase 1	10715
A_33_P3289960	-2.16	LINC00222	long intergenic non-protein coding RNA 222	387111
A_21_P0011832	-2.16	lnc-IL1R2-2	lnc-IL1R2-2:1	

A_21_P0001874	-2.16			
A_33_P3276159	-2.16	LOC100996890	uncharacterized LOC100996890	100996890
A_33_P3421118	-2.15	IL20RA	interleukin 20 receptor, alpha	53832
A_33_P3422025	-2.15	DNAH12	dynein, axonemal, heavy chain 12	201625
A_32_P489	-2.15	LOC100132735	uncharacterized LOC100132735	100132735
A_23_P324813	-2.14	BCL6B	B-cell CLL/lymphoma 6, member B	255877
A_21_P0003682	-2.14	LOC101928551	uncharacterized LOC101928551	101928551
A_23_P386384	-2.13	C1orf87	chromosome 1 open reading frame 87	127795
A_21_P0009975	-2.13	lnc-MOCS3-3	lnc-MOCS3-3:1	
A_21_P0000427	-2.13	SNORD114-30	small nucleolar RNA, C/D box 114-30	767611
A_21_P0008123	-2.12	LINC00403	long intergenic non-protein coding RNA 403	100505996
A_21_P0009770	-2.12	lnc-ZNF296-1	lnc-ZNF296-1:1	
A_21_P0004077	-2.12			
A_33_P3249837	-2.12	LINC00883	long intergenic non-protein coding RNA 883	344595
A_33_P3280955	-2.12	LOC100128079	uncharacterized LOC100128079	100128079
A_21_P0004436	-2.12	lnc-ZNF608-8	lnc-ZNF608-8:2	
A_23_P357351	-2.11	MPV17L	MPV17 mitochondrial membrane protein-like	255027
A_21_P0000862	-2.11	LINC00856	long intergenic non-protein coding RNA 856	100132987
A_33_P3331376	-2.11	EPHB2	EPH receptor B2	2048
A_24_P148836	-2.11	KLHDC8B	kelch domain containing 8B	200942
A_21_P0005265	-2.10			
A_21_P0007364	-2.09	lnc-CFL1-1	lnc-CFL1-1:2	
A_33_P3401726	-2.08	lnc-FMNL2-2	lnc-FMNL2-2:1	
A_21_P0006967	-2.08	lnc-C10orf31-7	lnc-C10orf31-7:6	
A_23_P31858	-2.07	ST18	suppression of tumorigenicity 18, zinc finger	9705
A_21_P0014906	-2.07	ANKRD62	ankyrin repeat domain 62	342850
A_19_P00321158	-2.07	CTD-3080P12,3	uncharacterized LOC101928857	101928857
A_21_P0004173	-2.07	LOC101927280	uncharacterized LOC101927280	101927280
A_32_P381593	-2.06	SLC26A7	solute carrier family 26 (anion exchanger), member 7	115111
A_33_P3514669	-2.06	LOC284632	uncharacterized LOC284632	284632
A_33_P3416634	-2.05	PRSS41	protease, serine, 41	360226
A_33_P3508541	-2.05	LOC400622	uncharacterized LOC400622	400622
A_21_P0003236	-2.05	lnc-ROBO2-4	lnc-ROBO2-4:3	
A_33_P3380076	-2.05			
A_19_P00800316	-2.05	LINC00544	long intergenic non-protein coding RNA 544	440131
A_21_P0006949	-2.04	lnc-PITRM1-3	lnc-PITRM1-3:1	
A_24_P350589	-2.04	RNF150	ring finger protein 150	57484
A_21_P0007158	-2.03	LOC102723894	uncharacterized LOC102723894	102723894
A_33_P3361287	-2.03	lnc-CDYL2-6	lnc-CDYL2-6:5	
A_33_P3321263	-2.03			
A_33_P3360611	-2.03	MPP2	membrane protein, palmitoylated 2 (MAGUK p55 subfamily member 2)	4355
A_32_P458472	-2.02	C1orf95	chromosome 1 open reading frame 95	375057

A_33_P3274701	-2.02			
A_21_P0012247	-2.01	DGCR5	DiGeorge syndrome critical region gene 5 (non-protein coding)	26220
A_19_P00316183	-2.01	LINC00607	long intergenic non-protein coding RNA 607	646324
A_23_P96383	-2.01	SRPX	sushi-repeat containing protein, X-linked	8406
A_21_P0010760	-2.01			
A_21_P0006524	-2.00			
A_21_P0008752	-2.00	lnc-ITGA11-2	lnc-ITGA11-2:2	
A_21_P0011507	-2.00	XLOC_l2_005602		
A_21_P0009344	2.00	lnc-NACA2-2	lnc-NACA2-2:1	
A_23_P12357	2.01	CRB1	crumbs family member 1, photoreceptor morphogenesis associated	23418
A_21_P0007394	2.02	lnc-GUCY1A2-2	lnc-GUCY1A2-2:1	
A_21_P0004639	2.02			
A_21_P0007882	2.03	LOC101928002	uncharacterized LOC101928002	101928002
A_23_P407583	2.03	PEG3	paternally expressed 3	5178
A_21_P0010556	2.07	XLOC_l2_000416		
A_21_P0008843	2.07	lnc-NDN-3	lnc-NDN-3:1	
A_24_P143301	2.08	KAAG1	kidney associated antigen 1	353219
A_33_P3420380	2.11	ITIH5	inter-alpha-trypsin inhibitor heavy chain family, member 5	80760
A_23_P47199	2.12	SLC22A11	solute carrier family 22 (organic anion/urate transporter), member 11	55867
A_21_P0006698	2.13			
A_21_P0001987	2.14	lnc-TMEM18-1	lnc-TMEM18-1:1	
A_21_P0011665	2.14	XLOC_l2_006548		
A_33_P3344339	2.15	KCNH5	potassium channel, voltage gated eag related subfamily H, member 5	27133
A_21_P0011096	2.17	XLOC_l2_003400		
A_21_P0008490	2.24	lnc-RTL1-6	lnc-RTL1-6:1	
A_19_P00809895	2.31	LINC01314	long intergenic non-protein coding RNA 1314	100996492
A_33_P3354836	2.34	OR4P4	olfactory receptor, family 4, subfamily P, member 4	81300
A_23_P35293	2.36	GJB5	gap junction protein, beta 5, 31,1kDa	2709
A_21_P0005345	2.42	lnc-FAM20C-4	lnc-FAM20C-4:3	
A_23_P19778	2.62	SLC13A4	solute carrier family 13 (sodium/sulfate symporter), member 4	26266
A_21_P0008111	2.66	lnc-DAOA-6	lnc-DAOA-6:1	
A_33_P3237854	2.81	LINC00293	long intergenic non-protein coding RNA 293	497634
A_21_P0005687	2.82	lnc-RP11-150O12,5,1-1	lnc-RP11-150O12,5,1-1:1	
A_33_P3339070	3.00	LINC00704	long intergenic non-protein coding RNA 704	100216001

Supplementary table 5 Genetic entities that reacted with a deregulation fold-change ≥ 2 (CTP/Ctrl.) after 24 and 48 hr of incubation with CTP in LCLs from non-responding patients

24 hr

Probe Name	FC (CTP/Ctrl.)	Gene Symbol	Gene Name	Entrez Gene ID
A_21_P0003414	-3.80			
A_21_P0007438	-3.09	lnc-LGALS12-2	lnc-LGALS12-2:2	
A_33_P3813561	-2.79	LOC283728	uncharacterized LOC283728	283728
A_23_P92885	-2.74	SLCO6A1	solute carrier organic anion transporter family, member 6A1	133482
A_21_P0013316	-2.64	XLOC_l2_013868		
A_21_P0001519	-2.60	lnc-ELTD1-2	lnc-ELTD1-2:1	
A_32_P928190	-2.57	LOC100130964	ADAM metallopeptidase domain 3A-like	100130964
A_21_P0001846	-2.49	lnc-EFR3B-3	lnc-EFR3B-3:5	
A_23_P94275	-2.46	DKK4	dickkopf WNT signaling pathway inhibitor 4	27121
A_23_P327605	-2.43	GPR123	G protein-coupled receptor 123	84435
A_23_P348257	-2.40	NUAK1	NUAK family, SNF1-like kinase, 1	9891
A_24_P99066	-2.40	RNF17	ring finger protein 17	56163
A_24_P271830	-2.39	LINC00670	long intergenic non-protein coding RNA 670	284034
A_21_P0008709	-2.39	LOC102725478	uncharacterized LOC102725478	102725478
A_19_P00321206	-2.37			
A_33_P3381832	-2.32	FAM166A	family with sequence similarity 166, member A	401565
A_21_P0000410	-2.31	SNORD114-13	small nucleolar RNA, C/D box 114-13	767591
A_24_P195134	-2.24			
A_24_P353905	-2.23	MXRA8	matrix-remodelling associated 8	54587
A_23_P320021	-2.22	TULP1	tubby like protein 1	7287
A_21_P0002898	-2.22			
A_23_P410469	-2.19	MGC15885	uncharacterized protein MGC15885	197003
A_21_P0010182	-2.19			
A_21_P0002308	-2.18	lnc-GCA-3	lnc-GCA-3:1	
A_33_P3260733	-2.16	GHR	growth hormone receptor	2690
A_23_P200728	-2.16	FCGR3A	Fc fragment of IgG, low affinity IIIa, receptor (CD16a)	2214
A_21_P0002813	-2.15			
A_23_P18913	-2.15	OR2V2	olfactory receptor, family 2, subfamily V, member 2	285659
A_23_P386310	-2.14	HRH4	histamine receptor H4	59340
A_33_P3412838	-2.14	LINC01193	long intergenic non-protein coding RNA 1193	348120
A_33_P3289386	-2.12			
A_23_P25698	-2.11	SLC10A1	solute carrier family 10 (sodium/bile acid cotransporter), member 1	6554
A_33_P3424826	-2.10			
A_21_P0001983	-2.10			
A_21_P0007445	-2.09	lnc-RP11-201M22,1,1-2	lnc-RP11-201M22,1,1-2:1	
A_33_P3215232	-2.09			
A_33_P3352382	-2.09	ARG1	arginase 1	383
A_23_P25176	-2.08	TBX5	T-box 5	6910
A_21_P0010898	-2.08	XLOC_l2_002069		
A_33_P3393010	-2.08	PKDCC	protein kinase domain containing, cytoplasmic	91461

A_24_P326398	-2.06	CRB2	crumbs family member 2	286204
A_32_P225816	-2.05	PRDM16	PR domain containing 16	63976
A_21_P0012817	-2.04	LOC100506272	uncharacterized LOC100506272	100506272
A_21_P0009455	-2.04	LINC01255	long intergenic non-protein coding RNA 1255	101927433
A_24_P82106	-2.03	MMP14	matrix metallopeptidase 14 (membrane-inserted)	4323
A_21_P0007884	-2.03	lnc-E2F7-2	lnc-E2F7-2:1	
A_33_P3853081	-2.02	ALDOAP2	aldolase A, fructose-bisphosphate pseudogene 2	228
A_23_P18362	-2.02	SLITRK3	SLIT and NTRK-like family, member 3	22865
A_21_P0014066	-2.02			
A_23_P131330	-2.01	LRRTM1	leucine rich repeat transmembrane neuronal 1	347730
A_24_P13285	-2.01	PPP1R1A	protein phosphatase 1, regulatory (inhibitor) subunit 1A	5502
A_33_P3302325	-2.01			
A_33_P3414689	2.00			
A_21_P0012801	2.00			
A_33_P3334155	2.01	GS1-24F4,2	uncharacterized LOC100652791	100652791
A_21_P0000626	2.01	LOC100288748	uncharacterized LOC100288748	100288748
A_21_P0007234	2.05	lnc-P2RY2-3	lnc-P2RY2-3:1	
A_21_P0009428	2.05	LOC100505853	uncharacterized LOC100505853	100505853
A_32_P145051	2.06	LOC646652	integral membrane glycoprotein-like	646652
A_21_P0011632	2.09			
A_21_P0013778	2.10	ARMCX4	armadillo repeat containing, X-linked 4	100131755
A_23_P85082	2.11	RHOXF1	Rhox homeobox family, member 1	158800
A_33_P3387985	2.12	LINC00957	long intergenic non-protein coding RNA 957	255031
A_21_P0011837	2.12	LOC102725293	uncharacterized LOC102725293	102725293
A_23_P146849	2.13	APBA2	amyloid beta (A4) precursor protein-binding, family A, member 2	321
A_33_P3261298	2.14	SLC6A7	solute carrier family 6 (neurotransmitter transporter), member 7	6534
A_33_P3362005	2.14	OR9A4	olfactory receptor, family 9, subfamily A, member 4	130075
A_33_P3336014	2.14	OR2T2	olfactory receptor, family 2, subfamily T, member 2	401992
A_33_P3589018	2.15			
A_33_P3405249	2.15			
A_21_P0000436	2.17	SNORD113-9	small nucleolar RNA, C/D box 113-9	767569
A_21_P0008644	2.20	lnc-ZNF609-4	lnc-ZNF609-4:1	
A_33_P3309506	2.20	SEBOX	SEBOX homeobox	645832
A_24_P222872	2.20	UGT1A6	UDP glucuronosyltransferase 1 family, polypeptide A6	54578
A_33_P3311073	2.23	KIR2DS3	killer cell immunoglobulin-like receptor, two domains, short cytoplasmic tail, 3	3808
A_32_P92489	2.23	PKD1L2	polycystic kidney disease 1-like 2 (gene/pseudogene)	114780
A_21_P0004876	2.25	lnc-AL353597,1-2	lnc-AL353597,1-2:1	
A_24_P75220	2.29	MAGI1	membrane associated guanylate kinase, WW and PDZ domain containing 1	9223
A_23_P380901	2.32	PTH2R	parathyroid hormone 2 receptor	5746
A_33_P3355708	2.32	C14orf180	chromosome 14 open reading frame 180	400258

A_21_P0008619	2.33			
A_21_P0002147	2.33	lnc-PER2-1	lnc-PER2-1:1	
A_21_P0013135	2.34			
A_21_P0013631	2.35	XLOC_l2_015170		
A_23_P411772	2.37	PCDHGB2	protocadherin gamma subfamily B, 2	56103
A_21_P0005555	2.44	LOC100506725	uncharacterized LOC100506725	100506725
A_21_P0001257	2.53	lnc-DFFB-4	lnc-DFFB-4:1	
A_21_P0003586	2.61	lnc-TBC1D19-1	lnc-TBC1D19-1:1	
A_21_P0003850	2.61	lnc-AC110373,1-1	lnc-AC110373,1-1:1	
A_21_P0001763	2.62	LOC100506929	uncharacterized LOC100506929	100506929
A_21_P0002425	2.70	lnc-AC013480,1,1-4	lnc-AC013480,1,1-4:1	
A_21_P0002789	2.81			
A_33_P3328883	3.78	HGC6,3	uncharacterized LOC100128124	100128124
A_21_P0009891	5.29	LINC01431	long intergenic non-protein coding RNA 1431	100505683

48 hr

Probe Name	FC (CTP/Ctrl.)	Gene Symbol	Gene Name	Entrez Gene ID
A_21_P0011105	-4.29	LRCOL1	leucine rich colipase-like 1	100507055
A_21_P0014047	-4.25	C4A	complement component 4A (Rodgers blood group)	720
A_24_P626951	-4.02			
A_33_P3226154	-3.87	LOC102724332	uncharacterized LOC102724332	102724332
A_33_P3263319	-3.81			
A_23_P312920	-3.76	POU2AF1	POU class 2 associating factor 1	5450
A_33_P3281444	-3.53			
A_32_P175934	-3.45	CD48	CD48 molecule	962
A_23_P389500	-3.39	REG1B	regenerating islet-derived 1 beta	5968
A_32_P190951	-3.34			
A_23_P74547	-3.32	CD53	CD53 molecule	963
A_21_P0006524	-3.30			
A_19_P00331623	-3.29	XIST	X inactive specific transcript (non-protein coding)	7503
A_33_P3214825	-3.24			
A_21_P0005723	-3.24	lnc-LY96-2	lnc-LY96-2:1	
A_23_P90626	-3.23	CYTIP	cytohesin 1 interacting protein	9595
A_21_P0011346	-3.22	XLOC_l2_004840		
A_33_P3331193	-3.21			
A_23_P13382	-3.20	LSP1	lymphocyte-specific protein 1	4046
A_23_P97141	-3.20	RGS1	regulator of G-protein signaling 1	5996
A_23_P30913	-3.14	HLA-DPA1	major histocompatibility complex, class II, DP alpha 1	3113
A_33_P3281985	-3.13	CR2	complement component (3d/Epstein Barr virus) receptor 2	1380
A_33_P3341686	-3.13	XIST	X inactive specific transcript (non-protein coding)	7503
A_23_P258769	-3.12	HLA-DPB1	major histocompatibility complex, class II, DP beta 1	3115
A_21_P0007918	-3.10			
A_32_P87697	-3.09	HLA-DRA	major histocompatibility complex, class II, DR alpha	3122

A_23_P113572	-3.08	CD19	CD19 molecule	930
A_23_P12082	-3.07	CHI3L2	chitinase 3-like 2	1117
A_33_P3337609	-3.07			
A_33_P3406567	-3.04	MS4A1	membrane-spanning 4-domains, subfamily A, member 1	931
A_33_P3271651	-3.04	HLA-DPB1	major histocompatibility complex, class II, DP beta 1	3115
A_23_P100730	-3.03	SKAP1	src kinase associated phosphoprotein 1	8631
A_33_P3211432	-3.02	NCF1	neutrophil cytosolic factor 1	653361
A_33_P3210798	-3.02	OR56A5	olfactory receptor, family 56, subfamily A, member 5	390084
A_23_P171074	-3.01	ITM2A	integral membrane protein 2A	9452
A_24_P357847	-3.01			
A_21_P0003905	-3.00	LOC102724809	uncharacterized LOC102724809	102724809
A_33_P3293049	-2.98	HLA-DQA1	major histocompatibility complex, class II, DQ alpha 1	3117
A_19_P00323692	-2.98	XIST	X inactive specific transcript (non-protein coding)	7503
A_23_P58132	-2.97	RHOH	ras homolog family member H	399
A_23_P128974	-2.97	BATF	basic leucine zipper transcription factor, ATF-like	10538
A_19_P00329511	-2.97	XIST	X inactive specific transcript (non-protein coding)	7503
A_23_P104464	-2.96	ALOX5	arachidonate 5-lipoxygenase	240
A_33_P3363637	-2.96	BLNK	B-cell linker	29760
A_21_P0002263	-2.94	LINC01102	long intergenic non-protein coding RNA 1102	150568
A_33_P3421351	-2.94	TRAF3IP3	TRAF3 interacting protein 3	80342
A_23_P64661	-2.94	ARHGAP9	Rho GTPase activating protein 9	64333
A_24_P161764	-2.92			
A_33_P3221748	-2.90	RUNX3	runt-related transcription factor 3	864
A_19_P00322705	-2.90	MIAT	myocardial infarction associated transcript (non-protein coding)	440823
A_23_P84596	-2.90	MZB1	marginal zone B and B1 cell-specific protein	51237
A_21_P0003128	-2.89	lnc-FOXP1-1	lnc-FOXP1-1:1	
A_23_P36658	-2.89	MGST1	microsomal glutathione S-transferase 1	4257
A_23_P86283	-2.89	LAPTM5	lysosomal protein transmembrane 5	7805
A_24_P206343	-2.87	MYO1G	myosin IG	64005
A_23_P161190	-2.87	VIM	vimentin	7431
A_23_P37736	-2.87	TNFRSF17	tumor necrosis factor receptor superfamily, member 17	608
A_32_P356316	-2.86	HLA-DOA	major histocompatibility complex, class II, DO alpha	3111
A_23_P25566	-2.86	GPR183	G protein-coupled receptor 183	1880
A_33_P3328559	-2.86	TBC1D10C	TBC1 domain family, member 10C	374403
A_24_P367432	-2.85			
A_23_P98910	-2.84	LRMP	lymphoid-restricted membrane protein	4033
A_23_P401700	-2.82	APBB1IP	amyloid beta (A4) precursor protein-binding, family B, member 1 interacting protein	54518
A_21_P0008803	-2.81	lnc-CHSY1-1	lnc-CHSY1-1:1	
A_33_P3229156	-2.80	SLC17A9	solute carrier family 17 (vesicular nucleotide transporter), member 9	63910
A_23_P208866	-2.80	GMFG	glia maturation factor, gamma	9535

A_33_P3231414	-2.80	LILRB1	leukocyte immunoglobulin-like receptor, subfamily B (with TM and ITIM domains), member 1	10859
A_24_P227927	-2.79	IL21R	interleukin 21 receptor	50615
A_32_P30905	-2.79	WDFY4	WDFY family member 4	57705
A_24_P159434	-2.79	CD300A	CD300a molecule	11314
A_23_P253321	-2.79	PNOC	prepronociceptin	5368
A_23_P86653	-2.77	SRGN	serglycin	5552
A_33_P3343120	-2.76	IRF8	interferon regulatory factor 8	3394
A_24_P82749	-2.76	CD37	CD37 molecule	951
A_23_P131024	-2.74	ZBTB32	zinc finger and BTB domain containing 32	27033
A_33_P3224800	-2.73	NCF1B	neutrophil cytosolic factor 1B pseudogene	654816
A_23_P85800	-2.73	CD52	CD52 molecule	1043
A_21_P0014612	-2.73	LOC100128095		
A_23_P214360	-2.72	IRF4	interferon regulatory factor 4	3662
A_33_P3220911	-2.71	BST2	bone marrow stromal cell antigen 2	684
A_24_P212024	-2.71			
A_23_P31725	-2.70	BLK	BLK proto-oncogene, Src family tyrosine kinase	640
A_33_P3351180	-2.69			
A_33_P3400273	-2.67	SELL	selectin L	6402
A_24_P237443	-2.67	SASH3	SAM and SH3 domain containing 3	54440
A_21_P0012683	-2.67	XLOC_l2_011283		
A_33_P3714341	-2.67			
A_23_P323761	-2.67	TRAF3IP3	TRAF3 interacting protein 3	80342
A_23_P73429	-2.67	HCLS1	hematopoietic cell-specific Lyn substrate 1	3059
A_23_P42746	-2.67	NCF1	neutrophil cytosolic factor 1	653361
A_23_P87879	-2.65	CD69	CD69 molecule	969
A_33_P3364821	-2.65	PTPRC	protein tyrosine phosphatase, receptor type, C	5788
A_23_P70095	-2.64	CD74	CD74 molecule, major histocompatibility complex, class II invariant chain	972
A_33_P3709150	-2.63	T	T, brachyury homolog (mouse)	6862
A_32_P44394	-2.63	AIM2	absent in melanoma 2	9447
A_23_P169017	-2.63	DEFB103B	defensin, beta 103B	55894
A_21_P0003419	-2.63	LOC100996286	uncharacterized LOC100996286	100996286
A_33_P3209651	-2.62	WDFY4	WDFY family member 4	57705
A_33_P3320563	-2.62	GLOD5	glyoxalase domain containing 5	392465
A_23_P39465	-2.61	BST2	bone marrow stromal cell antigen 2	684
A_33_P3294533	-2.61	PRKCB	protein kinase C, beta	5579
A_23_P23639	-2.61	MCOLN2	mucolipin 2	255231
A_33_P3333960	-2.60	LINC00426	long intergenic non-protein coding RNA 426	100188949
A_21_P0001141	-2.60			
A_23_P23279	-2.60	RCSD1	RCSD domain containing 1	92241
A_33_P3336587	-2.59	LOC283710	uncharacterized LOC283710	283710
A_21_P0010633	-2.59	LINC01057	long intergenic non-protein coding RNA 1057	101928079
A_24_P182947	-2.59	GCSAM	germinal center-associated, signaling and motility	257144
A_21_P0006685	-2.59			

A_24_P245838	-2.58	MGAT3	mannosyl (beta-1,4-)-glycoprotein beta-1,4-N-acetylglucosaminyltransferase	4248
A_33_P3655646	-2.58	RARB	retinoic acid receptor, beta	5915
A_23_P76538	-2.57	TESC	tescalcin	54997
A_24_P366509	-2.57	PIK3R6	phosphoinositide-3-kinase, regulatory subunit 6	146850
A_33_P3288409	-2.57	PSMA8	proteasome (prosome, macropain) subunit, alpha type, 8	143471
A_23_P343398	-2.56	CCR7	chemokine (C-C motif) receptor 7	1236
A_23_P133691	-2.56	RRAGD	Ras-related GTP binding D	58528
A_23_P79069	-2.55	RASAL3	RAS protein activator like 3	64926
A_23_P357104	-2.55	ANXA6	annexin A6	309
A_21_P0011776	-2.54	LOC100420587	SHC SH2-domain binding protein 1 pseudogene	100420587
A_23_P300600	-2.54	NEFH	neurofilament, heavy polypeptide	4744
A_23_P159316	-2.54	BFSP2	beaded filament structural protein 2, phakinin	8419
A_23_P410725	-2.53	ZNF491	zinc finger protein 491	126069
A_32_P148122	-2.52			
A_23_P45099	-2.52	HLA-DRB5	major histocompatibility complex, class II, DR beta 5	3127
A_23_P35045	-2.52	ARHGAP30	Rho GTPase activating protein 30	257106
A_23_P500614	-2.52	TNFRSF8	tumor necrosis factor receptor superfamily, member 8	943
A_23_P206806	-2.52	ITGAL	integrin, alpha L (antigen CD11A (p180), lymphocyte function-associated antigen 1; alpha polypeptide)	3683
A_21_P0008097	-2.52	lnc-NDFIP2-12	lnc-NDFIP2-12:1	
A_24_P228130	-2.52	CCL3L3	chemokine (C-C motif) ligand 3-like 3	414062
A_21_P0005747	-2.52			
A_23_P366098	-2.51	NUP210L	nucleoporin 210kDa-like	91181
A_33_P3842556	-2.51	IKZF1	IKAROS family zinc finger 1 (Ikaros)	10320
A_23_P40295	-2.51	LAMP5	lysosomal-associated membrane protein family, member 5	24141
A_33_P3281403	-2.51	TRAF3IP3	TRAF3 interacting protein 3	80342
A_23_P51231	-2.51	RUNX3	runt-related transcription factor 3	864
A_33_P3289246	-2.51			
A_23_P340019	-2.51	NLRC3	NLR family, CARD domain containing 3	197358
A_23_P207564	-2.51	CCL4L2	chemokine (C-C motif) ligand 4-like 2	9560
A_23_P209678	-2.50	PLEK	pleckstrin	5341
A_33_P3277514	-2.50	BTK	Bruton agammaglobulinemia tyrosine kinase	695
A_23_P211561	-2.50	MEI1	meiosis inhibitor 1	150365
A_23_P45871	-2.50	IFI44L	interferon-induced protein 44-like	10964
A_23_P145631	-2.50	GIMAP6	GTPase, IMAP family member 6	474344
A_23_P84705	-2.50	TNFRSF13B	tumor necrosis factor receptor superfamily, member 13B	23495
A_24_P203000	-2.50	IL2RB	interleukin 2 receptor, beta	3560
A_21_P0009398	-2.50	lnc-RAC3-1	lnc-RAC3-1:3	
A_33_P3273884	-2.50	HLA-DQA1	major histocompatibility complex, class II, DQ alpha 1	3117
A_32_P52018	-2.50	PHACTR1	phosphatase and actin regulator 1	221692
A_23_P46039	-2.49	FCRLA	Fc receptor-like A	84824

A_33_P3365621	-2.49	OR2AT4	olfactory receptor, family 2, subfamily AT, member 4	341152
A_33_P3358923	-2.49	BTLA	B and T lymphocyte associated	151888
A_32_P19294	-2.48	GLT1D1	glycosyltransferase 1 domain containing 1	144423
A_23_P126167	-2.48	KCNN3	potassium channel, calcium activated intermediate/small conductance subfamily N alpha, member 3	3782
A_24_P149124	-2.47	NREP	neuronal regeneration related protein	9315
A_33_P3244122	-2.47	HAAO	3-hydroxyanthranilate 3,4-dioxygenase	23498
A_23_P94230	-2.47	LY96	lymphocyte antigen 96	23643
A_23_P207201	-2.47	CD79B	CD79b molecule, immunoglobulin-associated beta	974
A_23_P357717	-2.46	TCL1A	T-cell leukemia/lymphoma 1A	8115
A_23_P140190	-2.46	KIAA0125	KIAA0125	9834
A_23_P385067	-2.46	CLIC6	chloride intracellular channel 6	54102
A_21_P0000859	-2.46	LOC100506207	uncharacterized LOC100506207	100506207
A_33_P3368014	-2.46	HVCN1	hydrogen voltage gated channel 1	84329
A_33_P3212172	-2.46	SNX22	sorting nexin 22	79856
A_19_P00321067	-2.46	MIAT	myocardial infarction associated transcript (non-protein coding)	440823
A_23_P334173	-2.46	LY75	lymphocyte antigen 75	4065
A_33_P3241021	-2.45	CD69	CD69 molecule	969
A_23_P64044	-2.45	FERMT3	fermitin family member 3	83706
A_24_P330263	-2.45	EDNRB	endothelin receptor type B	1910
A_23_P164773	-2.44	FCER2	Fc fragment of IgE, low affinity II, receptor for (CD23)	2208
A_23_P142075	-2.44	ACP5	acid phosphatase 5, tartrate resistant	54
A_23_P201211	-2.44	FCRL5	Fc receptor-like 5	83416
A_23_P36641	-2.44	AICDA	activation-induced cytidine deaminase	57379
A_19_P00319151	-2.44	XIST	X inactive specific transcript (non-protein coding)	7503
A_23_P30547	-2.44	LCP2	lymphocyte cytosolic protein 2 (SH2 domain containing leukocyte protein of 76kDa)	3937
A_23_P107336	-2.44	ACAP1	ArfGAP with coiled-coil, ankyrin repeat and PH domains 1	9744
A_19_P00321068	-2.43	MIAT	myocardial infarction associated transcript (non-protein coding)	440823
A_23_P251881	-2.43	NCR3	natural cytotoxicity triggering receptor 3	259197
A_24_P852756	-2.42	HLA-DQA2	major histocompatibility complex, class II, DQ alpha 2	3118
A_23_P14564	-2.42	GPR65	G protein-coupled receptor 65	8477
A_33_P3241984	-2.42	PTPN22	protein tyrosine phosphatase, non-receptor type 22 (lymphoid)	26191
A_33_P3354607	-2.42	CCL4L2	chemokine (C-C motif) ligand 4-like 2	9560
A_33_P3260733	-2.41	GHR	growth hormone receptor	2690
A_24_P64344	-2.41	BLNK	B-cell linker	29760
A_24_P295010	-2.41	SERPINB9	serpin peptidase inhibitor, clade B (ovalbumin), member 9	5272
A_24_P347378	-2.41	ALOX5AP	arachidonate 5-lipoxygenase-activating protein	241
A_33_P3383970	-2.40	TLR10	toll-like receptor 10	81793
A_23_P43369	-2.40	SIT1	signaling threshold regulating transmembrane adaptor 1	27240

A_24_P95723	-2.40	KIAA0125	KIAA0125	9834
A_24_P237036	-2.39	TNFSF14	tumor necrosis factor (ligand) superfamily, member 14	8740
A_23_P321984	-2.39	CLECL1	C-type lectin-like 1	160365
A_33_P3352827	-2.38	SLAMF1	signaling lymphocytic activation molecule family member 1	6504
A_23_P103932	-2.38	FGR	FGR proto-oncogene, Src family tyrosine kinase	2268
A_33_P3335506	-2.38	FCRL5	Fc receptor-like 5	83416
A_33_P3365432	-2.38	NCF4	neutrophil cytosolic factor 4, 40kDa	4689
A_24_P54390	-2.38	RASGRP3	RAS guanyl releasing protein 3 (calcium and DAG-regulated)	25780
A_23_P203173	-2.38	IL10RA	interleukin 10 receptor, alpha	3587
A_23_P320242	-2.38	KIAA1324L	KIAA1324-like	222223
A_23_P148473	-2.37	IL2RG	interleukin 2 receptor, gamma	3561
A_23_P202071	-2.37	CELF2	CUGBP, Elav-like family member 2	10659
A_24_P408704	-2.37	DOCK2	dedicator of cytokinesis 2	1794
A_23_P30900	-2.36	HLA-DQA2	major histocompatibility complex, class II, DQ alpha 2	3118
A_24_P166443	-2.36	HLA-DPB1	major histocompatibility complex, class II, DP beta 1	3115
A_23_P34233	-2.36	QPRT	quinolinate phosphoribosyltransferase	23475
A_24_P340128	-2.36	P2RY8	purinergic receptor P2Y, G-protein coupled, 8	286530
A_33_P3316273	-2.36	CCL3	chemokine (C-C motif) ligand 3	6348
A_33_P3330911	-2.36	BCAS1	breast carcinoma amplified sequence 1	8537
A_23_P161297	-2.36	OGDHL	oxoglutarate dehydrogenase-like	55753
A_23_P314250	-2.35	FAM78A	family with sequence similarity 78, member A	286336
A_23_P204847	-2.35	LCP1	lymphocyte cytosolic protein 1 (L-plastin)	3936
A_33_P3237674	-2.35			
A_21_P0011343	-2.35	LOC100128108	uncharacterized LOC100128108	100128108
A_23_P209055	-2.35	CD22	CD22 molecule	933
A_32_P84728	-2.35			
A_23_P349406	-2.35	RIMKLA	ribosomal modification protein rimK-like family member A	284716
A_24_P274831	-2.35	GIMAP7	GTPase, IMAP family member 7	168537
A_33_P3262537	-2.35			
A_24_P683861	-2.34			
A_32_P159192	-2.34			
A_33_P3399064	-2.34	RNA5-8S5	RNA, 5,8S ribosomal 5	100008587
A_24_P943894	-2.34	SCUBE3	signal peptide, CUB domain, EGF-like 3	222663
A_21_P0001820	-2.34			
A_33_P3215843	-2.34	KLK3	kallikrein-related peptidase 3	354
A_33_P3369716	-2.34	LOC100507195	uncharacterized LOC100507195	100507195
A_24_P241183	-2.33	CLEC2D	C-type lectin domain family 2, member D	29121
A_33_P3247175	-2.33	C4orf47	chromosome 4 open reading frame 47	441054
A_33_P3271635	-2.32	HLA-DPB1	major histocompatibility complex, class II, DP beta 1	3115
A_19_P00322611	-2.32	lnc-SPAG1-3	lnc-SPAG1-3:3	
A_33_P3424591	-2.32			
A_23_P414654	-2.32	RAB37	RAB37, member RAS oncogene family	326624

A_23_P119478	-2.32	EBI3	Epstein-Barr virus induced 3	10148
A_21_P0008248	-2.32			
A_21_P0009701	-2.32	LOC102724958	uncharacterized LOC102724958	102724958
A_24_P276576	-2.31	FCRLA	Fc receptor-like A	84824
A_21_P0005805	-2.31	lnc-CSGALNACT1-2	lnc-CSGALNACT1-2:1	
A_32_P217750	-2.31	IL3RA	interleukin 3 receptor, alpha (low affinity)	3563
A_23_P84154	-2.31	ARHGAP15	Rho GTPase activating protein 15	55843
A_23_P420692	-2.31	PPFIA4	protein tyrosine phosphatase, receptor type, f polypeptide (PTPRF), interacting protein (liprin), alpha 4	8497
A_21_P0009488	-2.31	lnc-MALT1-1	lnc-MALT1-1:1	
A_21_P0000117	-2.30	MID1	midline 1	4281
A_23_P155057	-2.30	CYTH4	cytohesin 4	27128
A_21_P0001156	-2.30			
A_23_P420863	-2.30	NOD2	nucleotide-binding oligomerization domain containing 2	64127
A_33_P3387766	-2.30	LINC00908	long intergenic non-protein coding RNA 908	284276
A_21_P0006538	-2.30	XIST	X inactive specific transcript (non-protein coding)	7503
A_21_P0014798	-2.29	LOC100128108	uncharacterized LOC100128108	100128108
A_19_P00317878	-2.29	LINC00659	long intergenic non-protein coding RNA 659	100652730
A_19_P00802872	-2.29	XIST	X inactive specific transcript (non-protein coding)	7503
A_23_P201778	-2.29	PTPN7	protein tyrosine phosphatase, non-receptor type 7	5778
A_33_P3291484	-2.29	ST8SIA4	ST8 alpha-N-acetyl-neuraminide alpha-2,8-sialyltransferase 4	7903
A_23_P13907	-2.29	IGF1	insulin-like growth factor 1 (somatomedin C)	3479
A_23_P21057	-2.28	Sep 01	septin 1	1731
A_19_P00315524	-2.28	MIAT	myocardial infarction associated transcript (non-protein coding)	440823
A_21_P0012042	-2.28			
A_33_P3284036	-2.28	CLDN14	claudin 14	23562
A_23_P128201	-2.28	NCKAP1L	NCK-associated protein 1-like	3071
A_33_P3414880	-2.28	LOC339192	uncharacterized LOC339192	339192
A_23_P61057	-2.28	IL16	interleukin 16	3603
A_23_P102000	-2.28	CXCR4	chemokine (C-X-C motif) receptor 4	7852
A_33_P3210399	-2.28	SLC14A1	solute carrier family 14 (urea transporter), member 1 (Kidd blood group)	6563
A_23_P26994	-2.28	GNGT2	guanine nucleotide binding protein (G protein), gamma transducing activity polypeptide 2	2793
A_21_P0001013	-2.28			
A_23_P48088	-2.27	CD27	CD27 molecule	939
A_21_P0011996	-2.27	LOC100506274	uncharacterized LOC100506274	100506274
A_21_P0013955	-2.27	lnc-TMEM18-12	lnc-TMEM18-12:1	
A_33_P3423445	-2.27	ZNF730	zinc finger protein 730	100129543
A_23_P209347	-2.27	ANKRD44	ankyrin repeat domain 44	91526
A_21_P0009306	-2.27	lnc-C17orf51-2	lnc-C17orf51-2:2	
A_33_P3397473	-2.27			

A_33_P3293918	-2.27	SH2D3C	SH2 domain containing 3C	10044
A_21_P0002491	-2.27	lnc-AC108938,5,1-3	lnc-AC108938,5,1-3:1	
A_19_P00809368	-2.26	LINC01215	long intergenic non-protein coding RNA 1215	101929623
A_33_P3718269	-2.26	MIR146A	microRNA 146a	406938
A_23_P420281	-2.26	PRKCB	protein kinase C, beta	5579
A_24_P348845	-2.26	KRTAP15-1	keratin associated protein 15-1	254950
A_23_P153662	-2.26	LGALS14	lectin, galactoside-binding, soluble, 14	56891
A_32_P8813	-2.26	LINC00926	long intergenic non-protein coding RNA 926	283663
A_23_P17065	-2.26	CCL20	chemokine (C-C motif) ligand 20	6364
A_33_P3379268	-2.26	SCIMP	SLP adaptor and CSK interacting membrane protein	388325
A_33_P3234277	-2.25	HLA-DPA1	major histocompatibility complex, class II, DP alpha 1	3113
A_33_P3295056	-2.25	PTPRCAP	protein tyrosine phosphatase, receptor type, C-associated protein	5790
A_24_P169048	-2.25	RFPL3S	RFPL3 antisense	10737
A_23_P170679	-2.25	COL4A3	collagen, type IV, alpha 3 (Goodpasture antigen)	1285
A_19_P00320628	-2.25	LOC101928682	uncharacterized LOC101928682	101928682
A_23_P26771	-2.25	CD300C	CD300c molecule	10871
A_33_P3303697	-2.25	CR2	complement component (3d/Epstein Barr virus) receptor 2	1380
A_23_P160720	-2.25	BATF3	basic leucine zipper transcription factor, ATF-like 3	55509
A_33_P3399150	-2.25	ORAOV1	oral cancer overexpressed 1	220064
A_33_P3317058	-2.24	STAG3	stromal antigen 3	10734
A_33_P3215834	-2.24	SORCS2	sortilin-related VPS10 domain containing receptor 2	57537
A_21_P0013554	-2.24			
A_33_P3492087	-2.24	LOC284191	uncharacterized LOC284191	284191
A_33_P3613605	-2.24			
A_24_P209455	-2.24	GIMAP4	GTPase, IMAP family member 4	55303
A_23_P133904	-2.23	MCCD1	mitochondrial coiled-coil domain 1	401250
A_32_P197561	-2.23	EBF1	early B-cell factor 1	1879
A_33_P3226212	-2.23	JAM2	junctional adhesion molecule 2	58494
A_23_P47704	-2.23	UCP2	uncoupling protein 2 (mitochondrial, proton carrier)	7351
A_23_P137139	-2.23	BTK	Bruton agammaglobulinemia tyrosine kinase	695
A_23_P123596	-2.23	GLDC	glycine dehydrogenase (decarboxylating)	2731
A_21_P0014177	-2.22	LOC101926963	uncharacterized LOC101926963	101926963
A_33_P3408152	-2.22	NEFH	neurofilament, heavy polypeptide	4744
A_33_P3218980	-2.22	ENTPD1	ectonucleoside triphosphate diphosphohydrolase 1	953
A_23_P38959	-2.22	VAV1	vav 1 guanine nucleotide exchange factor	7409
A_21_P0008953	-2.22	lnc-SETD6-6	lnc-SETD6-6:1	
A_21_P0007844	-2.22	LOC100507616	uncharacterized LOC100507616	100507616
A_23_P96599	-2.22	TMSB15B	thymosin beta 15B	286527
A_23_P156683	-2.22	LTA	lymphotoxin alpha	4049
A_24_P766716	-2.22	CMKLR1	chemokine-like receptor 1	1240

A_33_P3734384	-2.21	lnc-MYO1G-1	lnc-MYO1G-1:1	
A_33_P3281273	-2.20	S1PR4	sphingosine-1-phosphate receptor 4	8698
A_33_P3339376	-2.20	WIPF1	WAS/WASL interacting protein family, member 1	7456
A_23_P78092	-2.20	EVI2A	ecotropic viral integration site 2A	2123
A_23_P207911	-2.20	TRPV2	transient receptor potential cation channel, subfamily V, member 2	51393
A_21_P0013296	-2.20	XLOC_l2_013783		
A_33_P3320283	-2.19			
A_23_P140760	-2.19	GPR97	G protein-coupled receptor 97	222487
A_21_P0012893	-2.19	lnc-MYO10-1	lnc-MYO10-1:1	
A_33_P3309621	-2.19	SIGLEC17P	sialic acid binding Ig-like lectin 17, pseudogene	284367
A_24_P370472	-2.19	HLA-DRB4	major histocompatibility complex, class II, DR beta 4	3126
A_33_P3280157	-2.19	SNORD116-19	small nucleolar RNA, C/D box 116-19	727708
A_23_P427023	-2.18	GIMAP1	GTPase, IMAP family member 1	170575
A_33_P3236734	-2.18	CLEC17A	C-type lectin domain family 17, member A	388512
A_33_P3374723	-2.18	ZEB1	zinc finger E-box binding homeobox 1	6935
A_23_P64860	-2.18	SELPLG	selectin P ligand	6404
A_33_P3228612	-2.18	CACNA1E	calcium channel, voltage-dependent, R type, alpha 1E subunit	777
A_33_P3230048	-2.18			
A_21_P0013552	-2.18	XLOC_l2_014697		
A_23_P401076	-2.17	SUSD3	sushi domain containing 3	203328
A_21_P0000361	-2.17	SNORA79	small nucleolar RNA, H/ACA box 79	677845
A_23_P207632	-2.17	ATP2A3	ATPase, Ca++ transporting, ubiquitous	489
A_21_P0000969	-2.17			
A_23_P3014	-2.17	RNASE6	ribonuclease, RNase A family, k6	6039
A_24_P232365	-2.17	APBB1IP	amyloid beta (A4) precursor protein-binding, family B, member 1 interacting protein	54518
A_33_P3464555	-2.17	CAMK1D	calcium/calmodulin-dependent protein kinase ID	57118
A_21_P0008714	-2.17	lnc-GABRB3-2	lnc-GABRB3-2:1	
A_24_P126406	-2.16	DNAH17	dynein, axonemal, heavy chain 17	8632
A_24_P314477	-2.16	TUBB2B	tubulin, beta 2B class IIb	347733
A_24_P314515	-2.16	HNF1A-AS1	HNF1A antisense RNA 1	283460
A_23_P132515	-2.16	SIDT1	SID1 transmembrane family, member 1	54847
A_23_P39386	-2.16	HCST	hematopoietic cell signal transducer	10870
A_19_P00317760	-2.16	lnc-NR5A2-1	lnc-NR5A2-1:2	
A_24_P941359	-2.16	FAM65B	family with sequence similarity 65, member B	9750
A_23_P214627	-2.15	AIF1	allograft inflammatory factor 1	199
A_23_P29005	-2.15	SAMSN1	SAM domain, SH3 domain and nuclear localization signals 1	64092
A_21_P0014037	-2.15			
A_23_P16384	-2.15	NLRP7	NLR family, pyrin domain containing 7	199713
A_21_P0000434	-2.15	SNORD113-6	small nucleolar RNA, C/D box 113-6	767566
A_23_P152002	-2.15	BCL2A1	BCL2-related protein A1	597
A_23_P352266	-2.15	BCL2	B-cell CLL/lymphoma 2	596

A_23_P7503	-2.15	TIMD4	T-cell immunoglobulin and mucin domain containing 4	91937
A_33_P3407049	-2.15			
A_33_P3403102	-2.15	PRR18	proline rich 18	285800
A_33_P3226008	-2.14	GCSAM	germinal center-associated, signaling and motility	257144
A_23_P143713	-2.14	APOBEC3G	apolipoprotein B mRNA editing enzyme, catalytic polypeptide-like 3G	60489
A_33_P3296181	-2.14	CCL3L3	chemokine (C-C motif) ligand 3-like 3	414062
A_23_P160886	-2.14	TAS1R1	taste receptor, type 1, member 1	80835
A_21_P0007470	-2.14	lnc-BLID-1	lnc-BLID-1:17	
A_23_P151166	-2.14	HVCN1	hydrogen voltage gated channel 1	84329
A_33_P3236020	-2.14	TIMD4	T-cell immunoglobulin and mucin domain containing 4	91937
A_21_P0008336	-2.14	lnc-C14orf166-1	lnc-C14orf166-1:1	
A_23_P47102	-2.14	ACY3	aspartoacylase (aminocyclase) 3	91703
A_24_P944253	-2.13	KLHL6	kelch-like family member 6	89857
A_23_P166087	-2.13	RASSF2	Ras association (RalGDS/AF-6) domain family member 2	9770
A_23_P167509	-2.13	CYFIP2	cytoplasmic FMR1 interacting protein 2	26999
A_33_P3231437	-2.13			
A_21_P0001386	-2.13	lnc-PRRC2C-1	lnc-PRRC2C-1:1	
A_23_P250231	-2.13	ANKRD7	ankyrin repeat domain 7	56311
A_33_P3319126	-2.13	CR1L	complement component (3b/4b) receptor 1-like	1379
A_33_P3379039	-2.13	IGLL5	immunoglobulin lambda-like polypeptide 5	100423062
A_23_P330616	-2.13	WIPF1	WAS/WASL interacting protein family, member 1	7456
A_19_P00322183	-2.13	lnc-NR5A2-1	lnc-NR5A2-1:1	
A_23_P167328	-2.12	CD38	CD38 molecule	952
A_33_P3305780	-2.12	CCNI2	cyclin I family, member 2	645121
A_21_P0004516	-2.12	lnc-RASA1-4	lnc-RASA1-4:1	
A_32_P351968	-2.12	HLA-DMB	major histocompatibility complex, class II, DM beta	3109
A_23_P5002	-2.11	MAP4K1	mitogen-activated protein kinase kinase kinase kinase 1	11184
A_33_P3364811	-2.11	PTPRC	protein tyrosine phosphatase, receptor type, C	5788
A_23_P167168	-2.11	IGJ	immunoglobulin J polypeptide, linker protein for immunoglobulin alpha and mu polypeptides	3512
A_21_P0000813	-2.11	APELA	apelin receptor early endogenous ligand	100506013
A_23_P61149	-2.11	INPP5D	inositol polyphosphate-5-phosphatase, 145kDa	3635
A_33_P3684897	-2.11	FLJ30064	uncharacterized LOC644975	644975
A_24_P807031	-2.11	ATP6AP1L	ATPase, H+ transporting, lysosomal accessory protein 1-like	92270
A_32_P57810	-2.11	RNF157	ring finger protein 157	114804
A_33_P3694746	-2.11	SLC2A1-AS1	SLC2A1 antisense RNA 1	440584
A_21_P0003330	-2.11	LOC728175	uncharacterized LOC728175	728175
A_23_P315451	-2.11	KIRREL2	kin of IRRE like 2 (Drosophila)	84063
A_33_P3325285	-2.10	lnc-MIXL1-2	lnc-MIXL1-2:1	

A_23_P34644	-2.10	FCGR2B	Fc fragment of IgG, low affinity IIb, receptor (CD32)	2213
A_23_P48109	-2.10	NINJ2	ninjurin 2	4815
A_23_P346376	-2.10	P2RY10	purinergic receptor P2Y, G-protein coupled, 10	27334
A_21_P0010166	-2.10			
A_33_P3397995	-2.10	IPCEF1	interaction protein for cytohesin exchange factors 1	26034
A_23_P331049	-2.09	DPYSL4	dihydropyrimidinase-like 4	10570
A_33_P3351745	-2.09	PVRIG	poliovirus receptor related immunoglobulin domain containing	79037
A_23_P43476	-2.09	VLDLR	very low density lipoprotein receptor	7436
A_33_P3318841	-2.09	C5orf63	chromosome 5 open reading frame 63	401207
A_33_P3230444	-2.09			
A_32_P140139	-2.09	F13A1	coagulation factor XIII, A1 polypeptide	2162
A_21_P0004127	-2.09			
A_21_P0007372	-2.09	lnc-FCHSD2-3	lnc-FCHSD2-3:1	
A_21_P0009722	-2.09	lnc-ZNF227-1	lnc-ZNF227-1:2	
A_33_P3231357	-2.09	KISS1R	KISS1 receptor	84634
A_24_P118011	-2.09	PRORSD1P	prolyl-tRNA synthetase associated domain containing 1, pseudogene	344405
A_23_P157136	-2.08	SCIN	scinderin	85477
A_33_P3268555	-2.08	SP140	SP140 nuclear body protein	11262
A_21_P0010325	-2.08	lnc-CSTB-1	lnc-CSTB-1:6	
A_24_P289170	-2.08	CCDC88C	coiled-coil domain containing 88C	440193
A_23_P153897	-2.08	GNG7	guanine nucleotide binding protein (G protein), gamma 7	2788
A_32_P171313	-2.08	GNB4	guanine nucleotide binding protein (G protein), beta polypeptide 4	59345
A_32_P144421	-2.08	ZNF518B	zinc finger protein 518B	85460
A_21_P0011911	-2.08	LOC102723854	uncharacterized LOC102723854	102723854
A_21_P0005265	-2.07			
A_33_P3386547	-2.07	SGPP2	sphingosine-1-phosphate phosphatase 2	130367
A_23_P207367	-2.07	STAT5A	signal transducer and activator of transcription 5A	6776
A_21_P0005196	-2.07	LOC101927902	uncharacterized LOC101927902	101927902
A_33_P3221114	-2.07	JAKMIP1	janus kinase and microtubule interacting protein 1	152789
A_33_P3386935	-2.07	KIAA1841	KIAA1841	84542
A_33_P3330079	-2.07	LOC100128242	uncharacterized LOC100128242	100128242
A_23_P306941	-2.07	RGL4	ral guanine nucleotide dissociation stimulator-like 4	266747
A_33_P3226080	-2.07	SCIMP	SLP adaptor and CSK interacting membrane protein	388325
A_23_P42588	-2.07	GIMAP5	GTPase, IMAP family member 5	55340
A_23_P53763	-2.07	KIAA0226L	KIAA0226-like	80183
A_21_P0006498	-2.06	lnc-AL353698,1-1	lnc-AL353698,1-1:1	
A_23_P250413	-2.06	PARVG	parvin, gamma	64098
A_33_P3416712	-2.06	LOC400958	uncharacterized LOC400958	400958
A_23_P17420	-2.06	BCAS1	breast carcinoma amplified sequence 1	8537
A_24_P11506	-2.06	KYNU	kynureninase	8942
A_33_P3224803	-2.06	NCF1	neutrophil cytosolic factor 1	653361

A_33_P3354783	-2.06			
A_33_P3321130	-2.05	DENND3	DENN/MADD domain containing 3	22898
A_21_P0007795	-2.05	lnc-SLC15A4-8	lnc-SLC15A4-8:1	
A_23_P62647	-2.05	SLAMF1	signaling lymphocytic activation molecule family member 1	6504
A_23_P253791	-2.05	CAMP	cathelicidin antimicrobial peptide	820
A_33_P3262635	-2.05	CECR1	cat eye syndrome chromosome region, candidate 1	51816
A_33_P3369393	-2.05	NCF1	neutrophil cytosolic factor 1	653361
A_19_P00801412	-2.05			
A_33_P3307910	-2.05			
A_23_P162386	-2.05	BIN2	bridging integrator 2	51411
A_21_P0009528	-2.05	lnc-PIEZO2-3	lnc-PIEZO2-3:3	
A_32_P101352	-2.05	CXorf65	chromosome X open reading frame 65	158830
A_23_P430728	-2.05	ATP4A	ATPase, H+/K+ exchanging, alpha polypeptide	495
A_21_P0002729	-2.05	LOC101927829	uncharacterized LOC101927829	101927829
A_21_P0012165	-2.04			
A_23_P115645	-2.04	CELF2	CUGBP, Elav-like family member 2	10659
A_32_P19519	-2.04	LOC728175	uncharacterized LOC728175	728175
A_33_P3288275	-2.04			
A_33_P3415247	-2.04	LOC115110	uncharacterized LOC115110	115110
A_21_P0003418	-2.04			
A_23_P376060	-2.04	IKZF3	IKAROS family zinc finger 3 (Aiolos)	22806
A_23_P55828	-2.04	CCL25	chemokine (C-C motif) ligand 25	6370
A_21_P0003029	-2.04	lnc-KBTBD12-1	lnc-KBTBD12-1:1	
A_23_P147025	-2.04	RAB33A	RAB33A, member RAS oncogene family	9363
A_23_P216693	-2.04	MLLT3	myeloid/lymphoid or mixed-lineage leukemia (trithorax homolog, Drosophila); translocated to, 3	4300
A_21_P0008559	-2.03	LOC145837	uncharacterized LOC145837	145837
A_33_P3244117	-2.03	STARD9	StAR-related lipid transfer (START) domain containing 9	57519
A_21_P0009828	-2.03	lnc-C20orf187-2	lnc-C20orf187-2:3	
A_21_P0003915	-2.03	LOC102723766	uncharacterized LOC102723766	102723766
A_23_P46356	-2.03	TNFAIP8L2	tumor necrosis factor, alpha-induced protein 8-like 2	79626
A_33_P3325231	-2.03	XLOC_l2_001961		
A_33_P3292874	-2.03			
A_33_P3354291	-2.03	KIAA1656	KIAA1656 protein	85371
A_33_P3218316	-2.03	VSTM2B	V-set and transmembrane domain containing 2B	342865
A_23_P201181	-2.03	PTPN22	protein tyrosine phosphatase, non-receptor type 22 (lymphoid)	26191
A_33_P3405424	-2.03	IL4I1	interleukin 4 induced 1	259307
A_33_P3363355	-2.03	ICAM4	intercellular adhesion molecule 4 (Landsteiner-Wiener blood group)	3386
A_23_P91764	-2.03	TNFRSF13C	tumor necrosis factor receptor superfamily, member 13C	115650
A_21_P0002320	-2.02	lnc-HNRNPA3-4	lnc-HNRNPA3-4:1	
A_19_P00329048	-2.02	OTUD6B-AS1	OTUD6B antisense RNA 1 (head to head)	100506365

A_33_P3671291	-2.02	SNORA12	small nucleolar RNA, H/ACA box 12	677800
A_23_P14165	-2.02	GPR18	G protein-coupled receptor 18	2841
A_21_P0014399	-2.02	PLCG1-AS1	PLCG1 antisense RNA 1	101927117
A_33_P3402943	-2.02	LOC100128591	uncharacterized LOC100128591	100128591
A_33_P3369741	-2.02	LINC01553	long intergenic non-protein coding RNA 1553	283025
A_24_P162226	-2.02	RIMBP2	RIMS binding protein 2	23504
A_23_P167005	-2.02	GPR160	G protein-coupled receptor 160	26996
A_33_P3283651	-2.02			
A_23_P500741	-2.02	CBFA2T3	core-binding factor, runt domain, alpha subunit 2; translocated to, 3	863
A_19_P00327297	-2.02	lnc-CHIC1-2	lnc-CHIC1-2:1	
A_24_P248240	-2.02	SYT11	synaptotagmin XI	23208
A_23_P348146	-2.01	SLAIN1	SLAIN motif family, member 1	122060
A_24_P683011	-2.01	C8orf88	chromosome 8 open reading frame 88	100127983
A_21_P0012143	-2.01			
A_23_P360804	-2.01	CPNE5	copine V	57699
A_23_P411761	-2.01	CABP1	calcium binding protein 1	9478
A_33_P3336760	-2.01	ABCB4	ATP-binding cassette, sub-family B (MDR/TAP), member 4	5244
A_21_P0013553	-2.01			
A_33_P3257182	-2.01	MYBPC2	myosin binding protein C, fast type	4606
A_33_P3329898	-2.01	STARD9	StAR-related lipid transfer (START) domain containing 9	57519
A_23_P80551	-2.01	KRBOX1	KRAB box domain containing 1	100506243
A_33_P3212799	-2.01	C22orf34	chromosome 22 open reading frame 34	348645
A_21_P0006742	-2.00	lnc-MTPAP-2	lnc-MTPAP-2:1	
A_33_P3268652	-2.00			
A_23_P211909	2.00	PLS1	plastin 1	5357
A_33_P3324680	2.00			
A_32_P223173	2.00	LOC102725053	unconventional myosin-Vb-like	102725053
A_33_P3383326	2.00	LPAR1	lysophosphatidic acid receptor 1	1902
A_23_P214950	2.00	PERP	PERP, TP53 apoptosis effector	64065
A_23_P77493	2.00	TUBB3	tubulin, beta 3 class III	10381
A_24_P251841	2.00	SETD7	SET domain containing (lysine methyltransferase) 7	80854
A_33_P3399380	2.00			
A_24_P782308	2.00	NEDD4L	neural precursor cell expressed, developmentally down-regulated 4-like, E3 ubiquitin protein ligase	23327
A_23_P12363	2.00	ROR1	receptor tyrosine kinase-like orphan receptor 1	4919
A_33_P3338116	2.00	LAMB2	laminin, beta 2 (laminin S)	3913
A_24_P387875	2.00	KCNJ10	potassium channel, inwardly rectifying subfamily J, member 10	3766
A_23_P85703	2.01	SOX13	SRY (sex determining region Y)-box 13	9580
A_33_P3392192	2.01			
A_33_P3251841	2.01	DSEL	dermatan sulfate epimerase-like	92126
A_23_P132041	2.01	CNBD2	cyclic nucleotide binding domain containing 2	140894
A_33_P3479449	2.01	lnc-IL1R2-2	lnc-IL1R2-2:1	

A_33_P3267814	2.01	MICAL3	microtubule associated monooxygenase, calponin and LIM domain containing 3	57553
A_23_P70355	2.01	SERPINB6	serpin peptidase inhibitor, clade B (ovalbumin), member 6	5269
A_33_P3291379	2.01	MSGN1	mesogenin 1	343930
A_33_P3708413	2.01	MFAP5	microfibrillar associated protein 5	8076
A_24_P193093	2.01	KLRK1	killer cell lectin-like receptor subfamily K, member 1	22914
A_33_P3266010	2.01	RIN1	Ras and Rab interactor 1	9610
A_21_P0011145	2.01	XLOC_l2_003737		
A_23_P163235	2.01	CKMT1A	creatine kinase, mitochondrial 1A	548596
A_23_P64611	2.01	P2RY6	pyrimidinergic receptor P2Y, G-protein coupled, 6	5031
A_21_P0011483	2.01	XLOC_l2_005503		
A_32_P99100	2.01	PTPRK	protein tyrosine phosphatase, receptor type, K	5796
A_23_P35617	2.01	PLCE1	phospholipase C, epsilon 1	51196
A_23_P301521	2.01	KIAA1462	KIAA1462	57608
A_23_P352870	2.02	PVRL2	poliovirus receptor-related 2 (herpesvirus entry mediator B)	5819
A_23_P133408	2.02	CSF2	colony stimulating factor 2 (granulocyte-macrophage)	1437
A_33_P3393971	2.02	PKP1	plakophilin 1	5317
A_23_P309619	2.02	KIAA1671	KIAA1671	85379
A_21_P0007484	2.02	LINC00941	long intergenic non-protein coding RNA 941	100287314
A_23_P59738	2.02	MYL7	myosin, light chain 7, regulatory	58498
A_21_P0007535	2.02	lnc-LRMP-4	lnc-LRMP-4:1	
A_33_P3337627	2.02	TRPC6	transient receptor potential cation channel, subfamily C, member 6	7225
A_24_P401601	2.02			
A_24_P148026	2.02	lnc-C1orf86-1	lnc-C1orf86-1:2	
A_33_P3350726	2.02	PPARG	peroxisome proliferator-activated receptor gamma	5468
A_24_P344416	2.02	DSC3	desmocollin 3	1825
A_24_P753476	2.02	GAS2L1P2	growth arrest-specific 2 like 1 pseudogene 2	340508
A_33_P3265376	2.02	HOMER3	homer homolog 3 (Drosophila)	9454
A_23_P30254	2.02	PLK2	polo-like kinase 2	10769
A_33_P3599591	2.02	PAPPA	pregnancy-associated plasma protein A, pappalysin 1	5069
A_23_P119353	2.02	RASIP1	Ras interacting protein 1	54922
A_33_P3369436	2.02	lnc-GOLGA8J-3	lnc-GOLGA8J-3:2	
A_23_P426663	2.02	MITF	microphthalmia-associated transcription factor	4286
A_24_P228149	2.02	KRT13	keratin 13, type I	3860
A_21_P0003395	2.02	lnc-NDST3-3	lnc-NDST3-3:1	
A_21_P0002918	2.02			
A_23_P74799	2.02	SLC25A24	solute carrier family 25 (mitochondrial carrier; phosphate carrier), member 24	29957
A_23_P130027	2.02	EPN3	epsin 3	55040
A_33_P3381318	2.03	FAM160A1	family with sequence similarity 160, member A1	729830
A_33_P3415820	2.03	THBS1	thrombospondin 1	7057

A_32_P89899	2.03	GABRG1	gamma-aminobutyric acid (GABA) A receptor, gamma 1	2565
A_33_P3590673	2.03	SNHG18	small nucleolar RNA host gene 18 (non-protein coding)	100505806
A_23_P318904	2.03	SERTAD4	SERTA domain containing 4	56256
A_23_P117782	2.03	LARP6	La ribonucleoprotein domain family, member 6	55323
A_23_P203540	2.03	EHF	ets homologous factor	26298
A_33_P3258206	2.03	OR6N2	olfactory receptor, family 6, subfamily N, member 2	81442
A_33_P3354106	2.03	KPNA7	karyopherin alpha 7 (importin alpha 8)	402569
A_33_P3237135	2.03	MMP2	matrix metallopeptidase 2 (gelatinase A, 72kDa gelatinase, 72kDa type IV collagenase)	4313
A_32_P46571	2.03	RHBDL2	rhomboid, veinlet-like 2 (Drosophila)	54933
A_23_P312358	2.03	BEND7	BEN domain containing 7	222389
A_33_P3417589	2.03			
A_23_P44436	2.03	GKN1	gastrokine 1	56287
A_19_P00805272	2.03	KIAA1671	KIAA1671	85379
A_33_P3248997	2.03			
A_33_P3256920	2.04	WNT7B	wingless-type MMTV integration site family, member 7B	7477
A_33_P3307836	2.04	LRRC7	leucine rich repeat containing 7	57554
A_33_P3441639	2.04	lnc-ANP32A-3	lnc-ANP32A-3:1	
A_24_P185709	2.04	EPB41L1	erythrocyte membrane protein band 4,1-like 1	2036
A_23_P71316	2.04	RBPMS	RNA binding protein with multiple splicing	11030
A_23_P65506	2.04	SPTB	spectrin, beta, erythrocytic	6710
A_33_P3229815	2.04	LINC00656	long intergenic non-protein coding RNA 656	200261
A_23_P256413	2.04	CMTM7	CKLF-like MARVEL transmembrane domain containing 7	112616
A_23_P214267	2.05	GPR110	G protein-coupled receptor 110	266977
A_23_P27133	2.05	KRT15	keratin 15, type I	3866
A_32_P199884	2.05	HORMAD1	HORMA domain containing 1	84072
A_24_P810290	2.05	PPAPDC1A	phosphatidic acid phosphatase type 2 domain containing 1A	196051
A_23_P143817	2.05	MYLK	myosin light chain kinase	4638
A_33_P3218783	2.05	ANK3	ankyrin 3, node of Ranvier (ankyrin G)	288
A_21_P0010596	2.05	RNF223	ring finger protein 223	401934
A_33_P3359704	2.05	ZNF703	zinc finger protein 703	80139
A_32_P226186	2.05	KIAA1549	KIAA1549	57670
A_33_P3215575	2.06	ARHGEF10L	Rho guanine nucleotide exchange factor (GEF) 10-like	55160
A_23_P422724	2.06	PPIC	peptidylprolyl isomerase C (cyclophilin C)	5480
A_21_P0012961	2.06	LOC255187	uncharacterized LOC255187	255187
A_32_P204205	2.06	SIX4	SIX homeobox 4	51804
A_33_P3238290	2.06	FAM65C	family with sequence similarity 65, member C	140876
A_23_P57268	2.06	CXADR	coxsackie virus and adenovirus receptor	1525
A_23_P24555	2.06	PHLDB1	pleckstrin homology-like domain, family B, member 1	23187
A_32_P63562	2.06	lnc-DNTTIP2-1	lnc-DNTTIP2-1:1	
A_23_P153197	2.06	TGIF1	TGFB-induced factor homeobox 1	7050
A_23_P163682	2.06	RHBDF1	rhomboid 5 homolog 1 (Drosophila)	64285

A_23_P19657	2.06	LRP11	low density lipoprotein receptor-related protein 11	84918
A_33_P3375576	2.06	MAP7	microtubule-associated protein 7	9053
A_33_P3227457	2.06			
A_23_P76364	2.06	CD9	CD9 molecule	928
A_23_P39364	2.06	HOMER3	homer homolog 3 (Drosophila)	9454
A_23_P71379	2.06	PSCA	prostate stem cell antigen	8000
A_32_P305888	2.06	SH3TC2	SH3 domain and tetratricopeptide repeats 2	79628
A_23_P337262	2.07	APCDD1	adenomatosis polyposis coli down-regulated 1	147495
A_24_P355944	2.07	EFNB2	ephrin-B2	1948
A_23_P419714	2.07	BTBD11	BTB (POZ) domain containing 11	121551
A_21_P0004416	2.07	LOC102724530	uncharacterized LOC102724530	102724530
A_24_P129417	2.07	BMP1	bone morphogenetic protein 1	649
A_23_P61778	2.07	NXN	nucleoredoxin	64359
A_21_P0006263	2.07	lnc-RNF38-2	lnc-RNF38-2:1	
A_33_P3420442	2.07	CDK20	cyclin-dependent kinase 20	23552
A_23_P410700	2.07	C16orf46	chromosome 16 open reading frame 46	123775
A_33_P3303900	2.07	OR52B4	olfactory receptor, family 52, subfamily B, member 4 (gene/pseudogene)	143496
A_33_P3307363	2.07	LPHN2	latrophilin 2	23266
A_23_P114689	2.08	ASAP3	ArfGAP with SH3 domain, ankyrin repeat and PH domain 3	55616
A_23_P115091	2.08	RAB25	RAB25, member RAS oncogene family	57111
A_24_P2648	2.08	PTPN14	protein tyrosine phosphatase, non-receptor type 14	5784
A_32_P135336	2.08	LOC388242	coiled-coil domain containing 101 pseudogene	388242
A_23_P23966	2.08	ZNF488	zinc finger protein 488	118738
A_23_P43898	2.08	EPHX4	epoxide hydrolase 4	253152
A_33_P3242508	2.08	ZNF365	zinc finger protein 365	22891
A_33_P3388391	2.08	GJB4	gap junction protein, beta 4, 30,3kDa	127534
A_23_P404494	2.08	IL7R	interleukin 7 receptor	3575
A_23_P48550	2.08	CEP170B	centrosomal protein 170B	283638
A_33_P3374221	2.08	LOC643936	uncharacterized LOC643936	643936
A_33_P3404316	2.08	MIR100HG	mir-100-let-7a-2 cluster host gene (non-protein coding)	399959
A_33_P3265374	2.08	HOMER3	homer homolog 3 (Drosophila)	9454
A_33_P3416127	2.08	ZNF175	zinc finger protein 175	7728
A_32_P196142	2.08	LOC100130938	uncharacterized LOC100130938	100130938
A_23_P97990	2.08	HTRA1	HtrA serine peptidase 1	5654
A_24_P734953	2.08	TRNP1	TMF1-regulated nuclear protein 1	388610
A_23_P214026	2.08	FBN2	fibrillin 2	2201
A_33_P3273552	2.08	KRT83	keratin 83, type II	3889
A_21_P0005032	2.08	lnc-B3GAT2-3	lnc-B3GAT2-3:10	
A_24_P149036	2.09	DPYSL3	dihydropyrimidinase-like 3	1809
A_23_P103099	2.09	RBFOX2	RNA binding protein, fox-1 homolog (C, elegans) 2	23543
A_23_P137097	2.09	SLC16A2	solute carrier family 16, member 2 (thyroid hormone transporter)	6567
A_24_P131522	2.09	ANTXR1	anthrax toxin receptor 1	84168

A_23_P216610	2.09	SUSD1	sushi domain containing 1	64420
A_23_P29394	2.09	ATP13A4	ATPase type 13A4	84239
A_33_P3215113	2.10	LDOC1	leucine zipper, down-regulated in cancer 1	23641
A_23_P161686	2.10	ARHGAP32	Rho GTPase activating protein 32	9743
A_24_P77904	2.10	HOXA10	homeobox A10	3206
A_23_P162142	2.10	TSKU	tsukushi, small leucine rich proteoglycan	25987
A_24_P928217	2.10	FAM134A	family with sequence similarity 134, member A	79137
A_21_P0014114	2.10	GATA2-AS1	GATA2 antisense RNA 1	101927167
A_23_P58082	2.10	CCDC80	coiled-coil domain containing 80	151887
A_24_P406060	2.10	RNF144B	ring finger protein 144B	255488
A_33_P3772937	2.10	KRT8P12	keratin 8 pseudogene 12	90133
A_21_P0000597	2.10	CTSLP8	cathepsin L pseudogene 8	1518
A_23_P40880	2.10	CMTM8	CKLF-like MARVEL transmembrane domain containing 8	152189
A_33_P3467872	2.11	LINC00343	long intergenic non-protein coding RNA 343	144920
A_23_P30666	2.11	TNFRSF21	tumor necrosis factor receptor superfamily, member 21	27242
A_23_P60499	2.11	ZNF462	zinc finger protein 462	58499
A_33_P3410235	2.11	DUOXA1	dual oxidase maturation factor 1	90527
A_23_P15101	2.11	TMC5	transmembrane channel-like 5	79838
A_21_P0006968	2.11	SFTA1P	surfactant associated 1, pseudogene	207107
A_33_P3359047	2.11	LYPD6	LY6/PLAUR domain containing 6	130574
A_33_P3349637	2.11	PCDH1	protocadherin 1	5097
A_21_P0002135	2.11			
A_23_P139704	2.11	DUSP6	dual specificity phosphatase 6	1848
A_23_P171143	2.11	TSPAN6	tetraspanin 6	7105
A_24_P122337	2.11	SYTL4	synaptotagmin-like 4	94121
A_21_P0014829	2.11			
A_33_P3608210	2.11	MIR31HG	MIR31 host gene (non-protein coding)	554202
A_23_P158925	2.12	GPR125	G protein-coupled receptor 125	166647
A_23_P156327	2.12	TGFBI	transforming growth factor, beta-induced, 68kDa	7045
A_33_P3393170	2.12	CAPN5	calpain 5	726
A_21_P0002161	2.12	lnc-SOX11-4	lnc-SOX11-4:1	
A_33_P3306146	2.12	PLAU	plasminogen activator, urokinase	5328
A_33_P3217103	2.12	RBFOX2	RNA binding protein, fox-1 homolog (C, elegans) 2	23543
A_21_P0013256	2.12			
A_21_P0012734	2.12	lnc-MMRN1-2	lnc-MMRN1-2:4	
A_23_P10442	2.12	OSBPL1A	oxysterol binding protein-like 1A	114876
A_23_P92860	2.12	CCNO	cyclin O	10309
A_24_P31929	2.12	PRRG1	proline rich Gla (G-carboxyglutamic acid) 1	5638
A_23_P428887	2.13	KLHL34	kelch-like family member 34	257240
A_33_P3344477	2.13	FERMT2	fermitin family member 2	10979
A_33_P3327642	2.13	AIM1L	absent in melanoma 1-like	55057
A_19_P00321124	2.13	LINC01468	long intergenic non-protein coding RNA 1468	101928687
A_32_P213330	2.13	ARHGEF28	Rho guanine nucleotide exchange factor (GEF) 28	64283

A_24_P68908	2.13	LOC344887	NmrA-like family domain containing 1 pseudogene	344887
A_23_P147245	2.13	OSBPL10	oxysterol binding protein-like 10	114884
A_23_P23296	2.13	PKP1	plakophilin 1	5317
A_23_P395582	2.13	ZFP42	ZFP42 zinc finger protein	132625
A_19_P00319981	2.13	LINC01503	long intergenic non-protein coding RNA 1503	100506119
A_23_P123848	2.13	DAB2IP	DAB2 interacting protein	153090
A_23_P48561	2.13	EFS	embryonal Fyn-associated substrate	10278
A_33_P3238166	2.13	PXDN	peroxidasin	7837
A_33_P3369844	2.13	CD24	CD24 molecule	100133941
A_32_P169179	2.13	MSX2P1	msh homeobox 2 pseudogene 1	55545
A_33_P3397940	2.14	CALML3-AS1	CALML3 antisense RNA 1	100132159
A_33_P3270863	2.14	XDH	xanthine dehydrogenase	7498
A_33_P3824237	2.14	LINC00857	long intergenic non-protein coding RNA 857	439990
A_21_P0013242	2.14	XLOC_l2_013484		
A_33_P3307197	2.14	PTGFRN	prostaglandin F2 receptor inhibitor	5738
A_24_P49260	2.14	SPTLC3	serine palmitoyltransferase, long chain base subunit 3	55304
A_19_P00323413	2.14	PTPN14	protein tyrosine phosphatase, non-receptor type 14	5784
A_23_P37127	2.14	FOXA1	forkhead box A1	3169
A_23_P258410	2.14	WNT7A	wingless-type MMTV integration site family, member 7A	7476
A_24_P219474	2.14	MGAT5B	mannosyl (alpha-1,6-)-glycoprotein beta-1,6-N-acetyl-glucosaminyltransferase, isozyme B	146664
A_33_P3332547	2.14	IQCJ-SCHIP1	IQCJ-SCHIP1 readthrough	100505385
A_21_P0012384	2.15			
A_23_P58328	2.15	ANXA10	annexin A10	11199
A_33_P3322884	2.15			
A_33_P3263212	2.15	LRRC7	leucine rich repeat containing 7	57554
A_21_P0008826	2.15	lnc-UNC13C-2	lnc-UNC13C-2:1	
A_21_P0010245	2.15	lnc-WRB-2	lnc-WRB-2:1	
A_23_P118571	2.15	SOST	sclerostin	50964
A_32_P101031	2.16	LYPD1	LY6/PLAUR domain containing 1	116372
A_23_P410469	2.16	MGC15885	uncharacterized protein MGC15885	197003
A_24_P11575	2.16	CRIM1	cysteine rich transmembrane BMP regulator 1 (chordin-like)	51232
A_23_P38732	2.16	CDH2	cadherin 2, type 1, N-cadherin (neuronal)	1000
A_23_P49338	2.16	TNFRSF12A	tumor necrosis factor receptor superfamily, member 12A	51330
A_23_P167389	2.16	ARAP3	ArfGAP with RhoGAP domain, ankyrin repeat and PH domain 3	64411
A_23_P54291	2.16	DUOX1	dual oxidase 1	53905
A_23_P127565	2.16	LAYN	layilin	143903
A_33_P3274647	2.16	CAMK2A	calcium/calmodulin-dependent protein kinase II alpha	815
A_23_P128323	2.16	SCNN1A	sodium channel, non voltage gated 1 alpha subunit	6337
A_24_P152325	2.16			
A_32_P76627	2.16			
A_23_P24903	2.16	P2RY2	purinergic receptor P2Y, G-protein coupled, 2	5029

A_23_P339818	2.16	ARRDC4	arrestin domain containing 4	91947
A_23_P1331	2.16	COL13A1	collagen, type XIII, alpha 1	1305
A_33_P3230166	2.16	NALCN	sodium leak channel, non selective	259232
A_21_P0010605	2.17			
A_21_P0002685	2.17	lnc-PDE1A-1	lnc-PDE1A-1:3	
A_33_P3351999	2.17			
A_23_P120982	2.17	PKDREJ	polycystin (PKD) family receptor for egg jelly	10343
A_23_P79259	2.17	SH3BP4	SH3-domain binding protein 4	23677
A_23_P24884	2.17	ST5	suppression of tumorigenicity 5	6764
A_21_P0003854	2.17	lnc-FAM160A1-1	lnc-FAM160A1-1:2	
A_23_P92727	2.17	RAI14	retinoic acid induced 14	26064
A_33_P3283646	2.17			
A_23_P330788	2.17	IQSEC2	IQ motif and Sec7 domain 2	23096
A_23_P383819	2.18	TBX3	T-box 3	6926
A_23_P68487	2.18	BMP7	bone morphogenetic protein 7	655
A_23_P2271	2.18	PTHLH	parathyroid hormone-like hormone	5744
A_24_P362540	2.18	ASAP2	ArfGAP with SH3 domain, ankyrin repeat and PH domain 2	8853
A_24_P50801	2.18	NRP2	neuropilin 2	8828
A_24_P282309	2.18	MYOF	myoferlin	26509
A_33_P3446495	2.18	FRMD4B	FERM domain containing 4B	23150
A_23_P208788	2.19	C19orf33	chromosome 19 open reading frame 33	64073
A_23_P348257	2.19	NUAK1	NUAK family, SNF1-like kinase, 1	9891
A_33_P3343503	2.19	SAMD4A	sterile alpha motif domain containing 4A	23034
A_23_P52806	2.19	BACE1	beta-site APP-cleaving enzyme 1	23621
A_23_P45365	2.19	COL4A5	collagen, type IV, alpha 5	1287
A_23_P383986	2.19	CHST15	carbohydrate (N-acetylgalactosamine 4-sulfate 6-O) sulfotransferase 15	51363
A_33_P3291445	2.19	PIGK	phosphatidylinositol glycan anchor biosynthesis, class K	10026
A_23_P108404	2.19	AGAP1	ArfGAP with GTPase domain, ankyrin repeat and PH domain 1	116987
A_23_P46045	2.20	RGS5	regulator of G-protein signaling 5	8490
A_24_P345679	2.20	MLF1	myeloid leukemia factor 1	4291
A_23_P251293	2.20	SNCG	synuclein, gamma (breast cancer-specific protein 1)	6623
A_19_P00803151	2.20	LINC01503	long intergenic non-protein coding RNA 1503	100506119
A_33_P3280521	2.20	MFAP3L	microfibrillar-associated protein 3-like	9848
A_23_P6045	2.20	DEFB126	defensin, beta 126	81623
A_24_P915692	2.20	PHLDA1	pleckstrin homology-like domain, family A, member 1	22822
A_24_P200854	2.20	HOXA2	homeobox A2	3199
A_33_P3237257	2.20	AGBL1-AS1	AGBL1 antisense RNA 1	727915
A_23_P52336	2.20	UNC5B	unc-5 homolog B (C, elegans)	219699
A_33_P3237729	2.21	PDLIM4	PDZ and LIM domain 4	8572
A_24_P286114	2.21	SLC1A3	solute carrier family 1 (glial high affinity glutamate transporter), member 3	6507
A_24_P12626	2.21	CAV1	caveolin 1, caveolae protein, 22kDa	857
A_33_P3397865	2.21	TNNT1	troponin T type 1 (skeletal, slow)	7138

A_23_P436145	2.21	LOC100507431	uncharacterized LOC100507431	100507431
A_24_P348203	2.21	LRRC8E	leucine rich repeat containing 8 family, member E	80131
A_32_P437004	2.21	XG	Xg blood group	7499
A_21_P0009558	2.21	lnc-CCDC68-1	lnc-CCDC68-1:1	
A_33_P3416634	2.21	PRSS41	protease, serine, 41	360226
A_21_P0009960	2.21	lnc-NCOA3-2	lnc-NCOA3-2:1	
A_23_P110957	2.21	FOXF2	forkhead box F2	2295
A_33_P3227375	2.21	THBS2	thrombospondin 2	7058
A_33_P3409090	2.21	CNTN1	contactin 1	1272
A_33_P3252939	2.21	MYLK4	myosin light chain kinase family, member 4	340156
A_33_P3330264	2.21	CXCL1	chemokine (C-X-C motif) ligand 1 (melanoma growth stimulating activity, alpha)	2919
A_23_P161424	2.22	PLXDC2	plexin domain containing 2	84898
A_23_P76249	2.22	KRT6B	keratin 6B, type II	3854
A_33_P3302075	2.22	UGT1A8	UDP glucuronosyltransferase 1 family, polypeptide A8	54576
A_33_P3240747	2.22	LOC100130899	uncharacterized LOC100130899	100130899
A_23_P104798	2.22	IL18	interleukin 18	3606
A_33_P3423979	2.22	PALLD	palladin, cytoskeletal associated protein	23022
A_23_P252306	2.22	ID1	inhibitor of DNA binding 1, dominant negative helix-loop-helix protein	3397
A_23_P106682	2.22	EMP2	epithelial membrane protein 2	2013
A_24_P303480	2.22	RAB32	RAB32, member RAS oncogene family	10981
A_23_P217379	2.22	COL4A6	collagen, type IV, alpha 6	1288
A_23_P215790	2.22	EGFR	epidermal growth factor receptor	1956
A_23_P45011	2.22	PPP1R14C	protein phosphatase 1, regulatory (inhibitor) subunit 14C	81706
A_33_P3275350	2.22	NCS1	neuronal calcium sensor 1	23413
A_24_P331704	2.22	KRT80	keratin 80, type II	144501
A_33_P3255544	2.22	RNF130	ring finger protein 130	55819
A_23_P19030	2.23	ARSI	arylsulfatase family, member I	340075
A_23_P91081	2.23	EPCAM	epithelial cell adhesion molecule	4072
A_33_P3360665	2.23	ACVR1	activin A receptor, type I	90
A_33_P3307840	2.23	LRRC7	leucine rich repeat containing 7	57554
A_23_P34597	2.23	CDA	cytidine deaminase	978
A_23_P121120	2.23	GPR87	G protein-coupled receptor 87	53836
A_23_P147397	2.24	DYNC2H1	dynein, cytoplasmic 2, heavy chain 1	79659
A_23_P106024	2.24	JAG2	jagged 2	3714
A_23_P372308	2.24	RGMA	repulsive guidance molecule family member a	56963
A_23_P10194	2.24	SEZ6L2	seizure related 6 homolog (mouse)-like 2	26470
A_24_P234415	2.24	STAC	SH3 and cysteine rich domain	6769
A_33_P3382177	2.24	TIMP2	TIMP metallopeptidase inhibitor 2	7077
A_33_P3373805	2.24	LOC255187	uncharacterized LOC255187	255187
A_23_P58396	2.24	PDGFC	platelet derived growth factor C	56034
A_33_P3259228	2.24	LOC642943	SPATA31 subfamily A pseudogene	642943
A_33_P3315385	2.24	MPPED2	metallophosphoesterase domain containing 2	744
A_19_P00321671	2.24	lnc-MMRN1-2	lnc-MMRN1-2:2	

A_23_P7250	2.24	CDS1	CDP-diacylglycerol synthase (phosphatidate cytidylyltransferase) 1	1040
A_32_P151544	2.25	KRT18	keratin 18, type I	3875
A_33_P3389286	2.25	SFN	stratifin	2810
A_23_P134454	2.25	CAV1	caveolin 1, caveolae protein, 22kDa	857
A_33_P3336686	2.25	CLIC3	chloride intracellular channel 3	9022
A_24_P379233	2.25	GJB3	gap junction protein, beta 3, 31kDa	2707
A_21_P0013080	2.25	C6orf132	chromosome 6 open reading frame 132	647024
A_21_P0007297	2.25			
A_23_P169039	2.25	SNAI2	snail family zinc finger 2	6591
A_21_P0000058	2.26	PROM2	prominin 2	150696
A_33_P3285545	2.26	CLDN4	claudin 4	1364
A_33_P3303810	2.26	LAD1	ladinin 1	3898
A_23_P501933	2.26	CACNG6	calcium channel, voltage-dependent, gamma subunit 6	59285
A_21_P0005374	2.26	lnc-C7orf10-1	lnc-C7orf10-1:1	
A_33_P3725227	2.26	COBL	cordon-bleu WH2 repeat protein	23242
A_33_P3409159	2.26	SLC22A23	solute carrier family 22, member 23	63027
A_19_P00323737	2.26	PTPN14	protein tyrosine phosphatase, non-receptor type 14	5784
A_23_P397910	2.26	CBLC	Cbl proto-oncogene C, E3 ubiquitin protein ligase	23624
A_23_P13083	2.27	BARX2	BARX homeobox 2	8538
A_23_P7866	2.27	GPR115	G protein-coupled receptor 115	221393
A_23_P148990	2.27	HMCN1	hemicentin 1	83872
A_32_P167239	2.27	AFAP1L1	actin filament associated protein 1-like 1	134265
A_21_P0008868	2.27	lnc-RP11-82I10,1,1-4	lnc-RP11-82I10,1,1-4:3	
A_23_P748	2.27	IRF6	interferon regulatory factor 6	3664
A_24_P220485	2.27	OLFML2A	olfactomedin-like 2A	169611
A_23_P156445	2.27	DDX43	DEAD (Asp-Glu-Ala-Asp) box polypeptide 43	55510
A_33_P3228460	2.27	FXYD3	FXYD domain containing ion transport regulator 3	5349
A_32_P129752	2.27	TMEM30B	transmembrane protein 30B	161291
A_23_P337934	2.27	FBLIM1	filamin binding LIM protein 1	54751
A_24_P404033	2.28	ARPIN	actin-related protein 2/3 complex inhibitor	348110
A_23_P201636	2.28	LAMC2	laminin, gamma 2	3918
A_24_P206624	2.28	FGFR2	fibroblast growth factor receptor 2	2263
A_33_P3765708	2.28	LINC00692	long intergenic non-protein coding RNA 692	285326
A_24_P96403	2.28	RUNX1	runt-related transcription factor 1	861
A_24_P892472	2.28	EMX2OS	EMX2 opposite strand/antisense RNA	196047
A_23_P360797	2.28	NTF3	neurotrophin 3	4908
A_33_P3240787	2.28	LOC100131910	uncharacterized LOC100131910	100131910
A_33_P3399318	2.28	GNG12	guanine nucleotide binding protein (G protein), gamma 12	55970
A_21_P0012988	2.29			
A_33_P3339070	2.29	LINC00704	long intergenic non-protein coding RNA 704	100216001
A_23_P328323	2.29	RAVER2	ribonucleoprotein, PTB-binding 2	55225
A_19_P00322339	2.29	LINC00707	long intergenic non-protein coding RNA 707	100507127

A_23_P208293	2.29	PVRL2	poliovirus receptor-related 2 (herpesvirus entry mediator B)	5819
A_33_P3364348	2.29	JPH1	junctophilin 1	56704
A_23_P13094	2.29	MMP10	matrix metallopeptidase 10 (stromelysin 2)	4319
A_24_P408736	2.29	GALNT5	polypeptide N-acetylgalactosaminyltransferase 5	11227
A_23_P135257	2.29	PRSS3	protease, serine, 3	5646
A_23_P161439	2.29	ADIRF	adipogenesis regulatory factor	10974
A_33_P3364433	2.30	ACVR1B	activin A receptor, type IB	91
A_24_P649282	2.30	LUZP2	leucine zipper protein 2	338645
A_33_P3334877	2.30	KRTAP10-4	keratin associated protein 10-4	386672
A_32_P174572	2.30	HTR7P1	5-hydroxytryptamine (serotonin) receptor 7 pseudogene 1	93164
A_23_P36825	2.30	GPRC5A	G protein-coupled receptor, class C, group 5, member A	9052
A_23_P139912	2.30	IGFBP6	insulin-like growth factor binding protein 6	3489
A_23_P209978	2.30	VSNL1	visinin-like 1	7447
A_33_P3246418	2.30	MDFI	MyoD family inhibitor	4188
A_24_P925040	2.30	CAV2	caveolin 2	858
A_23_P124619	2.30	S100A14	S100 calcium binding protein A14	57402
A_32_P117354	2.31	LIMCH1	LIM and calponin homology domains 1	22998
A_23_P139143	2.31	STX3	syntaxin 3	6809
A_24_P238250	2.31	LGALS7	lectin, galactoside-binding, soluble, 7	3963
A_32_P14457	2.31	LOC101927418	uncharacterized LOC101927418	101927418
A_23_P256473	2.31	SEMA3C	sema domain, immunoglobulin domain (Ig), short basic domain, secreted, (semaphorin) 3C	10512
A_23_P41114	2.31	CSTA	cystatin A (stefin A)	1475
A_23_P211110	2.31	SIM2	single-minded family bHLH transcription factor 2	6493
A_23_P160559	2.31	ECM1	extracellular matrix protein 1	1893
A_23_P3038	2.31	GPX2	glutathione peroxidase 2 (gastrointestinal)	2877
A_33_P3225948	2.31	AJAP1	adherens junctions associated protein 1	55966
A_33_P3278362	2.31	ANKRD2	ankyrin repeat domain 2 (stretch responsive muscle)	26287
A_33_P3219527	2.31	RTKN2	rhotekin 2	219790
A_23_P13740	2.32	NAV3	neuron navigator 3	89795
A_19_P00802448	2.32	lnc-ANKRA2-3	lnc-ANKRA2-3:1	
A_24_P192301	2.32	SEMA3A	sema domain, immunoglobulin domain (Ig), short basic domain, secreted, (semaphorin) 3A	10371
A_24_P43810	2.32	FAM83A	family with sequence similarity 83, member A	84985
A_23_P159937	2.32	SLC6A8	solute carrier family 6 (neurotransmitter transporter), member 8	6535
A_33_P3215948	2.32	MPZL2	myelin protein zero-like 2	10205
A_33_P3365978	2.32	ST7-AS2	ST7 antisense RNA 2	93654
A_21_P0011578	2.32			
A_23_P53390	2.32	PTPRB	protein tyrosine phosphatase, receptor type, B	5787
A_23_P49155	2.33	CDH3	cadherin 3, type 1, P-cadherin (placental)	1001
A_23_P375372	2.33	FGA	fibrinogen alpha chain	2243
A_23_P154358	2.33	PROM2	prominin 2	150696

A_23_P92909	2.33	SPINK6	serine peptidase inhibitor, Kazal type 6	404203
A_23_P212469	2.33	ENTPD3	ectonucleoside triphosphate diphosphohydrolase 3	956
A_24_P35228	2.33	GRHL2	grainyhead-like 2 (Drosophila)	79977
A_33_P3243887	2.33	IL11	interleukin 11	3589
A_33_P3260430	2.33	SPRR2A	small proline-rich protein 2A	6700
A_21_P0006762	2.33	LINC01468	long intergenic non-protein coding RNA 1468	101928687
A_33_P3379076	2.33	LOC101929056	uncharacterized LOC101929056	101929056
A_33_P3216763	2.34	EYA1	EYA transcriptional coactivator and phosphatase 1	2138
A_23_P211007	2.34	NRIP1	nuclear receptor interacting protein 1	8204
A_23_P306987	2.34	SOX7	SRY (sex determining region Y)-box 7	83595
A_21_P0001527	2.34	lnc-GNG5-1	lnc-GNG5-1:1	
A_23_P307544	2.34	PLXNA2	plexin A2	5362
A_21_P0009781	2.34	UCA1	urothelial cancer associated 1 (non-protein coding)	652995
A_33_P3391796	2.34	NOG	noggin	9241
A_23_P63432	2.34	RHBDL2	rhomboid, veinlet-like 2 (Drosophila)	54933
A_21_P0011904	2.35	XLOC_l2_007884		
A_23_P142239	2.35	YIF1B	Yip1 interacting factor homolog B (S, cerevisiae)	90522
A_33_P3418209	2.35	ITGBL1	integrin, beta-like 1 (with EGF-like repeat domains)	9358
A_19_P00318539	2.35	lnc-BTBD10-3	lnc-BTBD10-3:9	
A_23_P122052	2.35	GPX8	glutathione peroxidase 8 (putative)	493869
A_23_P89431	2.36	CCL2	chemokine (C-C motif) ligand 2	6347
A_23_P167096	2.36	VEGFC	vascular endothelial growth factor C	7424
A_23_P96158	2.36	KRT17	keratin 17, type I	3872
A_23_P45059	2.36	DOCK1	dedicator of cytokinesis 1	1793
A_23_P332399	2.37	GULP1	GULP, engulfment adaptor PTB domain containing 1	51454
A_24_P319923	2.37	MYLK	myosin light chain kinase	4638
A_23_P201386	2.37	DDAH1	dimethylarginine dimethylaminohydrolase 1	23576
A_23_P112798	2.37	CRIP2	cysteine-rich protein 2	1397
A_24_P389608	2.37	PROSER2	proline and serine rich 2	254427
A_23_P501538	2.37	HOXA3	homeobox A3	3200
A_21_P0003359	2.37			
A_23_P26386	2.37	TPPP3	tubulin polymerization-promoting protein family member 3	51673
A_23_P94501	2.38	ANXA1	annexin A1	301
A_23_P215913	2.38	CLU	clusterin	1191
A_23_P304450	2.38	GATA6	GATA binding protein 6	2627
A_23_P250156	2.38	IGF2BP2	insulin-like growth factor 2 mRNA binding protein 2	10644
A_24_P256380	2.38	WLS	wntless Wnt ligand secretion mediator	79971
A_33_P3229953	2.39	EEF1A2	eukaryotic translation elongation factor 1 alpha 2	1917
A_32_P5276	2.39	ARHGEF26	Rho guanine nucleotide exchange factor (GEF) 26	26084
A_23_P73239	2.39	NCKAP1	NCK-associated protein 1	10787
A_23_P387184	2.39	NHSL1	NHS-like 1	57224

A_24_P158946	2.39	FGD4	FYVE, RhoGEF and PH domain containing 4	121512
A_23_P71530	2.39	TNFRSF11B	tumor necrosis factor receptor superfamily, member 11b	4982
A_24_P411749	2.39	GPR126	G protein-coupled receptor 126	57211
A_33_P3221203	2.40	MMP13	matrix metallopeptidase 13 (collagenase 3)	4322
A_23_P71328	2.40	MATN2	matrilin 2	4147
A_24_P156113	2.40	EHD2	EH-domain containing 2	30846
A_24_P928969	2.40	PTPN3	protein tyrosine phosphatase, non-receptor type 3	5774
A_33_P3308534	2.40	OSBPL1A	oxysterol binding protein-like 1A	114876
A_21_P0006656	2.40	LOC102724039	uncharacterized LOC102724039	102724039
A_33_P3293858	2.41	MTUS2	microtubule associated tumor suppressor candidate 2	23281
A_21_P0006730	2.41			
A_23_P204630	2.41	NTN4	netrin 4	59277
A_24_P348806	2.41	PLEKHA7	pleckstrin homology domain containing, family A member 7	144100
A_23_P111995	2.41	LOXL2	lysyl oxidase-like 2	4017
A_23_P259127	2.41	ESRP1	epithelial splicing regulatory protein 1	54845
A_24_P364236	2.41	NDUFC2	NADH dehydrogenase (ubiquinone) 1, subcomplex unknown, 2, 14,5kDa	4718
A_24_P67395	2.42	KRT8	keratin 8, type II	3856
A_23_P349566	2.42	CCDC85A	coiled-coil domain containing 85A	114800
A_32_P142440	2.42	PCSK9	proprotein convertase subtilisin/kexin type 9	255738
A_33_P3352019	2.42	SCARA3	scavenger receptor class A, member 3	51435
A_33_P3336257	2.42	IRX1	iroquois homeobox 1	79192
A_23_P252062	2.42	PPARG	peroxisome proliferator-activated receptor gamma	5468
A_32_P62863	2.42	SCHIP1	schwannomin interacting protein 1	29970
A_23_P376449	2.42			
A_33_P3332252	2.43	TUBAL3	tubulin, alpha-like 3	79861
A_23_P207213	2.44	ALDH3A1	aldehyde dehydrogenase 3 family, member A1	218
A_32_P47643	2.44	FAM110C	family with sequence similarity 110, member C	642273
A_23_P501007	2.44	EFEMP1	EGF containing fibulin-like extracellular matrix protein 1	2202
A_23_P53557	2.44	LTBR	lymphotoxin beta receptor (TNFR superfamily, member 3)	4055
A_23_P45304	2.44	XK	X-linked Kx blood group	7504
A_23_P393051	2.45	KDF1	keratinocyte differentiation factor 1	126695
A_23_P1602	2.45	CDC42EP2	CDC42 effector protein (Rho GTPase binding) 2	10435
A_23_P502747	2.45	RASAL2	RAS protein activator like 2	9462
A_24_P413126	2.46	PMEPA1	prostate transmembrane protein, androgen induced 1	56937
A_23_P166686	2.46	AMOTL2	angiomotin like 2	51421
A_19_P00315452	2.46	LOC100130938	uncharacterized LOC100130938	100130938
A_23_P33364	2.46	SH3D19	SH3 domain containing 19	152503
A_33_P3413821	2.47	KIRREL	kin of IRRE like (Drosophila)	55243
A_23_P353035	2.47	IGFBP7	insulin-like growth factor binding protein 7	3490

A_32_P200238	2.47	UCA1	urothelial cancer associated 1 (non-protein coding)	652995
A_23_P1682	2.47	TMEM45B	transmembrane protein 45B	120224
A_23_P74012	2.47	SPRR1A	small proline-rich protein 1A	6698
A_32_P35969	2.47	CHRNA7	cholinergic receptor, nicotinic, alpha 7 (neuronal)	1139
A_33_P3361067	2.47	ABCG2	ATP-binding cassette, sub-family G (WHITE), member 2 (Junior blood group)	9429
A_23_P143348	2.47	OVOL2	ovo-like zinc finger 2	58495
A_21_P0010854	2.47	AKR1C8P	aldo-keto reductase family 1, member C8, pseudogene	340811
A_21_P0002261	2.47	lnc-IL1R2-1	lnc-IL1R2-1:2	
A_23_P160968	2.48	LAMC2	laminin, gamma 2	3918
A_33_P3348782	2.48	CYP2S1	cytochrome P450, family 2, subfamily S, polypeptide 1	29785
A_23_P7144	2.48	CXCL1	chemokine (C-X-C motif) ligand 1 (melanoma growth stimulating activity, alpha)	2919
A_33_P3384462	2.48	THSD4	thrombospondin, type I, domain containing 4	79875
A_23_P135381	2.48	SP5	Sp5 transcription factor	389058
A_21_P0010477	2.49	lnc-SYN3-1	lnc-SYN3-1:1	
A_32_P85999	2.49	CDH13	cadherin 13	1012
A_21_P0005592	2.50			
A_23_P218068	2.50	PLEKHA5	pleckstrin homology domain containing, family A member 5	54477
A_23_P94030	2.50	LAMB1	laminin, beta 1	3912
A_24_P354689	2.50	SPOCK1	sparc/osteonectin, cwcv and kazal-like domains proteoglycan (testican) 1	6695
A_23_P393034	2.50	HAS3	hyaluronan synthase 3	3038
A_23_P18493	2.50	PTPN13	protein tyrosine phosphatase, non-receptor type 13 (APO-1/CD95 (Fas)-associated phosphatase)	5783
A_23_P113777	2.50	ITGBL1	integrin, beta-like 1 (with EGF-like repeat domains)	9358
A_23_P320553	2.51	PPFIA3	protein tyrosine phosphatase, receptor type, f polypeptide (PTPRF), interacting protein (liprin), alpha 3	8541
A_33_P3376249	2.51	S100A2	S100 calcium binding protein A2	6273
A_24_P55295	2.52	GJA1	gap junction protein, alpha 1, 43kDa	2697
A_33_P3392921	2.52	CTTN	cortactin	2017
A_24_P230057	2.52			
A_33_P3399778	2.52			
A_33_P3290562	2.52	GLI3	GLI family zinc finger 3	2737
A_23_P380614	2.52	ATP9A	ATPase, class II, type 9A	10079
A_21_P0012061	2.52			
A_32_P170925	2.52	TXNRD3	thioredoxin reductase 3	114112
A_23_P122924	2.53	INHBA	inhibin, beta A	3624
A_33_P3219651	2.53	BMPER	BMP binding endothelial regulator	168667
A_23_P251043	2.53	SYNDIG1	synapse differentiation inducing 1	79953
A_23_P39955	2.53	ACTG2	actin, gamma 2, smooth muscle, enteric	72
A_32_P204381	2.53	CIAPIN1	cytokine induced apoptosis inhibitor 1	57019
A_33_P3386723	2.54			
A_19_P00321941	2.54	LINC00704	long intergenic non-protein coding RNA 704	100216001

A_23_P104762	2.54	YAP1	Yes-associated protein 1	10413
A_23_P157865	2.54	TNC	tenascin C	3371
A_23_P211631	2.54	FBLN1	fibulin 1	2192
A_24_P256063	2.54			
A_23_P53081	2.54	OSBPL5	oxysterol binding protein-like 5	114879
A_23_P118158	2.55	HS3ST2	heparan sulfate (glucosamine) 3-O-sulfotransferase 2	9956
A_33_P3407424	2.56	CDC42EP1	CDC42 effector protein (Rho GTPase binding) 1	11135
A_24_P133253	2.56	KITLG	KIT ligand	4254
A_24_P921366	2.56	CALD1	caldesmon 1	800
A_23_P78980	2.56	B3GNT3	UDP-GlcNAc:betaGal beta-1,3-N-acetylglucosaminyltransferase 3	10331
A_33_P3284345	2.56	NRG1	neuregulin 1	3084
A_21_P0006451	2.56			
A_33_P3232945	2.57	F2RL1	coagulation factor II (thrombin) receptor-like 1	2150
A_33_P3238215	2.57	COBLL1	cordon-bleu WH2 repeat protein-like 1	22837
A_23_P18372	2.57	B3GNT5	UDP-GlcNAc:betaGal beta-1,3-N-acetylglucosaminyltransferase 5	84002
A_23_P14083	2.57	AMIGO2	adhesion molecule with Ig-like domain 2	347902
A_23_P389897	2.58	NGFR	nerve growth factor receptor	4804
A_23_P55477	2.58	ADORA2B	adenosine A2b receptor	136
A_23_P121716	2.59	ANXA3	annexin A3	306
A_32_P4199	2.59	RNF152	ring finger protein 152	220441
A_23_P39056	2.59	KLK7	kallikrein-related peptidase 7	5650
A_23_P141345	2.59	MPP3	membrane protein, palmitoylated 3 (MAGUK p55 subfamily member 3)	4356
A_23_P213102	2.59	PALLD	palladin, cytoskeletal associated protein	23022
A_23_P259071	2.60	AREG	amphiregulin	374
A_33_P3221980	2.60			
A_23_P392384	2.60	AIF1L	allograft inflammatory factor 1-like	83543
A_23_P106906	2.61	PPL	periplakin	5493
A_32_P387648	2.61	FLG	filaggrin	2312
A_23_P131935	2.61	FERMT1	fermitin family member 1	55612
A_33_P3228450	2.61	FXYD3	FXYD domain containing ion transport regulator 3	5349
A_23_P217319	2.61	FGF13	fibroblast growth factor 13	2258
A_24_P114249	2.61	GALNT3	polypeptide N-acetylgalactosaminyltransferase 3	2591
A_33_P3264662	2.61	CYP27C1	cytochrome P450, family 27, subfamily C, polypeptide 1	339761
A_24_P48204	2.62	SECTM1	secreted and transmembrane 1	6398
A_33_P3316539	2.62	SLC7A2	solute carrier family 7 (cationic amino acid transporter, y+ system), member 2	6542
A_33_P3214159	2.63	CDH2	cadherin 2, type 1, N-cadherin (neuronal)	1000
A_21_P0004922	2.63	lnc-RFPL4B-2	lnc-RFPL4B-2:1	
A_33_P3405474	2.63	lnc-CNTLN-2	lnc-CNTLN-2:1	
A_23_P146849	2.63	APBA2	amyloid beta (A4) precursor protein-binding, family A, member 2	321
A_23_P76488	2.63	EMP1	epithelial membrane protein 1	2012
A_24_P124370	2.64	PARVA	parvin, alpha	55742

A_33_P3350758	2.64	RASAL2	RAS protein activator like 2	9462
A_23_P1691	2.65	MMP1	matrix metallopeptidase 1 (interstitial collagenase)	4312
A_23_P92161	2.65	ARL14	ADP-ribosylation factor-like 14	80117
A_21_P0000073	2.65	OSMR	oncostatin M receptor	9180
A_24_P358131	2.66			
A_24_P13041	2.66	RTKN2	rhotekin 2	219790
A_33_P3348747	2.66	DSG3	desmoglein 3	1830
A_33_P3246833	2.67	IL1RN	interleukin 1 receptor antagonist	3557
A_33_P3280721	2.67	WLS	wntless Wnt ligand secretion mediator	79971
A_23_P315815	2.68	NRG1	neuregulin 1	3084
A_23_P22134	2.68	BNC1	basonuclin 1	646
A_24_P125469	2.68	LIPG	lipase, endothelial	9388
A_33_P3351175	2.69	WNK2	WNK lysine deficient protein kinase 2	65268
A_24_P65616	2.69	PVR	poliovirus receptor	5817
A_24_P251534	2.69	CTDSPL	CTD (carboxy-terminal domain, RNA polymerase II, polypeptide A) small phosphatase-like	10217
A_21_P0009868	2.69	lnc-C20orf197-2	lnc-C20orf197-2:1	
A_24_P15621	2.69	SLC6A10P	solute carrier family 6 (neurotransmitter transporter), member 10, pseudogene	386757
A_19_P00322184	2.69	LINC01503	long intergenic non-protein coding RNA 1503	100506119
A_23_P142849	2.70	RND3	Rho family GTPase 3	390
A_33_P3297562	2.71	IRX2	iroquois homeobox 2	153572
A_33_P3419190	2.71	AREG	amphiregulin	374
A_23_P66481	2.71	RTN4RL1	reticulon 4 receptor-like 1	146760
A_33_P3287785	2.71	NEFL	neurofilament, light polypeptide	4747
A_24_P937405	2.71	PRSS23	protease, serine, 23	11098
A_24_P7750	2.71			
A_24_P938614	2.72	CDS1	CDP-diacylglycerol synthase (phosphatidate cytidylyltransferase) 1	1040
A_23_P152235	2.72	IRX3	iroquois homeobox 3	79191
A_21_P0006534	2.72	lnc-FOXP3-1	lnc-FOXP3-1:1	
A_32_P218355	2.72	C6orf132	chromosome 6 open reading frame 132	647024
A_33_P3338121	2.73	LAMB3	laminin, beta 3	3914
A_23_P141802	2.73	SERPINB7	serpin peptidase inhibitor, clade B (ovalbumin), member 7	8710
A_23_P11800	2.74	CAMK2N1	calcium/calmodulin-dependent protein kinase II inhibitor 1	55450
A_24_P261417	2.75	DKK3	dickkopf WNT signaling pathway inhibitor 3	27122
A_23_P25150	2.76	HOXC9	homeobox C9	3225
A_23_P211039	2.76	ADAMTS1	ADAM metallopeptidase with thrombospondin type 1 motif, 1	9510
A_33_P3351554	2.77	ETNK2	ethanolamine kinase 2	55224
A_32_P215938	2.77	GPSM1	G-protein signaling modulator 1	26086
A_23_P373708	2.77	KRT18P55	keratin 18 pseudogene 55	284085
A_23_P123071	2.77	CAV2	caveolin 2	858
A_23_P163467	2.78	C15orf52	chromosome 15 open reading frame 52	388115
A_23_P431388	2.78	SPOCD1	SPOC domain containing 1	90853
A_23_P354387	2.78	MYOF	myoferlin	26509

A_23_P501010	2.78	COL17A1	collagen, type XVII, alpha 1	1308
A_23_P369899	2.79	TMEM158	transmembrane protein 158 (gene/pseudogene)	25907
A_19_P00315502	2.79	LOC102723721	uncharacterized LOC102723721	102723721
A_23_P164284	2.79	CLDN7	claudin 7	1366
A_33_P3613516	2.79	GATA2-AS1	GATA2 antisense RNA 1	101927167
A_24_P887857	2.80			
A_23_P503010	2.80	SLC24A4	solute carrier family 24 (sodium/potassium/calcium exchanger), member 4	123041
A_33_P3718274	2.80	LOC285629	uncharacterized LOC285629	285629
A_33_P3231447	2.80	ITGA6	integrin, alpha 6	3655
A_23_P500998	2.81	HOXA9	homeobox A9	3205
A_32_P231617	2.81	TM4SF1	transmembrane 4 L six family member 1	4071
A_23_P146946	2.82	CST6	cystatin E/M	1474
A_23_P151506	2.82	PLEK2	pleckstrin 2	26499
A_23_P304682	2.83	EMP2	epithelial membrane protein 2	2013
A_33_P3214665	2.84	MAP2	microtubule-associated protein 2	4133
A_23_P95930	2.84	HMGA2	high mobility group AT-hook 2	8091
A_32_P29118	2.85	SEMA3D	sema domain, immunoglobulin domain (Ig), short basic domain, secreted, (semaphorin) 3D	223117
A_23_P153480	2.85	KLK5	kallikrein-related peptidase 5	25818
A_23_P20743	2.86	TMEM246	transmembrane protein 246	84302
A_23_P215634	2.86	IGFBP3	insulin-like growth factor binding protein 3	3486
A_23_P70968	2.87	HOXA7	homeobox A7	3204
A_23_P57784	2.87	CLDN1	claudin 1	9076
A_23_P91390	2.88	THBD	thrombomodulin	7056
A_24_P403417	2.89	PTGES	prostaglandin E synthase	9536
A_33_P3402565	2.90	DSP	desmoplakin	1832
A_33_P3211014	2.90			
A_24_P882732	2.90			
A_23_P46429	2.91	CYR61	cysteine-rich, angiogenic inducer, 61	3491
A_23_P258612	2.91	ATP8A2	ATPase, aminophospholipid transporter, class I, type 8A, member 2	51761
A_33_P3405728	2.91	PKP2	plakophilin 2	5318
A_23_P94754	2.95	TNFSF15	tumor necrosis factor (ligand) superfamily, member 15	9966
A_24_P193435	2.95	TJP1	tight junction protein 1	7082
A_24_P95154	2.96	TUSC3	tumor suppressor candidate 3	7991
A_23_P110837	2.96	IRX4	iroquois homeobox 4	50805
A_21_P0003003	2.97	LOC152225	uncharacterized LOC152225	152225
A_23_P207507	2.97	ABCC3	ATP-binding cassette, sub-family C (CFTR/MRP), member 3	8714
A_33_P3846653	2.97	KRT19P2	keratin 19 pseudogene 2	160313
A_19_P00316914	2.98			
A_23_P159974	2.98	KLHL13	kelch-like family member 13	90293
A_33_P3401658	2.99	PSG2	pregnancy specific beta-1-glycoprotein 2	5670
A_32_P105549	3.00	ANXA8L1	annexin A8-like 1	728113

A_32_P164246	3.00	FOXQ1	forkhead box Q1	94234
A_24_P247454	3.04			
A_23_P33093	3.05	ST6GALNAC5	ST6 (alpha-N-acetyl-neuraminyl-2,3-beta-galactosyl-1,3)-N-acetylgalactosaminide alpha-2,6-sialyltransferase 5	81849
A_33_P3347193	3.06	VSTM2A	V-set and transmembrane domain containing 2A	222008
A_23_P107612	3.06	RAB27B	RAB27B, member RAS oncogene family	5874
A_21_P0003070	3.07	lnc-EIF2B5-2	lnc-EIF2B5-2:1	
A_23_P253484	3.08	AADAT	aminoadipate aminotransferase	51166
A_23_P203267	3.09	TRIM29	tripartite motif containing 29	23650
A_24_P169843	3.10			
A_23_P163087	3.11	NID2	nidogen 2 (osteonidogen)	22795
A_23_P369343	3.11	KLK8	kallikrein-related peptidase 8	11202
A_23_P51397	3.11	ENAH	enabled homolog (Drosophila)	55740
A_33_P3229107	3.12	MIR205HG	MIR205 host gene (non-protein coding)	642587
A_23_P64372	3.15	TCN1	transcobalamin I (vitamin B12 binding protein, R binder family)	6947
A_23_P83579	3.16	ARNT2	aryl-hydrocarbon receptor nuclear translocator 2	9915
A_23_P390068	3.17	MISP	mitotic spindle positioning	126353
A_21_P0012556	3.19			
A_23_P49499	3.20	ST6GALNAC2	ST6 (alpha-N-acetyl-neuraminyl-2,3-beta-galactosyl-1,3)-N-acetylgalactosaminide alpha-2,6-sialyltransferase 2	10610
A_23_P257003	3.20	PCSK5	proprotein convertase subtilisin/kexin type 5	5125
A_33_P3317628	3.20	PKP3	plakophilin 3	11187
A_32_P62963	3.21	KRT16P2	keratin 16 pseudogene 2	400578
A_24_P245379	3.22	SERPINB2	serpin peptidase inhibitor, clade B (ovalbumin), member 2	5055
A_21_P0011517	3.24	KRT14	keratin 14, type I	3861
A_23_P359245	3.24	MET	MET proto-oncogene, receptor tyrosine kinase	4233
A_23_P500381	3.25	HTR7	5-hydroxytryptamine (serotonin) receptor 7, adenylate cyclase-coupled	3363
A_23_P2041	3.26	MICALCL	MICAL C-terminal like	84953
A_24_P305570	3.28	RIN2	Ras and Rab interactor 2	54453
A_23_P30126	3.28	FGFBP1	fibroblast growth factor binding protein 1	9982
A_33_P3888629	3.29	MECOM	MDS1 and EVI1 complex locus	2122
A_23_P366936	3.30	KRT6C	keratin 6C, type II	286887
A_23_P205959	3.31	ALDH1A3	aldehyde dehydrogenase 1 family, member A3	220
A_33_P3329088	3.33	PRSS8	protease, serine, 8	5652
A_23_P897	3.34	C1orf116	chromosome 1 open reading frame 116	79098
A_23_P156025	3.34	IRX2	iroquois homeobox 2	153572
A_23_P24129	3.34	DKK1	dickkopf WNT signaling pathway inhibitor 1	22943
A_21_P0000176	3.36	CDH13	cadherin 13	1012
A_24_P42136	3.38	KRT18	keratin 18, type I	3875
A_23_P399078	3.38	TIMP3	TIMP metallopeptidase inhibitor 3	7078
A_23_P218047	3.39	KRT5	keratin 5, type II	3852
A_23_P214168	3.40	COL12A1	collagen, type XII, alpha 1	1303

A_33_P3226832	3.40	F3	coagulation factor III (thromboplastin, tissue factor)	2152
A_33_P3390013	3.40	ADAMTS1	ADAM metallopeptidase with thrombospondin type 1 motif, 1	9510
A_33_P3338733	3.41	MITF	microphthalmia-associated transcription factor	4286
A_24_P222872	3.47	UGT1A6	UDP glucuronosyltransferase 1 family, polypeptide A6	54578
A_23_P210176	3.51	ITGA6	integrin, alpha 6	3655
A_33_P3286349	3.53	DNAAF3	dynein, axonemal, assembly factor 3	352909
A_23_P164011	3.55	SOX15	SRY (sex determining region Y)-box 15	6665
A_33_P3857239	3.55	KRT42P	keratin 42 pseudogene	284116
A_33_P3292886	3.57	KRT6A	keratin 6A, type II	3853
A_23_P147918	3.58	S100A16	S100 calcium binding protein A16	140576
A_23_P141894	3.58	PVR	poliovirus receptor	5817
A_21_P0008964	3.59	lnc-CDH3-1	lnc-CDH3-1:1	
A_23_P149529	3.60	TACSTD2	tumor-associated calcium signal transducer 2	4070
A_23_P21092	3.62	CALB2	calbindin 2	794
A_21_P0008191	3.62	lnc-SLITRK6-6	lnc-SLITRK6-6:1	
A_23_P89780	3.64	LAMA3	laminin, alpha 3	3909
A_23_P60130	3.66	MAL2	mal, T-cell differentiation protein 2 (gene/pseudogene)	114569
A_23_P69537	3.73	NMU	neuromedin U	10874
A_23_P66798	3.75	KRT19	keratin 19, type I	3880
A_33_P3281745	3.78	lnc-C10orf71-1	lnc-C10orf71-1:1	
A_24_P541831	3.80	LINC00264	long intergenic non-protein coding RNA 264	645528
A_23_P35293	3.80	GJB5	gap junction protein, beta 5, 31,1kDa	2709
A_32_P157945	3.83	DSP	desmoplakin	1832
A_21_P0007862	3.83	lnc-TMEM132B-4	lnc-TMEM132B-4:9	
A_24_P3415	3.84	PPP2R2C	protein phosphatase 2, regulatory subunit B, gamma	5522
A_33_P3390057	3.89	TM4SF1	transmembrane 4 L six family member 1	4071
A_33_P3345534	3.89	KRT14	keratin 14, type I	3861
A_33_P3310104	3.90	SERPINB5	serpin peptidase inhibitor, clade B (ovalbumin), member 5	5268
A_21_P0003000	4.03	lnc-OR5AC2-1	lnc-OR5AC2-1:1	
A_21_P0011633	4.10	KRT14	keratin 14, type I	3861
A_23_P110531	4.22	FST	follistatin	10468
A_21_P0006957	4.92	lnc-AKR1C2-3	lnc-AKR1C2-3:1	
A_24_P87036	5.45	ANO1	anoctamin 1, calcium activated chloride channel	55107

Supplementary table 6. Enriched CTP-altered pathways in responders and non-responders

Altered pathways in NR after 24 hr CTP incubation	p-value	Matched Entities	Pathway Entities
Hs_FTO_Obesity_Variant_Mechanism_WP3407_89858	1.44E-02	1	8
Hs_EDA_Signalling_in_Hair_Follicle_Development_WP3930_90751	2.32E-02	1	13
Hs_Estrogen_metabolism_WP697_94757	2.32E-02	1	18
Hs_NRF2_pathway_WP2884_94787	2.33E-02	2	143
Hs_Integrin_cell_surface_interactions_WP1833_44861	2.50E-02	1	16

Hs_Prolactin_receptor_signaling_WP2678_76870	2.50E-02	1	15
Hs_Activation_of_Matrix_Metalloproteinases_WP2769_77041	2.85E-02	1	16
Hs_Syndecan_interactions_WP2787_77077	2.85E-02	1	16
Hs_Drug_Induction_of_Bile_Acid_Pathway_WP2289_88593	3.03E-02	1	17
Hs_Glucuronidation_WP698_94183	3.03E-02	1	26
Hs_Growth_hormone_receptor_signaling_WP2657_76835	3.20E-02	1	20
Hs_Farnesoid_X_Receptor_Pathway_WP2879_94789	3.38E-02	1	19
Hs_Urea_cycle_and_metabolism_of_amino_groups_WP497_94180	3.55E-02	1	37
Hs_Metapathway_biotransformation_WP702_73516	3.65E-02	2	188
Hs_Degradation_of_collagen_WP2708_76921	3.73E-02	1	21
Hs_Bile_acid_and_bile_salt_metabolism_WP1788_76958	3.90E-02	1	23
Hs_GPCRs,_Class_B_Secretin-like_WP334_79716	4.08E-02	1	23
Hs_Differentiation_of_white_and_brown_adipocyte_WP2895_79216	4.42E-02	1	25
Hs_YAP1-_and_WWTR1_(TAZ)-stimulated_gene_expression_WP2738_76971	4.42E-02	1	25
Hs_Constitutive_Androstane_Receptor_Pathway_WP2875_94791	4.59E-02	1	32
Hs_AhR_pathway_WP2100_47069	4.77E-02	1	28
Hs_Pregnane_X_Receptor_pathway_WP2876_94792	4.94E-02	1	33
Hs_Extracellular_vesicle-mediated_signaling_in_recipient_cells_WP2870_88052	5.28E-02	1	30
Hs_Matrix_Metalloproteinases_WP129_72054	5.28E-02	1	31
Hs_Oxidative_Stress_WP408_94131	5.28E-02	1	30

Altered pathways in RESP after 24 hr CTP incubation	p-value	Matched Entities	Pathway Entities
Hs_Role_of_Osx_and_miRNAs_in_tooth_development_WP3971_91525	1.17E-03	2	37
Hs_Elastic_fibre_formation_WP2666_76849	4.66E-03	2	32
Hs_Hypothetical_Network_for_Drug_Addiction_WP666_68893	4.66E-03	2	32
Hs_Melatonin_metabolism_and_effects_WP3298_91618	5.25E-03	2	42
Hs_Neurotransmitter_Receptor_Binding_And_Downstream_Transmission_In_The_Postsynaptic_Cell_WP2754_77001	6.55E-03	3	124
Hs_Parkinsons_Disease_Pathway_WP2371_87374	7.21E-03	2	76
Hs_NO-cGMP-PKG_mediated_Neuroprotection_WP4008_92677	9.05E-03	2	47
Hs_Tryptophan_metabolism_WP465_94086	9.45E-03	2	80
Hs_Serotonin_Receptor_2_and_STAT3_Signaling_WP733_74441	1.26E-02	1	4
Hs_SIDS_Susceptibility_Pathways_WP706_80056	1.53E-02	3	166
Hs_Endochondral_Ossification_WP474_87977	1.77E-02	2	64
Hs_Glucocorticoid_&_Mineralcorticoid_Metabolism_WP237_78497	2.51E-02	1	9
Hs_Common_Pathways_Underlying_Drug_Addiction_WP2636_89423	3.05E-02	3	41
Hs_Metabolism_of_Angiotensinogen_to_Angiotensins_WP2729_76948	3.13E-02	1	10
Hs_Mitotic_G2-G2-M_phases_WP1859_44913	3.13E-02	1	10
Hs_GPCRs,_Other_WP117_71231	3.83E-02	2	118
Hs_Dopamine_metabolism_WP2436_94675	4.05E-02	1	13
Hs_Serotonin_and_anxiety-related_events_WP3944_90836	4.05E-02	1	13
Hs_Biogenic_Amine_Synthesis_WP550_90171	4.66E-02	1	15
Hs_GPCRs,_Class_C_Metabotropic_glutamate,_pheromone_WP501_79715	4.66E-02	1	15

Hs_GPCRs,_Class_A_Rhodopsin-like_WP455_81793	4.66E-02	3	262
Hs_Serotonin_Receptor_2_and_ELK-SRF-GATA4_signaling_WP732_45038	4.96E-02	1	16
Hs_ACE_Inhibitor_Pathway_WP554_92084	5.26E-02	1	17
Hs_NOTCH1_regulation_of_human_endothelial_cell_calcification_WP3413_87953	5.26E-02	1	17
Hs_Serotonin_and_anxiety_WP3947_91925	5.26E-02	1	17
Altered pathways in NR after 48 hr CTP incubation	**p-value**	**Matched Entities**	**Pathway Entities**
Hs_Focal_Adhesion_WP306_94849	3.60E-10	29	207
Hs_Integrin_cell_surface_interactions_WP1833_77019	6.68E-10	14	64
Hs_Vitamin_D_Receptor_Pathway_WP2877_94793	8.02E-10	23	186
Hs_MHC_class_II_antigen_presentation_WP2679_76872	1.38E-09	15	90
Hs_TCR_signaling_WP1927_76950	1.41E-09	13	74
Hs_TYROBP_Causal_Network_WP3945_90843	3.45E-09	13	60
Hs_Interferon_gamma_signaling_WP1836_77096	3.96E-09	10	43
Hs_Cell_junction_organization_WP1793_77057	4.23E-09	13	61
Hs_Costimulation_by_the_CD28_family_WP1799_77064	4.84E-09	12	71
Hs_B_Cell_Receptor_Signaling_Pathway_WP23_92558	5.00E-09	16	98
Hs_Primary_Focal_Segmental_Glomerulosclerosis_FSGS_WP2572_76327	2.53E-08	13	74
Hs_Ectoderm_Differentiation_WP2858_94753	1.55E-07	17	144
Hs_Endochondral_Ossification_WP474_87977	7.88E-07	11	64
Hs_Cardiac_Progenitor_Differentiation_WP2406_89157	1.02E-06	10	53
Hs_Mesodermal_Commitment_Pathway_WP2857_87780	1.44E-06	16	153
Hs_Interleukin-3,_5_and_GM-CSF_signaling_WP1840_77073	3.39E-06	8	37
Hs_GPCR_ligand_binding_WP1825_76977	3.73E-06	26	371
Hs_Differentiation_Pathway_WP2848_89940	3.75E-06	9	50
Hs_Immunoregulatory_interactions_between_a_Lymphoid_and_a_non-Lymphoid_cell_WP1829_76993	5.20E-06	11	292
Hs_Calcium_Regulation_in_the_Cardiac_Cell_WP536_94305	1.03E-05	15	150
Hs_Inflammatory_Response_Pathway_WP453_80206	1.25E-05	7	33
Hs_Development_of_pulmonary_dendritic_cells_and_macrophage_subsets_WP3892_89703	1.32E-05	5	13
Hs_Allograft_Rejection_WP2328_76328	1.54E-05	11	100
Hs_Assembly_of_collagen_fibrils_and_other_multimeric_structures_WP2798_77089	1.57E-05	7	33
Hs_Cell_surface_interactions_at_the_vascular_wall_WP1794_77039	1.92E-05	11	91
Hs_Kit_receptor_signaling_pathway_WP304_78799	2.17E-05	9	59
Hs_Activation_of_Matrix_Metalloproteinases_WP2769_77041	4.18E-05	5	16
Hs_Spinal_Cord_Injury_WP2431_87678	4.66E-05	12	117
Hs_Myometrial_Relaxation_and_Contraction_Pathways_WP289_89548	6.22E-05	14	156
Hs_miR-targeted_genes_in_muscle_cell_-_TarBase_WP2005_75377	6.71E-05	22	409
Hs_Interleukin-2_signaling_WP2732_76959	7.30E-05	6	29
Hs_Muscle_cell_TarBase_WP2005_44926	7.66E-05	22	336
Hs_Integrated_Pancreatic_Cancer_Pathway_WP2377_71228	7.83E-05	16	200
Hs_EGF-EGFR_Signaling_Pathway_WP437_79266	1.00E-04	14	162
Hs_Pathogenic_Escherichia_coli_infection_WP2272_78594	1.00E-04	8	64
Hs_Senescence_and_Autophagy_WP615_71375	1.09E-04	11	106

Hs_Signaling_by_the_B_Cell_Receptor_(BCR)_WP2746_76984	1.09E-04	11	239
Hs_Matrix_Metalloproteinases_WP129_72054	1.10E-04	6	31
Hs_Senescence_and_Autophagy_in_Cancer_WP615_81193	1.18E-04	11	109
Hs_Degradation_of_collagen_WP2708_76921	1.75E-04	5	21
Hs_Alpha_6_Beta_4_signaling_pathway_WP244_85199	1.92E-04	6	33
Hs_Regulation_of_Insulin-like_Growth_Factor_(IGF)_Transport_and_Uptake_by_Insulin-like_Growth_Factor_Binding_Proteins_(IGFBPs)_WP2799_77094	2.77E-04	4	13
Hs_Chemokine_signaling_pathway_WP3929_90949	3.02E-04	13	166
Hs_GPCR_downstream_signaling_WP1824_76910	3.40E-04	23	406
Hs_VEGFA-VEGFR2_Signaling_Pathway_WP3888_90000	5.42E-04	16	236
Hs_Aryl_Hydrocarbon_Receptor_Pathway_WP2873_88902	6.53E-04	6	46
Hs_TGF-B_Signaling_in_Thyroid_Cells_for_Epithelial-Mesenchymal_Transition_WP3859_90120	8.47E-04	4	19
Hs_Lung_fibrosis_WP3624_92327	8.62E-04	7	64
Hs_NAD_Biosynthesis_II_(from_tryptophan)_WP2485_70025	9.08E-04	3	8
Hs_Epithelium_TarBase_WP2002_45243	9.58E-04	17	278
Hs_Gastrin-CREB_signalling_pathway_via_PKC_and_MAPK_WP2664_76844	1.12E-03	11	147
Hs_White_fat_cell_differentiation_WP4149_94399	1.18E-03	5	32
Hs_Muscle_contraction_WP1864_76895	1.36E-03	6	49
Hs_Oncostatin_M_Signaling_Pathway_WP2374_92557	1.54E-03	7	65
Hs_IL-3_Signaling_Pathway_WP286_78583	1.70E-03	6	49
Hs_Collagen_biosynthesis_and_modifying_enzymes_WP2725_76944	2.09E-03	6	51
Hs_miR-targeted_genes_in_epithelium_-_TarBase_WP2002_75319	2.12E-03	16	345
Hs_Blood_Clotting_Cascade_WP272_93044	2.34E-03	4	23
Hs_Regulation_of_Apoptosis_by_Parathyroid_Hormone-related_Protein_WP3872_89397	2.34E-03	4	22
Hs_miR-targeted_genes_in_lymphocytes_-_TarBase_WP2004_75374	2.44E-03	21	495
Hs_Classical_Pathway_with_Drug_Info_WP2228_49780	2.50E-03	14	225
Hs_Nucleotide_GPCRs_WP80_68938	2.52E-03	3	11
Hs_TGF-beta_Signaling_Pathway_WP366_90028	2.56E-03	10	132
Hs_ErbB_Signaling_Pathway_WP673_94739	2.81E-03	6	55
Hs_TGF-beta_Receptor_Signaling_WP560_94820	2.81E-03	6	55
Hs_Lymphocyte_TarBase_WP2004_46264	3.25E-03	21	420
Hs_Preimplantation_Embryo_WP3527_94671	3.38E-03	6	59
Hs_Endoderm_Differentiation_WP2853_88152	3.71E-03	10	146
Hs_NOD_pathway_WP1433_68991	3.75E-03	5	41
Hs_Nucleotide-binding_Oligomerization_Domain_(NOD)_pathway_WP1433_86035	3.75E-03	5	41
Hs_Differentiation_of_white_and_brown_adipocyte_WP2895_87889	3.81E-03	4	25
Hs_Fcgamma_receptor_(FCGR)_dependent_phagocytosis_WP2719_76936	4.04E-03	6	210
Hs_Netrin-1_signaling_WP1868_76847	4.18E-03	5	42
Hs_Signaling_by_Activin_WP2791_77082	4.20E-03	3	13
Hs_Cytokines_and_Inflammatory_Response_WP530_94763	4.41E-03	4	30
Hs_Signaling_by_NOTCH2_WP2718_76935	4.41E-03	4	28
Hs_Arylhydrocarbon_receptor_(AhR)_signaling_pathway_WP2100_74081	5.07E-03	4	28
Hs_Signaling_by_PDGF_WP1916_76874	5.15E-03	5	48

Hs_Semaphorin_interactions_WP1907_76850	5.61E-03	6	62
Hs_Apoptotic_execution_phase_WP1784_76813	5.68E-03	5	46
Hs_Selenium_Micronutrient_Network_WP15_94185	5.73E-03	7	84
Hs_Regulation_of_Actin_Cytoskeleton_WP51_94816	6.04E-03	10	151
Hs_GPCRs,_Class_A_Rhodopsin-like_WP455_81793	7.03E-03	14	262
Hs_Formation_of_Fibrin_Clot_(Clotting_Cascade)_WP1818_76965	7.45E-03	4	30
Hs_Prostaglandin_Synthesis_and_Regulation_WP98_88906	7.45E-03	4	31
Hs_AGE-RAGE_pathway_WP2324_89798	7.60E-03	6	66
Hs_Role_of_Osx_and_miRNAs_in_tooth_development_WP3971_91525	7.77E-03	3	37
Hs_Amplification_and_Expansion_of_Oncogenic_Pathways_as_Metastatic_Traits_WP3678_90110	9.25E-03	3	17
Hs_miR-509-3p_alteration_of_YAP1-ECM_axis_WP3967_94301	9.25E-03	3	18
Hs_Elastic_fibre_formation_WP2666_76849	9.38E-03	4	32
Hs_Wnt_Signaling_Pathway_WP428_94851	9.39E-03	6	70
Hs_Interleukin-7_signaling_WP2673_76857	9.58E-03	2	6
Hs_Nuclear_Receptors_in_Lipid_Metabolism_and_Toxicity_WP299_89331	1.05E-02	4	35
Hs_Prion_disease_pathway_WP3995_94740	1.05E-02	4	33
Hs_Apoptosis-related_network_due_to_altered_Notch3_in_ovarian_cancer_WP2864_79278	1.24E-02	5	53
Hs_Overview_of_nanoparticle_effects_WP3287_89371	1.27E-02	3	22
Hs_Signaling_by_Hippo_WP2714_76930	1.27E-02	3	20
Hs_Photodynamic_therapy-induced_NF-kB_survival_signaling_WP3617_88316	1.28E-02	4	35
Hs_Arrhythmogenic_Right_Ventricular_Cardiomyopathy_WP2118_71265	1.30E-02	6	78
Hs_Gap_junction_trafficking_and_regulation_WP1820_76886	1.32E-02	2	8
Hs_Neurotransmitter_Receptor_Binding_And_Downstream_Transmission_In_The_Postsynaptic_Cell_WP2754_77001	1.32E-02	8	124
Hs_Signaling_by_ERBB4_WP2781_77063	1.41E-02	4	44
Hs_Eicosanoid_Synthesis_WP167_89514	1.46E-02	3	25
Hs_Hypertrophy_Model_WP516_94803	1.46E-02	3	20
Hs_Microglia_Pathogen_Phagocytosis_Pathway_WP3937_94208	1.70E-02	4	40
Hs_Dissolution_of_Fibrin_Clot_WP1802_76989	1.73E-02	2	8
Hs_Dual_hijack_model_of_Vif_in_HIV_infection_WP3300_87896	1.73E-02	2	8
Hs_GPVI-mediated_activation_cascade_WP1826_42049	1.73E-02	2	8
Hs_Macrophage_markers_WP4146_94392	1.73E-02	2	9
Hs_Extracellular_matrix_organization_WP2703_76914	1.78E-02	5	58
Hs_miRNA_targets_in_ECM_and_membrane_receptors_WP2911_87847	1.90E-02	3	45
Hs_Complement_and_Coagulation_Cascades_WP558_90196	1.90E-02	5	60
Hs_Tgif_disruption_of_Shh_signaling_WP3674_88772	2.18E-02	2	9
Hs_Splicing_factor_NOVA_regulated_synaptic_proteins_WP4148_94396	2.20E-02	4	42
Hs_Apoptosis_WP254_93003	2.30E-02	6	87
Hs_IL-2_Signaling_Pathway_WP49_91243	2.38E-02	4	42
Hs_Angiogenesis_WP1539_95042	2.40E-02	3	24
Hs_IL1_and_megakaryotyces_in_obesity_WP2865_81650	2.40E-02	3	24
Hs_Signaling_by_VEGF_WP1919_76864	2.68E-02	2	10

Hs_IL-7_Signaling_Pathway_WP205_89854	2.68E-02	3	25
Hs_Corticotropin-releasing_hormone_WP2355_71393	3.09E-02	6	90
Hs_Pregnane_X_Receptor_pathway_WP2876_94792	3.60E-02	3	33
Hs_L1CAM_interactions_WP1843_76876	3.85E-02	5	75
Hs_Oxidative_Stress_WP408_94131	4.30E-02	3	30
Hs_EDA_Signalling_in_Hair_Follicle_Development_WP3930_90751	4.41E-02	2	13
Hs_Serotonin_and_anxiety-related_events_WP3944_90836	4.41E-02	2	13
Hs_Wnt_Signaling_Pathway_Netpath_WP363_78571	4.43E-02	4	51
Hs_Bladder_Cancer_WP2828_89143	4.67E-02	3	31
Hs_Gastric_Cancer_Network_2_WP2363_87523	4.67E-02	3	32
Hs_Neural_Crest_Differentiation_WP2064_79263	4.78E-02	6	101
Hs_Integrin-mediated_Cell_Adhesion_WP185_88160	4.97E-02	6	101
Hs_Fluoropyrimidine_Activity_WP1601_94711	5.06E-02	3	34
Hs_Prolactin_receptor_signaling_WP2678_76870	5.06E-02	2	15
Hs_Evolocumab_Mechanism_WP3408_88049	5.17E-02	1	2
Hs_Hypoxia-mediated_EMT_and_Stemness_WP2943_88661	5.17E-02	1	5
Hs_Influenza_A_virus_infection_WP1438_94766	5.17E-02	1	13
Hs_Proprotein_convertase_subtilisin-kexin_type_9_(PCSK9)_mediated_LDL_receptor_degradation_WP2846_89409	5.17E-02	1	2
Hs_Iron_uptake_and_transport_WP2670_75892	5.17E-02	6	105
Hs_Cardiac_Hypertrophic_Response_WP2795_85087	5.27E-02	4	54
Altered pathways in RESP after 48 hr CTP incubation	**p-value**	**Matched Entities**	**Pathway Entities**
Hs_Lung_fibrosis_WP3624_92327	1.30E-02	2	64
Hs_angiogenesis_overview_WP1993_44954	1.51E-02	2	65
Hs_L1CAM_interactions_WP1843_76876	1.84E-02	2	75
Hs_NLR_Proteins_WP288_80026	2.60E-02	1	10
Hs_Signaling_by_VEGF_WP1919_76864	2.88E-02	1	10
Hs_Potassium_Channels_WP2669_76853	3.41E-02	2	99
Hs_Alanine_and_aspartate_metabolism_WP106_94196	3.45E-02	1	40
Hs_TarBasePathway_WP1992_78296	3.45E-02	1	18
Hs_Keap1-Nrf2_Pathway_WP3_48217	4.01E-02	1	14
Hs_Biogenic_Amine_Synthesis_WP550_90171	4.29E-02	1	15
Hs_GABA_synthesis,_release,_reuptake_and_degradation_WP2685_76885	4.29E-02	1	16
Hs_Transcriptional_activation_by_NRF2_WP3_94689	4.29E-02	1	15
Hs_Activation_of_Matrix_Metalloproteinases_WP2769_77041	4.57E-02	1	16
Hs_Simplified_Interaction_Map_Between_LOXL4_and_Oxidative_Stress_Pathway_WP3670_90107	5.13E-02	1	18

Supplementary table 7. Gene expression measured with qPCR in SSRI exploratory cohort (n = 17).

Gene	Incubation	Time (hr)	ΔCp NR (mean)	ΔCp RESP (mean)	p-value	
PITX1	Ctrl.	24	7.86	9.66	*0.16*	#
PITX1	CTP	24	7.92	9.68	*0.17*	#
GAD1	Ctrl.	24	10.06	12.13	**0.05**	*
GAD1	CTP	24	9.94	11.86	**0.05**	*

NFIB	Ctrl.	24	4.51	6.91	*0.13*	#
NFIB	CTP	24	4.44	6.93	*0.12*	#
FYB	Ctrl.	24	6.80	4.75	**0.05**	*
FYB	CTP	24	6.64	4.60	**0.04**	*
RAMP1	Ctrl.	24	6.48	5.15	*0.07*	#
RAMP1	CTP	24	6.24	4.76	**0.02**	*
UNC13C	Ctrl.	24	14.57	14.66	0.86	
UNC13C	CTP	24	13.64	14.14	0.32	
TBC1D9	Ctrl.	24	2.88	1.19	**0.03**	*
TBC1D9	CTP	24	2.82	1.22	**0.04**	*
NINL	Ctrl.	24	9.06	9.30	0.68	
NINL	CTP	24	9.19	9.14	0.94	
GRIN2A	Ctrl.	24	7.62	7.16	0.65	
GRIN2A	CTP	24	7.59	6.96	0.54	
AADAT	Ctrl.	24	11.61	12.61	*0.20*	#
AADAT	CTP	24	11.30	11.72	0.51	
ITGB6	Ctrl.	24	13.89	14.51	0.34	
ITGB6	CTP	24	14.88	14.40	0.62	
EPHB2	Ctrl.	24	7.10	7.69	0.36	
EPHB2	CTP	24	7.04	7.60	0.38	
FGF7	Ctrl.	24	11.13	11.04	0.91	
FGF7	CTP	24	11.05	11.03	0.97	
NRP1	Ctrl.	24	9.81	9.47	0.67	
NRP1	CTP	24	9.38	9.14	0.71	
PITX1	Ctrl.	48	7.65	9.71	*0.07*	#
PITX1	CTP	48	7.52	9.75	**0.05**	*
GAD1	Ctrl.	48	10.08	11.89	**0.04**	*
GAD1	CTP	48	10.04	11.73	*0.07*	#
NFIB	Ctrl.	48	4.13	6.47	*0.11*	#
NFIB	CTP	48	4.19	6.64	*0.12*	#
FYB	Ctrl.	48	6.89	4.69	**0.03**	*
FYB	CTP	48	6.78	4.68	**0.02**	*
RAMP1	Ctrl.	48	5.67	4.93	0.40	
RAMP1	CTP	48	5.47	4.85	0.57	
UNC13C	Ctrl.	48	12.68	13.77	0.37	
UNC13C	CTP	48	12.88	14.08	0.37	
TBC1D9	Ctrl.	48	2.81	0.88	**0.01**	*
TBC1D9	CTP	48	2.81	0.94	**0.02**	*
NINL	Ctrl.	48	8.60	9.03	0.48	
NINL	CTP	48	8.78	8.84	0.96	
GRIN2A	Ctrl.	48	8.21	7.23	*0.20*	#
GRIN2A	CTP	48	8.19	7.50	0.51	
AADAT	Ctrl.	48	10.29	11.40	*0.20*	#
AADAT	CTP	48	10.13	11.16	0.35	
ITGB6	Ctrl.	48	14.63	15.21	0.74	
ITGB6	CTP	48	14.75	15.01	0.73	

EPHB2	Ctrl.	48	7.18	7.90	0.32
EPHB2	CTP	48	7.02	7.84	0.42
FGF7	Ctrl.	48	10.87	11.26	0.72
FGF7	CTP	48	10.60	10.72	0.96
NRP1	Ctrl.	48	10.23	9.65	0.48
NRP1	CTP	48	10.12	9.46	0.42

* $p \leq 0.05$, # $p \leq 0.2$.

Acknowledgements

I would like to sincerely thank Prof. Julia Stingl for giving me the opportunity to join her innovative research works and to complete my PhD in her group. I thank her for the close supervision of my work and for the scientific as well as personal support throughout my times at her department. Many thanks to Prof. Ulrich Jaehde for his co-supervision, for the fruitful cooperation and for the valuable, durable advice along my stay as an external member of his working group. I extend my thanks also to the examining committee for taking time to critically read my work.

Many thanks to Dr. Catharina Scholl for the continuous, close supervision in the lab and during writing the dissertation and for the many valuable discussions. Thanks also to Dr. Michael Steffens for carrying out the statistical analyses. Many thanks to Dr. Anya Staal for the smooth cooperation and the many interesting talks.

I would also like to cordially thank Kerstin Brandenburg, my officemate, for the unconditional technical and mental support throughout the good and hard times. Many thanks to Sandra Weickhardt, Martina Wiertz, Maria Wos-Maganga for the continuous technical support in the lab.

Thanks are extended to all the colleagues in the Research Division, particularly Vivien, Simone, Denna, Jörg, Sarah, Miriam, Matthias, Nina, Anna, Anna, Sabrina for all the good work as well as free times we spent together. I emphasize my thanks to Vivien for being so motivating and having ears for me before, during and also after my PhD. My thank goes also to Ilina Mansour for her dedicated support in the ubiquitination project.

My endless cordial gratitude goes to my family, my parents Anas and Maisa, my wife Ghaliah, my sisters Najwa and Farah and brother Eyad. Your emotional, mental and financial support was unconditional. You believed in me in times I did not. Without you, after God, I would never have made it. For the happy soul at home, my daughter Mayssa, many kisses and hugs for cheering me up; despite some long, sleepless nights.

God Almighty, without your blessings, it would have never been. Before all, and after all, Thank you, God!

List of Publications

Journal Article

- **Barakat AK**, Scholl C, Steffens M, Brandenburg K, Ising M, Lucae S, Holsboer F, Laje G, Kalayda GV, Jaehde U, Stingl JC. Citalopram-induced pathways regulation and tentative treatment-outcome-predicting biomarkers in lymphoblastoid cell lines from depression patients. *Transl Psychiatry* 2020; **10**(1):210. doi: 10.1038/s41398-020-00900-8. PMID: 32612257; PMCID: PMC7329820.

Congress Talks

- **A Barakat**, C Scholl, J Stingl (2016) Candidate Biomarkers for the Prediction of Antidepressant Response; Paul-Ehrlich-Institute Retreat; Ronneburg.
- **A Barakat**, C Scholl, J Stingl (2017); Expression and Intracellular Localization of Serotonin Transporter in LCLs as Putative Biomarker for Antidepressant Response; World Congress of Biological Psychiatry, Copenhagen.
- **A Barakat**, C Scholl, J Stingl (2017); Pharmacogenetic Factors in Neuroprotection During Neurodevelopment; World Congress of Biological Psychiatry, Copenhagen.

Poster presentation

- N Beyer, M Vogel, C Scholl, **A Barakat**, J C Stingl (2018): “Mimicking metabolism in the brain – analysis of cytochrome P450 mediated drug metabolism in iPSC-derived cortical organoids by highly sensitive LC–MS techniques”; German Pharm-Tox Summit, Göttingen, Deutschland.

References

1. Rehm J, Shield KD. Global Burden of Disease and the Impact of Mental and Addictive Disorders. *Curr Psychiatry Rep* 2019; **21**(2)**:** 10.

2. Kessler RC, Berglund P, Demler O, Jin R, Merikangas KR, Walters EE. Lifetime prevalence and age-of-onset distributions of DSM-IV disorders in the National Comorbidity Survey Replication. *Arch. Gen. Psychiatry* 2005; **62**(6)**:** 593-602.

3. Ebmeier KP, Donaghey C, Steele JD. Recent developments and current controversies in depression. *Lancet* 2006; **367**(9505)**:** 153-167.

4. World Health Organization (2017). Depression and other common mental disorders: global health estimates. World Health Organization: Geneva.

5. Twenge JM, Cooper AB, Joiner TE, Duffy ME, Binau SG. Age, period, and cohort trends in mood disorder indicators and suicide-related outcomes in a nationally representative dataset, 2005-2017. *J. Abnorm. Psychol.* 2019; **128**(3)**:** 185-199.

6. *Diagnostic and statistical manual of mental disorders : DSM-5*. American Psychiatric Association: Arlington, VA, 2013.

7. Montgomery SA, Asberg M. A new depression scale designed to be sensitive to change. *The British journal of psychiatry : J Ment Sci* 1979; **134:** 382-389.

8. Hamilton M. A rating scale for depression. *J Neurol Neurosurg Psychiatry* 1960; **23:** 56-62.

9. Rush AJ, Trivedi MH, Ibrahim HM, Carmody TJ, Arnow B, Klein DN*, et al*. The 16-Item Quick Inventory of Depressive Symptomatology (QIDS), clinician rating (QIDS-C), and self-report (QIDS-SR): a psychometric evaluation in patients with chronic major depression. *Biol psychiatry* 2003; **54**(5)**:** 573-583.

10. Fernandez-Pujals AM, Adams MJ, Thomson P, McKechanie AG, Blackwood DH, Smith BH*, et al*. Epidemiology and Heritability of Major Depressive Disorder, Stratified by Age of Onset, Sex, and Illness Course in Generation Scotland: Scottish Family Health Study (GS:SFHS). *PloS one* 2015; **10**(11)**:** e0142197.

11. Sullivan PF, Neale MC, Kendler KS. Genetic epidemiology of major depression: review and meta-analysis. *Am J Psychiatry* 2000; **157**(10)**:** 1552-1562.

12. Lohoff FW. Overview of the genetics of major depressive disorder. *Curr Psychiatry Rep* 2010; **12**(6)**:** 539-546.

13. Byrne EM, Carrillo-Roa T, Henders AK, Bowdler L, McRae AF, Heath AC*, et al*. Monozygotic twins affected with major depressive disorder have greater variance in methylation than their unaffected co-twin. *Transl Psychiatry* 2013; **3**(6)**:** e269.

14. Flint J, Kendler KS. The Genetics of Major Depression. *Neuron* 2014; **81**(5)**:** 1214.

15. Major Depressive Disorder Working Group of the Psychiatric GC, Ripke S, Wray NR, Lewis CM, Hamilton SP, Weissman MM*, et al*. A mega-analysis of genome-wide association studies for major depressive disorder. *Mol psychiatry* 2013; **18**(4)**:** 497-511.

16. McMahon FJ, Insel TR. Pharmacogenomics and personalized medicine in neuropsychiatry. *Neuron* 2012; **74**(5)**:** 773-776.

17. Schildkraut JJ. The catecholamine hypothesis of affective disorders: a review of supporting evidence. *Am J Psychiatry* 1965; **122**(5)**:** 509-522.

18. Bunney WE, Jr., Davis JM. Norepinephrine in depressive reactions. A review. *Arch. Gen. Psychiatry* 1965; **13**(6)**:** 483-494.

19. Bazan IS, Fares WH. Review of the Ongoing Story of Appetite Suppressants, Serotonin Pathway, and Pulmonary Vascular Disease. *Am J Cardiol* 2016; **117**(10)**:** 1691-1696.

20. Portas CM, Bjorvatn B, Ursin R. Serotonin and the sleep/wake cycle: special emphasis on microdialysis studies. *Prog Neurobiol* 2000; **60**(1)**:** 13-35.

21. Meneses A, Liy-Salmeron G. Serotonin and emotion, learning and memory. *Rev Neurosci* 2012; **23**(5-6)**:** 543-553.

22. Barkan T, Gurwitz D, Levy G, Weizman A, Rehavi M. Biochemical and pharmacological characterization of the serotonin transporter in human peripheral blood lymphocytes. *Eur Neuropsychopharmacol* 2004; **14**(3)**:** 237-243.

23. Adell A, Garcia-Marquez C, Armario A, Gelpi E. Chronic stress increases serotonin and noradrenaline in rat brain and sensitizes their responses to a further acute stress. *J Neurochem* 1988; **50**(6)**:** 1678-1681.

24. Mitchell HA, Weinshenker D. Good night and good luck: norepinephrine in sleep pharmacology. *Biochem Pharmacol* 2010; **79**(6)**:** 801-809.

25. Coppen A, Shaw DM, Farrell JP. Potentiation of the antidepressive effect of a monoamine-oxidase inhibitor by tryptophan. *Lancet* 1963; **1**(7272)**:** 79-81.

26. Shopsin B, Friedman E, Gershon S. Parachlorophenylalanine reversal of tranylcypromine effects in depressed patients. *Arch. Gen. Psychiatry* 1976; **33**(7)**:** 811-819.

27. Shopsin B, Gershon S, Goldstein M, Friedman E, Wilk S. Use of synthesis inhibitors in defining a role for biogenic amines during imipramine treatment in depressed patients. *Psychopharmacol Commun* 1975; **1**(2)**:** 239-249.

28. Leonard BE. Psychopathology of depression. *Drugs Today (Barc)* 2007; **43**(10)**:** 705-716.

29. Sulser F. New perspectives on the molecular pharmacology of affective disorders. *Eur Arch Psychiatry Neurol Sci* 1989; **238**(5-6)**:** 231-239.

30. Banerjee SP, Kung LS, Riggi SJ, Chanda SK. Development of beta-adrenergic receptor subsensitivity by antidepressants. *Nature* 1977; **268**(5619)**:** 455-456.

31. De Cesare D, Fimia GM, Sassone-Corsi P. Signaling routes to CREM and CREB: plasticity in transcriptional activation. *Trends Biochem Sci* 1999; **24**(7)**:** 281-285.

32. Hyman SE, Nestler EJ. Initiation and adaptation: a paradigm for understanding psychotropic drug action. *Am J Psychiatry* 1996; **153**(2)**:** 151-162.

33. Racagni G, Popoli M. Cellular and molecular mechanisms in the long-term action of antidepressants. *Dialogues Clin Neurosci* 2008; **10**(4)**:** 385-400.

34. Calabrese F, Rossetti AC, Racagni G, Gass P, Riva MA, Molteni R. Brain-derived neurotrophic factor: a bridge between inflammation and neuroplasticity. *Front Cell Neurosci* 2014; **8:** 430.

35. Amrein I, Isler K, Lipp HP. Comparing adult hippocampal neurogenesis in mammalian species and orders: influence of chronological age and life history stage. *Eur J Neurosci* 2011; **34**(6)**:** 978-987.

36. Fuchs E, Gould E. Mini-review: in vivo neurogenesis in the adult brain: regulation and functional implications. *Eur J Neurosci* 2000; **12**(7)**:** 2211-2214.

37. Gould E, Reeves AJ, Graziano MS, Gross CG. Neurogenesis in the neocortex of adult primates. *Science* 1999; **286**(5439)**:** 548-552.

38. Bernier PJ, Bedard A, Vinet J, Levesque M, Parent A. Newly generated neurons in the amygdala and adjoining cortex of adult primates. *PNAS USA* 2002; **99**(17)**:** 11464-11469.

39. Kuhn HG, Winkler J, Kempermann G, Thal LJ, Gage FH. Epidermal growth factor and fibroblast growth factor-2 have different effects on neural progenitors in the adult rat brain. *J Neurosci* 1997; **17**(15)**:** 5820-5829.

40. Gould E, Cameron HA, Daniels DC, Woolley CS, McEwen BS. Adrenal hormones suppress cell division in the adult rat dentate gyrus. *J Neurosci* 1992; **12**(9)**:** 3642-3650.

41. Brezun JM, Daszuta A. Depletion in serotonin decreases neurogenesis in the dentate gyrus and the subventricular zone of adult rats. *Neuroscience* 1999; **89**(4)**:** 999-1002.

42. Malberg JE, Eisch AJ, Nestler EJ, Duman RS. Chronic antidepressant treatment increases neurogenesis in adult rat hippocampus. *J Neurosci* 2000; **20**(24)**:** 9104-9110.

43. Mahar I, Bambico FR, Mechawar N, Nobrega JN. Stress, serotonin, and hippocampal neurogenesis in relation to depression and antidepressant effects. *Neurosci Biobehav Rev* 2014; **38:** 173-192.

44. Gronli J, Bramham C, Murison R, Kanhema T, Fiske E, Bjorvatn B*, et al*. Chronic mild stress inhibits BDNF protein expression and CREB activation in the dentate gyrus but not in the hippocampus proper. *Pharmacol Biochem Behav* 2006; **85**(4)**:** 842-849.

45. Wang Z, Hu SY, Lei DL, Song WX. Effect of chronic stress on PKA and P-CREB expression in hippocampus of rats and the antagonism of antidepressors. *J Zhong Univ Health Sci* 2006; **31**(5)**:** 767-771.

46. Pandey GN, Dwivedi Y, Ren X, Rizavi HS, Roberts RC, Conley RR. Cyclic AMP response element-binding protein in post-mortem brain of teenage suicide victims: specific decrease in the prefrontal cortex but not the hippocampus. *Int J Neuropsychopharmacol* 2007; **10**(5)**:** 621-629.

47. Bartova L, Dold M, Kautzky A, Fabbri C, Spies M, Serretti A*, et al*. Results of the European Group for the Study of Resistant Depression (GSRD) - basis for further research and clinical practice. *World J Biol Psychiatry* 2019; **20**(6)**:** 427-448.

48. Rethorst CD, South CC, Rush AJ, Greer TL, Trivedi MH. Prediction of treatment outcomes to exercise in patients with nonremitted major depressive disorder. *Depress Anxiety* 2017; **34**(12)**:** 1116-1122.

49. Kautzky A, Baldinger P, Souery D, Montgomery S, Mendlewicz J, Zohar J*, et al*. The combined effect of genetic polymorphisms and clinical parameters on treatment outcome in treatment-resistant depression. *Eur Neuropsychopharmacol* 2015; **25**(4)**:** 441-453.

50. Lim SW, Kim S, Carroll BJ, Kim DK. T-lymphocyte CREB as a potential biomarker of response to antidepressant drugs. *Int J Neuropsychopharmacol* 2013; **16**(5)**:** 967-974.

51. Liu Q, Dwyer ND, O'Leary DD. Differential expression of COUP-TFI, CHL1, and two novel genes in developing neocortex identified by differential display PCR. *J Neurosci* 2000; **20**(20)**:** 7682-7690.

52. Hillenbrand R, Molthagen M, Montag D, Schachner M. The close homologue of the neural adhesion molecule L1 (CHL1): patterns of expression and promotion of neurite outgrowth by heterophilic interactions. *Eur J Neurosci* 1999; **11**(3)**:** 813-826.

53. Schmid RS, Maness PF. L1 and NCAM adhesion molecules as signaling coreceptors in neuronal migration and process outgrowth. *Curr Opin Neurobiol* 2008; **18**(3)**:** 245-250.

54. Huang X, Zhu LL, Zhao T, Wu LY, Wu KW, Schachner M*, et al*. CHL1 negatively regulates the proliferation and neuronal differentiation of neural progenitor cells through activation of the ERK1/2 MAPK pathway. *Mol Cell Neurosci* 2011; **46**(1)**:** 296-307.

55. Chen S, Mantei N, Dong L, Schachner M. Prevention of neuronal cell death by neural adhesion molecules L1 and CHL1. *J Neurobiol* 1999; **38**(3)**:** 428-439.

56. Probst-Schendzielorz K, Scholl C, Efimkina O, Ersfeld E, Viviani R, Serretti A*, et al*. CHL1, ITGB3 and SLC6A4 gene expression and antidepressant drug response: results from the Munich Antidepressant Response Signature (MARS) study. *Pharmacogenomics* 2015; **16**(7)**:** 689-701.

57. Fabbri C, Crisafulli C, Gurwitz D, Stingl J, Calati R, Albani D*, et al*. Neuronal cell adhesion genes and antidepressant response in three independent samples. *Pharmacogenomics J* 2015; **15**(6)**:** 538-548.

58. Fabbri C, Crisafulli C, Calati R, Albani D, Forloni G, Calabro M*, et al*. Neuroplasticity and second messenger pathways in antidepressant efficacy: pharmacogenetic results from a prospective trial investigating treatment resistance. *Eur Arch Psychiatry Clin Neurosci* 2017; **267**(8)**:** 723-735.

59. Yao B, Christian KM, He C, Jin P, Ming GL, Song H. Epigenetic mechanisms in neurogenesis. *Nat Rev Neurosci* 2016; **17**(9)**:** 537-549.

60. Zhang RR, Cui QY, Murai K, Lim YC, Smith ZD, Jin S*, et al*. Tet1 regulates adult hippocampal neurogenesis and cognition. *Cell stem cell* 2013; **13**(2)**:** 237-245.

61. Ito S, D'Alessio AC, Taranova OV, Hong K, Sowers LC, Zhang Y. Role of Tet proteins in 5mC to 5hmC conversion, ES-cell self-renewal and inner cell mass specification. *Nature* 2010; **466**(7310)**:** 1129-1133.

62. Dawlaty MM, Ganz K, Powell BE, Hu YC, Markoulaki S, Cheng AW*, et al*. Tet1 is dispensable for maintaining pluripotency and its loss is compatible with embryonic and postnatal development. *Cell stem cell* 2011; **9**(2)**:** 166-175.

63. Wei Y, Melas PA, Wegener G, Mathe AA, Lavebratt C. Antidepressant-like effect of sodium butyrate is associated with an increase in TET1 and in 5-hydroxymethylation levels in the Bdnf gene. *Int J Neuropsychopharmacol* 2014; **18**(2).

64. Cheng Y, Sun M, Chen L, Li Y, Lin L, Yao B*, et al*. Ten-Eleven Translocation Proteins Modulate the Response to Environmental Stress in Mice. *Cell Rep* 2018; **25**(11)**:** 3194-3203 e3194.

65. Grebe KM, Takeda K, Hickman HD, Bailey AL, Embry AC, Bennink JR*, et al*. Cutting edge: Sympathetic nervous system increases proinflammatory cytokines and exacerbates influenza A virus pathogenesis. *J Immunol* 2010; **184**(2)**:** 540-544.

66. Glaser R, Kiecolt-Glaser JK. Stress-induced immune dysfunction: implications for health. *Nat Rev Immunol* 2005; **5**(3)**:** 243-251.

67. Slavich GM, Irwin MR. From stress to inflammation and major depressive disorder: a social signal transduction theory of depression. *Psychol Bull* 2014; **140**(3)**:** 774-815.

68. Schleimer RP. An overview of glucocorticoid anti-inflammatory actions. *Eur J Clin Pharmacol* 1993; **45 Suppl 1:** S3-7; discussion S43-44.

69. Schmaal L, Veltman DJ, van Erp TG, Samann PG, Frodl T, Jahanshad N*, et al*. Subcortical brain alterations in major depressive disorder: findings from the ENIGMA Major Depressive Disorder working group. *Mol psychiatry* 2016; **21**(6)**:** 806-812.

70. Stockmeier CA, Mahajan GJ, Konick LC, Overholser JC, Jurjus GJ, Meltzer HY*, et al*. Cellular changes in the postmortem hippocampus in major depression. *Biol psychiatry* 2004; **56**(9)**:** 640-650.

71. Campbell S, Macqueen G. The role of the hippocampus in the pathophysiology of major depression. *J Psychiatry Neurosci* 2004; **29**(6)**:** 417-426.

72. Galigniana NM, Ballmer LT, Toneatto J, Erlejman AG, Lagadari M, Galigniana MD. Regulation of the glucocorticoid response to stress-related disorders by the Hsp90-binding immunophilin FKBP51. *J Neurochem* 2012; **122**(1)**:** 4-18.

73. Denny WB, Valentine DL, Reynolds PD, Smith DF, Scammell JG. Squirrel monkey immunophilin FKBP51 is a potent inhibitor of glucocorticoid receptor binding. *Endocrinology* 2000; **141**(11)**:** 4107-4113.

74. Fabbri C, Hosak L, Mossner R, Giegling I, Mandelli L, Bellivier F*, et al*. Consensus paper of the WFSBP Task Force on Genetics: Genetics, epigenetics and gene expression markers of major depressive disorder and antidepressant response. *World J Biol Psychiatry* 2017; **18**(1)**:** 5-28.

75. Zimmermann P, Bruckl T, Nocon A, Pfister H, Binder EB, Uhr M*, et al*. Interaction of FKBP5 gene variants and adverse life events in predicting depression onset: results from a 10-year prospective community study. *Am J Psychiatry* 2011; **168**(10)**:** 1107-1116.

76. Wang Q, Shelton RC, Dwivedi Y. Interaction between early-life stress and FKBP5 gene variants in major depressive disorder and post-traumatic stress disorder: A systematic review and meta-analysis. *J Affect Disord* 2018; **225:** 422-428.

77. Binder EB, Bradley RG, Liu W, Epstein MP, Deveau TC, Mercer KB*, et al*. Association of FKBP5 polymorphisms and childhood abuse with risk of posttraumatic stress disorder symptoms in adults. *JAMA* 2008; **299**(11)**:** 1291-1305.

78. Ising M, Maccarrone G, Bruckl T, Scheuer S, Hennings J, Holsboer F*, et al*. FKBP5 Gene Expression Predicts Antidepressant Treatment Outcome in Depression. *Int J Mol Sci* 2019; **20**(3).

79. Le-Niculescu H, Roseberry K, Gill SS, Levey DF, Phalen PL, Mullen J*, et al*. Precision medicine for mood disorders: objective assessment, risk prediction, pharmacogenomics, and repurposed drugs. *Mol psychiatry* 2021; **26**(7)**:** 2776-2804.

80. Myint AM, Leonard BE, Steinbusch HW, Kim YK. Th1, Th2, and Th3 cytokine alterations in major depression. *J Affect Disord* 2005; **88**(2)**:** 167-173.

81. Sanjabi S, Zenewicz LA, Kamanaka M, Flavell RA. Anti-inflammatory and pro-inflammatory roles of TGF-beta, IL-10, and IL-22 in immunity and autoimmunity. *Curr Opin Pharmacol* 2009; **9**(4)**:** 447-453.

82. Mamdani F, Berlim MT, Beaulieu MM, Turecki G. Pharmacogenomic predictors of citalopram treatment outcome in major depressive disorder. *World J Biol Psychiatry* 2014; **15**(2)**:** 135-144.

83. Wicks SJ, Grocott T, Haros K, Maillard M, ten Dijke P, Chantry A. Reversible ubiquitination regulates the Smad/TGF-beta signalling pathway. *Biochem Soc Trans* 2006; **34**(Pt 5)**:** 761-763.

84. Anacker C, Zunszain PA, Cattaneo A, Carvalho LA, Garabedian MJ, Thuret S*, et al*. Antidepressants increase human hippocampal neurogenesis by activating the glucocorticoid receptor. *Mol psychiatry* 2011; **16**(7)**:** 738-750.

85. Möller H-J, Laux G, Deister A. Duale Reihe Psychiatrie und Psychotherapie. *Georg Thieme Verlag* 2009.

86. Tynan RJ, Weidenhofer J, Hinwood M, Cairns MJ, Day TA, Walker FR. A comparative examination of the anti-inflammatory effects of SSRI and SNRI antidepressants on LPS stimulated microglia. *Brain Behav Immun* 2012; **26**(3)**:** 469-479.

87. Qi H, Mailliet F, Spedding M, Rocher C, Zhang X, Delagrange P*, et al*. Antidepressants reverse the attenuation of the neurotrophic MEK/MAPK cascade in frontal cortex by elevated platform stress; reversal of effects on LTP is associated with GluA1 phosphorylation. *Neuropharmacology* 2009; **56**(1)**:** 37-46.

88. Morag A, Kirchheiner J, Rehavi M, Gurwitz D. Human lymphoblastoid cell line panels: novel tools for assessing shared drug pathways. *Pharmacogenomics* 2010; **11**(3)**:** 327-340.

89. Koch JM, Kell S, Aldenhoff JB. Differential effects of fluoxetine and imipramine on the phosphorylation of the transcription factor CREB and cell-viability. *J Psychiatr Res* 2003; **37**(1)**:** 53-59.

90. De Carlo V, Calati R, Serretti A. Socio-demographic and clinical predictors of non-response/non-remission in treatment resistant depressed patients: A systematic review. *Psychiatry Res* 2016; **240:** 421-430.

91. Fabbri C, Minarini A, Matsumoto Y, Serretti A. Chapter 26 - Pharmacogenetics of Antidepressant Drugs. In: Padmanabhan S (ed). *Handb Pharmacogen Strat Med*. Academic Press: San Diego, 2014, pp 543-562.

92. Gibson TB, Jing Y, Smith Carls G, Kim E, Bagalman JE, Burton WN*, et al*. Cost burden of treatment resistance in patients with depression. *Am J Manag Care* 2010; **16**(5)**:** 370-377.

93. Horstmann S, Binder EB. Pharmacogenomics of antidepressant drugs. *Pharmacol Ther* 2009; **124**(1)**:** 57-73.

94. Lerer B, Macciardi F. Pharmacogenetics of antidepressant and mood-stabilizing drugs: a review of candidate-gene studies and future research directions. *Int J Neuropsychopharmacol* 2002; **5**(3)**:** 255-275.

95. aan het Rot M, Mathew SJ, Charney DS. Neurobiological mechanisms in major depressive disorder. *CMAJ* 2009; **180**(3)**:** 305-313.

96. Schmidt HD, Shelton RC, Duman RS. Functional biomarkers of depression: diagnosis, treatment, and pathophysiology. *Neuropsychopharmacology* 2011; **36**(12)**:** 2375-2394.

97. Italiano A. Prognostic or predictive? It's time to get back to definitions! *J Clin Oncol* 2011; **29**(35)**:** 4718; author reply 4718-4719.

98. Perlis RH. Betting on biomarkers. *Am J Psychiatry* 2011; **168**(3)**:** 234-236.

99. McGuffin P, Cohen S, Knight J. Homing in on depression genes. *Am J Psychiatry* 2007; **164**(2)**:** 195-197.

100. Wei YB, McCarthy M, Ren H, Carrillo-Roa T, Shekhtman T, DeModena A*, et al*. A functional variant in the serotonin receptor 7 gene (HTR7), rs7905446, is associated with good response to SSRIs in bipolar and unipolar depression. *Mol psychiatry* 2020; **25**(6)**:** 1312-1322.

101. Horstmann S, Lucae S, Menke A, Hennings JM, Ising M, Roeske D*, et al*. Polymorphisms in GRIK4, HTR2A, and FKBP5 show interactive effects in predicting remission to antidepressant treatment. *Neuropsychopharmacology* 2010; **35**(3)**:** 727-740.

102. Hennings JM, Kohli MA, Czamara D, Giese M, Eckert A, Wolf C*, et al*. Possible associations of NTRK2 polymorphisms with antidepressant treatment outcome: findings from an extended tag SNP approach. *PloS one* 2013; **8**(6)**:** e64947.

103. Unschuld PG, Ising M, Specht M, Erhardt A, Ripke S, Heck A*, et al*. Polymorphisms in the GAD2 gene-region are associated with susceptibility for unipolar depression and with a risk factor for anxiety disorders. *American journal of medical genetics Part B, Am J Med Genet B Neuropsychiatr Genet* 2009; **150B**(8)**:** 1100-1109.

104. Uhr M, Tontsch A, Namendorf C, Ripke S, Lucae S, Ising M*, et al*. Polymorphisms in the drug transporter gene ABCB1 predict antidepressant treatment response in depression. *Neuron* 2008; **57**(2)**:** 203-209.

105. Kohli MA, Lucae S, Saemann PG, Schmidt MV, Demirkan A, Hek K*, et al*. The neuronal transporter gene SLC6A15 confers risk to major depression. *Neuron* 2011; **70**(2)**:** 252-265.

106. Hunter AM, Leuchter AF, Power RA, Muthen B, McGrath PJ, Lewis CM*, et al*. A genome-wide association study of a sustained pattern of antidepressant response. *J Psychiatr Res* 2013; **47**(9)**:** 1157-1165.

107. Garriock HA, Tanowitz M, Kraft JB, Dang VC, Peters EJ, Jenkins GD*, et al*. Association of mu-opioid receptor variants and response to citalopram treatment in major depressive disorder. *Am J Psychiatry* 2010; **167**(5)**:** 565-573.

108. Menke A, Klengel T, Binder EB. Epigenetics, depression and antidepressant treatment. *Curr Pharm Des* 2012; **18**(36)**:** 5879-5889.

109. Wigmore EM, Hafferty JD, Hall LS, Howard DM, Clarke TK, Fabbri C*, et al*. Genome-wide association study of antidepressant treatment resistance in a population-based cohort using health service prescription data and meta-analysis with GENDEP. *Pharmacogenomics J* 2020; **20**(2)**:** 329-341.

110. Investigators G, Investigators M, Investigators SD. Common genetic variation and antidepressant efficacy in major depressive disorder: a meta-analysis of three genome-wide pharmacogenetic studies. *Am J Psychiatry* 2013; **170**(2)**:** 207-217.

111. Uher R, Perroud N, Ng MY, Hauser J, Henigsberg N, Maier W*, et al*. Genome-wide pharmacogenetics of antidepressant response in the GENDEP project. *Am J Psychiatry* 2010; **167**(5)**:** 555-564.

112. Li QS, Tian C, Seabrook GR, Drevets WC, Narayan VA. Analysis of 23andMe antidepressant efficacy survey data: implication of circadian rhythm and neuroplasticity in bupropion response. *Transl Psychiatry* 2016; **6**(9)**:** e889.

113. Hennings JM, Owashi T, Binder EB, Horstmann S, Menke A, Kloiber S*, et al*. Clinical characteristics and treatment outcome in a representative sample of depressed inpatients - findings from the Munich Antidepressant Response Signature (MARS) project. *J Psychiatr Res* 2009; **43**(3)**:** 215-229.

114. Garriock HA, Kraft JB, Shyn SI, Peters EJ, Yokoyama JS, Jenkins GD*, et al*. A genomewide association study of citalopram response in major depressive disorder. *Biol psychiatry* 2010; **67**(2)**:** 133-138.

115. Thomas L, Mulligan J, Mason V, Tallon D, Wiles N, Cowen P*, et al*. GENetic and clinical predictors of treatment response in depression: the GenPod randomised trial protocol. *Trials* 2008; **9:** 29.

116. Tansey KE, Guipponi M, Perroud N, Bondolfi G, Domenici E, Evans D*, et al*. Genetic predictors of response to serotonergic and noradrenergic antidepressants in major depressive disorder: a genome-wide analysis of individual-level data and a meta-analysis. *PLoS medicine* 2012; **9**(10)**:** e1001326.

117. Perroud N, Bondolfi G, Uher R, Gex-Fabry M, Aubry JM, Bertschy G*, et al*. Clinical and genetic correlates of suicidal ideation during antidepressant treatment in a depressed outpatient sample. *Pharmacogenomics* 2011; **12**(3)**:** 365-377.

118. Mehta D, Menke A, Binder EB. Gene expression studies in major depression. *Curr Psychiatry Rep* 2010; **12**(2)**:** 135-144.

119. Tomita H, Vawter MP, Walsh DM, Evans SJ, Choudary PV, Li J*, et al*. Effect of agonal and postmortem factors on gene expression profile: quality control in microarray analyses of postmortem human brain. *Biol psychiatry* 2004; **55**(4)**:** 346-352.

120. Liew CC, Ma J, Tang HC, Zheng R, Dempsey AA. The peripheral blood transcriptome dynamically reflects system wide biology: a potential diagnostic tool. *J Lab Clin Med* 2006; **147**(3)**:** 126-132.

121. Sullivan PF, Fan C, Perou CM. Evaluating the comparability of gene expression in blood and brain. *American journal of medical genetics Part B, Am J Med Genet B Neuropsychiatr Genet* 2006; **141B**(3)**:** 261-268.

122. Menke A. Gene expression: biomarker of antidepressant therapy? *Int Rev Psychiatry* 2013; **25**(5)**:** 579-591.

123. Mamdani F, Berlim MT, Beaulieu MM, Labbe A, Merette C, Turecki G. Gene expression biomarkers of response to citalopram treatment in major depressive disorder. *Transl Psychiatry* 2011; **1**(6)**:** e13.

124. Belzeaux R, Bergon A, Jeanjean V, Loriod B, Formisano-Treziny C, Verrier L*, et al*. Responder and nonresponder patients exhibit different peripheral transcriptional signatures during major depressive episode. *Transl Psychiatry* 2012; **2**(11)**:** e185.

125. Hennings JM, Uhr M, Klengel T, Weber P, Putz B, Touma C*, et al*. RNA expression profiling in depressed patients suggests retinoid-related orphan receptor alpha as a biomarker for antidepressant response. *Transl Psychiatry* 2015; **5**(3)**:** e538.

126. Ma W, Xia C, Ling P, Qiu M, Luo Y, Tan TH*, et al*. Leukocyte-specific adaptor protein Grap2 interacts with hematopoietic progenitor kinase 1 (HPK1) to activate JNK signaling pathway in T lymphocytes. *Oncogene* 2001; **20**(14)**:** 1703-1714.

127. Caliskan M, Cusanovich DA, Ober C, Gilad Y. The effects of EBV transformation on gene expression levels and methylation profiles. *Hum Mol Genet* 2011; **20**(8)**:** 1643-1652.

128. Sie L, Loong S, Tan EK. Utility of lymphoblastoid cell lines. *J Neurosci Res* 2009; **87**(9)**:** 1953-1959.

129. Morag A, Pasmanik-Chor M, Oron-Karni V, Rehavi M, Stingl JC, Gurwitz D. Genome-wide expression profiling of human lymphoblastoid cell lines identifies CHL1 as a putative SSRI antidepressant response biomarker. *Pharmacogenomics* 2011; **12**(2)**:** 171-184.

130. Koide R, Kobayashi S, Shimohata T, Ikeuchi T, Maruyama M, Saito M*, et al*. A neurological disease caused by an expanded CAG trinucleotide repeat in the TATA-binding protein gene: a new polyglutamine disease? *Hum Mol Genet* 1999; **8**(11)**:** 2047-2053.

131. Kobayashi H, Kruger R, Markopoulou K, Wszolek Z, Chase B, Taka H*, et al*. Haploinsufficiency at the alpha-synuclein gene underlies phenotypic severity in familial Parkinson's disease. *Brain* 2003; **126**(Pt 1)**:** 32-42.

132. Gutekunst CA, Levey AI, Heilman CJ, Whaley WL, Yi H, Nash NR*, et al*. Identification and localization of huntingtin in brain and human lymphoblastoid cell lines with anti-fusion protein antibodies. *PNAS USA* 1995; **92**(19)**:** 8710-8714.

133. Abe K, St George-Hyslop PH, Tanzi RE, Kogure K. Induction of amyloid precursor protein mRNA after heat shock in cultured human lymphoblastoid cells. *Neurosci Lett* 1991; **125**(2)**:** 169-171.

134. Breitfeld J, Scholl C, Steffens M, Brandenburg K, Probst-Schendzielorz K, Efimkina O*, et al*. Proliferation rates and gene expression profiles in human lymphoblastoid cell lines from patients with depression characterized in response to antidepressant drug therapy. *Transl Psychiatry* 2016; **6**(11)**:** e950-e950.

135. Breitfeld J, Scholl C, Steffens M, Laje G, Stingl JC. Gene expression and proliferation biomarkers for antidepressant treatment resistance. *Transl Psychiatry* 2017; **7**(3)**:** e1061.

136. Tate CG, Blakely RD. The effect of N-linked glycosylation on activity of the Na(+)- and Cl(-)-dependent serotonin transporter expressed using recombinant baculovirus in insect cells. *J Biol Chem* 1994; **269**(42)**:** 26303-26310.

137. Rudnick G. Structure/function relationships in serotonin transporter: new insights from the structure of a bacterial transporter. *Handb Exp Pharmacol* 2006;(175)**:** 59-73.

138. Amara SG, Kuhar MJ. Neurotransmitter transporters: recent progress. *Annu Rev Neurosci* 1993; **16:** 73-93.

139. Uhl GR, Johnson PS. Neurotransmitter transporters: three important gene families for neuronal function. *J Exp Biol* 1994; **196:** 229-236.

140. Faraj BA, Olkowski ZL, Jackson RT. Expression of a high-affinity serotonin transporter in human lymphocytes. *Int J Immunopharmacol* 1994; **16**(7)**:** 561-567.

141. Launay JM, Geoffroy C, Mutel V, Buckle M, Cesura A, Alouf JE*, et al*. One-step purification of the serotonin transporter located at the human platelet plasma membrane. *J Biol Chem* 1992; **267**(16)**:** 11344-11351.

142. Balkovetz DF, Tiruppathi C, Leibach FH, Mahesh VB, Ganapathy V. Evidence for an imipramine-sensitive serotonin transporter in human placental brush-border membranes. *J Biol Chem* 1989; **264**(4)**:** 2195-2198.

143. Wade PR, Chen J, Jaffe B, Kassem IS, Blakely RD, Gershon MD. Localization and function of a 5-HT transporter in crypt epithelia of the gastrointestinal tract. *J Neurosci* 1996; **16**(7)**:** 2352-2364.

144. Sur C, Betz H, Schloss P. Localization of the serotonin transporter in rat spinal cord. *Eur J Neurosci* 1996; **8**(12)**:** 2753-2757.

145. Legutko R, Gannon RL. Serotonin transporter localization in the hamster suprachiasmatic nucleus. *Brain Res* 2001; **893**(1-2)**:** 77-83.

146. Sutcliffe JS, Delahanty RJ, Prasad HC, McCauley JL, Han Q, Jiang L*, et al*. Allelic heterogeneity at the serotonin transporter locus (SLC6A4) confers susceptibility to autism and rigid-compulsive behaviors. *Am J Hum Genet* 2005; **77**(2)**:** 265-279.

147. Lesch KP, Bengel D, Heils A, Sabol SZ, Greenberg BD, Petri S*, et al*. Association of anxiety-related traits with a polymorphism in the serotonin transporter gene regulatory region. *Science* 1996; **274**(5292)**:** 1527-1531.

148. Caspi A, Sugden K, Moffitt TE, Taylor A, Craig IW, Harrington H*, et al*. Influence of life stress on depression: moderation by a polymorphism in the 5-HTT gene. *Science* 2003; **301**(5631)**:** 386-389.

149. Sanchez C, Bergqvist PB, Brennum LT, Gupta S, Hogg S, Larsen A*, et al*. Escitalopram, the S-(+)-enantiomer of citalopram, is a selective serotonin reuptake inhibitor with potent effects in animal models predictive of antidepressant and anxiolytic activities. *Psychopharmacology (Berl)* 2003; **167**(4)**:** 353-362.

150. Rudnick G, Wall SC. The molecular mechanism of "ecstasy" [3,4-methylenedioxy-methamphetamine (MDMA)]: serotonin transporters are targets for MDMA-induced serotonin release. *PNAS USA* 1992; **89**(5)**:** 1817-1821.

151. Rudnick G, Wall SC. Binding of the cocaine analog 2 beta-[3H] carboxymethoxy-3 beta-(4-fluorophenyl)tropane to the serotonin transporter. *Mol Pharmacol* 1991; **40**(3)**:** 421-426.

152. D'Souza UM, Powell-Smith G, Haddley K, Powell TR, Bubb VJ, Price T*, et al*. Allele-specific expression of the serotonin transporter and its transcription factors following lamotrigine treatment in vitro. *American journal of medical genetics Part B, Am J Med Genet B Neuropsychiatr Genet* 2013; **162B**(5)**:** 474-483.

153. Chen NH, Reith ME, Quick MW. Synaptic uptake and beyond: the sodium- and chloride-dependent neurotransmitter transporter family SLC6. *Pflugers Arch* 2004; **447**(5)**:** 519-531.

154. Noordam R, Aarts N, Verhamme KM, Sturkenboom MC, Stricker BH, Visser LE. Prescription and indication trends of antidepressant drugs in the Netherlands between 1996 and 2012: a dynamic population-based study. *Eur J Clin Pharmacol* 2015; **71**(3)**:** 369-375.

155. Forns J, Pottegard A, Reinders T, Poblador-Plou B, Morros R, Brandt L*, et al*. Antidepressant use in Denmark, Germany, Spain, and Sweden between 2009 and 2014: Incidence and comorbidities of antidepressant initiators. *J Affect Disord* 2019; **249:** 242-252.

156. Bauer M, Monz BU, Montejo AL, Quail D, Dantchev N, Demyttenaere K*, et al*. Prescribing patterns of antidepressants in Europe: results from the Factors Influencing Depression Endpoints Research (FINDER) study. *Europ Psychiatr* 2008; **23**(1)**:** 66-73.

157. Abbing-Karahagopian V, Huerta C, Souverein PC, de Abajo F, Leufkens HG, Slattery J*, et al*. Antidepressant prescribing in five European countries: application of common definitions to assess the prevalence, clinical observations, and methodological implications. *Eur J Clin Pharmacol* 2014; **70**(7)**:** 849-857.

158. Omasits U, Ahrens CH, Muller S, Wollscheid B. Protter: interactive protein feature visualization and integration with experimental proteomic data. *Bioinformatics* 2014; **30**(6)**:** 884-886.

159. Lesch KP, Balling U, Gross J, Strauss K, Wolozin BL, Murphy DL*, et al*. Organization of the human serotonin transporter gene. *J Neural Transm Gen Sect* 1994; **95**(2)**:** 157-162.

160. Levinson DF. The genetics of depression: a review. *Biol psychiatry* 2006; **60**(2)**:** 84-92.

161. Canli T, Lesch KP. Long story short: the serotonin transporter in emotion regulation and social cognition. *Nat Neurosci* 2007; **10**(9)**:** 1103-1109.

162. Wendland JR, Martin BJ, Kruse MR, Lesch KP, Murphy DL. Simultaneous genotyping of four functional loci of human SLC6A4, with a reappraisal of 5-HTTLPR and rs25531. *Mol psychiatry* 2006; **11**(3)**:** 224-226.

163. Murphy DL, Lerner A, Rudnick G, Lesch KP. Serotonin transporter: gene, genetic disorders, and pharmacogenetics. *Mol Interv* 2004; **4**(2)**:** 109-123.

164. Gonda X. [The serotonin transporter gene and personality: association of the 5-HTTLPR s allele, anxiety, depression and affective temperaments]. *Orv Hetil* 2008; **149**(33)**:** 1569-1573.

165. Dorado P, Penas-Lledo EM, Gonzalez AP, Caceres MC, Cobaleda J, Llerena A. Increased risk for major depression associated with the short allele of the serotonin transporter promoter region (5-HTTLPR-S) and the CYP2C9*3 allele. *Fundam Clin Pharmacol* 2007; **21**(4)**:** 451-453.

166. Anguelova M, Benkelfat C, Turecki G. A systematic review of association studies investigating genes coding for serotonin receptors and the serotonin transporter: I. Affective disorders. *Mol psychiatry* 2003; **8**(6)**:** 574-591.

167. Kiyohara C, Yoshimasu K. Association between major depressive disorder and a functional polymorphism of the 5-hydroxytryptamine (serotonin) transporter gene: a meta-analysis. *Psychiatr Genet* 2010; **20**(2)**:** 49-58.

168. Clarke H, Flint J, Attwood AS, Munafo MR. Association of the 5- HTTLPR genotype and unipolar depression: a meta-analysis. *Psychol Med* 2010; **40**(11)**:** 1767-1778.

169. Uher R, Caspi A, Houts R, Sugden K, Williams B, Poulton R*, et al*. Serotonin transporter gene moderates childhood maltreatment's effects on persistent but not single-episode depression: replications and implications for resolving inconsistent results. *J Affect Disord* 2011; **135**(1-3)**:** 56-65.

170. Hu XZ, Rush AJ, Charney D, Wilson AF, Sorant AJ, Papanicolaou GJ*, et al*. Association between a functional serotonin transporter promoter polymorphism and citalopram treatment in adult outpatients with major depression. *Arch. Gen. Psychiatry* 2007; **64**(7)**:** 783-792.

171. Serretti A, Kato M, De Ronchi D, Kinoshita T. Meta-analysis of serotonin transporter gene promoter polymorphism (5-HTTLPR) association with selective serotonin reuptake inhibitor efficacy in depressed patients. *Mol psychiatry* 2007; **12**(3)**:** 247-257.

172. Taylor MJ, Sen S, Bhagwagar Z. Antidepressant response and the serotonin transporter gene-linked polymorphic region. *Biol psychiatry* 2010; **68**(6)**:** 536-543.

173. Iurescia S, Seripa D, Rinaldi M. Role of the 5-HTTLPR and SNP Promoter Polymorphisms on Serotonin Transporter Gene Expression: a Closer Look at Genetic Architecture and In Vitro Functional Studies of Common and Uncommon Allelic Variants. *Mol Neurobiol* 2016; **53**(8)**:** 5510-5526.

174. Reimold M, Knobel A, Rapp MA, Batra A, Wiedemann K, Strohle A*, et al*. Central serotonin transporter levels are associated with stress hormone response and anxiety. *Psychopharmacology (Berl)* 2011; **213**(2-3)**:** 563-572.

175. Gryglewski G, Lanzenberger R, Kranz GS, Cumming P. Meta-analysis of molecular imaging of serotonin transporters in major depression. *J Cereb Blood Flow Metab* 2014; **34**(7)**:** 1096-1103.

176. Uebelhack R, Franke L, Herold N, Plotkin M, Amthauer H, Felix R. Brain and platelet serotonin transporter in humans-correlation between [123I]-ADAM SPECT and serotonergic measurements in platelets. *Neurosci Lett* 2006; **406**(3)**:** 153-158.

177. Ellis PM, Salmond C. Is platelet imipramine binding reduced in depression? A meta-analysis. *Biol Psychiatry* 1994; **36**(5):292-9.

178. Lima L, Urbina M. Serotonin transporter modulation in blood lymphocytes from patients with major depression. *Cell Mol Neurobiol* 2002; **22**(5-6)**:** 797-804.

179. Blakely RD, Bauman AL. Biogenic amine transporters: regulation in flux. *Curr Opin Neurobiol* 2000; **10**(3)**:** 328-336.

180. Urban JD, Clarke WP, von Zastrow M, Nichols DE, Kobilka B, Weinstein H*, et al*. Functional selectivity and classical concepts of quantitative pharmacology. *J Pharmacol Exp Ther* 2007; **320**(1)**:** 1-13.

181. Zhu CB, Hewlett WA, Feoktistov I, Biaggioni I, Blakely RD. Adenosine receptor, protein kinase G, and p38 mitogen-activated protein kinase-dependent up-regulation of serotonin transporters involves both transporter trafficking and activation. *Mol Pharmacol* 2004; **65**(6)**:** 1462-1474.

182. Samuvel DJ, Jayanthi LD, Bhat NR, Ramamoorthy S. A role for p38 mitogen-activated protein kinase in the regulation of the serotonin transporter: evidence for distinct cellular mechanisms involved in transporter surface expression. *J Neurosci* 2005; **25**(1)**:** 29-41.

183. Urbina M, Pineda S, Pinango L, Carreira I, Lima L. [3H]Paroxetine binding to human peripheral lymphocyte membranes of patients with major depression before and after treatment with fluoxetine. *Int J Immunopharmacol* 1999; **21**(10)**:** 631-646.

184. Iga J, Watanabe SY, Numata S, Umehara H, Nishi A, Kinoshita M*, et al*. Association study of polymorphism in the serotonin transporter gene promoter, methylation profiles,

and expression in patients with major depressive disorder. *Hum Psychopharmacol* 2016; **31**(3)**:** 193-199.

185. Belzeaux R, Loundou A, Azorin JM, Naudin J, Ibrahim EC. Longitudinal monitoring of the serotonin transporter gene expression to assess major depressive episode evolution. *Neuropsychobiology* 2014; **70**(4)**:** 220-227.

186. Horschitz S, Hummerich R, Schloss P. Down-regulation of the rat serotonin transporter upon exposure to a selective serotonin reuptake inhibitor. *Neuroreport* 2001; **12**(10)**:** 2181-2184.

187. Lau T, Horschitz S, Berger S, Bartsch D, Schloss P. Antidepressant-induced internalization of the serotonin transporter in serotonergic neurons. *FASEB J* 2008; **22**(6)**:** 1702-1714.

188. Rivera-Baltanas T, Olivares JM, Calado-Otero M, Kalynchuk LE, Martinez-Villamarin JR, Caruncho HJ. Serotonin transporter clustering in blood lymphocytes as a putative biomarker of therapeutic efficacy in major depressive disorder. *J Affect Disord* 2012; **137**(1-3)**:** 46-55.

189. Sadowski M, Suryadinata R, Tan AR, Roesley SN, Sarcevic B. Protein monoubiquitination and polyubiquitination generate structural diversity to control distinct biological processes. *IUBMB Life* 2012; **64**(2)**:** 136-142.

190. Sadowski M, Sarcevic B. Mechanisms of mono- and poly-ubiquitination: Ubiquitination specificity depends on compatibility between the E2 catalytic core and amino acid residues proximal to the lysine. *Cell Div* 2010; **5:** 19.

191. Haglund K, Sigismund S, Polo S, Szymkiewicz I, Di Fiore PP, Dikic I. Multiple monoubiquitination of RTKs is sufficient for their endocytosis and degradation. *Nat Cell Biol* 2003; **5**(5)**:** 461-466.

192. Thrower JS, Hoffman L, Rechsteiner M, Pickart CM. Recognition of the polyubiquitin proteolytic signal. *EMBO J* 2000; **19**(1)**:** 94-102.

193. Jin L, Williamson A, Banerjee S, Philipp I, Rape M. Mechanism of ubiquitin-chain formation by the human anaphase-promoting complex. *Cell* 2008; **133**(4)**:** 653-665.

194. Passmore LA, Barford D. Getting into position: the catalytic mechanisms of protein ubiquitylation. *Biochem J* 2004; **379**(Pt 3)**:** 513-525.

195. Mouri A, Ikeda M, Koseki T, Iwata N, Nabeshima T. The ubiquitination of serotonin transporter in lymphoblasts derived from fluvoxamine-resistant depression patients. *Neurosci Lett* 2016; **617:** 22-26.

196. Barakat AK, Scholl C, Steffens M, Brandenburg K, Ising M, Lucae S*, et al*. Citalopram-induced pathways regulation and tentative treatment-outcome-predicting biomarkers

in lymphoblastoid cell lines from depression patients. *Transl Psychiatry* 2020; **10**(1)**:** 210.

197. Rush AJ, Fava M, Wisniewski SR, Lavori PW, Trivedi MH, Sackeim HA*, et al*. Sequenced treatment alternatives to relieve depression (STAR*D): rationale and design. *Controlled clinical trials* 2004; **25**(1)**:** 119-142.

198. Tosato G, Cohen JI. Generation of Epstein-Barr Virus (EBV)-immortalized B cell lines. *Curr Protoc Immunol* 2007; **Chapter 7:** Unit 7 22.

199. Berlin IL. Wirkstoffbestimmung von Psychopharmaka Teil IV Pharmakologische Besonderheiten ausgewählter SSRI und SSNRI. *Diagnostikinformation* (273).

200. Sidhu J, Priskorn M, Poulsen M, Segonzac A, Grollier G, Larsen F. Steady-state pharmacokinetics of the enantiomers of citalopram and its metabolites in humans. *Chirality* 1997; **9**(7)**:** 686-692.

201. Oved K, Morag A, Pasmanik-Chor M, Oron-Karni V, Shomron N, Rehavi M*, et al*. Genome-wide miRNA expression profiling of human lymphoblastoid cell lines identifies tentative SSRI antidepressant response biomarkers. *Pharmacogenomics* 2012; **13**(10)**:** 1129-1139.

202. O'Brien FE, O'Connor RM, Clarke G, Dinan TG, Griffin BT, Cryan JF. P-glycoprotein inhibition increases the brain distribution and antidepressant-like activity of escitalopram in rodents. *Neuropsychopharmacology* 2013; **38**(11)**:** 2209-2219.

203. Nedahl M, Johansen SS, Linnet K. Reference Brain/Blood Concentrations of Citalopram, Duloxetine, Mirtazapine and Sertraline. *J Anal Toxicol* 2018; **42**(3)**:** 149-156.

204. Brustolim D, Ribeiro-dos-Santos R, Kast RE, Altschuler EL, Soares MB. A new chapter opens in anti-inflammatory treatments: the antidepressant bupropion lowers production of tumor necrosis factor-alpha and interferon-gamma in mice. *Int Immunopharmacol* 2006; **6**(6)**:** 903-907.

205. Campos AC, Vaz GN, Saito VM, Teixeira AL. Further evidence for the role of interferon-gamma on anxiety- and depressive-like behaviors: involvement of hippocampal neurogenesis and NGF production. *Neurosci Lett* 2014; **578:** 100-105.

206. Dow AL, Russell DS, Duman RS. Regulation of activin mRNA and Smad2 phosphorylation by antidepressant treatment in the rat brain: effects in behavioral models. *J Neurosci* 2005; **25**(20)**:** 4908-4916.

207. Krampert M, Chirasani SR, Wachs FP, Aigner R, Bogdahn U, Yingling JM*, et al*. Smad7 regulates the adult neural stem/progenitor cell pool in a transforming growth factor beta- and bone morphogenetic protein-independent manner. *Mol Cell Biol* 2010; **30**(14)**:** 3685-3694.

208. Zoicas I, Schumacher F, Kleuser B, Reichel M, Gulbins E, Fejtova A*, et al*. The Forebrain-Specific Overexpression of Acid Sphingomyelinase Induces Depressive-Like Symptoms in Mice. *Cells* 2020; **9**(5).

209. Beckmann N, Sharma D, Gulbins E, Becker KA, Edelmann B. Inhibition of acid sphingomyelinase by tricyclic antidepressants and analogons. *Front Physiol* 2014; **5:** 331.

210. Gass P, Riva MA. CREB, neurogenesis and depression. *Bioessays* 2007; **29**(10)**:** 957-961.

211. Marsden WN. Synaptic plasticity in depression: molecular, cellular and functional correlates. *Prog Neuropsychopharmacol Biol Psychiatry* 2013; **43:** 168-184.

212. Karege F, Perret G, Bondolfi G, Schwald M, Bertschy G, Aubry JM. Decreased serum brain-derived neurotrophic factor levels in major depressed patients. *Psychiatry Res* 2002; **109**(2)**:** 143-148.

213. Kelder T, Pico AR, Hanspers K, van Iersel MP, Evelo C, Conklin BR. Mining biological pathways using WikiPathways web services. *PloS one* 2009; **4**(7)**:** e6447.

214. Kraft JB, Slager SL, McGrath PJ, Hamilton SP. Sequence analysis of the serotonin transporter and associations with antidepressant response. *Biol psychiatry* 2005; **58**(5)**:** 374-381.

215. Schurks M, Frahnow A, Diener HC, Kurth T, Rosskopf D, Grabe HJ. Bi-allelic and tri-allelic 5-HTTLPR polymorphisms and triptan non-response in cluster headache. *J Headache Pain* 2014; **15**(1)**:** 46.

216. Hu XZ, Lipsky RH, Zhu G, Akhtar LA, Taubman J, Greenberg BD*, et al*. Serotonin transporter promoter gain-of-function genotypes are linked to obsessive-compulsive disorder. *Am J Hum Genet* 2006; **78**(5)**:** 815-826.

217. Cell Signaling T, Weinberg RA, Comb MJ. *CST Guide: Pathways & Protocols*. Cell Signaling Technology, 2015.

218. Kim DS, Burt AA, Ranchalis JE, Wilmot B, Smith JD, Patterson KE*, et al*. Sequencing of sporadic Attention-Deficit Hyperactivity Disorder (ADHD) identifies novel and potentially pathogenic de novo variants and excludes overlap with genes associated with autism spectrum disorder. *Am J Med Genet B Neuropsychiatr Genet* 2017; **174**(4)**:** 381-389.

219. Ashley-Koch AE, Garrett ME, Gibson J, Liu Y, Dennis MF, Kimbrel NA*, et al*. Genome-wide association study of posttraumatic stress disorder in a cohort of Iraq-Afghanistan era veterans. *J Affect Disord* 2015; **184:** 225-234.

220. McLatchie LM, Fraser NJ, Main MJ, Wise A, Brown J, Thompson N*, et al*. RAMPs regulate the transport and ligand specificity of the calcitonin-receptor-like receptor. *Nature* 1998; **393**(6683)**:** 333-339.

221. Mathe AA, Agren H, Lindstrom L, Theodorsson E. Increased concentration of calcitonin gene-related peptide in cerebrospinal fluid of depressed patients. A possible trait marker of major depressive disorder. *Neurosci Lett* 1994; **182**(2)**:** 138-142.

222. Grant SG, O'Dell TJ, Karl KA, Stein PL, Soriano P, Kandel ER. Impaired long-term potentiation, spatial learning, and hippocampal development in fyn mutant mice. *Science* 1992; **258**(5090)**:** 1903-1910.

223. Scott LJ, Muglia P, Kong XQ, Guan W, Flickinger M, Upmanyu R*, et al*. Genome-wide association and meta-analysis of bipolar disorder in individuals of European ancestry. *PNAS USA* 2009; **106**(18)**:** 7501-7506.

224. Orsetti M, Di Brisco F, Rinaldi M, Dallorto D, Ghi P. Some molecular effectors of antidepressant action of quetiapine revealed by DNA microarray in the frontal cortex of anhedonic rats. *Pharmacogenet Genomics* 2009; **19**(8)**:** 600-612.

225. Tripp A, Oh H, Guilloux JP, Martinowich K, Lewis DA, Sibille E. Brain-derived neurotrophic factor signaling and subgenual anterior cingulate cortex dysfunction in major depressive disorder. *Am J Psychiatry* 2012; **169**(11)**:** 1194-1202.

226. Pu M, Zhang Z, Xu Z, Shi Y, Geng L, Yuan Y*, et al*. Influence of genetic polymorphisms in the glutamatergic and GABAergic systems and their interactions with environmental stressors on antidepressant response. *Pharmacogenomics* 2013; **14**(3)**:** 277-288.

227. Philippi A, Tores F, Carayol J, Rousseau F, Letexier M, Roschmann E*, et al*. Association of autism with polymorphisms in the paired-like homeodomain transcription factor 1 (PITX1) on chromosome 5q31: a candidate gene analysis. *BMC Med Gen* 2007; **8:** 74.

228. Hornberg H, Wollerton-van Horck F, Maurus D, Zwart M, Svoboda H, Harris WA*, et al*. RNA-binding protein Hermes/RBPMS inversely affects synapse density and axon arbor formation in retinal ganglion cells in vivo. *J Neurosci* 2013; **33**(25)**:** 10384-10395.

229. Goswami DB, Jernigan CS, Chandran A, Iyo AH, May WL, Austin MC*, et al*. Gene expression analysis of novel genes in the prefrontal cortex of major depressive disorder subjects. *Prog Neuropsychopharmacol Biol Psychiatry* 2013; **43:** 126-133.

230. Lee CH, Javed D, Althaus AL, Parent JM, Umemori H. Neurogenesis is enhanced and mossy fiber sprouting arises in FGF7-deficient mice during development. *Mol Cell Neurosci* 2012; **51**(3-4)**:** 61-67.

231. Zhen L, Shao T, Luria V, Li G, Li Z, Xu Y*, et al*. EphB2 Deficiency Induces Depression-Like Behaviors and Memory Impairment: Involvement of NMDA 2B Receptor Dependent Signaling. *Front Pharmacol* 2018; **9:** 862.

232. Wigner P, Czarny P, Synowiec E, Bijak M, Talarowska M, Galecki P*, et al*. Variation of genes encoding KAT1, AADAT and IDO1 as a potential risk of depression development. *Europ Psychiatr* 2018; **52:** 95-103.

233. Kaut O, Schmitt I, Hofmann A, Hoffmann P, Schlaepfer TE, Wullner U*, et al*. Aberrant NMDA receptor DNA methylation detected by epigenome-wide analysis of hippocampus and prefrontal cortex in major depression. *Eur Arch Psychiatry Clin Neurosci* 2015; **265**(4)**:** 331-341.

234. Jiang S, Yang W, Qiu Y, Chen HZ, Alzheimer's Disease Neuroimaging I. Identification of novel quantitative traits-associated susceptibility loci for APOE epsilon 4 non-carriers of Alzheimer's disease. *Curr Alzheimer Res* 2015; **12**(3)**:** 218-227.

235. Odgerel Z, Talati A, Hamilton SP, Levinson DF, Weissman MM. Genotyping serotonin transporter polymorphisms 5-HTTLPR and rs25531 in European- and African-American subjects from the National Institute of Mental Health's Collaborative Center for Genomic Studies. *Transl Psychiatry* 2013; **3**(9)**:** e307.

236. Massague J. TGF-beta signal transduction. *Annu Rev Biochem* 1998; **67:** 753-791.

237. Kubiczkova L, Sedlarikova L, Hajek R, Sevcikova S. TGF-beta - an excellent servant but a bad master. *J Transl Med* 2012; **10:** 183.

238. Schmitt E, Hoehn P, Huels C, Goedert S, Palm N, Rude E*, et al*. T helper type 1 development of naive CD4+ T cells requires the coordinate action of interleukin-12 and interferon-gamma and is inhibited by transforming growth factor-beta. *Eur J Immunol* 1994; **24**(4)**:** 793-798.

239. Musil R, Schwarz MJ, Riedel M, Dehning S, Cerovecki A, Spellmann I*, et al*. Elevated macrophage migration inhibitory factor and decreased transforming growth factor-beta levels in major depression--no influence of celecoxib treatment. *J Affect Disord* 2011; **134**(1-3)**:** 217-225.

240. Pallavi P, Sagar R, Mehta M, Sharma S, Subramanium A, Shamshi F*, et al*. Serum cytokines and anxiety in adolescent depression patients: Gender effect. *Psychiatry Res* 2015; **229**(1-2)**:** 374-380.

241. Davami MH, Baharlou R, Ahmadi Vasmehjani A, Ghanizadeh A, Keshtkar M, Dezhkam I*, et al*. Elevated IL-17 and TGF-beta Serum Levels: A Positive Correlation between T-helper 17 Cell-Related Pro-Inflammatory Responses with Major Depressive Disorder. *Basic Clin Neurosci* 2016; **7**(2)**:** 137-142.

242. Lee KM, Kim YK. The role of IL-12 and TGF-beta1 in the pathophysiology of major depressive disorder. *Int Immunopharmacol* 2006; **6**(8)**:** 1298-1304.

243. Slusarczyk J, Trojan E, Glombik K, Piotrowska A, Budziszewska B, Kubera M*, et al*. Targeting the NLRP3 Inflammasome-Related Pathways via Tianeptine Treatment-Suppressed Microglia Polarization to the M1 Phenotype in Lipopolysaccharide-Stimulated Cultures. *Int J Mol Sci* 2018; **19**(7).

244. Moore SR. Commentary: What is the case for candidate gene approaches in the era of high-throughput genomics? A response to Border and Keller (2017). *J Child Psychol Psychiatry* 2017; **58**(3)**:** 331-334.

245. Brunton L.L. H-DR, Knollmann B.C. Drug Therapy of Depression and Anxiety Disorders. *Goodman & Gilman's: The Pharmacological Basis of Therapeutics* 2017; **13e**.

246. Schwabe U P, D., Ludwig, W.-D., Klauber. Arzneimittelverbrauch in Deutschland. *Arzneiverordnungs-Report* 2019.

247. Erlander MG, Tillakaratne NJ, Feldblum S, Patel N, Tobin AJ. Two genes encode distinct glutamate decarboxylases. *Neuron* 1991; **7**(1)**:** 91-100.

248. Sanacora G, Treccani G, Popoli M. Towards a glutamate hypothesis of depression: an emerging frontier of neuropsychopharmacology for mood disorders. *Neuropharmacology* 2012; **62**(1)**:** 63-77.

249. Maguire J. Neuroactive Steroids and GABAergic Involvement in the Neuroendocrine Dysfunction Associated With Major Depressive Disorder and Postpartum Depression. *Front Cell Neurosci* 2019; **13:** 83.

250. Utge S, Soronen P, Partonen T, Loukola A, Kronholm E, Pirkola S*, et al*. A population-based association study of candidate genes for depression and sleep disturbance. *American journal of medical genetics Part B, Am J Med Genet B Neuropsychiatr Genet* 2010; **153B**(2)**:** 468-476.

251. Lin CH, Huang MW, Lin CH, Huang CH, Lane HY. Altered mRNA expressions for N-methyl-D-aspartate receptor-related genes in WBC of patients with major depressive disorder. *J Affect Disord* 2019; **245:** 1119-1125.

252. Thase ME. Evaluating antidepressant therapies: remission as the optimal outcome. *J Clin Psychiatry* 2003; **64 Suppl 13:** 18-25.

253. Ishibashi K, Kanno E, Itoh T, Fukuda M. Identification and characterization of a novel Tre-2/Bub2/Cdc16 (TBC) protein that possesses Rab3A-GAP activity. *Genes Cells* 2009; **14**(1)**:** 41-52.

254. Oguchi ME, Noguchi K, Fukuda M. TBC1D12 is a novel Rab11-binding protein that modulates neurite outgrowth of PC12 cells. *PloS one* 2017; **12**(4)**:** e0174883.

255. Herve M, Bergon A, Le Guisquet AM, Leman S, Consoloni JL, Fernandez-Nunez N*, et al*. Translational Identification of Transcriptional Signatures of Major Depression and Antidepressant Response. *Front Mol Neurosci* 2017; **10:** 248.

256. Patel V. Talking sensibly about depression. *PLoS medicine* 2017; **14**(4)**:** e1002257.

257. McGorry P, Nelson B. Why We Need a Transdiagnostic Staging Approach to Emerging Psychopathology, Early Diagnosis, and Treatment. *JAMA Psychiatry* 2016; **73**(3)**:** 191-192.

258. Herrman H, Kieling C, McGorry P, Horton R, Sargent J, Patel V. Reducing the global burden of depression: a Lancet-World Psychiatric Association Commission. *Lancet* 2019; **393**(10189)**:** e42-e43.

259. Strawbridge R, Young AH, Cleare AJ. Biomarkers for depression: recent insights, current challenges and future prospects. *Neuropsychiatr Dis Treat* 2017; **13:** 1245-1262.

260. O'Reardon JP, Brunswick DJ, Amsterdam JD. Treatment-resistant depression in the age of serotonin: Evolving strategies. *Curr Opin Psychiatry* 2000; **13**(1)**:** 93-98.

261. Fagiolini A, Kupfer DJ. Is treatment-resistant depression a unique subtype of depression? *Biol psychiatry* 2003; **53**(8)**:** 640-648.

262. Souery D, Amsterdam J, de Montigny C, Lecrubier Y, Montgomery S, Lipp O*, et al*. Treatment resistant depression: methodological overview and operational criteria. *Eur Neuropsychopharmacol* 1999; **9**(1-2)**:** 83-91.

263. Pies R. Are antidepressants effective in the acute and long-term treatment of depression? Sic et Non. *Innov Clin Neurosci* 2012; **9**(5-6)**:** 31-40.

264. Deneen B, Ho R, Lukaszewicz A, Hochstim CJ, Gronostajski RM, Anderson DJ. The transcription factor NFIA controls the onset of gliogenesis in the developing spinal cord. *Neuron* 2006; **52**(6)**:** 953-968.

265. Heng YH, McLeay RC, Harvey TJ, Smith AG, Barry G, Cato K*, et al*. NFIX regulates neural progenitor cell differentiation during hippocampal morphogenesis. *Cereb Cortex* 2014; **24**(1)**:** 261-279.

266. Piper M, Harris L, Barry G, Heng YH, Plachez C, Gronostajski RM*, et al*. Nuclear factor one X regulates the development of multiple cellular populations in the postnatal cerebellum. *J Comp Neurol* 2011; **519**(17)**:** 3532-3548.

267. Matuzelski E, Bunt J, Harkins D, Lim JWC, Gronostajski RM, Richards LJ*, et al*. Transcriptional regulation of Nfix by NFIB drives astrocytic maturation within the developing spinal cord. *Dev Biol* 2017; **432**(2)**:** 286-297.

268. Rolando C, Erni A, Grison A, Beattie R, Engler A, Gokhale PJ*, et al*. Multipotency of Adult Hippocampal NSCs In Vivo Is Restricted by Drosha/NFIB. *Cell stem cell* 2016; **19**(5)**:** 653-662.

269. Cotter D, Mackay D, Chana G, Beasley C, Landau S, Everall IP. Reduced neuronal size and glial cell density in area 9 of the dorsolateral prefrontal cortex in subjects with major depressive disorder. *Cereb Cortex* 2002; **12**(4)**:** 386-394.

270. Gos T, Schroeter ML, Lessel W, Bernstein HG, Dobrowolny H, Schiltz K*, et al*. S100B-immunopositive astrocytes and oligodendrocytes in the hippocampus are differentially afflicted in unipolar and bipolar depression: a postmortem study. *J Psychiatr Res* 2013; **47**(11)**:** 1694-1699.

271. Lisowski P, Stankiewicz AM, Goscik J, Wieczorek M, Zwierzchowski L, Swiergiel AH. Selection for stress-induced analgesia affects the mouse hippocampal transcriptome. *J Mol Neurosci* 2012; **47**(1)**:** 101-112.

272. Surget A, Wang Y, Leman S, Ibarguen-Vargas Y, Edgar N, Griebel G*, et al*. Corticolimbic transcriptome changes are state-dependent and region-specific in a rodent model of depression and of antidepressant reversal. *Neuropsychopharmacology* 2009; **34**(6)**:** 1363-1380.

273. Ponsuksili S, Du Y, Murani E, Schwerin M, Wimmers K. Elucidating molecular networks that either affect or respond to plasma cortisol concentration in target tissues of liver and muscle. *Genetics* 2012; **192**(3)**:** 1109-1122.

274. Schosser A, Serretti A, Souery D, Mendlewicz J, Zohar J, Montgomery S*, et al*. European Group for the Study of Resistant Depression (GSRD)--where have we gone so far: review of clinical and genetic findings. *Eur Neuropsychopharmacol* 2012; **22**(7)**:** 453-468.

275. Fabbri C, Kasper S, Kautzky A, Bartova L, Dold M, Zohar J*, et al*. Genome-wide association study of treatment-resistance in depression and meta-analysis of three independent samples. *The British journal of psychiatry : J Ment Sci* 2019; **214**(1)**:** 36-41.

276. Rush AJ, Trivedi MH, Wisniewski SR, Nierenberg AA, Stewart JW, Warden D*, et al*. Acute and longer-term outcomes in depressed outpatients requiring one or several treatment steps: a STAR*D report. *Am J Psychiatry* 2006; **163**(11)**:** 1905-1917.

277. Fabbri C, Crisafulli C, Calabro M, Spina E, Serretti A. Progress and prospects in pharmacogenetics of antidepressant drugs. *Expert Opin Drug Metab Toxicol* 2016; **12**(10)**:** 1157-1168.

278. Fabbri C, Porcelli S, Serretti A. From pharmacogenetics to pharmacogenomics: the way toward the personalization of antidepressant treatment. *Can J Psychiatry* 2014; **59**(2)**:** 62-75.

279. Martins-de-Souza D, Maccarrone G, Ising M, Kloiber S, Lucae S, Holsboer F*, et al*. Blood mononuclear cell proteome suggests integrin and Ras signaling as critical pathways for antidepressant treatment response. *Biol psychiatry* 2014; **76**(7)**:** e15-17.

280. Kaddurah-Daouk R, Boyle SH, Matson W, Sharma S, Matson S, Zhu H*, et al*. Pretreatment metabotype as a predictor of response to sertraline or placebo in depressed outpatients: a proof of concept. *Transl Psychiatry* 2011; **1**(7)**:** e26.

281. Gupta M, Neavin D, Liu D, Biernacka J, Hall-Flavin D, Bobo WV*, et al*. TSPAN5, ERICH3 and selective serotonin reuptake inhibitors in major depressive disorder: pharmacometabolomics-informed pharmacogenomics. *Mol psychiatry* 2016; **21**(12)**:** 1717-1725.

282. Rotroff DM, Corum DG, Motsinger-Reif A, Fiehn O, Bottrel N, Drevets WC*, et al*. Metabolomic signatures of drug response phenotypes for ketamine and esketamine in subjects with refractory major depressive disorder: new mechanistic insights for rapid acting antidepressants. *Transl Psychiatry* 2016; **6**(9)**:** e894.

283. Maes M. Evidence for an immune response in major depression: a review and hypothesis. *Prog Neuropsychopharmacol Biol Psychiatry* 1995; **19**(1)**:** 11-38.

284. Miller AH, Maletic V, Raison CL. Inflammation and its discontents: the role of cytokines in the pathophysiology of major depression. *Biol psychiatry* 2009; **65**(9)**:** 732-741.

285. Fabbri C, Marsano A, Albani D, Chierchia A, Calati R, Drago A*, et al*. PPP3CC gene: a putative modulator of antidepressant response through the B-cell receptor signaling pathway. *Pharmacogenomics J* 2014; **14**(5)**:** 463-472.

286. Mossner R, Mikova O, Koutsilieri E, Saoud M, Ehlis AC, Muller N*, et al*. Consensus paper of the WFSBP Task Force on Biological Markers: biological markers in depression. *World J Biol Psychiatry* 2007; **8**(3)**:** 141-174.

287. Castera L, Zigante F, Bastie A, Buffet C, Dhumeaux D, Hardy P. Incidence of interferon alfa-induced depression in patients with chronic hepatitis C. *Hepatology* 2002; **35**(4)**:** 978-979.

288. Feinstein A, O'Connor P, Feinstein K. Multiple sclerosis, interferon beta-1b and depression A prospective investigation. *Journal of neurology* 2002; **249**(7)**:** 815-820.

289. Malaguarnera M, Laurino A, Di Fazio I, Pistone G, Castorina M, Guccione N*, et al*. Neuropsychiatric effects and type of IFN-alpha in chronic hepatitis C. *J Interferon Cytokine Res* 2001; **21**(5)**:** 273-278.

290. Elangbam CS, Qualls CW, Jr., Dahlgren RR. Cell adhesion molecules--update. *Veter Pathol* 1997; **34**(1)**:** 61-73.

291. Stewart LT. Cell adhesion proteins and the pathogenesis of autism spectrum disorders. *J Neurophysiol* 2015; **113**(5)**:** 1283-1286.

292. Wang KS, Liu X, Arana TB, Thompson N, Weisman H, Devargas C*, et al*. Genetic association analysis of ITGB3 polymorphisms with age at onset of schizophrenia. *J Mol Neurosci* 2013; **51**(2)**:** 446-453.

293. Kao CF, Jia P, Zhao Z, Kuo PH. Enriched pathways for major depressive disorder identified from a genome-wide association study. *Int J Neuropsychopharmacol* 2012; **15**(10)**:** 1401-1411.

294. Bergstrom A, Jayatissa MN, Thykjaer T, Wiborg O. Molecular pathways associated with stress resilience and drug resistance in the chronic mild stress rat model of depression: a gene expression study. *J Mol Neurosci* 2007; **33**(2)**:** 201-215.

295. Lin E, Chen PS. Pharmacogenomics with antidepressants in the STAR*D study. *Pharmacogenomics* 2008; **9**(7)**:** 935-946.

296. Kraft JB, Peters EJ, Slager SL, Jenkins GD, Reinalda MS, McGrath PJ*, et al*. Analysis of association between the serotonin transporter and antidepressant response in a large clinical sample. *Biol psychiatry* 2007; **61**(6)**:** 734-742.

297. Huezo-Diaz P, Uher R, Smith R, Rietschel M, Henigsberg N, Marusic A*, et al*. Moderation of antidepressant response by the serotonin transporter gene. *The British journal of psychiatry : J Ment Sci* 2009; **195**(1)**:** 30-38.

298. Porcelli S, Fabbri C, Serretti A. Meta-analysis of serotonin transporter gene promoter polymorphism (5-HTTLPR) association with antidepressant efficacy. *Eur Neuropsychopharmacol* 2012; **22**(4)**:** 239-258.

299. Mrazek DA, Rush AJ, Biernacka JM, O'Kane DJ, Cunningham JM, Wieben ED*, et al*. SLC6A4 variation and citalopram response. *American journal of medical genetics Part B, Am J Med Genet B Neuropsychiatr Genet* 2009; **150B**(3)**:** 341-351.

300. Jang YJ, Lim SW, Moon YK, Kim SY, Lee H, Kim S*, et al*. 5-HTTLPR-rs25531 and Antidepressant Treatment Outcomes in Korean Patients with Major Depression. *Pharmacopsychiatry* 2021; **54**(6)**:** 269-278.

301. Heils A, Wichems C, Mossner R, Petri S, Glatz K, Bengel D*, et al*. Functional characterization of the murine serotonin transporter gene promoter in serotonergic raphe neurons. *J Neurochem* 1998; **70**(3)**:** 932-939.

302. Yammamoto H, Tanaka S, Tanaka A, Hide I, Seki T, Sakai N. Long-term exposure of RN46A cells expressing serotonin transporter (SERT) to a cAMP analog up-regulates SERT activity and is accompanied by neural differentiation of the cells. *J Pharmacol Sci* 2013; **121**(1)**:** 25-38.

303. Nyarko JNK, Quartey MO, Heistad RM, Pennington PR, Poon LJ, Knudsen KJ*, et al*. Glycosylation States of Pre- and Post-synaptic Markers of 5-HT Neurons Differ With Sex and 5-HTTLPR Genotype in Cortical Autopsy Samples. *Front Neurosci* 2018; **12:** 545.

304. Zitterl W, Stompe T, Aigner M, Zitterl-Eglseer K, Ritter K, Zettinig G*, et al*. Diencephalic serotonin transporter availability predicts both transporter occupancy and treatment response to sertraline in obsessive-compulsive checkers. *Biol psychiatry* 2009; **66**(12)**:** 1115-1122.

305. Kambeitz JP, Howes OD. The serotonin transporter in depression: Meta-analysis of in vivo and post mortem findings and implications for understanding and treating depression. *J Affect Disord* 2015; **186:** 358-366.

306. Chamba A, Holder MJ, Barnes NM, Gordon J. Characterisation of the endogenous human peripheral serotonin transporter SLC6A4 reveals surface expression without N-glycosylation. *J Neuroimmunol* 2008; **204**(1-2)**:** 75-84.

307. Pena S, Baccichet E, Urbina M, Carreira I, Lima L. Effect of mirtazapine treatment on serotonin transporter in blood peripheral lymphocytes of major depression patients. *Int Immunopharmacol* 2005; **5**(6)**:** 1069-1076.

308. Fazzino F, Montes C, Urbina M, Carreira I, Lima L. Serotonin transporter is differentially localized in subpopulations of lymphocytes of major depression patients. Effect of fluoxetine on proliferation. *J Neuroimmunol* 2008; **196**(1-2)**:** 173-180.

309. Ellis PM, Salmond C. Is platelet imipramine binding reduced in depression? A meta-analysis. *Biol psychiatry* 1994; **36**(5)**:** 292-299.

310. Watanabe SY, Numata S, Iga JI, Kinoshita M, Umehara H, Ishii K*, et al*. Gene expression-based biological test for major depressive disorder: an advanced study. *Neuropsychiatr Dis Treat* 2017; **13:** 535-541.

311. Tsao CW, Lin YS, Chen CC, Bai CH, Wu SR. Cytokines and serotonin transporter in patients with major depression. *Prog Neuropsychopharmacol Biol Psychiatry* 2006; **30**(5)**:** 899-905.

312. Belzeaux R, Azorin JM, Ibrahim EC. Monitoring candidate gene expression variations before, during and after a first major depressive episode in a 51-year-old man. *BMC Psychiatry* 2014; **14:** 73.

313. Gomez F, Venero C, Viveros MP, Garcia-Garcia L. Short-term fluoxetine treatment induces neuroendocrine and behavioral anxiogenic-like responses in adolescent male rats. *Exp Brain Res* 2015; **233**(3)**:** 983-995.

314. Keck ME, Sartori SB, Welt T, Muller MB, Ohl F, Holsboer F*, et al*. Differences in serotonergic neurotransmission between rats displaying high or low

anxiety/depression-like behaviour: effects of chronic paroxetine treatment. *J Neurochem* 2005; **92**(5)**:** 1170-1179.

315. Iwakawa HO, Tomari Y. The Functions of MicroRNAs: mRNA Decay and Translational Repression. *Trends Cell Biol* 2015; **25**(11)**:** 651-665.

316. Baudry A, Pietri M, Launay JM, Kellermann O, Schneider B. Multifaceted Regulations of the Serotonin Transporter: Impact on Antidepressant Response. *Front Neurosci* 2019; **13:** 91.

317. Qian Y, Galli A, Ramamoorthy S, Risso S, DeFelice LJ, Blakely RD. Protein kinase C activation regulates human serotonin transporters in HEK-293 cells via altered cell surface expression. *J Neurosci* 1997; **17**(1)**:** 45-57.

318. Odaira T, Nakagawasai O, Takahashi K, Nemoto W, Sakuma W, Lin JR*, et al*. Mechanisms underpinning AMP-activated protein kinase-related effects on behavior and hippocampal neurogenesis in an animal model of depression. *Neuropharmacology* 2019; **150:** 121-133.

319. Guo X, Mao R, Cui L, Wang F, Zhou R, Wang Y*, et al*. PAID study design on the role of PKC activation in immune/inflammation-related depression: a randomised placebo-controlled trial protocol. *Gen Psychiatr* 2021; **34**(2)**:** e100440.

320. Lau T, Heimann F, Bartsch D, Schloss P, Weber T. Nongenomic, glucocorticoid receptor-mediated regulation of serotonin transporter cell surface expression in embryonic stem cell derived serotonergic neurons. *Neurosci Lett* 2013; **554:** 115-120.

321. Willeit M, Sitte HH, Thierry N, Michalek K, Praschak-Rieder N, Zill P*, et al*. Enhanced serotonin transporter function during depression in seasonal affective disorder. *Neuropsychopharmacology* 2008; **33**(7)**:** 1503-1513.

322. Hershenberg R, McDonald WM, Crowell A, Riva-Posse P, Craighead WE, Mayberg HS*, et al*. Concordance between clinician-rated and patient reported outcome measures of depressive symptoms in treatment resistant depression. *J Affect Disord* 2020; **266:** 22-29.

323. Reilly TJ, MacGillivray SA, Reid IC, Cameron IM. Psychometric properties of the 16-item Quick Inventory of Depressive Symptomatology: a systematic review and meta-analysis. *J Psychiatr Res* 2015; **60:** 132-140.

324. Park DI, Dournes C, Sillaber I, Ising M, Asara JM, Webhofer C*, et al*. Delineation of molecular pathway activities of the chronic antidepressant treatment response suggests important roles for glutamatergic and ubiquitin-proteasome systems. *Transl Psychiatry* 2017; **7**(4)**:** e1078.

325. Camara ML, Almeida TB, de Santi F, Rodrigues BM, Cerri PS, Beltrame FL*, et al*. Fluoxetine-induced androgenic failure impairs the seminiferous tubules integrity and

increases ubiquitin carboxyl-terminal hydrolase L1 (UCHL1): Possible androgenic control of UCHL1 in germ cell death? *Biomed Pharmacother* 2019; **109:** 1126-1139.

326. Rossi M, Rotblat B, Ansell K, Amelio I, Caraglia M, Misso G*, et al*. High throughput screening for inhibitors of the HECT ubiquitin E3 ligase ITCH identifies antidepressant drugs as regulators of autophagy. *Cell Death Dis* 2014; **5**(5)**:** e1203.

327. Tramarin M, Rusconi L, Pizzamiglio L, Barbiero I, Peroni D, Scaramuzza L*, et al*. The antidepressant tianeptine reverts synaptic AMPA receptor defects caused by deficiency of CDKL5. *Hum Mol Genet* 2018; **27**(12)**:** 2052-2063.

328. Peters EJ, Slager SL, Kraft JB, Jenkins GD, Reinalda MS, McGrath PJ*, et al*. Pharmacokinetic genes do not influence response or tolerance to citalopram in the STAR*D sample. *PloS one* 2008; **3**(4)**:** e1872.

329. Collins PY, Insel TR, Chockalingam A, Daar A, Maddox YT. Grand challenges in global mental health: integration in research, policy, and practice. *PLoS medicine* 2013; **10**(4)**:** e1001434.

330. Cianconi P, Betro S, Janiri L. The Impact of Climate Change on Mental Health: A Systematic Descriptive Review. *Front Psychiatry* 2020; **11:** 74.

331. World Health O (2022). COVID-19 pandemic triggers 25% increase in prevalence of anxiety and depression worldwide. World Health Organization: Geneva.

332. Uher R, Tansey KE, Malki K, Perlis RH. Biomarkers predicting treatment outcome in depression: what is clinically significant? *Pharmacogenomics* 2012; **13**(2)**:** 233-240.